

**IMPACT OF ACID ATMOSPHERIC DEPOSITION
ON SOILS:**

**QUANTIFICATION OF CHEMICAL AND
HYDROLOGIC PROCESSES**

5 5 000 000

CR-KADDEX

CENTRALE LANDBOUWCATALOGUS



0000 0298 6558

BIBLIOTHEEK
LANDBOUWUNIVERSITEIT
WAGENINGEN

40951

Promotoren: dr. ir. N. van Breemen
hoogleraar in de bodemvorming en ecopedologie

dr. ir. F.A.M. de Haan
hoogleraar in de bodemhygiëne en bodemverontreiniging

Co-promotor: dr. ir. W.H. van Riemsdijk
universitair hoofddocent in de bodemhygiëne en
bodemverontreiniging

UNO8201, 1233

J.J.M. van Grinsven

**IMPACT OF ACID ATMOSPHERIC DEPOSITION
ON SOILS:
QUANTIFICATION OF CHEMICAL AND
HYDROLOGIC PROCESSES**

Proefschrift
ter verkrijging van de graad van
doctor in de landbouwwetenschappen,
op gezag van de rector magnificus,
dr. H.C. van der Plas,
in het openbaar te verdedigen
op vrijdag 16 september 1988
des namiddags te vier uur in de aula
van de Landbouwuniversiteit te Wageningen

ISW 415 716

Aan mijn ouders

STELLINGEN:

1. Substantial differences exist in the magnitudes of rate estimates from the field and the laboratory. At present there is not a good mechanistic understanding why these differences exist, so this will be a fruitful area for future research.

George Holdren and Patricia Speyer, *Geochim. Cosmochim. Acta* 51: p. 2311-2318, 1987.

2. De effecten van waterbeweging op verweringskinetiek, welke werkzaam zijn vanaf de schaal van verweringsplekken op een bodemdeeltje, tot op de schaal van een vanggebied, worden sterk onderschat. Effecten van waterbeweging verklaren een belangrijk deel van de waargenomen verschillen tussen verweringsnelheden van experimenten onderling, en van experiment en veld.

dit proefschrift

3. De ruwheid van het oppervlak van mineralen als gevolg van heterogene oppervlaktereacties zou niet verdwijnen bij overheersing van de verweringsnelheid door diffusietransport (Michael Velbel, In: J.A. Davis and K.F. Hayes (eds.) "Geochemical Processes at Mineral Surfaces", ACS Symposium series no. 323: p. 615-640, 1986), maar slechts verminderen.

dit proefschrift

4. Aangezien de toestand van het mineraaloppervlak de oplosnelheid bepaalt, hebben oplosnelheden van gezuiverde of kunstmatige mineralen slechts in relatieve zin betekenis voor verweringsnelheden in het veld.

dit proefschrift

5. Bij handhaving van de huidige snelheden van zure depositie gedurende de volgende 50 jaar, is uitputting van de voorraad van secundaire oxiden en hydroxiden van Al in de bodem een reëel probleem voor Nederlandse zandgronden. Hierdoor zal een ingrijpende verandering van het buffergedrag van de bodem optreden.

dit proefschrift

6. De verandering van de zuurgraad van de bodemoplossing is een slechte indicator voor veranderingen in het bodem-ecosysteem. Het proton is bij vrijwel alle bodemchemische processen betrokken, waardoor de zuurgraad relatief constant blijft, zelfs bij ingrijpende veranderingen in het ecosysteem zoals na reductie van zure depositie, bemesting of kap. Onder deze omstandigheden uiten veranderingen zich met name in veranderingen van concentraties en fluxen van stikstof en aluminium.

dit proefschrift

7. The failure to detect a leached layer using X-ray Photoelectron Spectroscopy is no proof of non-existence of such a layer.

Lei Chou and Roland Wollast, *Geochim. Cosmochim. Acta* 48: p. 2205-2217, 1984.

8. Uncertainties in estimating the area of mineral surface in contact with percolating fluids cause several orders of magnitude of variability of mineral weathering rates.
Michael Velbel, Geochemical mass balances and weathering rates in forested watersheds of the Southern Blue Ridge. *Amer. J. Sci.* 283: 904-930, 1985.
9. There is no statistically significant, positive correlation between the observed reaction rate and the exposed surface of the starting material.
George Holdren and Patricia Speyer, *Geochim. Cosmochim. Acta* 49: p. 675-681, 1985.
10. Since the increase in weathering rate upon increase of $[H^+]$ is less than linear, increased acidification resulting from atmospheric input cannot be fully compensated by increase in neutralization rate in the watershed.
Werner Stumm, Gerhard Furrer, Erich Wieland and Bettina Zinder, In: J.I. Drever (ed.) "The chemistry of weathering": p. 1997-2016, 1985.
11. Na het lezen van "Chaos; Making a new science" door James Gleick, en "Gaia; A new look on life on earth" door Jim Lovelock, blijft de vraag of het uitoefenen van grote druk op complexe systemen zoals, de mens, de bodem en de aarde, kan leiden tot onomkeerbare ontregeling van dergelijke systemen.
12. De ervaring dat motorrijders vaak doodrijders zijn, betekent niet dat een motorrijwiel een onveilig voertuig is dan een auto.
13. Het academisch of Wagenings kwartiertje heeft vaak onterecht een negatieve bijklank aangezien het meestal ook inhoudt dat men minstens een kwartier langer beschikbaar is.
14. Taalkundig is het juist om gebruikers van simulatiemodellen simulanten te noemen.
15. Met betrekking tot mogelijkheden ter bestrijding van zure atmosferische depositie, bevindt Nederland zich in een relatief gunstige positie aangezien 40% van de zure depositie door ammoniak veroorzaakt wordt en afkomstig is uit lokale bronnen. Hierdoor is reductie van emissie van ammoniak "slechts" een nationaal probleem, welke bovendien zeer snel tot verbetering van de bodemwaterkwaliteit onder bossen en natuurterreinen zal leiden.
16. Mogelijk zullen enkele bomen gered worden door inzicht uit computer-simulaties, maar zeker één boom is geveld voor de computer-simulatie beschreven in dit proefschrift.
17. Een onderschat probleem bij de evaluatie van experimenteel onderzoek betreft de verwerping van afwijkende meetwaarden. Vroegtijdige verwerping kan leiden tot een verarmd beeld van de onderliggende dynamiek van natuurlijke processen.

ABSTRACT

Van Grinsven, J.J.M., 1988. Impact of acid atmospheric deposition on soils: Quantification of chemical and hydrologic processes. Doctoral thesis. Agricultural University, Wageningen, The Netherlands.

Atmospheric deposition of SO_x , NO_x and NH_x will cause major changes in the chemical composition of solutions in acid soils, which may affect the biological functions of the soil. This thesis deals with quantification of soil acidification by means of chemical budgets, kinetics of mineral weathering of aluminum and base cations, and simulation of soil acidification. Most results apply to an acid forest soil on the Hackfort estate, for which monitoring data were available from 1981 to 1987.

Spatial variability of soil solution composition was found to be the dominant source of uncertainty in determining chemical budgets. Uncertainty in annual chemical budgets due to simulation of unsaturated soil water fluxes generally does not exceed 10%. A new method was developed for in situ measurement of unsaturated soil water fluxes at a similar accuracy as obtained by numerical simulation.

Weathering of Al is the dominant process for proton buffering in acid soils. In dutch acid soils, the most reactive pool for Al is present in hydrated oxides, often in association with organic matter. On average the weathering rate of Al increases nearly proportional with (H^+) , and decrease strongly with increasing depletion of reactive Al. Total exhaustion of the reactive pool of hydrated oxides may become a problem in the coming century.

A new column percolation technique was developed to measure weathering rates at controlled pH in absence of mechanical disturbance. In all cases base cation weathering rates from laboratory experiments were considerably higher than estimated from field mass balance studies. A yet unconsidered effect for explanation of this discrepancy, is the increase of weathering rate with (by approximation the square root of) the percolation rate. Moreover, evidence was found that assumed patchy coatings of secondary Al may be protective against weathering of Ca from plagioclases.

The ILWAS model was adapted for simulation of soil acidification. The model proved to be appropriate to simulate annual budgets and seasonal variation of concentrations for all major components. Concentration peaks near the end of summer appeared to be overestimated, but also scarce field observations may be biased. The model seemed somewhat too crude to predict N-dynamics. The model was used to analyze the response of the soil system to 50% reduction of deposition, fertilization, and removal of forest vegetation. Scenario analyses, demonstrated that pH is not a sensitive indicator for changes in soil chemistry. Simple models, using large time steps, may be adequate to evaluate average annual changes of soil solution characteristics over periods of several decades.

Additional Index Words: unsaturated soil hydrology, flux measurement, chemical budget, pH buffering, weathering kinetics, column experiment, field mass balance, aluminum, base cations, percolation rate, etch pit, coating, simulation, sensitivity analysis, scenario analysis.

VOORWOORD

Na zes jaren van onderzoek aan een breed scala van onderwerpen is mijn proefschrift daar, hetgeen ik ervaar als de bekroning van twaalf jaren in het Wageningse. Dit proefschrift is het produkt van een gezamenlijke inspanning zoals tot uitdrukking gebracht in de namen van de vele mede-auteurs van de opgenomen publicaties en manuscripten.

Op de eerste plaats wil ik mijn ouders bedanken die mij altijd gestimuleerd en ondersteund hebben in mijn nieuwsgierigheid en studieambities. Helaas heeft mijn vader de Wageningse periode niet meer mee mogen maken, en heb ik hem maar kort als vriend mogen ervaren.

Dit proefschrift heeft in belangrijke mate vorm gekregen door de inspanningen en interesse van mijn promotoren Nico van Breemen, Willem van Riemsdijk en Frans de Haan. Nico, jou wil ik bedanken voor de grote vrijheid die je me hebt toegestaan in een overbelast projekt en voor de niet aflatende stroom van creatieve ideeën. Willem, jou bedank ik voor het "echte" chemische inzicht en voor de vele inspirerende wetenschappelijke steekspelen. Frans, jou bedank ik voor de gastvrijheid op de vakgroep en voor het aandeel dat ik mocht genieten in het geven van doctoraalonderwijs.

Ook wil ik alle medewerkers in het zure regenprojekt bedanken voor de warme collegialiteit en de vanzelfsprekende bereidwilligheid om me altijd van dienst te zijn wanneer ik analyses, data of een helpende hand nodig had; bedankt Eef Velthorst, Harrie Bootink, Tom Pape, Marcel Lubbers, Neel Nakken, Frans Lettink, en Leo Begheijn.

Een belangrijk deel van het proefschrift handelt over minerale verwerking, en is gebaseerd op kolomexperimenten in het kader van een samenwerkingsverband tussen de vakgroep Bodemkunde en Geologie en het Energie Centrum Nederland te Petten. Hierbij wil ik in het bijzonder René Otjes bedanken voor het geduld en vakmanschap waarmee hij mijn vaak amorphe ideeën vorm gaf, en Tjip Lub voor zijn inhoudelijke ondersteuning.

In de loop van de jaren hebben een groot aantal doctoraalstudenten aan het onderzoek meegewerkt en zijn hun resultaten verwerkt in dit proefschrift. De samenwerking met, en de begeleiding van deze studenten heb ik altijd als plezierig ervaren en heeft een aantal vriendschappen voortgebracht. Hierbij bedank ik jullie; Egbert Brouwer, Dave Kloeg, Wolf Knab, Chris Kooge, Marjan Sperna Weiland, Hans Postma, Egbert Heslinga, Gijs Breedveld, Hans Kros, Hugo Denier van der Gon, Erik van Eek, Hans van den Dool en Bart Wesselink.

Verder wil ik Chris Dirksen bedanken als aangename buurman en als altijd beschikbare vraagbaak voor mijn problemen op gebied van onverzadigde waterstroming en de Engelse taal.

Tijdens mijn onderzoek ben ik altijd gevrijwaard gebleven voor grote hoeveelheden werk m.b.t projectorganisatie en -beleid. Naast Nico van Breemen wil ik ook Fré Schelbergen hiervoor bedanken die als een waar tovenaer in zeer korte tijd de meest fantastische "klusjes" voor mij heeft kunnen klaren.

Leen van der Plas en de sectie mineralogie ben ik erkentelijk voor hun bijdragen aan mijn late mineralogische inhaaloperatie.

Verder wil ik hier Egbert Nab en Simon Maasland van de vakgroep Bodemkunde en Plantenvoeding bedanken voor hun hulp bij vele klussen en ook voor de schier eindeloze stroom van relativerende uitspraken.

Het werken op en met twee grote vakgroepen leidt onvermijdelijk tot het vergeten van persoonlijke dankwoorden. Daarom wil ik hier tot slot nog even kwijt dat ik de afgelopen zes jaren met veel plezier tussen jullie vertoefd heb, en met vrucht van de samenwerking heb kunnen profiteren.

Auch möchte ich das Staatliches Amt für Wasser und Abfallwirtschaft in Münster, vor allem Dr. Manfred Schroeder, danken für die Zustimmung zur Anwendung der Lysimeteranlage in St. Arnold und für die angenehme Zusammenarbeit.

De afgelopen jaren zijn er een aantal hechte vriendschappen op beide vakgroepen ontstaan waaruit ik veel plezier en inspiratie heb kunnen putten; Hein ten Berge, Sjoerd van der Zee, Pieter de Visser, Jan Mulder, Tom Feijtel en Carla Konsten, let's stick together.

De eerste drie jaren van mijn contractperiode werden gefinancierd door de EEG, onder projekt ENV-650-NL. De laatste drie jaren zijn gefinancierd door het ministerie van Volkshuisvesting, Ruimtelijke ordening en Milieuhygiëne in het kader van het Nationaal Programma Zure Regen. In verband met het laatstgenoemde wil ik Tom Bresser en Dr. Schneider van het RIVM bedanken voor de vrijheid waarmee ik mijn onderzoek richting kon geven.

Tot slot wil ik mijn huisgenoten bedanken voor het geduld waarmee ze mijn niet altijd even sociale werklust hebben gedoogd; Flip, Tanja, Johanneke, Sandra, Marg, Erik, Frens en Dirk bedankt.

CONTENTS

| | |
|---|----------|
| 1. GENERAL INTRODUCTION | 1 |
| 2. EFFECTS OF ACID ATMOSPHERIC DEPOSITION ON SOIL AND GROUNDWATER | |
| 2.1 Introduction | 7 |
| 2.2 Soil Acidification; The concept of acid neutralizing capacity | 8 |
| 2.3 Natural and enhanced soil acidification | 10 |
| 2.4 Chemical characteristics of acidified soils | 11 |
| 2.5 Effects on groundwater and drinking water | 12 |
| 2.6 Key processes and critical parameters | 13 |
| 2.7 Some conclusive remarks | 17 |
| 3. IMPACTS OF ACID ATMOSPHERIC DEPOSITION ON WOODLAND SOILS IN THE NETHERLANDS: I. CALCULATION OF HYDROLOGIC AND CHEMICAL BUDGETS | |
| 3.1 Introduction | 19 |
| 3.2 Materials and methods | 20 |
| 3.2.1 Soil sites and monitoring | 20 |
| 3.2.2 Water retention and hydraulic conductivity | 21 |
| 3.2.3 The flow model | 22 |
| 3.2.4 Evapotranspiration | 23 |
| 3.2.5 Parameter choice and sensitivity analysis | 24 |
| 3.3 Results and discussion | 28 |
| 3.3.1 Model calibration for plot A | 28 |
| 3.3.2 Error analysis for simulated soil water fluxes | 30 |
| 3.3.3 Differences between plots | 32 |
| 3.4 Summary and conclusions | 33 |
| 4. AUTOMATED IN SITU MEASUREMENT OF UNSATURATED SOIL WATER FLUX | |
| 4.1 Introduction | 35 |
| 4.2 Materials and methods | 37 |
| 4.2.1 Description of the fluxmeter | 37 |
| 4.2.2 Description of laboratory setup | 38 |
| 4.2.3 Field test | 39 |
| 4.3 Results and discussion | 40 |
| 5. A COMPARISON BETWEEN BATCH AND COLUMN TECHNIQUES TO MEASURE WEATHERING RATES IN SOILS. DISCREPANCIES WITH RATES OBSERVED IN FIELD MASS BALANCE STUDIES | |
| 5.1 Introduction | 45 |
| 5.1.1 Mineral weathering in soils | 45 |
| 5.1.2 Discrepancy between weathering rates in the laboratory and in the field | 46 |
| 5.1.3 Rate controlling processes and reactive surface area | 47 |
| 5.2 Review of laboratory methods to study weathering kinetics | 48 |
| 5.2.1 Batch techniques | 48 |
| 5.2.2 Column techniques | 49 |
| 5.2.3 Improved methods to study weathering kinetics in soil samples | 49 |

| | | |
|---------------|---|-----|
| 5.3..... | Materials and methods | 52 |
| 5.3.1 | Soil material and chemical analysis | 52 |
| 5.3.2.... | Batch experiments | 53 |
| 5.3.3.... | Column experiments | 54 |
| 5.3.4 | The effectiveness of diffusion transport | 55 |
| 5.4..... | Results and discussion | 57 |
| 5.4.1 | Effect of sample pretreatment | 57 |
| 5.4.2.... | Effect of experimental method | 59 |
| 5.4.3.... | Effect of percolation rate | 61 |
| 5.5..... | Conclusions | 65 |
| 6..... | KINETICS OF THE DISSOLUTION OF ALUMINUM AND BASE | |
| | CATIONS FROM A SOIL AT pH VALUES BELOW 4 | |
| 6.1..... | Introduction | 67 |
| 6.2..... | Materials and methods | 68 |
| 6.3..... | Results and discussion | 69 |
| 6.3.1 | Solid phase characteristics | 69 |
| 6.3.2.... | A mechanistic interpretation of experiment I | 69 |
| 6.3.3.... | A kinetic illite dissolution model for experiment I | 71 |
| 6.3.4.... | Dissolution kinetics in experiment II | 75 |
| 6.3.5.... | Comparison of H ⁺ consumption rates for the surface soil and the | |
| | subsoil in experiment III | 76 |
| 6.4..... | Conclusions | 77 |
| 7..... | WEATHERING KINETICS IN ACID SANDY SOILS FROM COLUMN | |
| | EXPERIMENTS: I. ALUMINUM | |
| 7.1..... | Introduction | 79 |
| 7.2..... | Materials and methods | 80 |
| 7.2.1 | Soil samples and chemical analysis | 80 |
| 7.2.2.... | Column percolation at constant pH | 82 |
| 7.2.3.... | Unstirred batch experiments | 85 |
| 7.2.4.... | The empirical model | 85 |
| 7.3..... | Results and discussion | 86 |
| 7.3.1 | General features of the experiments | 86 |
| 7.3.2.... | Weathering stoichiometry | 87 |
| 7.3.3.... | Experimental artefacts | 88 |
| 7.3.4.... | Application of the empirical model | 90 |
| 7.3.5.... | Effects of pH and depletion on the Al dissolution rate | 92 |
| 7.3.6.... | Effect of mineral saturation on dissolution rate of Al | 94 |
| 7.3.7 | Pools of reactive Al | 96 |
| 7.3.8.... | Effect of temperature | 97 |
| 7.4..... | Summary and conclusions | 99 |
| 8..... | WEATHERING KINETICS IN ACID SANDY SOILS FROM COLUMN | |
| | EXPERIMENTS: II. BASE CATIONS | |
| 8.1..... | Introduction | 101 |
| 8.2..... | Materials and methods | 103 |
| 8.3..... | Results and discussion | 106 |
| 8.3.1 | General features of the column experiments | 106 |
| 8.3.2.... | Comparison of percolation with CsCl and soil extracts | 107 |
| 8.3.3.... | The role of cation exchange in the A-horizon of the Dystrichrept | 108 |
| 8.3.4.... | Mineral pools of base cations | 111 |
| 8.3.5.... | Weathering of K, Na, and Mg from the C-horizon | 112 |

| | | |
|-----------|---|-----|
| 8.3.6.... | Comparison of weathering rates of Na from different soil horizons | 114 |
| 8.3.7.... | Comparison of weathering rates from column, batch and field experiments | 114 |
| 8.3.8.... | Hydrodynamic effect of percolation rate on weathering rate | 116 |
| 8.4..... | Summary and conclusion | 117 |

**9..... EVIDENCE FOR INCREASED WEATHERING OF Ca FROM
..... PLAGIOCLASES AS A RESULT OF DISSOLUTION OF PROTECTIVE
..... Al COATINGS IN ACID SOLUTIONS**

| | | |
|-----------|--|-----|
| 9.1..... | Introduction | 119 |
| 9.2..... | Materials and methods | 120 |
| 9.2.1.... | Soil samples and chemical analysis | 120 |
| 9.2.2.... | Column and unstirred batch experiments | 122 |
| 9.3..... | Results and discussion | 122 |
| 9.4..... | Summary and conclusion | 128 |

**10..... THE ILWAS MODEL TO ANALYSE THE RESPONSE OF AN ACID
..... FOREST SOIL TO ACID DEPOSITION AND MITIGATION
..... MEASURES**

| | | |
|-----------|---|-----|
| 10.1..... | Introduction | 131 |
| 10.2..... | Materials and methods | 132 |
| 10.2..... | 1The ILWAS model | 133 |
| 10.2.2.. | Modification of the ILWAS model | 137 |
| 10.2.3.. | Site characteristics and model parameterization | 138 |
| 10.2.4.. | Model calibration | 141 |
| 10.2.5.. | Scenarios | 142 |
| 10.3..... | Results and discussion | 143 |
| 10.3.1.. | Simulation of waterfluxes and [Cl] | 143 |
| 10.3.2.. | Simulation of annual solute fluxes and flux weighted concentrations | 147 |
| 10.3.3.. | Simulation of time series of concentration | 149 |
| 10.3.4.. | 50% reduction of atmospheric deposition of $(NH_4)_2SO_4$ | 153 |
| 10.3.5.. | Addition of K_2SO_4 and $MgSO_4$ | 155 |
| 10.3.6.. | Removal of forest vegetation | 157 |
| 10.4..... | Conclusions | 159 |

**11..... THE SENSITIVITY OF ACID FOREST SOILS TO ACID
..... DEPOSITION**

| | | |
|-----------|---------------------------------|-----|
| 11.1..... | Introduction | 161 |
| 11.2..... | The model | 162 |
| 11.3..... | Field data and model parameters | 165 |
| 11.4..... | Simulation procedures | 166 |
| 11.5..... | Results and discussion | 169 |

**12..... THE EFFECT OF PERCOLATION RATE ON WEATHERING
..... KINETICS**

| | | |
|-----------|------------------------------------|-----|
| 12.1..... | Introduction | 173 |
| 12.2..... | Materials and methods | 174 |
| 12.2.1.. | Soil samples and chemical analysis | 174 |
| 12.2.2.. | Column experiments | 175 |
| 12.2.3.. | Computational procedures | 175 |
| 12.3..... | Results and discussion | 176 |
| 12.4..... | Conclusions | 180 |

| | |
|---|-----|
| 13..... WEATHERING RATES FROM LONG-TERM COLUMN | |
| EXPERIMENTS | |
| 13.1 Introduction | 181 |
| 13.2 Materials and methods | 182 |
| 13.3 Results and discussion | 183 |
| 13.3.1 .. Aluminum and hydrogen | 183 |
| 13.3.2 .. Base cations and silica | 186 |
| 13.4 Conclusions | 190 |
| | |
| SUMMARY | 191 |
| | |
| SAMENVATTING | 197 |
| | |
| MAJOR CONCLUSIONS | 203 |
| | |
| REFERENCES | 205 |
| | |
| Curriculum Vitae | 215 |

Chapter 1

GENERAL INTRODUCTION

Since the onset of the Industrialization in the previous century, emission and atmospheric deposition of potentially acid substances, particularly SO_x , NO_x and their derivatives, have increased considerably. The main source of SO_x - and NO_x -emission is burning of fossil fuels, particularly coal and oil, for energy supply, chemical industry and transportation. In areas with high industrial activity, eg. in central and western Europe and the north-east of the USA, increases of emission and deposition were observed by a factor five to ten, for individual components. Long-distance transport of air-borne pollutants and acidic substances lead to enhanced deposition in remote, hardly industrialized areas, like northern Scandinavia, Canada, southern Bavaria and Switzerland. More recently, emission and deposition of acidic substances in quickly industrializing countries of south-east Asia and South America has also started to increase at a high rate.

Large lake and forest areas in Scandinavia, Canada, the north-east of USA, central Europe, and also in the tropics, receiving acid atmospheric deposition from industrialized areas, are underlain by acid soils and rocks. Due to the absence of adequate buffering capacity in these remote areas, acid atmospheric deposition has led to acidification of water in soils, regolith, streams and lakes. Typical acidification phenomena in surface and sub-surface waters are a decrease of pH and alkalinity, an increase of the concentration of Al and a decrease of concentrations of Ca, Mg and K (so-called base cations).

In the Netherlands, atmospheric deposition of NH_x , represents an additional source of acidification to surface and sub-surface water, which has caused large changes in solution composition in soils under forests and nature reserves. NH_x is emitted mainly by intensive animal husbandry. After infiltration in the soil profile, NH_x may be nitrified and will acidify the soil, provided that nitrogen is not taken up by the vegetation. Increased atmospheric deposition of nitrogen may be judged favorably, in case it will increase forest production. However, even without nitrification increased deposition of N may be regarded as unwelcome in areas with valuable plant communities associated with specific (often low) nutrient availability (eg. heath ecosystems).

In the sixties and seventies a decrease of forest vitality and abundance of fish-, plant- and fungi-species was observed in central and northern Europe and northern America, even in remote areas. In many cases, this decrease could be attributed to the specific impact of air pollution and acid atmospheric deposition.

Impairment of the vegetation by air pollution and acid atmospheric deposition can both result from direct effects on leaf tissue and from indirect effects on the root environment. Examples of direct effects of acid atmospheric deposition on leaf tissue are leaching of cations, and damage of foliar tissue by action of sulfuric acid, nitric acid and ozone. Indirect effects on the root environment are caused by increased concentrations of H, Al and NH_4 in the soil solution. These ions can both have toxic effects on root tissues, and may counteract uptake of essential plant nutrients, like Mg, K, Ca and P. Furthermore, soil acidification may affect the microflora and -fauna in the soil, which play an important intermediate role in nutrient uptake.

Internationally there seems to be a consensus on the nature and magnitude of changes in the chemical composition of soil water and surface water, in large areas of the world as a result of acid atmospheric deposition. Many examples of adverse effects of soil acidification and increased nitrogen deposition on plant growth and abundance of plant species have been demonstrated. However, no consensus exists about the extent of damage caused by acid atmospheric deposition on the biota in forest-soil- and lake-ecosystems. As long as effects of these changes in water chemistry on living organisms remain uncertain or a matter of discussion, the long-term fate of forest- and lake-ecosystems is a matter of great concern. Another pressing question concerns the reversibility of the acknowledged effects of atmospheric deposition on the soil environment. Typical soil acidification phenomena like decrease of pH, increase of Al-concentration, depletion of the buffering capacity and the availability of exchangeable K, Ca and Mg, are theoretically reversible by addition of lime or fertilizers. Addition of these substances may be feasible for the relatively small forested areas in the Netherlands but is hardly possible from a practical point of view in vast, poorly accessible forest regions in Scandinavia and Canada. Excessive liming may enhance mineralization of organic matter, which may result in leaching losses of N and base cations, and a decrease of CEC. Irreversible, more speculative, effects associated with acid atmospheric deposition are erosion after forest dieback, and blocking of exchange sites by Al-precipitation.

In strongly acidified areas in the Ertz-Gebirge in Tsjechslowakia, it was observed that within one century a flourishing forest of spruce (*Picea excelsa* L.) appeared and was gradually replaced by birch (*Betula pendula* L.) and mountain-ash berry (*Sorbus aucuparia* L.), which are more resistant to soil acidity. In many cases soil acidification will probably lead to changes in plant species composition rather than to a man-made desert. The appraisal of these changes is rather arbitrary. However, the intermediate stage in ecosystems, after soil cover has strongly decreased due to effects of acid deposition and before

re-establishment of a new vegetation, may have catastrophic consequences. Increased drainage due to decreased evapotranspiration and shorter residence times of water in the catchment may cause disastrous flooding in urban areas along river banks, and may cause soil erosion due to the increase of surface runoff. So, irrespective of the acceptability of man-induced changes in the biological variety of extensively managed ecosystems, international measures will have to be taken to prevent the large scale reduction of vegetation cover in mountainous areas.

The previous discussion is not always directly relevant for the situation in the Netherlands, as only 10% of the total area is covered by forest, which are located in flat or slightly undulating regions. However, the rate of soil acidification in the Netherlands is high compared to that in more remote forest areas in Scandinavia and Canada, because of high levels of atmospheric deposition of NH_x . Moreover, forested areas in our highly urbanized and densely populated country have many important functions. The direct economical use of our forests and nature reserves is rather small, but their recreational and social function, and their importance to accommodate typically Dutch plant-animal communities is invaluable.

After recognition of the importance of man-induced soil acidification, scientific research in the Netherlands was strongly stimulated. Important issues for research on soil acidification were and are:

- The definition of soil acidification.
- The measurement of soil acidification rates and the composition of the soil solution in the field, and the comparison of these rates for different soil types, vegetation types and regimes of soil acidification.
- Indication of the key processes involved in soil acidification, proton buffering and supply of plant nutrients. Quantification of these soil processes and the derivation of relationships between the rate and nature of these processes and the chemical and physical environment.
- Integration of the individual process formulations into a general simulation model for interaction and transport of chemical components in the soil. Prediction of changes in rates of soil acidification and changes in the composition of the soil solution as a result of changing boundary condition with respect to atmospheric deposition and vegetation characteristics.

The crux of soil acidification research in particular, and of integrated chemical, physical and biological soil research in general, is to increase the insight in the dynamic interactions of the soil system with its environment. The dynamic soil-ecosystem responds to a changing environment through a variety of physical, chemical and biological processes, which determine the characteristics of the solid phase, the aqueous and the gas phase of the soil. At the same time the aqueous phase and the gas phase act as transporting agents. The key principle for interaction is feed-back. Many beautiful examples can be given to illustrate the potential of the soil-ecosystem to control moisture content and pore volume, temperature and chemical composition. For maintaining a specific ecosystem, of moisture content, temperature and chemical composition should be confined to rather narrow ranges. The impact of man on the ecosystem is still increasing, and more than ever we are faced with the uncertainty about the potential of the soil-water-ecosystems to maintain a livable environment.

This book is one of two theses with the common title: "Impact of acid atmospheric deposition on soils". The first thesis is written by Jan Mulder and subtitled: "Field monitoring and aluminum chemistry". The studies underlying both theses were carried out as part of one research project, at the Department of Soil Science and Geology, into the effects of acid atmospheric deposition on soils. A large part of the project was financed by the European Economical Community and more recently by the Dutch Ministry of Environment, as part of the Dutch Priority Programme on Acidification. This thesis is a collection of publications and manuscripts on various subjects. The main topics are unsaturated soil hydrology, kinetics of mineral weathering, and computer simulation of transport and interactions of chemical constituents in soil. Detailed information on characteristics of the soil sites, field monitoring procedures and the chemistry of aluminum is given in the thesis by Jan Mulder.

- The definition and general features of soil acidification are discussed in Chapter 2.
- The quantification of elemental fluxes, which are needed to quantify soil acidification, are discussed in Chapter 3. Elemental fluxes are calculated by multiplying unsaturated soil water fluxes with concentrations in soil solution. Chapter 3 is focussed on the simulation of unsaturated soil water fluxes.
- Chapter 4 describes a new method to measure unsaturated soil water fluxes in the field, which may enable direct quantification of elemental fluxes in undisturbed plant-soil systems.

Chapters 5 to 9 are dealing with mineral weathering, in particular with reaction kinetics.

- In Chapter 5 various experimental techniques to study mineral weathering in the laboratory are compared and discussed. In this chapter kinetic artifacts of the experimental methods are emphasized.
- Chapter 6 discusses weathering kinetics in batch experiments, and evaluates a kinetic model which assumes rate control by the degree of mineral undersaturation.

- Chapter 7 describes a new technique to determine mineral weathering rates from packed soil columns at constant pH. Results are focussed on the dissolution of Al from oxides in the soil, which are the dominant sources of proton buffering in acid soils in the Netherlands.
- Chapter 8 deals with the slow release of base cations from acid soils as observed by the method described in chapter 7 and with unstirred batch experiments. The relations between the observed dissolution rates and the mineral composition, and field budget studies are emphasized.
- Chapter 9 reports anomalous dissolution behaviour of Ca from plagioclases giving evidence for the presence of protective coatings of aluminum-oxides.
- Chapter 10 describes an application of the ILWAS model for simulation of transport and biogeochemical interactions in an acid forest soil. The model is calibrated and used to evaluate the effects of decreased acid atmospheric deposition, fertilizer application and removal of the forest vegetation. The period from March 1981 to March 1987 is considered.
- Chapter 11 describes a simple simulation model for transport and interaction of H, Al, K, Na, Ca and Mg, NH_4 , NO_3 , SO_4 and Cl in soils, which is used to evaluate long-term (50 years) effects of altered rates of acid atmospheric deposition using data from long-term field monitoring studies. A new simulation procedure is proposed which allows the use of long time steps, and prevent excessive numerical dispersion.
- Chapter 12 deals with the effect of percolation rate on the rate of mineral weathering, which was studied by means of column experiments at percolation rate varying by a factor of 50.
- Chapter 13 describes results of column percolation experiments which were carried out over a period of 9 months, on both undisturbed and packed soil columns.

Chapter 2

EFFECTS OF ACID ATMOSPHERIC DEPOSITION ON SOIL AND GROUNDWATER

ABSTRACT

Acid atmospheric deposition will result in soil acidification, which may cause serious harm to forest production. Soil acidification involves the change of several soil properties. The decrease of the acid neutralizing capacity is a suitable parameter to quantify soil acidification. A decreased pH and increased concentrations of aluminum and ammonium as compared to concentrations of cationic plant nutrients affect biological functions. The magnitudes and time scales of changes in soil chemistry depend on cation exchange properties and the nature and rate of silicate weathering. Knowledge about these two processes is also essential to evaluate strategies to abate acid conditions in soils.

2.1 INTRODUCTION

Soil acidification is a natural process which can be strongly enhanced by atmospheric deposition of SO_2 , NO_x and NH_3 . Enhanced soil acidification due to acid deposition is an important example of soil degradation because the land area involved is very large and effects on biology develop very gradually and are often difficult to distinguish from natural phenomena and effects from other changes in the environment. Evidence grows that degradation of soil conditions due to acid deposition seriously harms forest production and the functioning of valuable ecosystems in north and central Europe and the north-west of the North American continent.

In the absence of a clear-cut definition of soil acidification several scientific controversies arose about the true nature of this process and about the relative importance of man-induced soil acidification versus natural soil acidification. Soil acidification can exert itself in various ways; by a decrease of pH or base saturation, by an increase in soil acidity, by an unbalanced availability of nutrients in the root environment or by a decrease of the acid neutralizing capacity (ANC) of the soil. From which angle one wishes to approach the soil acidification process depends on the question to be answered. Relevant questions are:

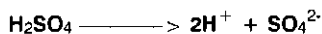
- To what extent is acid deposition deteriorating soil conditions now, and will it do in the future, and what are the effects on ecosystems in general and forest growth in particular?
- Which situations need amelioration and how should this amelioration of soil conditions be brought about?

To answer these questions we need a thorough understanding of chemical interactions in the soil related to the acidification process. Forest soils in general have a great capability to delay effects of acid deposition due to the presence of a large, mainly bio-organic, exchange complex. However the ultimate process for acid neutralization and supply of plant nutrients in (un-fertilized) soils is dissolution of silicate minerals. Compared to current deposition rates the capacity of silicate minerals to neutralize acid is nearly infinite. However the rates of dissolution are far more important as they seem to be similar to current deposition rates. Exchange reactions and mineral dissolution need to be understood to evaluate present and future effects of acid deposition on soil and to develop abatement strategies.

2.2 SOIL ACIDIFICATION; THE CONCEPT OF ACID NEUTRALIZING CAPACITY

The soil matrix generally consists of a large bulk of inert quartz in which various amounts of clay minerals, amorphous (hydr)oxides of aluminum and iron, primary minerals and organic matter are present. Clay minerals and organic matter have predominantly negatively charged surfaces (partly) neutralized by cations. If strong acid enters the soil it can react with the soil matrix in various ways:

- 1) If the protons do not react with soil constituents a pH decrease will take place.

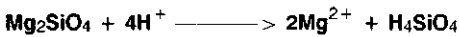


- 2) The positively charged protons can exchange against base cations (Na, K, Ca and Mg) bound to clay minerals or organic matter. The pH decrease will be less than in case (1) and will be insignificant when the proton input is

negligible compared to the total amount of base cations bound to clay minerals and organic matter.



3) The protons can react with primary minerals or (hydr)oxides. Protons will be bound in carbonic acid, water or silicic acid and cations will be brought into solution. This can be exemplified by the following reactions:



The pH decrease will be less than in (1). If the mineral is relatively reactive, as in the case of CaCO_3 the pH will remain approximately constant, as long as the mineral is present. If the mineral is not very reactive, the increase in pH will be noticeable only if the residence time of the percolating soil solution is long.

The above reactions illustrate the complexity of the soil acidification problem. Definition of soil acidification as a decrease of soil pH is obviously too narrow, although from an ecological point of view it might suffice because an unchanged pH generally indicates unchanged conditions for plant growth. Recently the definition of soil acidification as a decrease of the acid neutralizing capacity (ANC) was introduced (Van Breemen et al., 1983; 1984). The ANC of a soil is defined as the sum of cations minus the sum of strong acid anions, expressed as their potential to consume or produce protons above a pH of 3:

$$\text{ANC} = 6(\text{Al}_2\text{O}_3) + 2(\text{CaO}) + 2(\text{MgO}) + 2(\text{K}_2\text{O}) + 2(\text{Na}_2\text{O}) + 2(\text{MnO}) \\ 2(\text{FeO}) - 2(\text{SO}_3) - 2(\text{P}_2\text{O}_5) - \text{HCl} - \text{oxalate}$$

The terms correspond to the total amounts of the respective elements in an inorganic bulk soil sample, expressed eg. as capacity to consume moles of protons per kg of a bulk soil. Some consequences of the above definition are that any introduction of strong acid, eg. H_2SO_4 , will decrease the ANC. However when the strong acid would pass the soil unneutralized the ANC would remain unchanged. If a weak acid would be introduced to the soil, eg. H_2CO_3 or organic acids, the ANC would not be changed unless these acids mobilize cations which are subsequently leached from the soil system for which the ANC was defined. As in most areas in north and central Europe and the north-east of North America

precipitation exceeds evapotranspiration, leaching of cation from the soil, and consequently soil acidification according to the above mechanism, is very common.

Changes of ANC can be expressed in $\text{kmol}\cdot\text{ha}^{-1}\cdot\text{yr}^{-1}$.

2.3 NATURAL AND ENHANCED SOIL ACIDIFICATION

In a clean pre-industrial situation there are two sources of protons input to soil, carbonic acid (H_2CO_3) and organic acids. Carbonic acid will only dissociate protons at pH value above 5. Soil acidification due to carbonic acid therefore is of particular interest in soils with near neutral pH, including those rich in carbonate minerals. The overall reaction in calcareous soils is:



The net effect will be leaching of Ca from the soil profile and thus a decrease of ANC. Resulting soil acidification rates can be as high as $10\text{-}20 \text{ kmol}\cdot\text{ha}^{-1}\cdot\text{yr}^{-1}$, as compared to $4 \text{ kmol}\cdot\text{ha}^{-1}\cdot\text{yr}^{-1}$ due to acid deposition in the more exposed areas in the Netherlands, FRG and CSSR.

If a soil is decalcified and is covered by a vegetation, biological activity will produce organic acids, which can dissociate and cause pH values less than 4. Furthermore the organic anions can mobilize cations which are subsequently leached from the soil. This may result in a decrease of ANC in the order of 0.1 to $0.5 \text{ kmol}\cdot\text{ha}^{-1}\cdot\text{yr}^{-1}$ (De Vries and Breeuwsma, 1984).

Vegetation under unfertilized conditions tend to take up more cations than anions. For charge balance purposes this difference is compensated by an excretion of protons from the roots. Resulting soil acidification is of similar magnitude as that due to organic acids.

Regular removal of vegetation or litter by man will increase soil acidification, due to the concurrent net removal of cations from the inorganic soil system. Removal of forest litter for use in agriculture, which was common on poor soils until the beginning of this century, can increase soil acidification with 0.1 to 1, modern agricultural (fertilizer use, high harvests) with 2 to $3 \text{ kmol}\cdot\text{ha}^{-1}\cdot\text{yr}^{-1}$ (Pâces, 1985).

Wet and dry deposition of acid or potentially acid substances can increase soil acidification by 1 to $2 \text{ kmol}\cdot\text{ha}^{-1}\cdot\text{yr}^{-1}$ in Scandinavia and the north-west of North America and by 2 to $8 \text{ kmol}\cdot\text{ha}^{-1}\cdot\text{yr}^{-1}$ in west and central Europe.

2.4 CHEMICAL CHARACTERISTICS OF ACIDIFIED SOILS

Definition of soil acidification as a decrease of the ANC is unambiguous, but does not provide ecologically useful information. In this chapter we will describe some typical chemical features of naturally and anthropogenically acidifying soils.

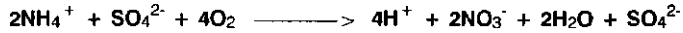
Interesting parameters are concentrations of a number of solutes in the soil solution especially of H, commonly expressed as pH ($-\log(\text{H}^+)$), Ca + Mg, hereafter addressed as M, and Al. Apart from the concentrations the fluxes of these components from the soil to the groundwater are of interest too.

In a carbonate holding soil the dominant anion will be HCO_3^- , the dominating cation will be M, the pH will be about 7, Al will be insignificant. The equivalent leachate flux ($\text{kmol}\cdot\text{ha}^{-1}\cdot\text{yr}^{-1}$) of Ca (and HCO_3) will equal the acidification rate. Concentrations also depend on the difference between precipitation and evapotranspiration. The smaller the difference, the higher concentrations tend to be. The difference between precipitation and evapotranspiration increases going from coniferous forest to deciduous forest to ground vegetation (eg. heath land) to bare soil. In the same range acid atmospheric deposition tends to decrease. Discussion from here on will deal with acid soils ($\text{pH} < 6$) which are not used for agriculture. Although soil acidification is a relevant process in agricultural soils, it poses no problem as adequate liming is common practice. In fact in agriculture the ANC of the soil may remain constant or even increase due to application of lime and some fertilizers as ANC contributors.

In naturally acid soils the anions in the leachate are mainly organic, while concentrations of Al can range between 30 and 100 $\text{mmol}\cdot\text{m}^{-3}$. Concentrations within the root zone are the overall result of a complex series of processes. Soils covered by a vegetation are involved in a cycle of nutrients (eg. NH_4 , NO_3 , M and K) which are mobilized at the surface by biodegradation of organic material, mineralization, and gradually taken up again by the roots from the percolating soil solution. The effects of atmospheric deposition on the soil solution composition is superimposed on the effects of the biocycle.

Atmospheric deposition of acid or potentially acid substances will increase the total amount of solutes in the soil. Generally concentrations of SO_4 and NO_3 will increase. The latter depends on whether deposited NO_3 or NH_4 is taken up by the vegetation. In the east of the Netherlands and the north-west of FRG deposition of NH_4 , up to $2 \text{ kmol}\cdot\text{ha}^{-1}\cdot\text{yr}^{-1}$ is common in woodlands, next to a

deposition of $1 \text{ kmol} \cdot \text{ha}^{-1} \cdot \text{yr}^{-1}$ of NO_3 . The NH_4 in many cases is, at least partly, nitrified in the soil, leading to increased soil acidification.



If all deposited NH_3 is taken up there will be no acidifying effect, if all deposited NH_3 is nitrified and not taken up soil acidification will be 1 mole per 1 mole of deposited NH_3 . In an early stage of soil acidification the generated acid will be neutralized by dissolution of Ca, K, Na and Mg. With progressing soil acidification, especially when at high rates, acid deposition will be neutralized by dissolution of Al. The capacity of the soil to produce Al is nearly infinite; compared to base cations Al is an abundant constituent of the soil matrix. Aluminum can be toxic, especially when the concentration is high compared to M. The same is true for NH_4 , when the concentration is high compared to that of K and Mg. Toxic effect of Al and NH_4 is diminished in the surface soil by mineralization of base cations.

Absolute concentrations of Al, SO_4 , NO_3 and NH_4 depend on vegetation type and deposition rate. For Dutch forests with deposition rates of 2 (deciduous) to 3 (coniferous) $\text{kmol} \cdot \text{ha}^{-1} \cdot \text{yr}^{-1}$, ionic equivalent concentrations of Al can amount to 2 and 4, of SO_4 1 and 2 and of NO_3 1 and 2 $\text{mmol} \cdot \text{m}^{-3}$, for deciduous and coniferous forests respectively. Concentrations of NH_4 in solutions of forest soils are generally low. Under heath land ionic equivalent concentrations of NH_4 can be as high as $0.5 \text{ mmol} \cdot \text{m}^{-3}$ due to less nitrification, which is still comparably low compared to concentrations of, for example, NO_3 in forest soils. This difference results from low evapotranspiration and deposition. Absolute concentrations in, generally coniferous, forests in Scandinavia will be up to ten times lower due to lower deposition rates and higher precipitation surpluses.

2.5 EFFECTS ON GROUNDWATER AND DRINKING WATER

Soil leachates rich in NO_3 , SO_4 , Al and possibly NH_4 , will eventually reach deeper groundwater. For example concentrations of NO_3 in soil water and shallow groundwater under Dutch woodland soils range between 50 and 200 $\text{mg} \cdot \text{l}^{-1}$ (Hoeks, 1986). These concentrations are alarming as they exceed the current drinking water standards of 50 $\text{mg} \cdot \text{l}^{-1}$ and are comparable to concentrations under heavily manured farmland. However the velocity of the nitrate front under forest (about $0.5 \text{ m} \cdot \text{yr}^{-1}$) is lower than under farmland ($1 \text{ m} \cdot \text{yr}^{-1}$),

due to a lower precipitation surplus. Current drinking water standards for NO_3 likely will be aggravated in the near future. Drinking water stations in the Netherlands are commonly located on sandy sediments under forest in areas with high ammonia deposition.

Due to denitrification the NO_3 concentration in groundwater may further decrease when moving down. However, low organic C contents and low pH may limit denitrification rates. High NO_3 concentrations in groundwater may also cause oxidation of sulfide containing sediments and explain occasionally reported low pH values at greater depths (≈ 10 m) (Hoeks, 1986).

Recently one drinking water pumping station has been closed already in an area in the Netherlands with high NO_3 concentrations due to excessive manure application. Groundwater quality near pumping stations is threatened and will be threatened, also under forest areas. Sulphate concentrations in soil water under woodlands due to acid deposition, $50\text{-}100\text{ mg.l}^{-1}$, also gradually approach the Dutch drinking water standard of 100 mg.l^{-1} (EC 250 mg.l^{-1}). A special problem is posed by drinking water from private wells, either for use by cattle or by man. Problems with NO_3 for cattle have been reported in the Netherlands. Recently a relation was suggested between the increasing occurrence of senile dementia and increased Al levels in drinking water from private wells in the UK.

2.6 KEY PROCESSES AND CRITICAL PARAMETERS

In order to obtain more insight in the present and future effects of acid deposition on the soil chemistry some key soil chemical processes will be discussed briefly.

Surface soils of forest generally have a large organic exchange complex, with equivalent capacities (CEC) up to 100 mmol.kg^{-1} . Cation equivalent exchange capacity for the rooted soil profile (0.3-1 m), converted to areal units, ranges from 200 to 500 kmol.ha^{-1} , which is considerable compared to deposition rates of 2 to $8\text{ kmol.ha}^{-1}\text{.yr}^{-1}$. Such a large exchange capacity strongly buffers concentrations of all cations in the soil solution. In an early stage of acid deposition a considerable portion of the exchange complex will be occupied by base cations. This fraction is generally indicated as base saturation value (BS). Protons will at first be exchanged against these base cations. As a result the pH in the soil solution remains relatively constant, while concentrations of base

cations are increased and are leached from the soil. In order to lower an initial BS of 30% to 10% in a soil with an equivalent CEC of $400 \text{ kmol} \cdot \text{ha}^{-1}$, 27 years of acid deposition at a rate of $3 \text{ kmol} \cdot \text{ha}^{-1} \cdot \text{yr}^{-1}$ would be necessary, assuming no resupply of bases from additional processes. In advanced stages of soil acidification the BS often lies below 10%, while the remainder of the CEC is occupied by H and Al. In order to restore the initial BS forest soils could be limed or deposition rates could be lowered. In the latter case natural resupply of bases (to balance net loss) would occur by mineral weathering, which will be discussed later in this chapter. To bring the BS from 10 to 30% 400 kg CaCO_3 per ha would be needed. Natural resupply by mineral weathering at a common rate of $0.5 \text{ kmol} \cdot \text{ha}^{-1} \cdot \text{yr}^{-1}$ would take at least 160 years. These examples clearly illustrate the delaying effect of the cation exchange complex on adverse effects of acid deposition and beneficial effects of lowering the deposition rate.

In all cases the exchange complex will prevent the occurrence of temporarily, extremely low pH values and associated high concentrations of Al. Such low pH conditions can prevail after dry periods in summer, when accumulated dry deposition is washed, all at once, from the forest canopy and infiltrates in the soil. Also acid pulses may occur at the start of snowmelt or right after a dry period.

A second crucial process is mineral weathering, which is the dissolution of primary and secondary soil minerals. The driving force for weathering is the attack of the mineral surfaces by protons. Primary minerals are generally aluminosilicates, that contain small amounts of base cations in their crystals, like eg. microcline (Na), albite and muscovite (K), anorthite and plagioclase (Ca), biotite (Ca and Mg) etc. Secondary minerals are residues of incomplete dissolution of primary minerals, or minerals newly formed from the reaction products of dissolution of primary minerals. The two main groups of secondary minerals are clay minerals, which in fact are a special group of aluminosilicates, and oxides and hydroxides of aluminum and iron. Secondary minerals generally have large surface areas and exchange capacities. Mineral dissolution is the primary source of base cations and plant nutrients in natural systems. The proportion of secondary minerals in the soil strongly varies and can amount to several tens of percentages, depending on rock type and geological history. Mineral weathering can be characterized by (1) the capacity to consume protons and to produce base cations and Al and (2) the dissolution rate, (3) the stoichiometry, which gives the nature and the relative occurrence of the dissolved ions.

The capacity of weathering to consume protons is very large. For an average soil with 20% silicate minerals, and a root zone of 0.5 m, the buffering capacity approximately is $20.000 \text{ kmol} \cdot \text{ha}^{-1}$. Capacities to produce base cations are also very large. Typical ionic equivalent pools for podzolic soils are 200 to 400 kmol Ca or Mg, 1000 kmol Na or K and 10.000 to 20.000 kmol Al per ha.

The dissolution rate is a far more important parameter than the capacity for mineral weathering. In the field, weathering rates of 0.5 to $5 \text{ kmol} \cdot \text{ha}^{-1} \cdot \text{yr}^{-1}$ (base cations + Al) are measured in chemical balance studies (Van Breemen et al., 1984; Ulrich, 1982). High weathering rates correspond to situations with high acidification rates and, for acid soils, with high fractions of aluminum in the dissolved ions. In general the larger part of proton production due to acid deposition is consumed in soil, suggesting that proton consumption rates are sufficiently high to meet present deposition rates. However, of more concern are the rates of base cation weathering; these determine whether the BS, which is the readily available pool of cationic plant nutrients will decrease, increase or remain constant. If the rate of exchange and subsequent leaching of base cations is larger than the rate of resupply by mineral weathering the pool will become smaller, if it is smaller the pool will increase if they are equal the pool will remain constant. Dissolution kinetics of primary minerals are still not sufficiently understood to predict weathering rates in field situations. It is generally accepted that weathering rates increase with decreasing pH and reactive surface area, and decrease with increasing accumulation of dissolved ions in the soil solution. Theoretically, weathering rates under different field conditions may vary by a factor of 10 to 100. High weathering rates can occur during short-lasting pH drops (!) or excessive flushing of the soil solution (dilution).

The amount of dissolved base cations and aluminum from the overall weathering reaction (the reaction stoichiometry) is important as it determines the absolute concentration of Al and its ratio to the concentration of M, which are both important parameters with respect to damage to the vegetation. The fraction of aluminum, which dissolves from silicate minerals, tends to be high at low pH and for high acid loadings, but will gradually decrease with increasing residence times of soil solutions. The underlying mechanism is not yet clear. If the fraction of dissolving aluminum decreases with decreased acid loading, the ratio between concentrations of Al and M will eventually improve when deposition rates would be lowered (Figure 2.1).

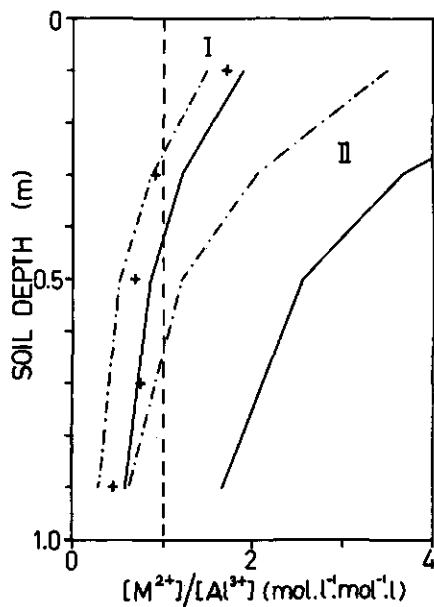
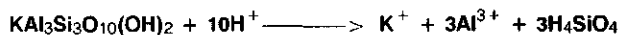
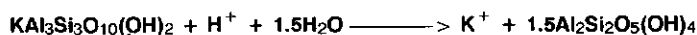
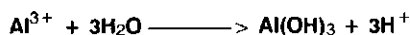


Fig. 2.1
Theoretical relationship between the ratio of concentrations of base cations (M^{2+}) and aluminum (Al^{3+}) in soil solution as a function of depth. The effect of increasing the dissolution rate of base cations from the mineral phase from 0.5 (---) to 1.0 (—) $kmol.ha^{-1}.yr^{-1}$ is demonstrated for soil acidification rates of 4 (I) and 2 (II) $kmol.ha^{-1}.yr^{-1}$. It is assumed that mineral weathering is the only acid neutralizing process, and that, besides the base cations, aluminum is the only dissolving ion. The present ratios between concentrations of M^{2+} and Al^{3+} in the field (+) are close to the presumably critical value of 1 (----).

Soils generally contain several percents of amorphous aluminum-(hydr)oxides, which could dissolve relatively fast after a high input of protons. High initial aluminum concentrations could also result from complete (congruent) dissolution of mineral crystals.



In the course of time Al could slowly reprecipitate as a hydroxide, gradually releasing protons in solution again, which will now be consumed by base cation weathering from primary minerals.



The net result of the weathering reaction is an incomplete (incongruent) dissolution of a primary mineral. By dissolution of aluminum-hydroxide or temporarily congruent dissolution of primary minerals the soil has a mechanism to quickly consume high loads of protons.

A third process which can be critical is nitrification. Nitrification is important in situations with high deposition of NH_3 , which occur in areas with intensive animal husbandry (bioindustry), for example in the eastern part of the Netherlands and the north-west of the FRG. In contradiction with general experience nitrification in forest soils also takes place at pH values below 4, as indicated by high leachate fluxes of NO_3 when nitrogen is deposited mainly as NH_3 . A fair availability of base cations seems a prerequisite for nitrification.

2.7 SOME CONCLUSIVE REMARKS

Soil acidification is a complex process which will affect various soil parameters. Definition of soil acidification as a decrease of the acid neutralizing capacity, gives us a tool to compare rates of acidification in various soil types in various stages of natural and anthropogenic acidification. In order to evaluate ecological consequences of changes in soil chemistry due to atmospheric deposition, pH and concentrations of aluminum as compared to base cations need to be assessed. For understanding the changes of these soil chemical properties cation exchange and mineral weathering are key processes. Critical parameters are cation exchange capacity, base saturation, and the rate and the stoichiometry of mineral dissolution reactions. Soils with a low CEC and low base saturation and low base weathering rates are most susceptible to adverse effects of acid deposition. Soils with a high CEC and high amount of exchangeable H and Al will be most difficult to ameliorate by liming. If, additionally, the dissolution rates of base cations from silicate minerals are low, natural recovery of the soil after deposition rates are lowered will be very slow. Experimental studies to obtain critical parameters in combination with the use of simulation models will be important to predict future changes in soil chemistry for different emission/deposition scenarios and to preevaluate mitigation strategies for forest soils.

This chapter was published in: T. Schneider (ed); Acidification and it policy implications, Elsevier, Amsterdam, pp. 65-75, 1986.

J.J.M. van Grinsven, F.A.M. de Haan and W.H. van Riemsdijk.

Chapter 3

IMPACTS OF ACID ATMOSPHERIC DEPOSITION ON WOODLAND SOILS IN THE NETHERLANDS:

I. CALCULATION OF HYDROLOGIC AND CHEMICAL BUDGETS.

ABSTRACT

To study effects of acidic atmospheric deposition on woodland soils in The Netherlands, chemical budgets were determined from simulated water fluxes and measured soil solution concentrations. Solute concentrations were determined in soil solutions, that were sampled monthly over a three year period at various depths in four different soils. Soil water fluxes were calculated with the SWATRE model. Rainfall and canopy throughfall were measured at the study site. Potential evapotranspiration was estimated by an adapted Penman method. Hydraulic conductivity was calculated from the soil water retentivity curves according to the Van Genuchten method. Simulated pressure heads could be fitted to field observations after reduction of conductivities by a factor between 6 and 60. Coefficients of variation (CV) for chemical budgets were determined by sensitivity analysis of the simulated soil water flux, and by measuring spatial, temporal and analytical variability of the solute concentrations. CV-values of solute fluxes for Al and NO₃ ranged from 10 to 30% between 10 and 90-cm depth, with spatial variability as the most important source of uncertainty. CV-values of chemical budgets (difference between inputs and outputs of solutes) for soil compartments which include the soil surface were also 10 to 30%, while those for deeper soil layers were larger, ranging from 40 to 200%.

3.1 INTRODUCTION

Atmospheric deposition of strong acids has been implicated in the degradation of forested ecosystems in northwestern and central Europe and northeastern North America. Chemical budgets can be a useful tool to quantify rates of soil acidification (Van Breemen et al., 1984). Chemical budgets are determined from the difference of solute inputs and outputs, preferably over time periods where changes in water storage in the hydrologic unit are negligible. A solute flux is the product of a water flux and a solute concentration. In unsaturated soil profiles, water fluxes cannot be measured directly but have to

be calculated by computer simulation (Wagenet, 1986). Apart from errors in simulated water fluxes, errors in chemical fluxes for unsaturated soil profiles result from spatial and temporal variation of chemical concentrations in soil solutions.

This paper describes a method to calculate chemical budgets for unsaturated soil profiles and discusses the uncertainty of budgets of N, Al and H. In two companion papers, chemical budgets are used to evaluate the effects of acid atmospheric deposition on N-transformations (Van Breemen et al., 1987) and Al-chemistry (Mulder et al., 1987) in soils.

3.2 MATERIALS AND METHODS

3.2.1 Soil sites and monitoring

The study site (Figure 3.1) is located in a 3.2-ha woodland near the Hackfort estate in The Netherlands.

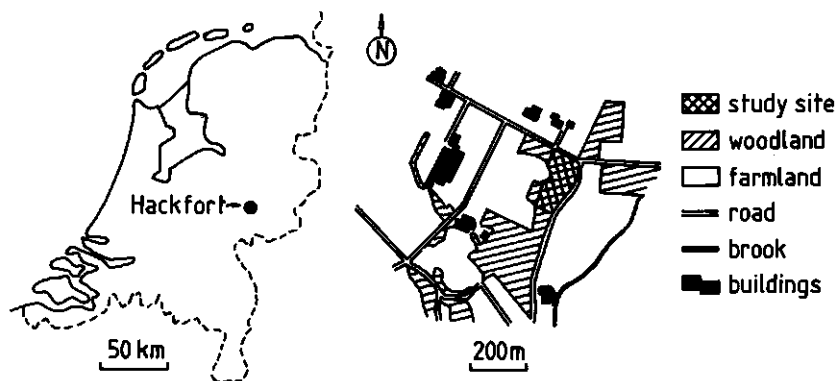


Fig. 3.1 Location of the Hackfort Estate in the Netherlands and the land use in the area surrounding the research sites.

Soils are developed in sandy to loamy Pleistocene sediments of the river Rhine, with a flat topography. Four 10x20-m² plots, A to D, were studied, which have different soil types, classified (Soil Survey Staff, 1975) as coarse loamy, mixed, acid, mesic Aeric Haplaquept (A); sandy, mixed, acid, mesic Umbric

Dystrochrept (B); mixed, acid, mesic Aquic Udipsamment (C); and sandy, mixed, calcareous, mesic Typic Haplaquoll (D). The three acidic soils have a well-developed organic forest floor, 2 to 5-cm thick, which is lacking in the calcareous soil. Predominant tree species are oak (*Quercus robur L.*) and birch (*Betula pendula L.*) at plot A, oak at plot B and C and a mixture of oak, birch, alder (*Alnus glutinosa L.*) and poplar (*Populus tremulus L.*) at D. The woodland was last coppiced in 1939 and has been left undisturbed since then. Groundwater in the woodland fluctuates between 0.5 and 1.5 m depth. From spring 1980 onwards quantities of rainfall were monitored hourly, canopy throughfall fortnightly and the chemical composition of volume-weighted rain and throughfall samples was determined monthly. From March 1981 soil solutions were collected monthly at 10, 20, 40, 60 and 90-cm depths using porous ceramic cups. During a few months in winter and spring groundwater levels are higher than 90-cm depth and saturated soil water will be sampled. The chemistry of this soil water is similar to water extracted under unsaturated conditions. High groundwater tables apparently result from local downward flow, which is supported by the hydrologic simulations. Details on soils, and collection and chemical analyses of water samples are described elsewhere (Van Breemen et al., 1987; 1988).

At plots A and B, four sets of water-filled ceramic tensiometers (home-made, 1-cm diameter, 5-cm long) were installed at 10-cm depth intervals. At two sets pressure head was measured from 10 to 90-cm and at the other two sets from 60 to 90-cm depth. Pressure head was measured weekly or biweekly between April and November in 1981 and 1982, using a pressure transducer (type National Semiconductor 1604 GB). At plot D pressure head was measured monthly in the summer of 1983, at 10, 30 and 50-cm depth, in duplicate. Soil water content was measured monthly in duplicate at plot A and B, and for one profile at plot C, at intervals of 5.1-cm (2 inch) down to 94.4-cm (36 inches) depth, using a double access gamma attenuation probe (type Troxler, model 2600), which was calibrated twice. Groundwater depth was measured weekly at all plots by means of piezometers.

3.2.2 Water retention and hydraulic conductivity

Undisturbed soil cores (100 cm³) were sampled at 10 cm intervals to a depth of 120 cm, from two soil pits at plot A, B and C (total of 6 to 18 replicates) and from one soil pit at D (total of 3 to 12 replicates). Soil water contents (θ) were

measured at pressure heads (h) of -10, -50, -100, -200, -500, -2500 and -16000 cm. Hydraulic conductivity (K) was measured by the two-plate method (Klute 1972) on 10-cm long (5-cm diameter) cores at $h = -10$ cm, for two to four soil horizons per plot, with an average of four replicates per horizon. For all four plots, soil horizons with similar water retentivity functions ($h(\theta)$) were defined. Parameters for the closed form equation by Van Genuchten (1981) were optimised for average experimental $h(\theta)$ relationships of the soil horizons. For the simulations, the maximum θ was fixed at the average of θ_{sat} and $\theta(h = -10)$ (Hillel, 1980). The $K(h)$ - function was calculated according to Mualem's model and fitted to the experimental $K(h = -10)$ data. Calibration of $K(h)$ with $K(h = -10)$ will be inaccurate when Mualem's model predicts a strong decrease of K for h -values near -10 cm, which is the case for the surface horizons of all plots (K decreases by a factor of about 10 per cm decrease of h).

3.2.3 The flow model

SWATRE (Soil Water Actual Transpiration Rate Extended) is an extended version (Belmans et al., 1983) of the SWATR model developed by Feddes et al. (1978). SWATRE is a non-stationary flow model based on the Darcy (Eq. [1]) and the continuity (Eq. [2]) equation:

$$J = -K(h) [dh/dz + 1] \quad [1]$$

$$dh/dt = -1/C(h) dJ/dz - S(h) \quad [2]$$

where J is the water flux density (m/d), z is depth (m), C is the slope of the water retentivity curve $h(\theta)$ (m^{-1}), t is time (d) and S is the root water uptake (m/d).

To predict water fluxes at monthly and 10-cm depth intervals, we used a flow model based on the Darcy equation. The SWATRE model predicts the pressure head, which is necessary for model calibration and for calculation of transpiration reduction in case of water stress. The surface boundary flux used in the simulations was obtained from measured throughfall and calculated potential evapotranspiration. The lower boundary condition was $h=0$ at measured groundwater depths. In view of the flat topography, lateral flow was not considered.

3.2.4 Evapotranspiration

The study site is one of many small parcels of woodland adjacent to grassland (Figure 3.1). Due to the lower aerodynamic resistance of forest (10 s/m) as compared to grassland (50 s/m), local advection (Brakke et al., 1978) is important in our plots, and methods to predict potential evapotranspiration from global meteorological data (Penman, 1948; Monteith, 1965) cannot be used directly. Due to specific enhancement by local advection, evaporation of intercepted water in our woodland was approximately 40% of total forest evapotranspiration, and similar to values reported for extensive coniferous forests (Gash and Stewart, 1977). If the canopy is dry and there is no water deficit grassland and forest have a similar transpiration (Roberts, 1983) and local advection will be small. It was assumed that lateral heat advection due to lower temperatures inside the woodland than above the grassland was negligible.

Actual interception (I_{act}) was calculated from the measured difference between gross rainfall and throughfall. Potential evapotranspiration without enhanced evaporation of intercepted water (ET_{pot}) was calculated from open water evaporation (E_0) according to Penman (1948) and a "crop" factor (f_1). ET_{pot} is the sum of potential transpiration (T_{pot}) and soil evaporation (E_{pot}) based on the fraction of soil surface covered by green vegetation (f_2). Potential transpiration was reduced by a fraction of the actual interception (f_3); the ratio of the rates of transpiration to evaporation of intercepted water. Based on daily rates, values of f_3 in a hardwood forest range from 1 to 0.3 (Singh and Szeicz, 1979).

The equations used to calculate potential values of evapotranspiration, soil evaporation and transpiration are:

$$ET_{pot} = f_1 E_0 \quad [3]$$

$$E_{pot} = (1-f_2) ET_{pot} \quad [4]$$

$$T_{pot} = (f_2 ET_{pot}) - (f_3 I_{act}) \quad [5]$$

E_0 was calculated from 10 day cumulative values provided by the Royal Dutch Meteorological Institute for the nearest weather station, which was Winterswijk, 40 km SE of the study site. Daily values of I_{act} were calculated from daily measurements of rainfall and biweekly measurements of throughfall:

$$i_{act} = P \left(\frac{P_{14} - T_{14}}{P_{14}} \right) \quad (\text{for } P > IC)$$

$$i_{act} = P \quad (\text{for } P < IC)$$

[6]

where i_{act} is the daily evaporation of intercepted water, IC is the interception capacity, P the daily precipitation, P_{14} is the cumulative precipitation over 14 days (for $P > IC$), T_{14} is the cumulative throughfall over 14 days. Daily throughfall was calculated as $(P - i_{act})$. The interception capacity was set at 0.8 mm, as reported for a mixed deciduous forest (Mitscherlich 1971).

Actual transpiration was calculated according to a dimensionless sink-term variable α (Feddes 1978), which relates the ratio of actual and potential water uptake for all rooted soil compartments to the pressure head.

| | | | |
|-------------------------|-----|------------------|-----|
| $\alpha = 0$ | for | $h > -10$ | |
| $\alpha = (h + 10)/-15$ | | $-10 > h > -25$ | |
| $\alpha = 1$ | | $-25 > h > -500$ | [7] |
| $\alpha = R/h$ | | $R > h > -16000$ | |
| $\alpha = 0$ | | $h < -16000$ | |

3.2.5 Parameter choice and sensitivity analysis

To define evapotranspiration parameters, the year was divided into three periods: (I) a fully developed canopy from May 22 to September 30, (II) canopy development in spring, from May 7 to 21, and canopy decay in autumn, from October 1 to 15 and (III) a leafless period from October 15 to May 7. Selected values for f_1 were 0.9 (I), 0.7 (II) and 0.5 (III), for f_2 were 0 (I), 0.5 (II) and 1 (III) respectively. A value of 0.8 for f_3 was estimated from average rates in 1981 of transpiration (2.4 mm/d) and interception (3 mm/d, on days with rainfall or drying canopy).

The distribution of potential root water uptake with depth ($S(z)$) was assumed to be proportional to the mass of fine (< 5 mm) roots ($R(z)$). At plots A, B and C 25% of the fine roots (including those in the litter layer) was concentrated in the top 10 cm, decreasing linearly to 0% at 80-cm depth. At plot D almost 60% of the roots was present in the top 10 cm, decreasing linearly to 0% at 40-cm. R

was set at -500 cm, which is a normal value for agricultural crops (Feddes et al., 1978). The above set of evapotranspiration parameters will be considered as a reference case for the sensitivity analysis. The conductivity functions were optimised by fitting the simulated pressure heads to the field measurements.

The sensitivity of the water flux calculations to the choice of f_1 , f_3 , R and $S(z)$ was investigated by the parameter perturbation method for plot B. For $S(z)$ a parabolic relation was assumed:

$$S(z) = az^2 + bz + c \quad [8]$$

which was solved for (1) $S(0) = 2S(40)$, (2) $S(80) = 0$ and (3) $\int_0^{80} S(z)dz = 1$. Thirty combinations of four parameters were generated by randomly selecting values from assumed normal distributions of f_1 ($\mu = 0.90$, $\sigma = 0.10$), f_2 ($\mu = 0.75$, $\sigma = 0.25$), R ($\mu = -750$ cm, $\sigma = 250$) and c in $S(z)$ (eq. 8) ($\mu = 2.50$, $\sigma = 0.75$). The mean value for C corresponds to a linear $S(z)$ relationship, which is in agreement with the measured distribution of fine roots.

To investigate spatial variability 20 lysimeters were installed a few tens of m outside the study plots, in similar soils. Lysimeters were placed at 20-cm depth, at 0.5 to 13-m distance from each other. Soil solutions were sampled on April 29, May 1, June 4 and September 9, 1985. Coefficients of variation ($CV = \frac{sd}{\bar{x}}$, where sd is the standard deviation and \bar{x} is the sample mean) for concentrations of Al , NO_3 and Cl at the 4 sample dates were similar (0.330 ± 0.10). Observations were pooled to create a new variable on which semi-variance analysis (Journel and Huijbregts, 1978) was conducted:

$$\gamma(l) = 1/2 E([z(x+l) - z(x)]^2), \quad [9]$$

where γ is the semi-variance, E is the expectation, z is the variable, x is the distance and l is the lag.

Temporal variability within the monthly sampling period was investigated by sampling soil solutions 10 times during November 1985, using 5 porous cup lysimeters at a depth of 50 cm. Time intervals between sampling ranged from 2 to 27 days. Observations at the 5 sample points ($CV = 0.140 \pm 0.05$) were grouped into a new variable on which semi-variance analysis was conducted. Analytical errors were determined by repeated analysis of standard solutions.

Spatial (x), temporal (t), analytical (a) and water flux simulation (j) errors were combined to obtain the CV for the monthly chemical flux:

$$CV_f = (CV_x^2 + CV_t^2 + CV_j^2 - CV_a^2)^{1/2} \quad [10]$$

CV_a^2 is preceded by a minus sign as both CV_x and CV_t already include the analytical error. The observed values of CV_x and CV_t were assumed to be representative for all depths and for all months of the year. CV_j was estimated per month. Values of CV_f were converted again to standard deviations (Table 3.3).

Semi-variance analysis showed that concentrations of Al (Figure 3.2 and 3.3) and NO_3 are independent between 0.5 and 13-m sample distance and between 7 and 20 days sample intervals. Distances between duplicate soil solution

| Coefficient of Variation (%) | | | | |
|------------------------------|------------|----------|---------|-------|
| Element | Analytical | Temporal | Spatial | Total |
| Al | 9.8 | 10.0 | 31.5 | 34.5 |
| NO_3 | 4.7 | 14.2 | 33.7 | 36.9 |
| Cl | 14.7 | 3.0 | 29.5 | 33.1 |
| NH_4 | 5.0 | 14.1 | 32.6 | 35.9 |

Table 3.1 Coefficients of variation for concentrations in soil solution, sampled monthly in a 10x20-m² plot, for an arbitrary depth and month.

sampling points in plots A to D varied between 2 and 10 m. The dominant source of error is spatial variation (Table 3.1).

Rainfall was sampled monthly using two collectors outside the woodland. Throughfall was sampled monthly using 7 collectors placed at the apices and in the centre of a hexagon, which covered the complete area of each plot. The standard errors ($SE = sd/n^{1/2}$) for the estimate of the monthly mean solute fluxes in throughfall and rainfall are negligible compared to those in soil solution, as sampling is continuous in time. The SE for the spatial mean solute flux in throughfall is also smaller, as 7 replicate samples are taken per plot, instead of 1 or 2 for the soil solution. CV-values for throughfall fluxes of NO_3 and NH_4 ranged between 5.2 and 14.2%.

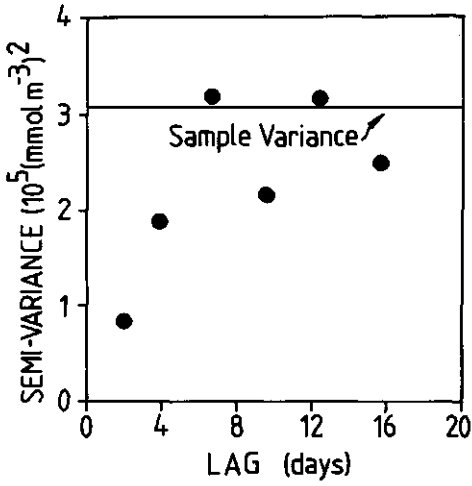


Fig. 3.2 Semi-variogram of concentrations of Al in soil solution at 20-cm depth, sampled in April, May, June and September, 1985, in a 200-m² soil plot.

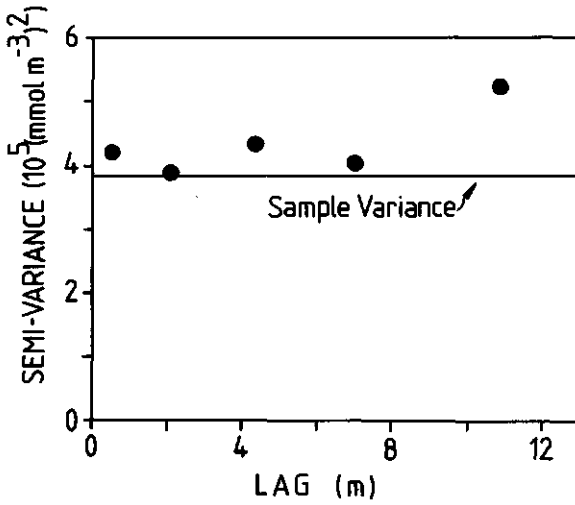


Fig. 3.3 Semi-variogram of a time series of concentrations of Al in soil solution at 50-cm depth, sampled in November, 1985.

Annual solute fluxes were divided by corresponding water fluxes to give annual flux-weighted soil solution concentrations. Unsubscripted CV-values refer to overall lumped values.

3.3 RESULTS AND DISCUSSION

3.3.1 Model calibration for plot A

Pressure heads observed in the field and simulated pressure heads for plot A, from April 1981 to March 1982, using the parameters for the reference case are shown in Figure 3.4.

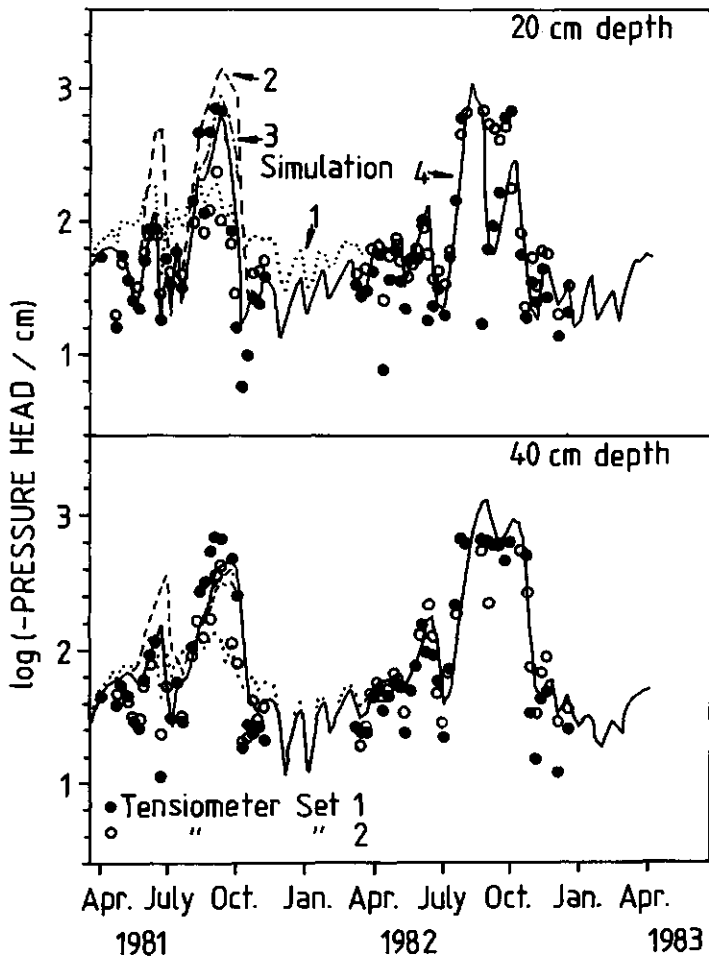


Fig. 3.4 Pressure heads from duplicate tensiometers (●,○) at 20 and 40- cm depth at plot A from April 1981 to March 1982 and simulated (1) before calibration (-----), (2) after calibration of $K(h)$ (-----), (3) after reducing transpiration due to the leaf roller infestation (.....) and (4) decreasing potential water uptake linearly with depth (———). The hydrologic year from April 1982 to March 1983 serves for model validation.

Pressure heads were overestimated during the growing season and underestimated in the dormant season. These discrepancies could result from overestimates of $K(h)$. Therefore, $K(h)$ for each layer was progressively reduced until simulated pressure heads fitted observations (Figure 3.4). Optimised $K(h)$ functions were 5 to 60 times lower than calculated according to Van Genuchten, which illustrates the inaccuracy of the calibration of $K(h)$ with laboratory measurements of $K(h = -10)$. The discrepancy between simulated and observed pressure heads could also be related to not considering short-circuiting of flow. Macro-pores are abundant but the soil matrix is too permeable and precipitation intensities are too low for the surface soil to become water saturated. Surface ponding was never observed in the 3-yr monitoring program.

After optimization of $K(h)$, h was still overestimated in June. Each year in June our oak woodlands are infested by the leaf roller *Tortrix viridiana* (L.), which severely damages leaves and presumably reduces transpiration. Extension of period II from May 21 to July 7 improved the agreement between simulated and observed h (Figure 3.4). Agreement was further improved when assuming an even distribution of water uptake over a 60-cm root zone, suggesting a relatively high efficiency of deeper roots.

The validity of the optimised model parameters is illustrated by the good agreement between simulated and observed pressure heads in the hydrologic year starting in April, 1982 (Figure 3.4). The set of optimised parameters was also used to calculate water fluxes for the other plots. For plot D a rooting depth of 30 cm was used. $K(h)$ was optimised independently for all plots, but for plot C and D field data were limited.

Average annual ET_{act} for all plots from April 1981 to March 1984 was 50.1 cm ($sd = 3.7$), which is very close to 52.2 cm ($sd = 3.6$) for ET_{pot} . This difference is small because the reduction of ET due to soil water deficit and the infestation of the leaf roller is almost balanced by the enhancement of evaporation of intercepted water (due to local advection). Average ET_{act} for our sites agrees well with values of 45 to 55 cm reported by Rutter (1968). The average annual value of T_{act} (29.5 cm, $sd = 2.2$) agrees well with values of forest transpiration for northern Europe reported by Galoux (1981) and Roberts (1983).

3.3.2 Error analysis for simulated soil water fluxes

The results of the sensitivity analysis of the soil water fluxes for plot B are summarized per month and depth in Table 3.2.

| | Water Flux (cm) | | | | | | T _{act} |
|-----------|-----------------|---------------|---------------|---------------|---------------|---------------|------------------|
| | Soil Depth (cm) | | | | | | |
| | 0 | 10 | 20 | 40 | 60 | 90 | |
| January | -6.35 ± 0.00 | -7.09 ± 0.00 | -6.68 ± 0.00 | -6.56 ± 0.00 | -5.96 ± 0.01 | -5.44 ± 0.01 | 0.00 ± 0.00 |
| February | -5.05 ± 0.00 | -4.88 ± 0.00 | -4.99 ± 0.00 | -5.04 ± 0.00 | -5.31 ± 0.00 | -8.41 ± 0.00 | 0.00 ± 0.00 |
| March | -2.58 ± 0.00 | -1.61 ± 0.00 | -1.26 ± 0.00 | -1.20 ± 0.00 | -1.53 ± 0.00 | -2.60 ± 0.00 | 0.00 ± 0.00 |
| April | -1.47 ± 0.00 | -0.21 ± 0.00 | -0.43 ± 0.00 | -0.93 ± 0.00 | -1.60 ± 0.00 | -3.75 ± 0.00 | 0.00 ± 0.00 |
| May | -3.65 ± 0.00 | -2.55 ± 0.07 | -1.95 ± 0.10 | -1.40 ± 0.07 | -1.23 ± 0.03 | -1.25 ± 0.04 | 2.05 ± 0.15 |
| June | -5.70 ± 0.00 | -4.29 ± 0.40 | -2.31 ± 0.50 | -0.15 ± 0.39 | -0.47 ± 0.06 | 0.11 ± 0.14 | 6.84 ± 0.43 |
| July | -4.35 ± 0.00 | -4.06 ± 0.21 | -3.40 ± 0.30 | -2.20 ± 0.46 | -0.81 ± 0.52 | -0.17 ± 0.49 | 9.24 ± 0.65 |
| August | -5.94 ± 0.00 | -3.93 ± 0.39 | -1.50 ± 0.55 | 0.26 ± 0.13 | 0.55 ± 0.08 | 0.52 ± 0.12 | 6.54 ± 0.29 |
| September | -0.71 ± 0.00 | -0.61 ± 0.11 | -0.64 ± 0.13 | -0.07 ± 0.15 | 0.40 ± 0.10 | 0.71 ± 0.06 | 4.45 ± 0.12 |
| October | -6.26 ± 0.00 | -4.58 ± 0.19 | -2.90 ± 0.31 | -0.08 ± 0.16 | 0.43 ± 0.06 | 0.68 ± 0.03 | 1.14 ± 0.05 |
| November | -5.31 ± 0.00 | -4.73 ± 0.02 | -4.06 ± 0.04 | -2.86 ± 0.42 | 0.13 ± 0.35 | 1.00 ± 0.17 | 0.00 ± 0.00 |
| December | -5.25 ± 0.00 | -5.38 ± 0.01 | -5.24 ± 0.01 | -5.50 ± 0.09 | -4.18 ± 0.32 | 0.56 ± 0.53 | 0.00 ± 0.00 |
| Year | -52.62 ± 0.00 | -43.89 ± 1.36 | -35.33 ± 1.87 | -25.30 ± 1.72 | -18.64 ± 1.34 | -18.06 ± 1.43 | 30.26 ± 1.28 |

Table 3.2 Means and standard deviations of unsaturated soil water fluxes and actual transpiration (T_{act}), all calculated with the SWATRE model using the parameter perturbation method.

The relative errors for the annual fluxes (expressed as CV) are small with a maximum of 8% at 90-cm depth. However, for specific months during the growing season the CV's for monthly fluxes can be greater than 100%, deeper than 40 cm. The relative insensitivity of annual soil water fluxes to f_1 , f_2 , R and S(z) can be explained by:

- (1) accurate throughfall measurements,
- (2) much smaller CV's of T_{act} (4.2%) than of T_{pot} (7.9%), due to the effect of R (Equation 7) and
- (3) the small absolute error in T_{act} (1.3 cm) compared to the difference between infiltration and T_{act} (18 cm).

The low but uncertain monthly soil water fluxes could result in relatively large errors in annual solute fluxes if those low monthly water fluxes coincide with high concentrations. Annual variation of monthly concentrations of Al and NO_3 rarely exceeded a factor of 4.

| Plot | A | | B | | C | | D | |
|--|--------------------------|------|-------|------|-------|------|-------|------|
| | Flux | S.d. | Flux | S.d. | Flux | S.d. | Flux | S.d. |
| cm | $kmol_c ha^{-1} yr^{-1}$ | | | | | | | |
| Al | | | | | | | | |
| 10 | -3.27 | 0.37 | -2.52 | 0.30 | -2.94 | 0.34 | | |
| 40 | -6.56 | 0.89 | -5.07 | 0.67 | -2.65 | 0.33 | | |
| 90 | 0.07 | 0.04 | -3.27 | 0.61 | -2.62 | 0.57 | | |
| NO_3 | | | | | | | | |
| 0 [†] | -0.95 | 0.06 | -1.00 | 0.09 | -0.85 | 0.05 | -1.03 | 0.15 |
| 10 | -7.64 | 0.93 | -6.01 | 0.73 | -3.21 | 0.41 | -9.55 | 1.18 |
| 90 | -5.03 | 1.22 | -1.90 | 0.52 | -1.56 | 0.48 | -6.23 | 1.52 |
| Al-Budgets | | | | | | | | |
| 10-40 | -3.29 | 1.26 | -2.55 | 0.97 | 0.29 | 0.66 | | |
| 40-90 | 6.63 | 0.86 | 1.80 | 1.29 | 0.03 | 0.90 | | |
| Proton production due to N-transformations | | | | | | | | |
| 0-10 | 8.68 | 1.26 | 7.22 | 1.09 | 4.03 | 0.70 | 11.80 | 1.69 |
| 10-90 | -1.67 | 2.26 | -3.22 | 1.31 | -1.00 | 1.00 | -3.17 | 2.71 |
| 0-90 | 7.01 | 1.44 | 3.90 | 0.78 | 3.05 | 0.65 | 8.63 | 2.01 |

[†] Flux in throughfall

Table 3.3 Average annual fluxes, budgets, and their respective standard deviations for Al, NO_3 and proton production due to N-transformations for various soil plots and depths.

The resulting CV's for the annual fluxes of Al and NO_3 in the mineral soil (Equation 10, Table 3.3) ranged from 10% at 10-cm depth to 30% at 90-cm depth and demonstrate that large errors in water fluxes in the growing season do not

greatly influence annual solute fluxes. The large uncertainty of the Al flux at 90-cm depth for plot A is due to very low mean Al concentrations.

Errors for input-output budgets for soil profiles or soil compartments can be high when the difference between solute fluxes at the compartment boundaries is small. CV-values in average annual budgets for Al (Mulder et al., 1987) and proton production due to N-transformations (Van Breemen et al., 1987) (Table 3.3) for soil compartments that include the soil surface are similar to those for individual fluxes, i.e. 10 to 30%. CV-values for deeper soil compartments are larger and range from 40 to 200%.

3.3.3 Differences between the plots

Plots were distinguished on the basis of differences in profile development. Some key hydrologic and hydrochemical characteristics are summarized in Table 3.4 for the different plots.

| Plot | A | B | C | D |
|---|-----------------------------------|------|-----|------|
| Precipitation | 706 | 706 | 706 | 706 |
| Actual Evapotranspiration | 511 | 497 | 478 | 518 |
| Unsaturated soil water flux ⁺ | 191 | 198 | 247 | 203 |
| Soil water storage change ⁺ | 3 | 6 | -20 | -11 |
| | mmol _c m ⁻³ | | | |
| Flux-weighted [NO ₃] ⁺ | 2648 | 1448 | 545 | 1847 |
| Flux-weighted [Al] ⁺ | 497 | 1847 | 742 | 8 |

⁺ At or down to (Soil water storage change) 60 cm depth.

Table 3.4 Annual values of some key hydrological and soil chemical parameters for plots A, B, C and D, averaged for three hydrologic years from April 1981 to March 1984.

Hydrologic differences between plots were generally small. Only differences between monthly soil water fluxes at 90-cm depth for plot C and A, and C and D were significant (Table 3.5).

| Significance level (%) | | | | | | | | | |
|------------------------|---------------------------------------|----|----|--|-----|-----|---|-----|-----|
| Plot | Soil water flux at 90-cm depth (n=36) | | | Concentration of NO ₃ at 60-cm depth (n=28) | | | Concentration of Al at 60-cm depth (n=24) | | |
| | B | C | D | B | C | D | B | C | D |
| A | 23 | 80 | 38 | 48 | 100 | 93 | 100 | 85 | 100 |
| B | | 61 | 12 | | 100 | 95 | | 100 | 100 |
| C | | | 75 | | | 100 | | | 100 |

Table 3.5 Significance levels for the paired Student's t-statistic: H₀: monthly means of unsaturated soil water fluxes at 90-cm depth and concentrations of NO₃ and Al at 60-cm depth are identical.

Monthly soil water fluxes at 10 and 20-cm depth for plot D differ from the other plots due to a difference in rooting depth.

Chemical differences between the plots were much more significant. This is illustrated in Table 3.5 for monthly concentrations of NO₃ and Al at 60-cm depth. All significance levels of differences between plots are higher than 90%, except for plot A and B (NO₃) and for plot A and C (Al).

3.4 SUMMARY AND CONCLUSIONS

Chemical fluxes for soil profiles have been calculated by multiplying simulated unsaturated soil water fluxes and measured soil solution concentrations. Errors in simulated soil water fluxes are small because throughfall was measured accurately and the difference between precipitation and actual evapotranspiration is large compared to the absolute error in actual evapotranspiration. Errors in soil solution concentration mainly result from large spatial variability. Resulting coefficients of variation in soil fluxes of NO₃ and Al, and budgets for soil compartments which include the soil surface, range from 10 to 30%; those for budgets for deeper soil compartments are often much larger (40 to 200%) and should be viewed with caution.

ACKNOWLEDGEMENTS

This research was supported in part by the EEC (ENV 650-NL) and by the Netherlands Directorate General for Science. We want to thank Dr. R. Feddes and Ir. M. de Graaf (Institute for Land and Water Management, Wageningen) for providing the SWATRE model. Thanks are due to B. Kroesbergen (Dept. of Soil Tillage, Agricultural University) for determining the water retentivity curves, to J. Kipp for doing the root mass analyses, to E.J. Velthorst for help during sampling and chemical analysis, to H. Postma for assistance with the uncertainty analyses, to Th. Pape for help with data management, to J. van Roestel for valuable discussions on evapotranspiration and to the Dept. of Soil Science and Plant Nutrition, Agricultural University, for providing hospitality to J.J.M. van Grinsven.

This chapter was published in the Soil Sci. Soc. Am. J. 51: p. 1629-1634, 1987. J.J.M van Grinsven, N. van Breemen and J. Mulder

Chapter 4

AUTOMATED IN SITU MEASUREMENT OF UNSATURATED SOIL WATER FLUX

ABSTRACT

A device is presented which, based on new operation principles, intercepts unsaturated soil water fluxes within an error of 10% and can yield samples for subsequent chemical analysis and calculation of convective solute fluxes. Operation is controlled by a microprocessor which automatically adjusts the vacuum imposed on a porous filter cloth such that identical matric potentials are maintained just above the cloth and at the same depth in the neighboring soil. Contact resistances and internal resistance of the device are implicitly corrected by adjustment of suction. Laboratory and field tests in a loamy sand under steady and transient flow conditions showed that cumulative water fluxes could be measured within 10% of those calculated from storage changes, and from numerical and analytical flow models.

4.1 INTRODUCTION

Unsaturated soil water flux densities must be estimated for any study which includes water balance or chemical budgets in the unsaturated zone (Ingestad, 1987, Jordan 1982, Van Breemen et al. 1987). Unsaturated convective chemical fluxes can be calculated from unsaturated soil water flux densities and concentrations in soil solution (Wagenet, 1986; Van Grinsven et al., 1987^b). Unsaturated soil water flux densities can be obtained indirectly either by simulation, or by integration of a time series of water content and matric potential measurements. Few methods are available for direct measurement of the unsaturated soil water flux directly (Wagenet, 1986). Two general principles are used for flux measurement. The first principle involves measurement of the displacement of a thermal field due to convective heat transport by soil water (Byrne et al., 1967; 1968). This method can only measure rather large flux densities and has not been thoroughly tested in the field. The second principle involves intercepting part or all of the soil water flux and determining its magnitude by measuring the hydraulic head loss across a known hydraulic resistance (Cary, 1968, 1970). Since the hydraulic resistance of the meter cannot be matched to that in the undisturbed neighboring soil, the soil water flux

streamlines will converge to or diverge from the fluxmeter. Correct flux densities can only be derived with extensive in situ calibrations for each combination of soil type and fluxmeter. Dirksen (1972, 1974) improved this type of fluxmeter by using fine-metering valves with micrometer dials as known variable hydraulic resistances and by installing the meter perpendicular to the flow direction. By matching the head loss across the meter with that measured with two tensiometers across an equal length of soil nearby within 10%, the measured flux density through the meter could be corrected for convergence and divergence of flow. Unfortunately, the calibration of the fine-metering valve proved to be a problem due to unpredictable effects of air dissolution, precipitation of solutes and bacterial growth on the resistance of the very narrow opening. This problem was later eliminated by using the fine-metering valve only to match the hydraulic resistances of meter and soil. The flux through the meter was derived from the convective heat transport in an unstricted part of the hydraulic path (Cary, 1973). Small head losses across the meter and soil need to be measured within 10 Pa (Dirksen, 1972; 1974). This accuracy was difficult to obtain due to the sensitivity of pressure transducer measurements to temperature variations, which inevitably occurred when taking readings and changing valve settings.

The fluxmeter described in this paper eliminates some of the previous problems by performing all control manipulations remotely and automatically with the help of a microprocessor. The method combines features of the methods by Dirksen (1974) and by Duke and Haise (1973). Soil water flow is intercepted by a porous plate, in which the suction is automatically adjusted to maintain identical matric potentials above the plate and in the surrounding undisturbed soil. A major new feature is that the fluxmeter no longer is a passive element through which soil water must find its way solely driven by the prevailing soil hydraulic gradient. Instead, soil water can be sucked into the fluxmeter, irrespective of larger hydraulic resistances in the path through the meter than through the soil. This makes the device insensitive to air bubbles, which unavoidably will occur in filter cloth and tubing (Peck, 1969), and which are disastrous in passive measuring systems such as that used by Dirksen (1972, 1974).

The water extracted by the fluxmeter can be used for subsequent chemical analysis and calculation of the local convective unsaturated chemical flux density.

4.2 MATERIAL AND METHODS

4.2.1 Description of the fluxmeter

The fluxmeter is schematically presented in Figure 4.1 as part of a field setup.

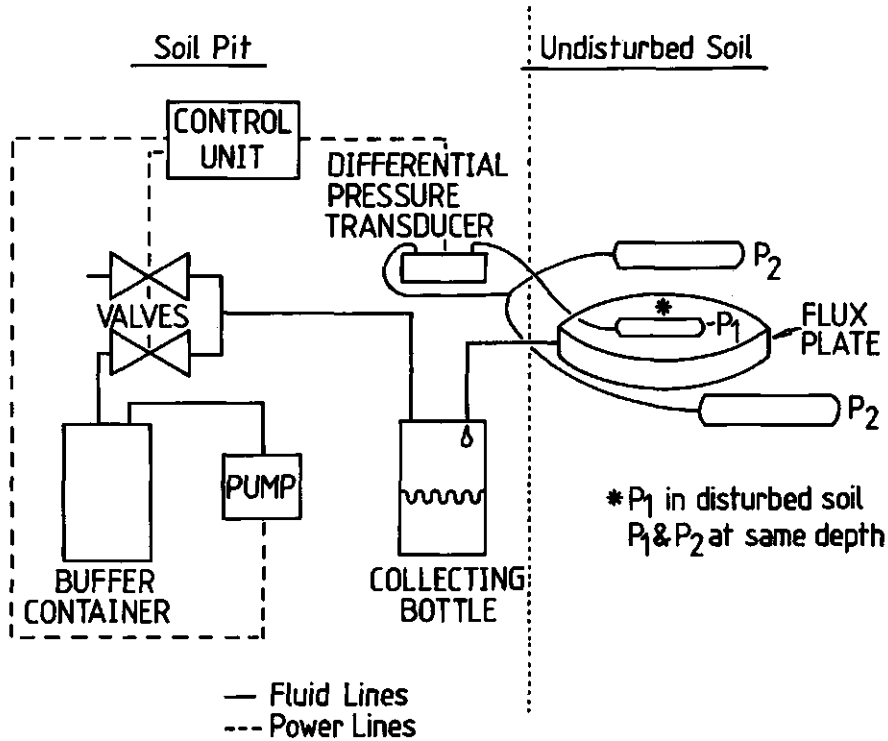


Fig. 4.1 Schematic diagram of flux meter components in assembly of field experiment.

The flux plate consists of a round polyacrylic filter cloth (Gelman, Versapor 200, a pore size of $0.2 \mu\text{m}$, area 79 cm^2) supported by a polyacrylate body. A thin tensiometer (P_1 , diameter 0.7 cm) is installed, together with the plate, in disturbed soil 0.5 cm above the plate. At the same level in the undisturbed soil, two tensiometers (diameter 1.8 cm) are installed at both sides of the plate, with a joined outlet (P_2). P_1 and P_2 are connected with tygon tubing to a differential pressure transducer (Honeywell Bull Microswitch 160 PC). All tensiometer tubing was installed horizontally to avoid hydraulic head differences along the length of

the tubing. The suction is applied by means of a pump connected to a buffer container. Adjustment of the suction inside the plate starts by bringing the buffer container to a suction of approximately 50 kPa. The differential transducer is read at pre-set time intervals (6 to 3 min). When the suction difference between P1 and P2 exceeds 100 Pa, either the valve to atmospheric air or the buffer container is opened for a short period, decreasing or increasing the suction in the collecting bottle and the flux plate.

4.2.2 Description of laboratory setup

Experiments were carried out under steady-state flow conditions. The flux plate and the tensiometers P₁ and P₂ were installed in a packed soil column (50 cm high, 45 cm in diameter) of loamy sand (Table 4.1).

| Suction (kPa) | 0.25 | 2.5 | 5. | 10. |
|---------------|---|------|------|------|
| | Water Content (cm ³ /cm ³) | | | |
| Lab Soil | 0.35 | 0.22 | 0.20 | 0.15 |
| Field Soil | 0.36 | 0.26 | 0.23 | 0.21 |
| | Conductivity (cm/d) | | | |
| Lab Soil | 20. | 2. | 1. | 0.8 |

Table 4.1 Hydraulic conductivity and water content at 0.25, 2.5, 5 and 10 kPa suction, for soils in laboratory and field experiments.

Tubing from the flux plate to the collecting bottle was 3 cm in diameter, air-filled and slanting: the intercepted water flowed by gravity in a thin film to the collecting bottle. The suction in the collecting bottle thus acted directly on the filter cloth. The soil was homogeneously packed at field capacity in layers of 5 cm. The flux plate and tensiometers P₁ and P₂ were installed at 20 cm below the soil surface during filling, so contact resistances were small. Additional tensiometers were installed at 10-cm depth intervals to verify steady-state flow. The matric potential at the bottom of the soil column was controlled by a hanging water column. At the bottom of the soil column a filter cloth (Gelman, Versapor 1200, pore size 1.2 μm) prevented air-entry. The surface flux was applied with a dripping device

consisting of a 5-cm-high closed vessel, with the same diameter as the soil column, and perforated at the bottom by 150 hypodermic needles. Puddling was prevented by a layer of gravel on the soil surface. The surface flux density was regulated by a pulse pump. Matric potentials and suction in the collecting bottle were measured with a pressure transducer. The volumetric outflow of the fluxmeter and the of column were recorded manually.

4.2.3 Field test

The flux plate was installed in an undisturbed loamy sand profile (Table 4.1) at 20 cm depth through a horizontal tunnel from an adjacent soil pit. In contrast to the laboratory setup, tubing was thin (1 mm diameter), water-filled and horizontal, to avoid problems with installing a wide slanting tube in undisturbed soil. The frequent adjustment of the suction in the collecting bottle proved to be adequate for compensating variable hydraulic resistance in the tubing due to air bubbles. Hydraulic contact between soil and plate was secured by using a spring-loaded support. The plate was covered with loose soil (containing P_1) before installation. Tensiometers were installed in duplicate at 10-cm intervals down to a depth of 50 cm. The matric potential at P_2 , the matric potential difference between P_1 and P_2 , and the total amount of collected water were measured continuously by means of a Hewlett Packard-75 computer/Hewlett Packard-3421A datalogger combination. Also the air temperature near the datalogger next to the soil pit was recorded. Additional tensiometers were recorded manually at intervals of 30 to 60 min during daytime.

Two similar experiments were carried out with the field setup described above, one (I) during fall 1986 and the other (II) in spring 1987. In both experiments soil was initially wetted to near saturation by applying 22 mm and 24 mm water, respectively. After irrigation, the plot was covered by plastic to prevent evaporation. Monitoring was carried out during 4 (I) and 6 (II) days. Twice a day soil cores were sampled for gravimetric water content. The collecting bottle was a 80 cm long and 3.5 cm wide tube. In the first experiment the increase of water volume in the tube was determined from the increase of hydraulic head which was measured by means of a pressure transducer at the bottom of the tube. In the second experiment the volume increase was derived from the increase of electrical capacitance, measured by means of two opposite copper plates along the length of the tube. Soil water fluxes obtained with the fluxmeter were compared with fluxes calculated from storage changes derived from tensiometer data, the water retention curves and gravimetric water contents.

4.3 RESULTS AND DISCUSSION

In a steady-state laboratory experiment with a surface flux density of 9.2 mm d^{-1} and a matric potential of -5 kPa at the bottom of the column, linear regression of cumulative flux with time over 4.3 d gave a flux density 9.0 mm d^{-1} ($r^2=0.967$, $n=33$) for the fluxmeter, as compared to 8.9 ($r^2=0.999$, $n=33$) mm d^{-1} for column outflow. The applied surface flux density was rather high compared to normal field values, but lower fluxes could not be controlled accurately. Suction differences between P_1 and P_2 seldom exceeded 0.2 kPa . The suction applied to the filter plate was generally between P_1 and P_2 , which confirms that contact resistance between plate and soil and the resistance of the filter cloth in the packed column were small.

Matric potential at P_1 and P_2 and air temperature during the two field experiments are shown in Figure 4.2.

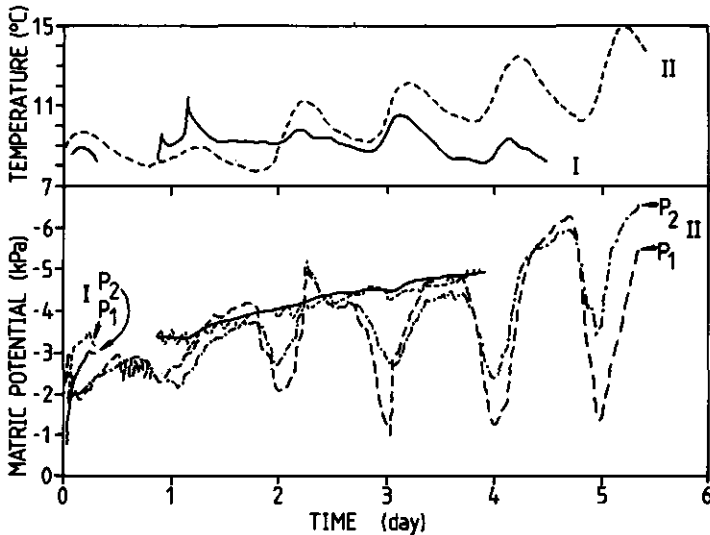


Fig. 4.2 Air temperature, and matric potential 0.5 cm above the fluxmeter and at the same depth in undisturbed soil during field experiment (I) in fall 1986 and (II) in spring

In experiment I soil was wetted to -1 kPa , in experiment II to -2 kPa . In both experiments the average potential difference between P_1 and P_2 was small: $-51 \pm 199 \text{ Pa}$ ($n = 805$) for experiment I and $-183 \pm 722 \text{ Pa}$ ($n = 317$) for experiment II. In experiment II the recorded matric potential had a strong diurnal fluctuation,

which was clearly associated with temperature. Although air temperature near the data logger did not fluctuate more than 5 °C, the temperature in the pit, where transducers and tubing were stored, probably fluctuated more strongly due to absorption of sunlight by the black plastic cover. In spite of this marked variation of the recorded suction, the average difference between P₁ and P₂ was small, although larger and more variable than in experiment I. Cumulative measured flux densities and flux densities obtained from measured storage changes are shown in Figure 4.3 for both experiments.

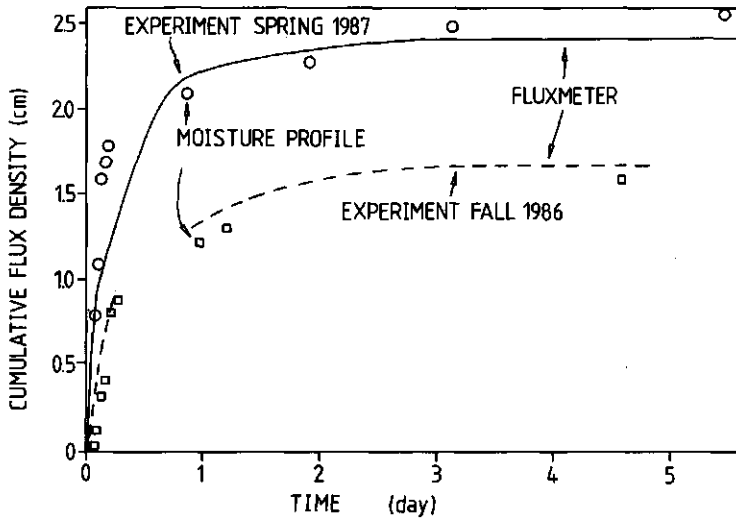


Fig. 4.3 Cumulative soil water flux density for field experiments as measured by fluxmeter and calculated from soil water changes.

At the end of monitoring, the difference between alternative flux density measurements did not exceed 5%. Apparently temperature fluctuations did not affect the accuracy of the flux measurement.

Cumulative flux density measured for field tests (II) was compared with two analytical solutions for vertical non-steady drainage by Jackson and Whisler (1970):

$$\frac{Q/Q_{\infty}}{1 - Q/Q_{\infty}} = \tau \quad [1]$$

$$\frac{0.03 Q/Q_{\infty}}{(1 - Q/Q_{\infty})^2} - 0.9 \ln(1 - Q/Q_{\infty}) = \tau \quad [2]$$

where Q is cumulative flux density (cm^3/cm^2), Q_{∞} is Q at infinite time, q_0 is the initial flux density, $\tau = q_0 t/Q_{\infty}$ and t is time (d). Both solutions predict the general shape of non-steady drainage with time, without requiring a conductivity and water retention function, and are calibrated by using the initial measured flux density. Eq. 1 assumes capillaries of equal radii, Eq. 2 capillaries of variable radii. The comparison for experiment II (Figure 4.4) shows that the measured cumulative flux density did fall in between the two analytical solutions.

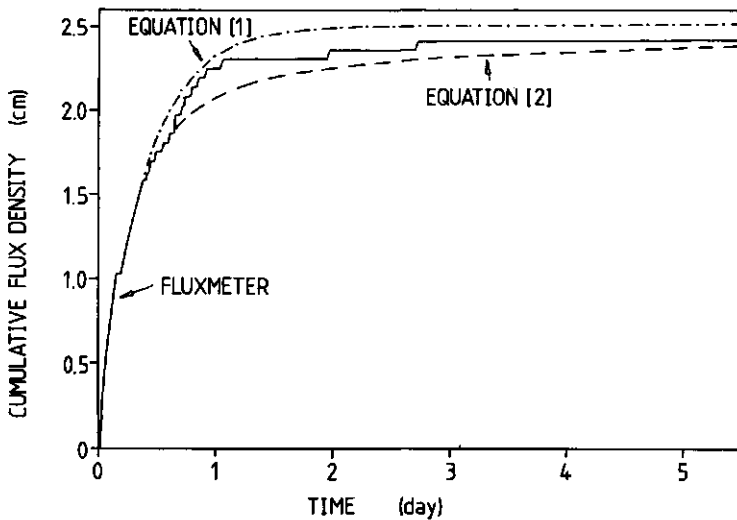


Fig. 4.4 Cumulative soil water flux density for second field experiment as measured by fluxmeter and calculated by two analytical solutions of Jackson and Whisler (1970).

Our fluxmeter measured cumulative flux densities in the field within 10% of the true value, which is similar to the accuracy obtained by existing fluxmeters or by numerical simulation. However, installation and operation are easier than for existing fluxmeters (Dirksen, 1972; 1974; Duke and Haise, 1973), and no time series of water content and water potential are needed to calibrate and validate simulation models (Van Grinsven et al., 1987^b). Tests were carried out under high downward flow conditions in loamy sand. By inversion of the flux plate, our

fluxmeter is also suitable to intercept upward flow. When using the fluxmeter in coarser or finer soil material under low flow conditions, the response of tensiometers will be more sluggish and flux measurement will be less accurate. Less accurate performance in dry soil is not a serious limitation since water transport and convective solute transport during high downward flow conditions (flux > 1 mm/d) often dominate annual fluxes. If matric potential varies strongly on a short distance, eg. in very heterogeneous soils or in case of macropore flow, flux measurement by control of the difference of matric potential between P_1 and P_2 is not possible. If the scale of spatial variability is larger than the dimensions of the fluxmeter setup (about 300 cm^2 for our prototype), the intercepted flux is not representative for the area. Theoretically, the principle of our flux measurement can be used to intercept fluxes over larger areas, similar to experiments by Montgomery et al. (1987).

ACKNOWLEDGEMENTS

The authors wish to thank Mr. Oudshoorn of TFDL Wageningen for the development of the electronic parts of the fluxmeter, S. Maasland of the Department of Soil Science and Plant Nutrition for building the fluxmeter and laboratory setup, and W. Bouten of the University of Amsterdam for providing the device for capacitive measurement of the volumetric flux.

This chapter is in press for Soil Sci. Soc. Am. J. 52 (1988)

J.J.M. van Grinsven, H.W.G. Booltink, C. Dirksen, N. van Breemen, N. Bongers, and N. Waringa

Chapter 5

A COMPARISON BETWEEN BATCH AND COLUMN TECHNIQUES TO MEASURE WEATHERING RATES IN SOILS.

DISCREPANCIES WITH RATES FROM FIELD MASS BALANCE STUDIES.

ABSTRACT

Dissolution experiments, both in batch and in columns, were carried out on soil material from a C-horizon of a Dystrochrept, to measure weathering rates of K, Na, Ca, Mg, Al and Si. Sieving and freeze drying of the soil material before the experiments did slightly increase the dissolution rate of Al. Observed weathering rates strongly depended on experimental conditions. Intensive stirring in batch systems increased rates of release of cations, in particular of Al, by more than one order of magnitude as compared to column experiments, even in an identical chemical environment. Observed silicate weathering rates in column experiments and unstirred batch experiments were of similar magnitude. Still these rates were 5 to 10 times higher than inferred from field studies, even when accounting for lower pH values in the laboratory than in the field. The larger part of the discrepancy could be explained by hydrodynamic factors. Column experiments with variable percolation rates showed that dissolution rate increased with the square root of percolation rate. This increase may be associated with a decreasing thickness of stagnant water films, which limit diffusion transport from etch pits in nearly stagnant hydrodynamic conditions.

5.1 INTRODUCTION

5.1.1 Mineral weathering in soils

The need for estimates of mineral weathering rates in soils is growing. Large areas covered by forest, both in temperate and tropic regions, are increasingly affected by human action. Intensified timber-felling, shifting cultivation and acid rain cause global deforestation, and increase erosion and leaching losses of base cations (K, Ca, Mg) from the soil for plant growth. Estimates of long-term mineral weathering rates are needed to assess the vulnerability of soil-ecosystems. The best estimates available come from budget studies of soils

or hydrological catchments (Páces, 1983, 1985, 1986^{a,b}; Velbel, 1985; Van Breemen et al., 1986; Mulder, 1988). However, these estimates are rather inaccurate due to interference by production or consumption of base cations by nutrient mineralization and uptake, by variable atmospheric inputs and cation exchange. Alternative estimates of mineral weathering rates may be obtained from dissolution experiments in the laboratory. Laboratory experiments involving soil samples are fast, cheap and relatively simple, but rather difficult to interpret, due to the complex nature of the solid phase. Soil is a mixture of feldspars, heavy minerals, clay minerals and organics. Interpretation of short-term soil dissolution studies in an uncontrolled chemical environment is arduous because the change in solution composition will be the sum of salt displacement, cation exchange, mineralization and mineral weathering. By pretreatment of the soil material it is possible to exclude all processes but mineral weathering, but such pretreatments likely will change the mineral surfaces and thus influence weathering kinetics. Observed weathering kinetics may also be influenced by experimental conditions like stirring or shaking. Therefore, in each dissolution experiment with soil material maximum control on dissolution conditions should be combined with minimal disturbance of the solid phase before and during the experiment.

5.1.2 Discrepancy between weathering rates in the laboratory and the field

Most studies on mineral weathering have been carried out using pure minerals, obtained from standard rock samples (Chou and Wollast, 1984; Holdren and Speyer, 1985^a) or picked from soil samples (Berner and Holdren, 1979). Before an experiment, mineral samples are generally conditioned to obtain a well-defined starting material. Common pretreatments are crushing, grinding, sonic cleaning, sieving, washing and drying. Experimental conditions rarely resemble natural conditions with respect to ionic strength and temperature. Moreover the solid material is mechanically kept in suspension, which will change the hydrodynamic conditions and also may affect the state of the solid-solution interface.

It is commonly accepted that the initial observations in dissolution experiments are mainly artifacts of the sample pretreatments. Crushing and grinding creates fine particles and fresh mineral surfaces causing initial non-linear dissolution behaviour (Holdren and Speyer 1985^b). Observed laboratory dissolution rates are commonly much higher than those concluded from catchment studies

(Páces, 1983; Velbel, 1986). The cause of this discrepancy is a matter of contention. Velbel (1986) lists as possibilities: different characteristics of the mineral surfaces in the laboratory as compared to nature, biased estimates of the reactive surface area, overestimates of the contact area between minerals and percolating solution in nature, and a higher degree of undersaturation in short-lasting dilute laboratory experiments. Other factors proposed to explain the discrepancy between weathering rates under natural and laboratory conditions include adsorption of trace compounds inhibiting crystal dissolution in nature, and the action of organic ligands and living organisms (Berner, 1978; Stumm and Furrer, 1985; Eckhardt, 1985).

5.1.3 Rate controlling processes and reactive surface area.

Early laboratory weathering experiments were designed primarily to elucidate weathering mechanisms and not to obtain estimates of weathering rates in natural systems. Laboratory experiments have generated several weathering theories. Until the mid-seventies the weathering rate was believed to be limited by the transport rate of reactants to and from the reacting surface (Correns and von Engelhardt, 1938; Helgeson, 1971; Paces, 1973; Busenberg and Clemency, 1976;). Transport-controlled weathering kinetics appeared less likely after X-ray photoelectron spectroscopy (XPS) and scanning electron microscopy (SEM) did not confirm the existence of a hypothetical diffusion limiting layer of leached material or secondary products covering the mineral surfaces (Wilson, 1973; Berner and Holdren 1979). Earlier Berner (1978) had stated that dissolution rates predicted by diffusion control were much higher than actual rates observed in laboratory experiments. At present the prevailing theory is that the rate of the surface reaction determines the overall dissolution rate (Berner, 1979; Aagaard and Helgeson, 1982; Lasaga, 1983; Blum and Lasaga; 1985). Two possible rate limiting surface reactions are surface protonation, and detachment of the surface complex (Stumm et al., 1985; Aagaard and Helgeson, 1982). Simultaneous with the rejection of diffusion control the insight grew that surface reactions were confined to specific sites on the mineral surface, resulting in the appearance of etch pits (Wilson, 1975; Berner and Holdren, 1979). If mineral dissolution is indeed a highly local phenomenon the specific surface area and the chemical composition of the surface of the bulk mineral, emphasized in earlier studies, become rather meaningless (Holdren and Speyer, 1987). At the same time however, the diffusion control hypothesis was rejected on the basis of either calculation of the maximum diffusion flux from the magnitude of the reactive

surface area (Berner, 1978) or on XPS observations of macroscopic portions of the mineral surface (Berner and Holdren, 1979). So it seems that the etch pit concept refutes the arguments for rejection of the diffusion hypothesis. Therefore the explanation by Chou and Wollast (1984) of dissolution peaks after sudden pH changes by diffusion control on etch pit scale, which was criticized by Berner et al. (1984), may have to be reconsidered.

5.2 REVIEW OF LABORATORY METHODS TO STUDY WEATHERING KINETICS

5.2.1 Batch Techniques

The classical method for studying weathering kinetics is the batch method (Wollast, 1967; Busenberg and Clemency, 1976; Petrovic, 1976; Holdren and Berner, 1979;) Generally a small mineral sample (5 to 100 g) is put in a large volume of water (0.5 to 1 L), to which a buffer solution (eg. Boric acid) is added to control pH. Small liquid samples (5 to 30 mL) are withdrawn from the reaction vessel at increasing time intervals over a time period up to 6 weeks (1000 hr). The suspension is stirred continuously at moderate (Petrovic, 1976) to high rates (3 cycles/s, Holdren and Speyer, 1985^c). Furthermore temperature is controlled.

Recently two new, similar methods have been introduced; the fluidized bed reactor (Chou and Wollast, 1984) and the flow cell (Holdren and Speyer, 1985^c). The principle of both methods is a forced flow of reactants through a mineral suspension, while part or all of the outflow is sampled. Advantages of these new methods over common batch techniques are better homogenization of the soil solution mixture, easier control of solution composition, more straightforward calculation of reaction rates and prevention of accumulation of reaction products

Batch studies on soil material often are aimed at determining the overall buffering behaviour of the soil and not at dissolution rates of specific minerals (Federer and Hornbeck, 1985; James and Riha, 1986; Kinniburgh, 1986). Soil samples are titrated by equilibrating soil samples with various amounts of strong acid or base. When organic surface horizons are used in combination with short reaction times, exchange processes will often overshadow mineral dissolution in these experiments.

5.2.2 Column techniques

Column techniques are rarely used in dissolution studies using pure mineral samples but are common for studying soil material (Abrahamsen and Stuanes, 1986; Skeffington and Brown, 1986). Experimental conditions in column experiments agree better with natural conditions than in batch experiments. Cronan (1985) leached undisturbed soil columns (12 cm diameter and 5-50 cm length) over a period of 60 weeks, adding 35 mm of acidified solutions (pH 3.5 and 4) weekly to simulate acid rain. He found cation ($K + Na + Ca + Mg$) weathering rates equivalent to 1.5 and 7.9 $\text{kmol}_c \cdot \text{ha}^{-1} \cdot \text{yr}^{-1}$ for 50 cm profiles of a Spodosol and an Inceptisol respectively. The error due to undetected cation exchange was estimated to be at least 50%. Moreover cation production from mineralization in the O-horizon could not be distinguished from mineral weathering. Acid was added once every week, which may have caused preferential flow paths.

5.2.3 Improved methods to study weathering kinetics in soil samples

The soil minerals have been affected by soil forming processes, resulting in cracks, etch pits and patchy coatings of clay minerals, oxides and organic substances on the mineral surfaces. Because these features influence the overall reactivity of the material, mechanical disturbance will likely affect dissolution kinetics of soil minerals. Sample pretreatment is undesirable when meaningful weathering rates in soil are to be derived from laboratory experiments. Overall mineral dissolution rates in soil material may be very low, first because reactive soil material is often diluted by inert quartz, and second because of earlier long-term exposure to acidifying substances (Berner and Holdren, 1979). The concentration changes in solution due to mineral weathering will be very small unless high soil/solution ratios are used, or long reaction times are allowed. For example the potassium weathering rate in an acid sandy soil is approximately $0.5 \text{ kmol} \cdot \text{ha}^{-1} \cdot \text{yr}^{-1}$ for a 0.9 m profile (Van Breemen et al., 1986). The concentration increase of K in a batch experiment (20 g of soil in 50 mL of solution) would be $0.06 \text{ mmol} \cdot \text{L}^{-1} \cdot \text{d}^{-1}$. In order to obtain a detectable (eg. by AAS) increase of the K concentration change, say to $1 \mu\text{mol}_c/\text{L}$, the product of soil-solution ratio and reaction time should be increased by a factor 20. An alternative would be to separate the reactive feldspars non-destructively from the inert bulk (Berner and Holdren, 1979).

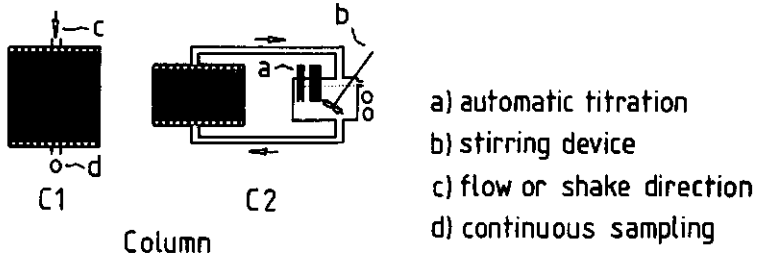
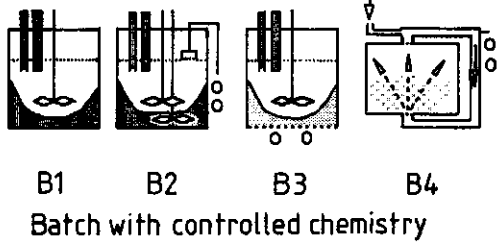
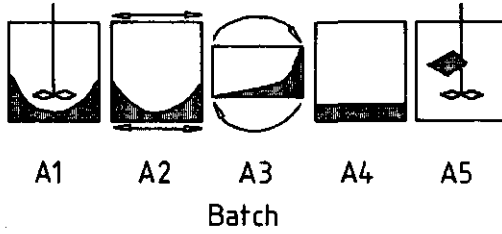


Fig. 5.1

Characteristics of methods to measure mineral weathering rates.

A: Batch-type; uncontrolled chemistry: (1) Stirred; (2) Reciprocal shaker; (3) Head-over-end; (4) Unstirred; (5) Sediment in dialysis bag.

B: Batch-type; controlled chemistry: (1) Stationary pH by automatic titration with concentrated acid using one fast stirring device; (2) Two stirring devices; a slow one for the sediment and a fast one for the solution: Optional titration with dilute acid and continuous extraction of solution samples to maintain a constant ionic strength and reaction volume; (3) Flow cell: One stirring device and constant addition of reactants and extraction of solution through a porous bottom; and (4) Fluidized bed reactor: homogenization by fast upward flow.

C: Column-type: (1) Fixed flow rate and variable outflow pH, or adjustment of flow rate proportional to buffer rate to control outflow pH; (2) Titration of solution in a separate vessel, which is continuously sampled and recirculated. Additional options: (a) Upward or downward flow direction, (b) disturbed or undisturbed soil material, (c) saturated or unsaturated hydrologic conditions, (d) zero or finite input concentrations.

Considering the problems discussed so far, methods to measure chemical weathering rates in soil material should;

- 1) use starting material as undisturbed as possible;
- 2) cause minimal disturbance of the solid phase during the experiment;
- 3) control the chemical composition of the solution during the experiment;
- 4) impose experimental conditions such that reaction rates can be calculated on basis of soil mass for a well defined chemical and hydrodynamic environment;
- 5) should not require impractically long reaction times.

Figure 5.1 gives a diagrammatic overview of existing laboratory methods to measure weathering rates and possible modifications along the lines of thought described above. Mechanical disturbance in batch-type experiments can be reduced by using slow head-over-end rotation (A3) instead of fast stirring devices (A1) or reciprocal shakers (A2). If weathering rates are slow compared to diffusion rates in the aqueous phase, unstirred batch systems, with a thin water film on top of a thin soil layer (A4), may be most appropriate. Chemical conditions in batch systems can be controlled by solution replacement (James and Riha, 1986; Chapter 6: Van Grinsven et al., 1986). However the repeated separation of sediment and solution may cause loss of fine (reactive) particles and undesirable disturbance of the solids. Frequent separation can be circumvented by using high solution to soil ratios. If diffusion across the dialysis membrane is not rate limiting the sediment can be put in a dialysis bag (A5).

The pH in batch studies can be controlled by automatically adding strong acid to a fast stirred suspension proportional to the buffer rate, which is recorded continuously by a pH electrode. Abrasion of the mineral surfaces due to fast stirring may enhance buffer kinetics but can be reduced by using a separate slow stirring device for the sediment at the bottom of the reaction vessel (B2). Accumulation of reaction products, and the subsequent increase in ionic strength and decrease in degree of undersaturation with the weathering minerals, can be reduced by titrating with a dilute acid, while maintaining a constant batch volume by continuously extracting solution through a porous plug (B3). This approach is similar to the flow cell (B4) (Holdren and Speyer, 1985^c), where reactants are added continuously to a stirred batch while continuously extracting solution through a porous bottom plate, and the fluidized bed reactor (Chou and Wollast, 1984) where solution is recirculated by fast upward flow through a batch, to suspend the solids, while continuously adding reactants and extracting samples.

Mechanical abrasion of the soil material will be minimal in column experiments (C1). pH can be controlled either by automatically adjusting the input flow proportional to the buffer rate (Chapter 7: Van Grinsven et al., 1988^b) or by recirculating a separate batch solution, which is titrated to constant pH (C2) (Van Riemsdijk and van der Linden, 1984). Accumulation of reaction products in such a recirculation experiment can be prevented by titration with dilute acid and using a overflow pipe to maintain a constant batch volume, as in B2. Column experiments can involve disturbed or undisturbed soil cores and water saturated (forced flow) or unsaturated (gravitational flow) conditions. Finite initial input concentrations for all relevant components may be applied to prevent large changes in the degree of undersaturation with dissolving minerals in the percolate during column passage.

In the following sections the effect of experimental conditions on observed dissolution kinetics is evaluated by comparing dissolution data from batch (A2, A3, A4 and B2) and column (C1) experiments, exposing one type of soil material to solutions of variable composition. Data were collected rather from rather independent studies over four years. Observed dissolution rates are compared to estimated weathering rates from field mass balance studies.

5.3 MATERIAL AND METHODS

5.3.1 Soil Material and chemical analysis.

The soil material (Table 5.1) was sampled from a C-horizon of a sandy, mixed, acid, mesic Umbric Dystrochrept (Van Breemen et al., 1986). Soil was sampled from a soil pit, sieved (1 mm mesh) to remove stones and roots, freeze dried and mixed. Freeze-drying was preferred over air drying to prevent formation of soil lumps requiring subsequent grinding to obtain a homogeneous sample. The elemental composition of the soil was determined by X-ray fluorescence spectrometry. The composition of the cation exchange complex was determined by an unbuffered BaCl₂ extraction (Bascomb, 1964). The concentrations of field soil solutions are flux-weighted means based on a three-year period of monthly sampling. For methods reference is made to Van Breemen et al. (1986, 1987). The mineral composition was determined by counting using the optical microscope. All experiments were carried out in duplicate unless stated otherwise.

| | <2 | 2-50 | 50-150 | 150-300 | >300 | (μm) | | | | | |
|--|-----------------------------------|-------------------|--------|---------|--------------------------------|-------------------|------|------|-----------------|-----------------|--|
| Texture | (mass fraction %) | | | | | | | | | | |
| | 3.8 | 4.7 | 39.0 | 47.8 | 8.5 | | | | | | |
| Elemental composition | K ₂ O | Na ₂ O | CaO | MgO | Al ₂ O ₃ | SiO ₂ | | | | | |
| | (mass fraction %) | | | | | | | | | | |
| | 1.10 | 0.55 | 0.10 | 0.10 | 3.08 | 94.5 | | | | | |
| Exchangeable | K | Na | Ca | Mg | Al | Si | H | Cl | SO ₄ | NO ₃ | |
| | (mmol _c /kg) | | | | | | | | | | |
| | <0.1 | <0.1 | 0.1 | 0.1 | 3.9 | | 5.1 | | | | |
| Solutions | mmol _c /m ³ | | | | | | | | | | |
| Average field | 100 | 250 | 350 | 220 | 1850 | | 100 | 410 | 1450 | 960 | |
| Experiments: | | | | | | | | | | | |
| C2(saturated), A5 | 7 | 60 | 8 | 10 | 2 | 0 | 1010 | 1035 | 65 | 0 | |
| C2(unsaturated) | 120 | 250 | 390 | 240 | 2370 | 0 | 775 | 4145 | 0 | 0 | |
| Mineralogical composition (mass fraction of fine earth%) | | | | | | | | | | | |
| "free" Al-oxides | | | | | 0.12 | | | | | | |
| K-feldspar | | | | | 14 | | | | | | |
| Plagioclase | | | | | 5 | | | | | | |
| Micas (muscovite) | | | | | 3 | | | | | | |
| Heavy minerals | | | | | 0.8 | | | | | | |
| of which: pure aluminosilicates | | | | | 0.1 | | | | | | |
| pyroboles | | | | | 0.2 | | | | | | |

Table 5.1 Texture, chemical and selected mineralogical characteristics of the soil material, and chemical composition of average field soil solutions and initial batch solutions and column percolates.

In the solutions of the experiments Ca and Mg were analyzed by atomic absorption spectrometry, K and Na by atomic emission spectrometry. Si and Al were analyzed by inductive coupled plasma spectrometry and H potentiometrically. Samples were passed through a 0.45 μm filter before analysis.

5.3.2 Batch Experiments.

For the A3-type experiments (Figure 5.1) 10 g of soil were mixed with 30 mL of 1 mmol/L HCl (pH is 3) in 50 mL centrifuge tubes. Separate batches were analyzed after 1, 2, 5, 15, 29, 90, 240 and 720 h. The soil material was prewashed 7 times for 1 hr with 30 mL 1 mmol/L HCl.

In the unstirred type-A4 experiments, about 30 g of soil were added to 150 mL of solution in a plastic container with a diameter of 10 cm. The soil material was leached beforehand for two days with 1 mmol/L HCl. The initial concentrations were equal to concentrations determined previously by recirculation of demineralized water through a prewashed soil column for two days (Table 5.1). The batch solutions were acidified to pH 3 with HCl. When pH had increased by more than 0.1 unit, 100 mL of the solution was sampled and replaced by a fresh solution. Experiments were continued for 90 d.

In the stirred type-B2 experiment a batch of 20 g of soil in 120 mL was maintained at pH 3 by automatic titration with 0.1 mol/L HCl. A fast (400 rpm) and a slowly (4 rpm) revolving magnetic stirring bar were used to mix solution and sediment respectively. The experiment lasted for 10 d. Only the final composition of the batch was analyzed.

5.3.3 Column Experiments.

Percolation experiments were carried out while soil cores were either completely (saturated conditions) or partly (unsaturated conditions) saturated with water.

Soil columns were percolated under unsaturated conditions at a flow rate of 45 mL/d (=23 mm/d) (C1a). Both packed columns, with soil pretreated as described earlier, and undisturbed soil columns, excavated at the field site, were leached with a 3 mmol/L HCl solution. The soil cores were 5 cm high and 5 cm in diameter, weighed about 120 g, and were enclosed between 2 cm thick layers of inert quartz to obtain homogeneous throughflow. The percolate was sampled daily over a period for 200 d.

In similar experiments the flow was adjusted manually to maintain an output pH ranging between 3.2 and 3.3. (C1b). Flow was lowered from 100 mL/d to 10 mL/d in the course of the experiment. In the experiments columns were packed with a mixture of 20 g of soil and 20 g of inert quartz to increase the hydraulic conductivity. The composition of the input solution was equal to that observed in the field (Table 5.1) but acidified to pH 3.1. Experiments lasted for 75 d.

Cores of 20 g of soil mixed with quartz were also percolated under saturated conditions for 10 d (C1c). The pH in the outflow was controlled by automated adjustment of the flow rate proportional to the rate of proton consumption (C3). Input concentrations were equal to those used for the unstirred batch experiments (Table 5.1).

5.3.4 The effectiveness of diffusion transport

The effectiveness of diffusion to homogenize solutions in absence of stirring was tested. In order to precondition the soil material, four plastic 250 mL containers filled with 30 g of soil and 150 mL 1 mmol/L HCl, were first stirred head-over-end during 4 d, while daily replacing 100 mL of the solution with a fresh HCl solution. After the fifth addition two experiments were continued without stirring while the other two were continued with stirring. After 1, 5 and 23 h pH was measured and 25 mL samples were taken for analysis. After 23 h 75 mL of fresh HCl was added and measurements were repeated at 30 and 47 h.

In the first day following the pretreatment, the proton buffering in the unstirred batch experiment was about 10% lower than in the head-over-end stirred experiment (Figure 5.2).

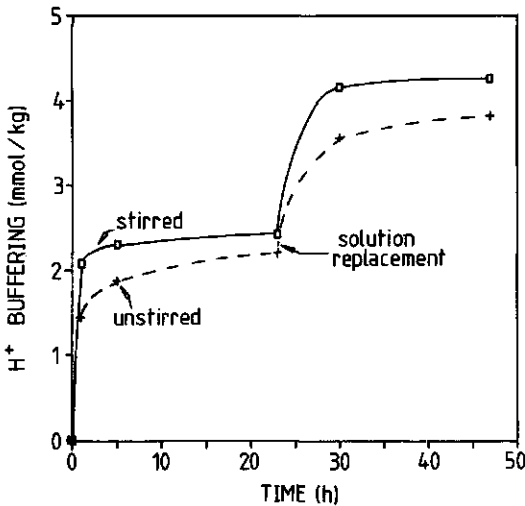


Fig. 5.2 Cumulative proton buffering in stirred and unstirred batch experiments after two consecutive solution replacements.

Dissolution of Al was the main buffering process (Table 5.2). Buffer rates decreased strongly with time, which may be attributed to increased saturation of solutions with respect to $Al(OH)_3$ (Equation 2); activity products during the experiment increased from $10^{4.6}$ to $10^{7.5}$.

| | H | Al | Mg | Si |
|----------|---|------|-------|-------|
| | (mmol _c ·kg ⁻¹ ·d ⁻¹) | | | |
| Addition | | | | |
| | Stirred | | | |
| 1 | -2.53 | -- | 0.047 | 0.339 |
| 2 | -1.84 | 1.91 | 0.048 | 0.330 |
| | Unstirred | | | |
| 1 | -2.32 | -- | 0.024 | 0.152 |
| 2 | -1.61 | 1.64 | 0.005 | 0.099 |

Table 5.2 The rates of release of H, Al, Mg and Si (kg⁻¹ soil) in stirred and unstirred batch experiments for 2 consecutive solution replacements.

The rates of release of Mg and Si (in the form of H₄SiO₄), in the stirred experiment were considerably higher than in the unstirred system (Table 5.2). The concentration gradients across the overlying stagnant solution, required to allow the dissolution rates observed in the stirred experiment, can be estimated from the equation for steady-state diffusion:

$$W = \frac{A D \Delta C}{\Delta X} \tag{1}$$

Where W is the dissolution rate (mol·s⁻¹), A is the area of a cross-section of the interface between solution and sediment (79 cm²), ΔC is the concentration difference (mol/cm³), D is the molecular diffusion coefficient (10⁻⁵ cm²/s) and ΔX is the thickness of the overlying solution layer (2 cm). Using the rate data for the stirred experiment (Table 5.2) resulting values for ΔC are 1.8 mmol/L for H, 0.29 mmol/L for Si and 0.02 mmol/L for Mg. Actual concentrations in the overlying solutions in the unstirred experiment after 1 d were 0.2 mmol/L for H, 0.67 mmol/L for Si and 0.005 mmol/L for Mg. For simplicity assuming that the [H⁺] in the sediment is negligible, dissolution of Al apparently was limited by bulk diffusion of protons to the sediment. However, the diffusion flux of H to the sediment will be adequate for the proton requirement for dissolution of silicate minerals, which is only a minor fraction of the total proton consumption. The concentrations in the interstitial water required for back-diffusion of Si and Mg, at the rates of release observed in the stirred experiment, are 0.96 and 0.025 mmol/L respectively. These concentrations are not unrealistic considering that the volume of the interstitial water is only about 10 mL.

If differences in rates of release of Mg and Si between stirred and unstirred batches are not caused by limited diffusion in the bulk solution, they may be

attributed to effects of mechanical abrasion of the mineral surfaces or to enhanced transport of reactants from the mineral surfaces to the bulk solution in the stirred experiment. Continuous formation of reactive surface sites by abrasion may also explain why dissolution rates of Mg and Si in the stirred system after both acid additions were identical, while particularly the dissolution rate of Mg decreased strongly in the unstirred system.

5.4 RESULTS AND DISCUSSION

5.4.1 Effect of sample pretreatment

The dissolution rate of Al in packed and undisturbed soil columns at a constant input of 45 mL/d of 3 mmol/L HCl is shown in Figure 5.3.

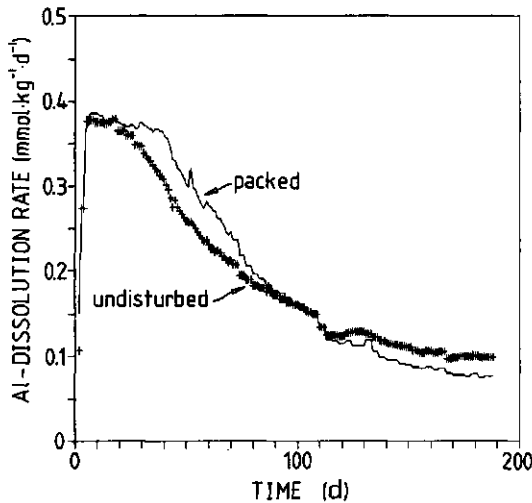
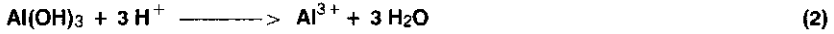


Fig. 5.3 The Al-dissolution rate in column experiments percolated with 45 mL/d of 0.003 mmol/L HCl, comparing undisturbed and packed soil cores under unsaturated hydrologic conditions.

The results for packed and undisturbed columns were very similar. Dissolution of Al was the dominating proton buffering process. Within 3 d, which is the approximate time needed to flush the columns, the dissolution rates of Al reached a stationary value of $0.38 \mu\text{mol.g}^{-1}.\text{d}^{-1}$. This rate was maintained for about 20 d. In this stage solutions were slightly undersaturated ($\log(Q_{\text{SO}}) = 8$)

with respect to dissolution of natural $\text{Al}(\text{OH})_3$ ($\log(K_{\text{so}})=8.8$) (Driscoll and Bisogni, 1984).



After 20 d dissolution rates of Al started to decrease, causing a decrease of pH in the pore water and outflow. This decrease was somewhat stronger for the undisturbed columns. However, from d 110 onwards dissolution rates of Al in the undisturbed columns were somewhat higher than in the packed columns. The overall decrease of the Al dissolution rate, which is counteracted by the decreasing pH in the pore water, is attributed to depletion of the most reactive Al-bearing minerals. In this soil the reactive pool of Al probably consists of amorphous aluminum-hydroxides, included in the "free" Al fraction (Table 5.1). The initially higher dissolution rates of Al in the packed columns as compared to the undisturbed columns can be explained by the creation of additional reactive Al sites by mechanical disturbance during sample pretreatment. Because the total pool of reactive Al is fixed, higher dissolution rates of Al cause faster depletion of this pool, eventually causing lower dissolution rates of Al in the packed columns than in the undisturbed columns. No such difference between dissolution rates in packed and undisturbed columns are observed for the alkali cations and Si, where exhaustion effects may be expected to be less prominent than for Al. The average output concentrations are summarized in Table 5.3.

| | | K | | Na | | Ca | | Mg | | Si | |
|-------------|---|--|------|------|------|------|------|------|------|-------|------|
| | | ($\mu\text{mol}_c \cdot \text{kg}^{-1} \cdot \text{d}^{-1}$) | | | | | | | | | |
| | | Mean | s.d. | Mean | s.d. | Mean | s.d. | Mean | s.d. | Mean | s.d. |
| Disturbed | 1 | 3.7 | 0.3 | 6.0 | 1.2 | 2.8 | 0.6 | 5.5 | 0.7 | 75.8 | 16.4 |
| | 2 | 3.5 | 0.4 | 6.0 | 0.5 | 3.1 | 0.6 | 5.8 | 0.8 | 98.8 | 29.5 |
| Undisturbed | 1 | 3.9 | 0.4 | 6.7 | 0.6 | 3.4 | 0.8 | 5.9 | 0.7 | 104.6 | 18.8 |
| | 2 | 3.5 | 0.5 | 5.9 | 0.5 | 2.8 | 0.5 | 3.8 | 0.6 | 90.8 | 17.6 |

Table 5.3 Mean rates of release of cations and Si (kg^{-1} soil) from duplicate (1 and 2) disturbed and packed soil columns percolating with 42 mL/d 3 mmol/L HCl for 260 d.

5.4.2 Effect of experimental method

Dissolution of Al proceeds much faster than dissolution of K, Na, Mg and Si and, moreover, slows down quickly during reaction progress. Therefore, the effect of experimental method on dissolution kinetics was evaluated separately for Al on the one side and for K, Na, Mg and Si on the other side. Figure 5.4 shows the logarithm of the proton buffer rate as function of reaction progress for the column experiments (C1b, C1c) and the stirred batch experiment (B2).

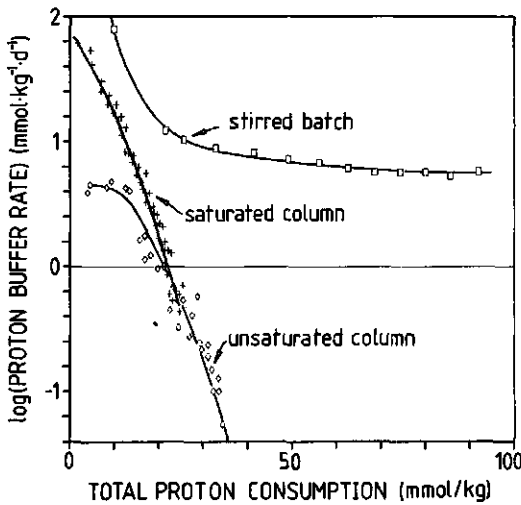


Fig. 5.4 Comparison of the proton buffer rates with reaction progress, at pH 3 during a stirred batch titration and two column experiments under saturated and unsaturated flow conditions, with low ($10 \text{ mmol} \cdot \text{m}^{-3}$) and high ($240 \text{ mmol} \cdot \text{m}^{-3}$) input concentrations of Al.

Dissolution of Al was the main buffering process, as was observed previously. Buffer rates obviously depend strongly on the experimental method. In the stirred batch experiment rates are much higher and decrease more slowly with reaction progress, than in the column experiments.

These differences cannot be attributed to pH differences (Stumm et al., 1985, Stumm and Furrer., 1986) or to differences in the degree of saturation with $\text{Al}(\text{OH})_3$. pH in all experiments was controlled at a value near 3. Differences in degree of saturation with $\text{Al}(\text{OH})_3$ were small: $\text{Al}(\text{OH})_3$ activity products (Equation 2) in the column experiments were $10^{5.1}$ (C1b) and $10^{6.5}$ (C1c) respectively, while they reached $10^{6.5}$ towards the end of the batch experiment. The most likely cause for the much higher and more slowly decreasing buffer

rates in the batch experiment seems to be mechanical disturbance of the surfaces. Stirring may continuously create reactive surface area. Continuous stirring of the sediment (Figure 5.1) may have stronger effects than sample pretreatment or head-over-end shaking. Amorphous hydrous oxides of Al, such as the Al extracted by oxalate-dithionite extraction, are the most likely source of Al. Mechanical disturbance of these secondary oxides is feasible: SEM photomicrographs (Berner and Holdren, 1979) suggest that secondary Al is present as small particles, often weakly adhering to surfaces of primary minerals.

Inadequate pH control in the experiment with unsaturated soil (C1b) was the main cause for initial lower buffer rates than in the experiment with saturated soil (C1c). The highest gravitational flow rates in the experiments with unsaturated soil were too low to maintain a pH value of 3.2 during the initial rapid dissolution of Al. After 25 mmol/kg of H⁺ has been consumed, the buffer rate curves for the saturated and unsaturated experiments seem to merge, suggesting that differences in water content and mineral saturation with respect to Al(OH)₃ do not influence rates of Al-release.

The results for the other cations and for Si are summarized in Table 5.4.

| Type | pH | Na | K | Mg | Si | Flow Volume | Weight | Duration |
|-----------------------|---------|---|-----|-----|------------|----------------|--------|----------|
| | | (μmol.kg ⁻¹ .d ⁻¹) | | | (mL/d, mL) | (g) | (d) | |
| Batch | | | | | | | | |
| Head-over-end | 3-4 | 4 | 33 | 43 | 110 | 30 | 10 | 30 |
| Unstirred | 3.0 | 3 | 2 | 4 | 33 | 150 | 16 | 50 |
| Stirred titration | 3.0 | 230 | --- | 185 | 1350 | 120 | 20 | 10 |
| Column | | | | | | | | |
| Fixed flow | 2.6-3.3 | 6 | 4 | 3 | 88 | 45 | 120 | 150 |
| Variable Gravim. flow | 3.1 | 20 | 10 | --- | 20 | 30 | 20 | 60 |
| Variable forced flow | 3.0 | 20 | 4 | 1 | 50 | 70 | 20 | 14 |

Table 5.4 Rates of release of K, Na, Mg and Si observed in six different types of dissolution experiments at pH 3.

The rates were corrected for initial salt displacement and cation exchange. Again, observed rates of release of Na, K, Mg and Si were markedly higher in the stirred pH-stat experiments (B2) than in all other experiments. Apparently, continuous stirring of the sediment also affected surfaces of silicate minerals, as was suggested earlier to explain differences in release of Mg and Si from stirred

and unstirred batch experiments (Table 5.2). The second highest rates for K, Mg and Si were found in the head-over-end experiment. Rates in the unstirred batch experiment and the column experiments were very similar, which may have been expected because during both types of experiments solids were not mechanically disturbed and solutions were stagnant or nearly stagnant. The duration and the total proton consumption of the experiments varied over a wide range; duration from 10 to 150 d and proton consumption from 3 to 110 $\mu\text{mol/g}$. Depletion effects after the initial salt displacement and exchange phase were considered unimportant; relative to total pools of silicate minerals, depletion over the duration of the experiments certainly was negligible.

5.4.3 Effect of percolation rate

The lowest weathering rates for K and Mg and Si observed in the laboratory experiment were 0.002, 0.002 and 0.02 $\mu\text{mol}_c\text{g}^{-1}\text{d}^{-1}$ respectively (Table 5.4). Extrapolated to field weathering rates for a 1 m soil profile, we find 7.3, 7.3 and 73 $\text{kmol}_c\text{ha}^{-1}\text{yr}^{-1}$ respectively. Budget studies based on three years of field monitoring revealed weathering values in the order of 0.5 for K and Mg and 1 $\text{kmol}_c\text{ha}^{-1}\text{yr}^{-1}$ for Si, for a 0.9 m soil profile (Van Breemen et al., 1986). Weathering rates for the C-horizon may be somewhat higher than the profile average, because silicate weathering rates in the leached A- and B-horizon may be expected to be lower than in the C-horizon. The discrepancy for Si may be attributed in part to reprecipitation of dissolved Si deeper in the soil profile, but it is clear that weathering rates for K and Mg are overestimated in the laboratory by at least one order of magnitude. As shown previously, enhanced weathering due to mechanical disturbance played no role in the column experiments and in the unstirred batch experiments. Moreover, the experiments were continued long enough to exclude the effects of salt displacement and cation exchange. Depression of weathering rates in the field due to chemical saturation effects with respect to K- and Mg-bearing silicates is unlikely at ambient values of pH in soil solution below 4. Remaining explanations may have to be sought either in effects of pH, by means of the surface protonation mechanism (Stumm et al., 1985), or in effects of hydraulics, eg. through imperfect contact between solids and percolating solution (Velbel, 1986). In general a power relationship is found between silicate dissolution rates and hydrogen activity in solution, where the exponent varies between 0.33 and 0.8 (Stumm and Furrer, 1986). If the weathering rate would increase with the square root of the hydrogen activity, the

pH difference between field (4) and experiments (3) would imply a three times lower weathering rate in the field than in the laboratory.

In Figure 5.5 the relationship between dissolution of Mg and residence time is compared at pH 3 for a batch experiment (head-over-end, A3) and a column experiment (forced variable flow, C1c).

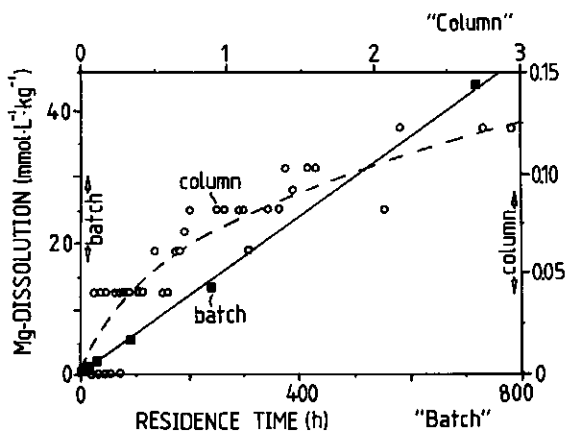


Fig. 5.5 The dissolution of Mg in a batch and a column experiment with increasing residence time.

In batch experiments, rates of silicate dissolution tend to become constant with time (Busenberg and Clemency, 1976), as was indeed observed in the batch experiment. However, for the column experiments, the concentration of Mg appears to increase less than linearly with residence time (Figure 5.5), with residence time calculated as the ratio of pore volume and percolation rate. This non-linear behaviour was also found for K, Na, Mn and Si. The outflow concentrations in the column experiments could be described as a function of the square root of residence time, implying that the weathering rate increases with the square root of the percolation rate. The essential difference between the batch and column experiment is that hydraulic conditions in batch are independent of residence time, while in column experiments residence time is inversely proportional to percolation rate. The lowest flow applied in the column experiments is about 70 mL/d, which is equivalent to 4 cm/d. By comparison, the average flow rate in the field ranges from 0.05 to 0.15 cm/d (Van Breemen et al., 1986). When assuming a square root relationship between weathering rate and percolation rate, the lowest dissolution rate observed in the column

experiment should be 5 to 9 times higher than field rates, what accounts for the larger part of the observed discrepancy of a factor of 15 for K and Mg.

Explanation of the effect of flow rate on dissolution rate requires a reconsideration of transport control (Berner, 1978; Berner and Holdren, 1979). Our observations are consistent with the existence of a stagnant water film at the interface of the reactive surface and solution, rather than a residual product layer, as the factor limiting diffusion transport. The etch pit concept implies that the reactive surface area is much smaller than the total surface area. The effect of a stagnant water film limiting diffusion of K from etch pits to the bulk solution can be illustrated by Equation 1. The observed dissolution rate of K in the saturated column experiment was $2 \cdot 10^{-9} \text{ mol} \cdot \text{g}^{-1} \cdot \text{d}^{-1}$ (Table 5.4). Let us assume that all K dissolves from microcline, present in a concentration of 0.05 g/g soil (Table 5.1), and having a total surface area of $104 \text{ cm}^2/\text{g}$ (Busenberg and Clemency, 1976). From SEM photomicrographs of the soil material (Figure 5.6) we further estimate that 1% of the total surface consists of etch pits. The reactive surface area (A) would then be $5 \text{ cm}^2/\text{g}$ soil. We finally assume that proton transport from bulk solution to the reactive surface is rate limiting, and a concentration difference (ΔC) of $10^{-6} \text{ mol}/\text{cm}^3$ between bulk solution (pH=3) and solution near the reactive surface (negligible (H^+)). Then Equation 1 predicts that a stagnant water film (ΔX) of $4.6 \times 10^{-4} \text{ cm}$ (about $5 \mu\text{m}$) thickness would limit diffusion transport. Such a thickness does not seem to be unrealistic, considering the scale of the surface roughness and the depth of etch pits, as shown on the SEM photomicrographs for a K-feldspar (Figure 5.6), which can amount to several mm. The thickness of this stagnant water film will depend on flow and stirring rate. In fact, variation of the stirring rate is used as a test to distinguish between transport and surface reaction control (Berner, 1978). However, rate control by stagnant water films overlying etch pits is not easily detected unless stirring rates are made very low. It may be impossible to establish a theoretical relationship between flow rate and the thickness of a stagnant water film on etched mineral surfaces using concepts of fluid dynamics. The theory for laminar capillary flow (Hagen and Poiseuille), which applies to flow in the column experiments where Reynold numbers do not exceed 0.01, states that the thickness of the region with flow rates less than the bulk rate decreases proportionally to the square root of the flow rate (Koorevaar et al., 1983):

$$v_r = 0.25 \eta^{-1} \nabla H (r^2 - R^2) \quad (3)$$

Where v_r is the fluid velocity (m/s), η is the viscosity (Pa.s), ∇H is pressure gradient (Pa/m), r is the radial distance from the capillary wall (m), and R is the capillary radius (m).

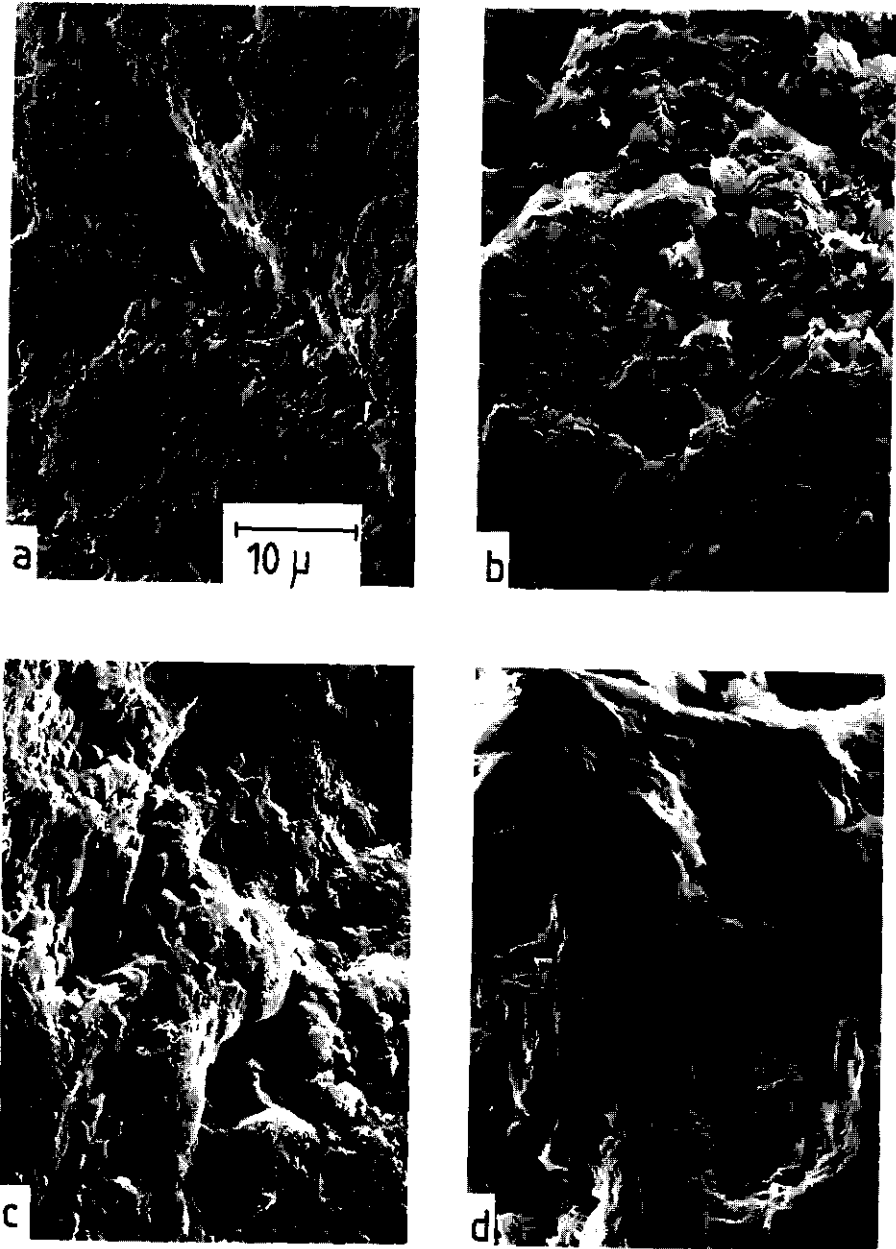


Fig. 5.6 Scanning electron micrographs of K-feldspars in a C-horizon of a Umbric Dystrachrept with increasing (a-d) etch pit depths and degree of surface roughness.

Equation 3 is consistent with the observed square root increase of dissolution rates with flow rate, provided that the effect of flow rate on the thickness of a stagnant water film is similar for smooth capillaries and rough mineral surfaces.

5.5 CONCLUSIONS

Knowledge of mineral dissolution kinetics in soils is important to evaluate the long-term mobilization of cation nutrients to extensively managed forest systems. Most dissolution studies were carried out on pure minerals, using experimental techniques which are not suitable to estimate mineral dissolution rates in soil. Usual mechanical pretreatments of soil material will increase the reactivity of minerals, especially of Al-oxides. Mild pretreatments like sieving and freeze drying will hardly affect the kinetics.

Observed weathering kinetics strongly depend on experimental conditions. Controlled pH is a prerequisite when studying kinetics of Al dissolution. Intensive stirring in batch systems can increase rates of release of cations, in particular of Al, by at least one order of magnitude as compared to column experiments, even in an identical chemical environment. Theoretically, rates of diffusion in unstirred batch experiments should be sufficient to maintain homogeneous solutions during slow silicate weathering. This could be tested by comparing stirred and unstirred experiments, but such a comparison is complicated by mechanical disturbance caused by stirring. Observed silicate weathering rates in column experiments and unstirred batch experiments are of similar magnitude. Still these rates are 5 to 10 times higher than inferred from field studies, even when accounting for lower pH values in the laboratory than in the field. The larger part of the discrepancy could be explained by hydrodynamic factors. Column experiments with variable percolation rates showed that dissolution rate increased with the square root of percolation rate. This increase may be associated with a decreasing thickness of stagnant water films, which limit diffusion transport from etch pits in nearly stagnant hydrodynamic conditions. Further research is needed to study weathering kinetics in nearly stagnant batch or column systems, at constant solution chemistry.

ACKNOWLEDGEMENTS

This research was sponsored by the Dutch Ministry of Environment as part of the Dutch Priority Programme on Acidification. Thanks are due to Professor N. van Breemen of the Department of Soil Science and Geology and Professor F.A.M. de Haan of the Department of Soil Science and Plant Nutrition for supervising the research program and critically reviewing this paper. We also thank the Netherlands Energy Research Foundation (ECN) in Petten, in particular Mr. R. Otjes and Dr. T. Lub, for carrying out the column experiments under forced flow. Furthermore we would like to thank Mrs. M. Sperna-Weiland, Mr. H. Denier van der Gon and Mr. C. Kooge for their experimental contributions as part of their MSc. program. Finally we wish to thank Mr. E. Nab for carrying out the long-term column experiments.

A revised version of this Chapter will be submitted to Geoderma.
J.J.M. van Grinsven and W.H. van Riemsdijk.

Chapter 6

KINETICS OF THE DISSOLUTION OF ALUMINUM AND BASE CATIONS FROM A SOIL AT pH VALUES BELOW 4

ABSTRACT

Kinetics of H^+ consumption by mineral dissolution in a surface soil and a subsoil of an acid woodland soil were studied by means of batch type experiments and stationary pH titrations. Mineral dissolution in the subsoil could effectively be described by congruent dissolution of illite ($K_{0.6}Mg_{0.25}Al_{2.3}Si_3O_{10}(OH)_2$) followed by an incongruent dissolution stage. In the incongruent stage the concentration of Al decreased while concentrations of K and Mg continued to increase. Congruent dissolution rates of illite could be predicted with power type relationships from transition state theory. In the incongruent dissolution stage the activities of H and Al appeared to be controlled by precipitation of $Al(OH)_3$. Results of this kind of experiments could be helpful to understand the behaviour of Al and base cations in acid soils and soils with high atmospheric loadings of acid. Comparison of the results of batch experiments for a surface soil and a subsoil showed that initially proton consumption in the surface soil is faster and more effective due to the presence of a relatively high cation exchange capacity and base saturation value. However with progressive proton consumption and increasing reaction times proton consumption in the subsoil becomes faster than in the surface soil, presumably due to higher rates of mineral dissolution in the subsoil. Lower dissolution rates in the surface soil may result from lower contents of easily weatherable minerals, due to excessive leaching in the past which is reflected in a 17% lower acid neutralizing capacity than in the subsoil.

6.1 INTRODUCTION

Ultimately consumption of protons in acid soils always originates from the dissolution of aluminosilicates. Exchange of base cations and dissolution of oxides are faster buffer processes than dissolution of aluminosilicates, however the origin, and therefore also the capacity of fast buffer mechanisms lies in continued dissolution of aluminosilicates. The difference between the rates of mineral dissolution and atmospherically derived H^+ production controls the long-term changes in soil chemistry. If the H^+ input exceeds the dissolution rate of base cations, acidity levels ($H + Al$) both in solution and on the exchange

complex will increase. If dissolution rates of base cations can keep up H^+ production rates, acidity levels will not increase and no adverse effects on biota will result. Generally in acid soils Al is the main product of mineral dissolution.

In order to evaluate long-term sensitivity of acid soils to harmful effects of acid atmospheric deposition by means of simulation models such as ILWAS (EPRI, 1983), dissolution of aluminosilicates must be described in terms of rate (r_i), acid neutralizing capacity (ANC) and stoichiometry. Present knowledge of the kinetics of dissolution of aluminosilicates applies mainly to pure mineral systems (Helgeson et al., 1984; Busenberg and Clemency, 1976; Lasaga, 1983), and not (quantitatively) to soils, which are complex mixtures of various minerals and organic substances. A budget study for an acid woodland soil (Van Breemen et al., 1984) showed that atmospheric H^+ loads of $4 \text{ kmol} \cdot \text{ha}^{-1} \cdot \text{yr}^{-1}$ are largely consumed between 0 and 10 cm depth, producing almost equivalent amounts of Al.

Batch type experiments were carried out on the surface soil and the subsoil of this woodland to study the rates and mechanisms of mineral dissolution.

6.2 MATERIALS AND METHODS

Soil samples (sandy mixed acid mesic Umbric Dystrachrept (USDA, 1975)) were taken every 10 cm, air dried and mixed well in bulk samples for 0 to 20 and 60 to 100 cm depth. Prior to all batch experiments soils were prewetted 24 hr with demineralized water. In experiment I 30 mL of a 1:1 mixture of 0.001 M HNO_3 and 0.0005 M H_2SO_4 (pH 3) were added per 10 g of dry soil. Experiments were carried out in duplicate and with one blank, in which soil was shaken with demineralized water. Batches were shaken, end over end, during 0.5, 2, 8, 23, 47, 96, 191, 336 and 672 hr. In experiment II 20 g of subsoil and 120 mL of demineralized water were titrated with a 1:1 mixture of 0.1 M HNO_3 and 0.05 M H_2SO_4 at an automatically adjustable rate in order to maintain a constant pH (Radiometer, ABU 80 autoburette and TTT 60 titrator). Sediment and solution were stirred at respective rates of 4 and 500 rpm in order to minimize abrasion of the soil grains that may result in an artificial increase of reactive surface. Titrations were carried out at pH values of 3.0, 3.2, 3.5 and 3.8. Experiment III was comparable to experiment I except that the batch solution was replaced five times by a fresh acid solution. The time intervals between the replacements were 1, 24 and 168 hr.

Elemental analysis of soil extracts and the solid phase was carried out according to procedures as described by Begheijn (1980). Ca and Mg were

measured by atomic absorption spectrometry, Na and K by atomic emission spectrometry, Al by colorimetry (pyrocatecholoviolet), SO_4 by ion chromatography and H_4SiO_4 by colorimetry (blue silica molybdic acid complex). The cation exchange complex was analyzed by an adapted unbuffered BaCl_2 extraction. Exchangeable H and Al were separated by titration of the extract up to a pH of 8.2, followed by an independent analysis of Al. Elemental analyses were done by X-ray fluorescence spectrometry.

6.3 RESULTS AND DISCUSSION

6.3.1 Solid phase characteristics

The acid neutralizing capacity (ANC) was estimated by the component composition (Van Breemen et al., 1984) according to:



For the surface soil ANC was 1365, (371 in the clay fraction) and for the subsoil 1623 mmol.kg^{-1} (dry soil). In the surface soil 30% of Al, 50% of Mg and 6% of K is present in the clay fraction. The CEC of the surface soil ranged from 60 to 100 mmol/kg and is mainly occupied by H (50%) and Al (25%) (on ionic equivalent basis). CEC and clay content in the subsoil are negligible. X-ray diffraction showed the presence of both illite and expandable three-layer clay minerals. The surface soil and the subsoil contain 20% (mass fraction) of K- and Na-feldspars.

6.3.2 A mechanistic interpretation of experiment I

Mineral dissolution kinetics were studied first in the subsoil because due to the small CEC cation exchange reactions caused by acid additions will be unimportant. Figure 6.1 shows concentrations of Al, Mg, K, H and SO_4 for experiment I. Initial concentrations of H and SO_4 were 1 and 0.25 mmol.L^{-1} , respectively. All concentration changes in the blank experiment were small compared to those in the experiment with acid addition except for Si. Therefore Si was not further considered.

Apparent is the occurrence of a maximum in the Al concentration at 47 hr. Concentrations of K and Mg increase throughout the experiment. In contrast concentrations of Ca and Na (not shown) hardly change after 2 hr.

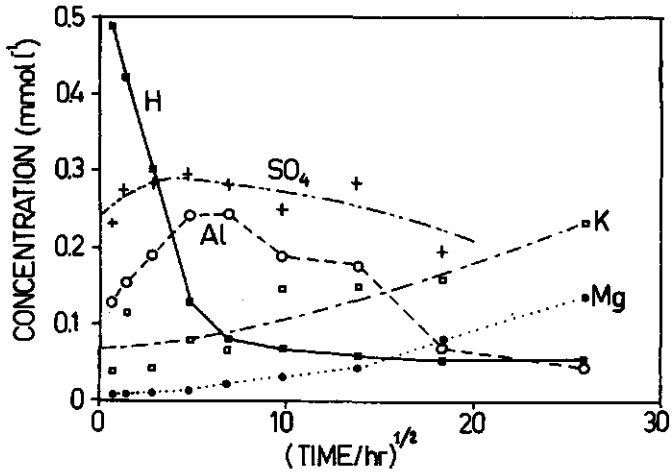


Fig. 6.1 Concentrations of Al, K, Mg, H and SO₄ for experiment I, after addition of 30 mL of a 1:1 mixture of 1 mmol/L HNO₃ and 0.5 mmol/L H₂SO₄ to 10 g of subsoil.

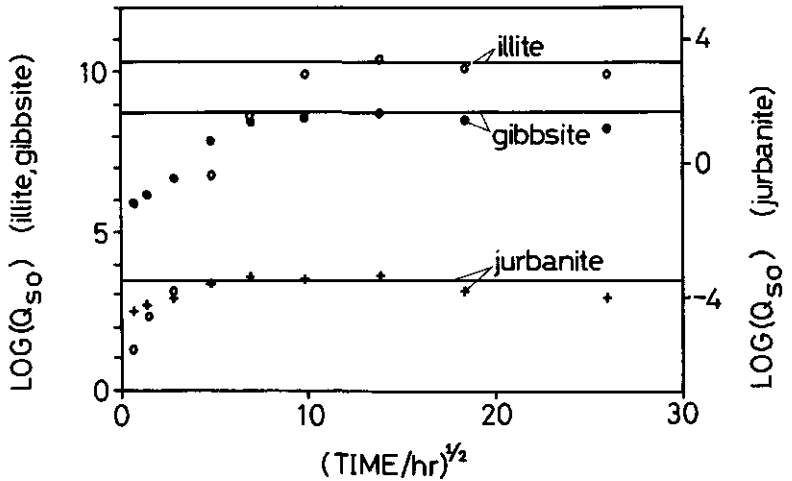
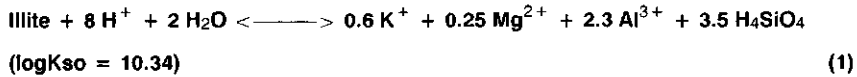


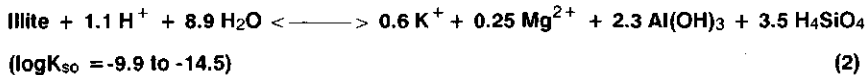
Fig. 6.2 Saturation of batch solutions in experiment I with respect to illite, ($\log(K_{so}) = 10.34$), natural gibbsite ($\log(K_{so}) = 8.77$) and jurbanite ($\log(K_{so}) = -3.50$).

The experimental results may be explained by an initial, congruent dissolution of a silicate mineral, releasing Al, K and Mg until the solution becomes oversaturated with respect to a secondary Al-mineral.

Up to 47 hr the ratio of the concentration changes of H and Al is -8/2.2, which agrees well with the theoretical ratio of -8/2.3 for congruent illite ($K_{0.6}Mg_{0.25}Al_{2.3}Si_3O_{10}(OH)_2$) dissolution:



Furthermore the batch solutions gradually become saturated with respect to illite (Figure 6.2), and after 191 hr remain slightly undersaturated. The decrease of [Al] after 47 hr suggests the formation of a secondary Al-mineral. At 47 hr log(Al)-3log(H) is 8.42 and fluctuates between 8.68 and 8.21 afterwards (Figure 6.2). These values suggest the formation of a precipitate of Al(OH)₃ intermediate between synthetic (log(K_{so}) = 8.11) and natural gibbsite (log(K_{so}) = 8.8). After 47 hr the net release of Al from illite stops. Because the pH will still slowly increase due to continued, incongruent dissolution of illite, Al released earlier will precipitate as Al(OH)₃ and supply the major part of the H⁺ for further release of K and Mg from illite. The incongruent dissolution reaction for illite is:



The observed decrease of SO₄ after 191 hr (Figure 6.1) and the presence of some correspondence between activities of H, Al and SO₄ and stability lines for jurbanite (Al(SO₄)(OH)·5H₂O) (Figure 6.2) suggest the precipitation of jurbanite. Yet jurbanite was not further considered as its formation remains obscure (Mulder et al., 1986) and the balance between the concentration changes of H and Al does not agree with the stoichiometry of jurbanite precipitation.

6.3.3 A kinetic illite dissolution model for experiment I

To illustrate the validity of the proposed dissolution mechanism for experiment I, a simple simulation model was developed. The required kinetic parameters and the equilibrium constant for gibbsite were derived from the experiment itself.

A general expression for the rate of mineral dissolution in terms of the transition theory (Aagaard and Helgeson, 1982) is:

$$r^* = K^* (H^+) (1 - \exp(A/(r RT))) \quad (3)$$

where r^* stands for the dissolution rate of the mineral ($\text{mol}\cdot\text{cm}^{-2}\cdot\text{s}^{-1}$), (H^+) represents the proton activity, A stands for the chemical affinity of the overall reaction ($\text{J}\cdot\text{mol}^{-1}$), R is the gas constant ($\text{J}\cdot\text{mol}^{-1}\cdot\text{K}^{-1}$), T represents the temperature ($^{\circ}\text{K}$), r is the ratio between the rate of decomposition of the activated complex and the overall reaction, and K^* is the rate constant ($\text{mol}\cdot\text{cm}^{-2}\cdot\text{s}^{-1}$). Equation (3) can be rewritten as:

$$r = K (H^+) (1 - (Q/K_{so})^p) \quad (4)$$

where r and K are the dissolution rate and rate constant in $\text{mol}\cdot\text{kg}^{-1}\cdot\text{hr}^{-1}$ (the reactive surface area was not measured), Q is the activity product for the dissolution reaction, which is:

$$\prod_i^n a_i$$

where n stands for the reaction coefficient for the i^{th} reactant species, K_{so} is the equilibrium constant for overall dissolution of the mineral and p is $1/r$. According to Aagaard and Helgeson (1982) the last term of Equation (4) is negligible far from equilibrium. At equilibrium Q is equal to K_{so} and r is equal to 0.

The non-linear optimization package OPTPAC (Kilsdonk, 1977) was used to determine parameters for Equation (4) for the congruent dissolution stage. The function to be minimized was:

$$\sum_{i=1}^n (r'_i - r_i) / r'_i)^2 \quad (5)$$

in which r'_i is the experimentally found mineral dissolution rate, which is calculated from the rate at which ions are released to solution assuming congruent illite stoichiometry, and n is the number of observations. The standard error of estimate and prediction accuracy (SEE) was calculated by dividing the result of Equation (5) by $(n-2)$. Values for p and C were calculated for rates of release of H alone ($n=5$) and of H, Al and Mg ($n=15$). Equation (4) could not be fitted to the incongruent dissolution stage because Q essentially remained constant (Figure 6.2) and the changes in the rates of release of K and Mg did not show a trend. Results are shown in Table 6.1.

| n | K (mol g ⁻¹ hr ⁻¹) | p | K _{SO} (illite) | SEE |
|----|--|------------------------|-----------------------------|-------|
| 5 | -3.06 10 ⁻² | -4.45 10 ⁻² | 2.19 10 ¹⁰ | 0.480 |
| 5 | -2.63 10 ⁻¹ | -6.51 10 ⁻³ | 1.00 10 ¹¹ | 0.407 |
| 15 | -2.02 | -1.51 10 ⁻¹ | 2.19 10 ¹⁰ | 0.565 |
| 15 | -1.12 | -1.68 10 ⁻¹ | 1.00 10 ¹¹ | 0.569 |

Table 6.1 Optimised kinetic parameters for incongruent dissolution of illite according to Equation 4.

In contradiction with transition state theory values of p are negative, which makes the last term of Equation (4) not negligible. Although apparently transition state theory does not apply, Equation (4) still fits the rate data.

Simulation of the congruent stage of experiment I using values for K and p, based on the consumption rates for H, gave the best prediction of the starting point of the incongruent stage. Exactly at 47 hr saturation was predicted with gibbsite ($\log(K_{SO}) = 8.40$). From this point several combinations of [H] and [Al] in equilibrium with $Al(OH)_3$ were calculated iteratively with the Newton-Raphson procedure for increasing values of H^+ consumption. The resulting concentrations of K and Mg were calculated from the total proton consumption and Equation (2). The reaction times to attain the newly calculated sets of concentrations in the incongruent stage were calculated both from Equation (4) (Figure 6.3) and by assuming a constant dissolution rate after equilibrium is attained with gibbsite (Figure 6.4). The simulation results show that the congruent dissolution stage is described well. In the incongruent stage the observed decrease of [Al] and increase of [Mg] are predicted best when assuming a constant illite dissolution rate. However, the latter assumption causes oversaturation with respect to illite after 230 hr (Figure 6.5). After 191 hr the predicted concentrations of K are too high, probably due to neglecting the observed decrease of $[SO_4]$. The fact that Equation (4) does not apply to the incongruent stage may also be caused by a too low equilibrium constant for illite. If we assume higher values for $\log(K_{SO})$, e.g. 11 (Table 6.1), undersaturation is maintained longer, but predicted illite dissolution rates in the incongruent stage remain too low.

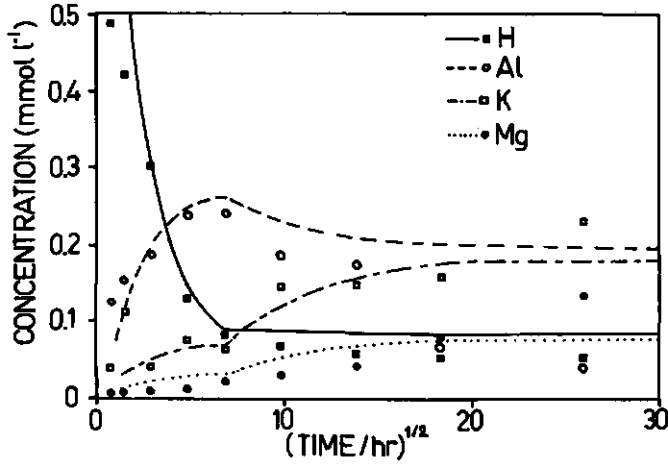


Fig. 6.3 Simulated and measured concentrations for experiment I, assuming congruent dissolution of illite until saturation with gibbsite ($\log(K_{so}) = 8.40$) occurs at 47 h. Illite dissolution rates are a function of the degree of saturation with respect to illite.

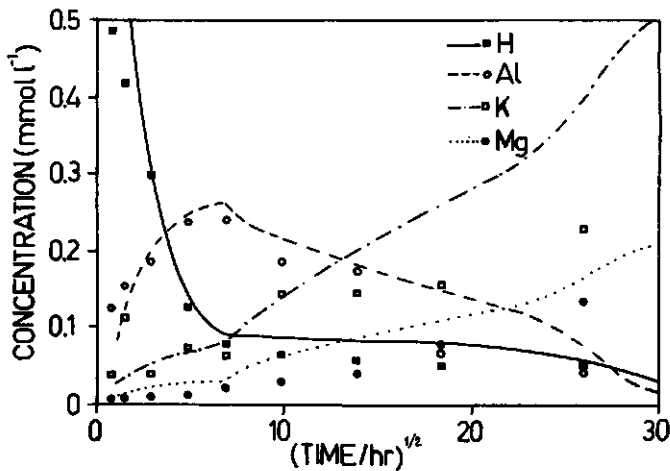


Fig. 6.4 Simulated and measured concentrations for experiment I, assuming congruent dissolution of illite until saturation with gibbsite ($\log(K_{so}) = 8.40$) occurs at 47 h. Before 47 h, illite dissolution rates are a function of the degree of saturation with respect to illite. After 47 h illite dissolution rates are assumed constant.

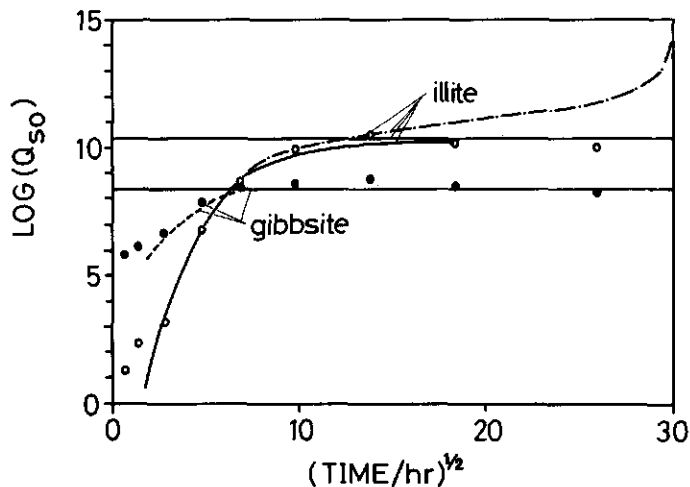


Fig. 6.5 Simulated and observed ion activity products (Q_{50}) for illite and gibbsite. After saturation with gibbsite, Q_{50} for illite is calculated assuming the illite dissolution rate to be a function of Q_{50} (—) or to remain constant (---).

6.3.4 Dissolution kinetics in experiment II

Only the final composition of the batches in experiment II was available. The overall reaction stoichiometry of the stationary pH titrations, i.e. H:Al:Mg was -10.8:2.5:0.25 and is close to illite stoichiometry. Stationary pH titrations were intended to establish a simple relationship between (H^+) and r far from equilibrium:

$$r = K' (H^+)^s. \tag{6}$$

As effects of ANC are not considered in Equation (6), r values for H were compared at ANC fixed at 12.5, 17.5, 22.5 and 27.5 mmol.kg⁻¹. Linear regression on the logarithmic form of Equation (6) gave 0.8 for s (correlation coefficient 0.95). For experiment I, using r values from H, Al and Mg, a value of 2.4 (correlation coefficient 0.76) was found. Disagreement between both s values most likely is caused by not considering effects of ANC, amounting to 3 mmol.kg⁻¹ in experiment I and to 40 mmol.kg⁻¹ in experiment II, or to artifacts from comparing a shaken to a stirred batch experiment.

6.3.5 Comparison of H^+ consumption rates for the surface soil and the subsoil in experiment III

Figure 6.6 shows H^+ consumption per batch experiment as a function of the number of times the acid solution was replaced. At the same time the effect of reaction time per batch experiment is illustrated.

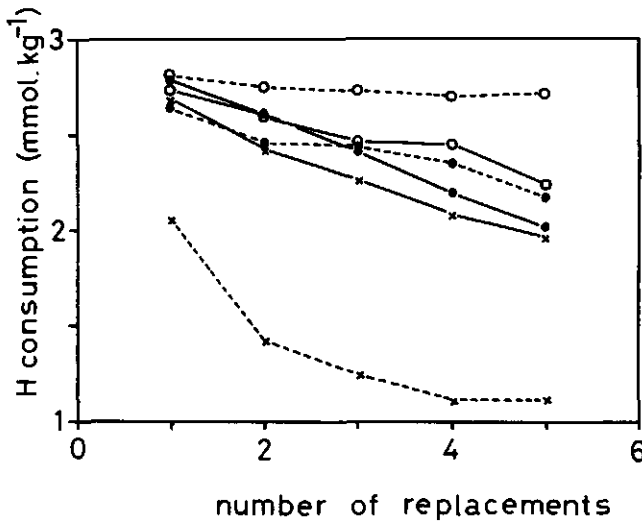


Fig. 6.6 The consumption of protons within one batch (10 g of soil and 30 mL of solution) as a function of the number of times the solution is replaced by a fresh acid solution (0.5 mmol/L HNO_3 and 0.25 mmol/L H_2SO_4) for the surface soil (—) and the subsoil (---), equilibrating for 1 h (x), 1 d (●) and 7 d (○).

In all cases H^+ consumption within one batch decreases with increasing number of acid solution replacements, but the effect is most clear in the subsoil for the shortest reaction time. This cannot be explained by Equation (4) as undersaturation and (H^+) tend to increase with repeated acid additions. More likely decreased H^+ consumption rates are a result of a decreasing ANC. The decrease of H^+ consumption rates with decreasing reaction time and increasing number of replacements is smallest in the surface soil, because here the main neutralizing process will be fast exchange of base cations. Observations for the subsoil for 1 hr reaction time, might agree with diffusion type dissolution mechanisms (Busenberg and Clemency, 1976): A step change in acid input and the resulting drop of pH will cause an extension of the diffusion layer, which will be expressed in a peak increase of r_i . Proton consumption in the surface soil

was largely balanced by mobilization of base cations and in the subsoil by dissolution of Al. Total H^+ consumption after 5 solution replacements in the surface soil is $12.5 \text{ mmol.kg}^{-1}$, which corresponds to 112% of the exchangeable bases. As a result it can be expected that during the last acid additions H^+ consumption due to mineral dissolution will also be important in the surface soil. This seems to be reflected by the observation that for a reaction time of 1 week H^+ consumption in the subsoil becomes increasingly higher than in the surface soil possibly due to higher mineral dissolution rates. It should be noted that ANC for the surface soil is 16% lower than for the subsoil. As parent material for the surface soil and the subsoil is similar this might indicate removal of reactive silicate minerals from the surface soil.

6.4 CONCLUSIONS

For a full description of mineral dissolution in acid soils we need to consider effects of saturation with respects to the dissolving minerals in addition to effects of a decreasing ANC. Experiment I and II clearly illustrate that the dissolution rate is very sensitive to small changes of ANC, which does not seem to be caused by exhaustion of a specific reactive mineral but more likely by a fast decrease of reactive spots such as dislocations and etch pits (Lasaga, 1983) on the mineral surfaces.

ACKNOWLEDGEMENTS

This research was supported in part by the Netherlands Directorate General for Science.

This chapter is published in *Water, Air and Soil Pollution* 31: p. 981-990, 1986.
J.J.M. van Grinsven, G.D.R. Kloeg and W.H. van Riemsdijk

Chapter 7

WEATHERING KINETICS IN ACID SANDY SOILS FROM COLUMN EXPERIMENTS

I. ALUMINUM

ABSTRACT

A new method was developed to measure weathering rates in small, packed soil columns in a controlled chemical environment. Cumulative leaching was described with a simple three-parameter model, facilitating interpolation and extrapolation of experimental data. Dissolution of Al was the main buffering process in samples from two acid forest soils, viz. a Dystrochrept and an Udipsamment. Leached Al was correlated with the contents of "free" Al-oxides, which consists mainly of hydrated oxides of Al. The importance of dissolution of Al-oxides was also indicated by the effect of temperature on the solubility and dissolution rate of Al. Dissolution rates of Al decreased exponentially with Al depletion from the soil sample (mol/kg) and on average increased with $(H^+)^{0.7}$. Depletion of reactive Al-oxides in forest soils as a result of acid atmospheric deposition may be a future environmental problem.

7.1 INTRODUCTION

Knowledge about rates of mineral weathering is crucial for the evaluation of the long-term response of extensively managed soil-vegetation systems to changing environmental factors (Cronan, 1985; Velbel, 1986). Dissolution of Al is the main process for buffering acid atmospheric deposition in large areas of acid forest soils (David and Driscoll, 1984; Mulder et al., 1987). Increased ionic concentrations of Al in soil solution due to acid atmospheric deposition may have adverse effects on soil biology and on tree vitality (Andersson and Kelly, 1984). In the absence of proton buffering by dissolution of Al, pH values could drop as low as 2.5 in western and central Europe (Hoeks, 1983).

Geochemical simulation models are useful to analyze the behaviour of soil-vegetation systems under changing environmental factors (Goldstein et al., 1984; Cosby et al., 1985^a; Chapter 11: Grinsven et al., 1987). Dissolution of Al is a key process in computer models simulating soil acidification. Many models assume equilibrium between soil solution and gibbsite (Christophersen and Wright 1981; Cosby et al; 1985^a). Near equilibrium with Gibbsite is indeed typical

for surface water, groundwater and soil water below the root zone, in areas with low to moderate levels of acid atmospheric deposition, but not for surface soils or under high levels of acid atmospheric deposition (Mulder et al., 1987). In organic soil horizons, the absence of equilibrium with gibbsite may be caused by equilibrium of Al concentrations with a humic adsorbent (Cronan et al., 1986). Distinction between equilibrium with a humic adsorbent and kinetic constraints on Al dissolution from gibbsite is difficult, not in the least because hydrated oxides of Al in soils very likely will be associated with organic substances (Kwong and Huang, 1979). Kinetic data for dissolution of Al from laboratory experiments (May et al., 1981, Stumm et al., 1985; Bloom and Erich 1987) often apply to commercial $\text{Al}(\text{OH})_3$ and rarely to aluminum in soil. An adequate model for dissolution of soil-Al should describe the effects of pH, mineral saturation, temperature and depletion of pools of reactive Al, and should relate these pools of reactive Al to determinable fractions of Al in soil. In addition, the nature of the anion may strongly influence the Al dissolution rate (Bloom and Erich, 1987). In Chapter 5 (Van Grinsven and Van Riemsdijk, 1988) an important effect of stirring on the dissolution rates of aluminum was demonstrated. Minimal sample disturbance and maximum control on solution chemistry are requirements for reliable measurements of dissolution rates of Al in soil material in the laboratory. This paper describes a new percolation method which meets these prerequisites, and provides part of the necessary data to built an adequate model for dissolution of Al in soil.

7.2 MATERIAL AND METHODS

7.2.1 Soil samples and chemical analysis

The soil samples used came from two sandy acid forest soils: an Umbric Dystrochrept (Van Breemen et al., 1986) and a Typic Udipsamment (Mulder et al., 1988). For the Dystrochrept, samples were taken from the A- (5 to 10), B- (20 to 30) and C-horizon (70 to 80 cm depth), for the Udipsamment samples from the A- (0.5 to 25) and C-horizon (100 to 125 cm depth). Soil samples were sieved over 2 mm mesh to remove stones and roots. Samples of the Dystrochrept were freeze-dried before storage. Freeze-drying was preferred soil material that was loamy or rich in organics to prevent formation of soil lumps which would require subsequent grinding. The sandy samples of the Udipsamment were air-dried.

| DYSTROCHREPT: UDIPSAMENT: | | D-A) 5-10, D-B) 20-30, D-C) 70-80 cm depth. U-A) 0.5-25, U-C) 100-125 cm depth. | | | | |
|------------------------------|-------------|--|------|------|-----------------|------|
| | | D-A | D-B | D-C | U-A | U-C |
| Particle size fraction (µm) | | Particle size distribution: (mass fraction %) | | | | |
| <2 | | 8.1 | 6.6 | 2.3 | 1.1 | 0.7 |
| 2-50 | | 12.7 | 12.7 | 1.1 | 1.4 | 1.4 |
| 50-150 | | 23.0 | 23.4 | 34.0 | 43.0 | 43.8 |
| 150-300 | | 30.1 | 29.7 | 46.5 | 50.0 | 46.8 |
| 300-420 | | 18.7 | 19.3 | 8.3 | 3.2 | 5.2 |
| 420-2000 | | 7.4 | 8.2 | 7.9 | 1.2 | 2.4 |
| | | Total Al ₂ O ₃ Contents analysis: (mass fraction %) | | | | |
| <2 | | 16.2 | 18.2 | 20.6 | -- ¹ | -- |
| 50-150 | | 2.83 | 3.13 | 6.55 | 3.09 | 3.21 |
| 150-300 | | 1.79 | 1.99 | 4.93 | 1.98 | 1.96 |
| 300-420 | | 0.80 | 0.85 | 1.55 | -- | 1.16 |
| <2000 | | 2.87 | 3.45 | 3.47 | 2.33 | 2.34 |
| | | Free Al ₂ O ₃ | | | | |
| <2000 | | 0.39 | 0.76 | 0.12 | 0.17 | 0.29 |
| | | Exchange complex (mmol _c /kg of fine earth) | | | | |
| Al | | 31 | 11 | 10 | 18 | 1 |
| H | | 52 | 16 | 3 | 30 | 4 |
| Base Cations | | 6.6 | 0.2 | 0.2 | 4 | <0.1 |
| Sum | | 89.6 | 27.2 | 13.2 | 52 | 5 |
| | | Recirculation Extracts (µmol _c /L) | | | | |
| Al | Anal. Error | 217. | 126. | 10. | 241. | 69. |
| H | | 197. | 27. | 14. | 62. | 17. |
| K | 0.2 | 53. | 9.8 | 6.6 | 22. | 8.5 |
| Na | 1.1 | 30. | 5.8 | 56. | 77. | 84. |
| Ca | 0.7 | 89. | 15. | 7.8 | 37. | 13. |
| Mg | 0.5 | 59. | 5.3 | 1.2 | 29. | 2.0 |
| | | Field soil solution (µmol _c /L) | | | | |
| Depth: (cm) | | 10 | 20 | 75 | 40 | 100 |
| Al | | 520 | 970 | 1830 | 1130 | 1520 |
| H | | 510 | 520 | 100 | 80 | 70 |
| Base Cations | | 1110 | 1290 | 995 | 850 | 780 |

¹ Not available.

Table 7.1 Chemical and physical characteristics of used soil samples and solutions.

Elemental analyses were carried out by X-ray fluorescence spectrometry; the cation exchange complex was analyzed by an adapted unbuffered BaCl_2 extraction (Bascomb, 1964); free Al-oxides were determined by oxalate-dithionite extraction (Begheijn, 1980). The average field soil solution chemistry is based on monthly, water-flux-weighted concentrations in samples, extracted by means of ceramic cups (Van Breemen et al., 1987).

Chemical and texture characteristics of the soil samples are given in Table 7.1. Free Al-oxides occur in distinctly higher concentrations in samples of the B-material of the Dystrochrept than in other samples. CEC values are highest in the surface soils due to relatively high contents of organic material. Base saturation is extremely low. The pH values of the field soil solutions vary between 3.3 in the surface soil of the Dystrochrept and 4.2 in the Udipsamment. Al is the dominating cation.

Percolates from the column experiments were acidified before storage at room temperature. K, Na, Cs, Ca and Mg were analyzed by atomic absorption spectrometry, Al and Si by inductive coupled plasma emission spectrometry.

7.2.2 Column percolation at constant pH

A new method was developed to study mineral weathering in a controlled chemical environment. Small columns of packed soil (20 cm^3) were percolated while maintaining a constant pH in the outflow, by adjusting the flow rate. So in fact, the proton supply was varied in proportion to the varying buffer rate. The difference between input and output proton concentration was about $200 \mu\text{mol/L}$, corresponding to 0.05-0.5 pH units. Percolation was continued until the flow rate became constant, or dropped lower than 50 mL/d and flow control became inaccurate. Most experiments lasted for about 3 d, but some experiments were continued up to 10 d. The total volume of solution passing the column varied between 1 and 15 L.

The composition of the input solutions for most column experiments was that of a recirculation extract (Table 7.1). This extract was obtained by recirculating demineralized water through a prewashed soil column for two days. Chemical analysis of these extracts indicated small anion deficits, probably caused by the presence of organic anions. These anion deficits were compensated for by adding Cl. In the actual percolation experiments the pH was varied between 2.5 and 4.8 by adding HCl. Concentrations for H, K, Na, Ca, Mg and all anions in the input solutions were higher than the observed concentration changes after column passage. Variation of the chemical composition of the pore water along

the length of the column generally was less than 50%, as compared to nearly infinite variation if zero input concentration are used. Finite input concentrations were used to minimize contributions of exchange processes and chromatography, and to prevent extremely low degrees of mineral saturation (Chapter 6: Van Grinsven et al., 1986). Yet, concentrations in the recirculation extracts were far lower than in soil solution under field conditions (Table 7.1). The extracts were generally strongly undersaturated with respect to all relevant minerals (Table 7.2), except for kaolinite and gibbsite in the solution for the C-material of the Udipsamment and for gibbsite for the B-material of the Dystrochrept.

The experimental setup is illustrated in Figure 7.1.

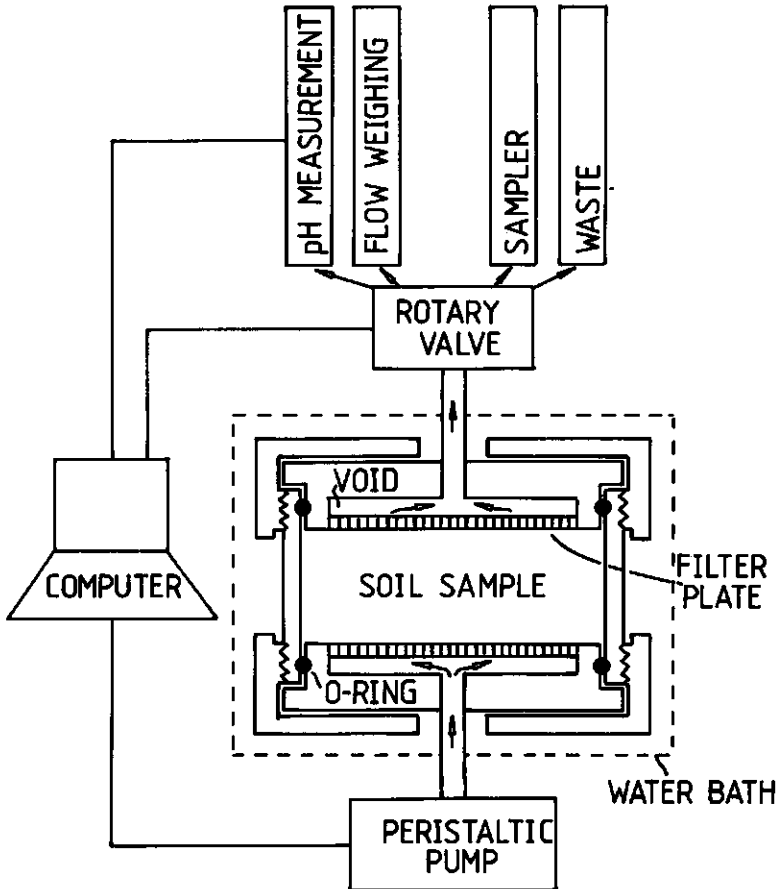


Fig. 7.1 Schematic overview of experimental setup for column experiments at constant pH.

Soil columns were 5 cm in diameter and approximately 1 cm high. Columns were filled with a water-saturated slurry. Loamy soil samples or samples rich in organics were mixed with inert coarse (50 μm) quartz sand to increase the hydraulic conductivity. The total core mass was 40 g. The soil core was enclosed between hollow glass filter plates (Figure 7.1) to facilitate homogeneous throughflow. Flow was upward and the filter plates were covered by a 0.45 μm filter to prevent loss of fine particles. Homogeneous throughflow was confirmed by means of breakthrough experiments with concentrated KCl using a conductivity electrode for detection of the breakthrough. The flow was varied by means of a computer-controlled Watson & Marlow 202U peristaltic pump. Soil columns were permanently water saturated but did not become anaerobic. The outflow pH was measured continuously by means of a Ingold continuous flow cell. Outflow was sampled by a ISCO (type Foxy) automatic sampler, which was stored in a plastic box, where air was kept near 100% humidity to minimize sample evaporation. The flow rate was measured continuously and independently from the pump setting by means of weighing using a Mettler PE360 balance. The soil columns were submerged in a water bath of 10 $^{\circ}\text{C}$, unless stated otherwise. The fate of the outflow was regulated by means of Cheminert rotary valves. All operations and datalogging were performed by an Apple IIe computer (programmed in BASIC), which could control four columns simultaneously.

All experiments were carried out in duplicate and accompanied by one unacidified column subject to the same flow programme. In addition experiments were carried out at pH 3 with CsCl solutions of identical ionic strength as the equilibrium solutions. CsCl was applied to check the effect of background concentrations in the input solutions on the analytical detection of the concentration increases of K, Na, Ca and Mg in the outflow, and on dissolution kinetics. The effect of temperature was studied in soil samples from the B-horizon of the Dystrochrept varying temperature between 5 and 25 $^{\circ}\text{C}$. The effect of pH and the degree of mineral saturation with $\text{Al}(\text{OH})_3$ on dissolution of Al were studied for samples from the C-horizon of the Dystrochrept by variation of pH and Al concentration simultaneously while maintaining a constant activity product with respect to $\text{Al}(\text{OH})_3$.

7.2.3 Unstirred batch experiments

Column titrations for the B- and C-material of the Dystrochrept were continued in batch, after buffer rates had decreased to such a low level that automatic flow adjustment became superfluous. The soil residues were transferred to plastic containers with a diameter of 10 cm, and 150 mL of acidified equilibrium solution was added. When the $[H^+]$ had decreased by about 200 $\mu\text{mol/L}$, 100 mL of the batch solution was sampled and replaced by a fresh solution.

7.2.4 The empirical model

Cumulative component output from the column as a function of time was fitted by means of an empirical three parameter model:

$$X = \frac{P_1 t}{P_2 + t} + P_3 t \quad (1)$$

where: X is cumulative production (mmol_c/kg , the subscript c indicating charge equivalents, t is time (d) and P_1 , P_2 and P_3 are parameters. The main purpose of the empirical model was to summarize, interpolate and extrapolate the experimental data. P_1 can be interpreted as the non-linear dissolution capacity (mmol_c/kg), which is the sum of salt displacement, cation exchange and amounts of very (possibly artificially) reactive material. P_2 refers to the half-life time of this non-linear pool (d). P_3 can be interpreted as the long-term weathering rate constant ($\text{mmol}_c.\text{kg}^{-1}.\text{d}^{-1}$), which is assumed to remain unaffected by depletion effects in the course of the experiment. The model was fitted to experimental data by means of a non-linear optimization programme based on the Levenberg-Marquardt method (Press et al., 1986).

The first derivative of equation (2) gives the dissolution rate:

$$R = \frac{dX}{dt} = \frac{P_1 P_2}{(t + P_2)^2} + P_3 \quad (2)$$

where R is the dissolution rate ($\text{mmol}_c.\text{kg}^{-1}.\text{d}^{-1}$). For large values of t, R converges to P_3 . Ideally experiments continue until R is practically equal to P_3 .

7.3 RESULTS AND DISCUSSION

7.3.1 General features of the experiments

Figure 7.2 summarizes some general features of the results of a percolation experiment at controlled pH using material of the C-horizon of the Dystrochrept.

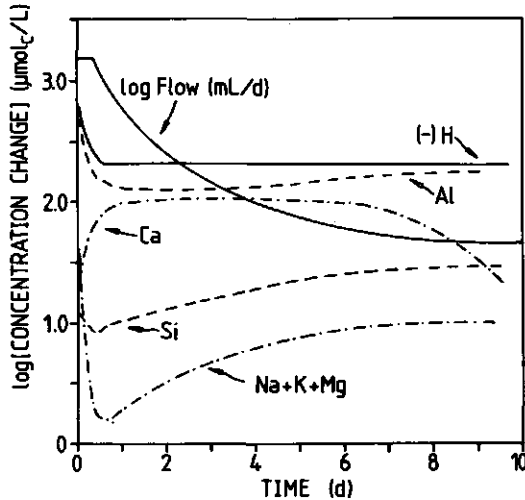


Fig. 7.2 Example of flow rate and concentration changes of H, Al, (K + Na + Mg) and of Ca in percolates from a column experiment at pH 3 for the D-C sample.

In the first few hours to one day, the pH in the outflow could not be controlled because the maximum possible flow rate was insufficient to meet the buffer rate of the soil column. In all soil samples dissolution of Al was the main process buffering the added H^+ . The concentration increase of the base cations (K, Na, Ca and Mg) generally was 1 to 2 orders of magnitude lower than that of Al. Concentrations of base cations and Si decreased very rapidly during the first pore volume replacements, primarily due to salt displacement and cation exchange, and remained constant or increased afterwards. Weathering rates were calculated as the product of flow rate and concentration change, so we implicitly assumed that weathering rate was independent of flow. Berner (1978) stated that weathering rates are independent of flow rate when reaction rates are not limited by diffusion transport and when solutions are strongly

undersaturated with respect to the dissolving minerals. In the acidified experiments solutions were indeed strongly undersaturated with respect to the feldspars, Al-oxides and clay minerals (Table 7.2).

| DEPTH (cm) | DYSTROCHREPT | | | UDIPSAMMENT | |
|-------------------------------|--------------|--------|--------|-------------|---------|
| | 5-10 | 20-30 | 70-80 | 0.5-25 | 100-125 |
| Synthetic Gibbsite | -7.83 | -2.06 | -6.38 | -4.50 | -0.55 |
| Natural Gibbsite | -8.49 | -2.72 | -7.04 | -5.16 | -1.21 |
| Amorphous Al(OH) ₃ | -10.52 | -4.75 | -9.07 | -7.19 | -3.24 |
| Microcline | -11.46 | -5.56 | -9.52 | -8.25 | -3.25 |
| Albite | -15.86 | -7.50 | -11.12 | -10.90 | -4.69 |
| Anortite | -31.01 | -17.55 | -24.98 | -23.70 | -12.69 |
| Kaolinite | -13.16 | -1.61 | -10.20 | -6.52 | 1.42 |
| Illite | -21.34 | -7.66 | -17.37 | -13.58 | -3.27 |

Table 7.2 Saturation indices with respect to relevant minerals after recirculating (originally) demineralized water through a column for 2 d.

The release of Ca from the sample of the C-horizon of the Dystrochrept was much higher than the release of the other base cations and than the release of Ca from the other samples. Experimental evidence was found for an anomalous weathering mechanism for Ca in U-C sample, which is discussed elsewhere (Chapter 9: Van Grinsven et al., 1988^d).

7.3.2 Weathering stoichiometry

Dissolution of Al was the dominant buffering process in all samples except D-C (Table 7.2). The release of Fe and Mn was negligible indicating that aerobic conditions were maintained throughout the experiment. The release of Al from the D-C, U-A and U-C samples exceeded proton consumption, indicating that part of the aqueous Al had a lower than trivalent charge, and so was complexated or colloidal (Mulder et al., 1987). In the U-A sample proton buffering exceeded cation release, possibly as a result of protonation of organic groups. The release of base cations and of silica were too low to be explained by either congruent dissolution of aluminosilicates. Precipitation of Si in the column was unlikely because column percolates were undersaturated with respect to quartz, with concentrations of Si ranging from 20 to 50 $\mu\text{mol/L}$. The release of Al by cation exchange reactions cannot explain the low Si/Al ratios, because near the end of

the column experiments solution composition was constant, suppressing exchange reactions. Apparently Al-oxides and -hydroxides are the main sources of soluble Al.

7.3.3 Experimental artifacts

In Chapter 5 (Van Grinsven and Van Riemsdijk, 1988) it was shown that after our sample pretreatments the dissolution rate of Al may be temporarily increased slightly, but that the overall effect on the kinetics of Al dissolution is minor. The dissolution rates of Al at the end of the column experiments were 5 to 20 times higher than rates during the consequent unstirred batch experiments for D-B and The D-C sample (Table 7.3).

| Sample | Al | Base Cations (mol _e) | Total Cations | Si | Estim. Si (mol) |
|--------|------|-------------------------------------|---------------|-----------------|--------------------|
| D-A | 5.7 | 0.9 | 6.5 | -- ¹ | 1.7 |
| D-B | 9.1 | 0.1 | 9.2 | 0.3 | 0.2 |
| D-C | 7.5 | 5.1 | 12.5 | 1.2 | 10.1 |
| U-A | 12.3 | 0.5 | 12.7 | -- | 0.9 |
| U-C | 12.4 | 0.3 | 12.7 | 1.5 | 0.5 |

¹ Not available

Table 7.3 Release of Al, base cations and Si in column experiments per 10 moles of protons consumed at pH 3 and averaged over the five last percolate samples.

Mechanical disturbance of the mineral surfaces during the experiments will strongly enhance the release of Al from soil (Chapter 5: Van Grinsven and Van Riemsdijk, 1988) but this effect should be negligible for both the column experiments and the unstirred batch experiments. Dissolution rates for Al in the unstirred batch experiment more likely will be limited by diffusion transport, as suggested earlier in Chapter 5 (Van Grinsven and Van Riemsdijk, 1988). The effectiveness of diffusion to homogenize the 2 cm thick stagnant water layer on top of the sediment was checked by applying the steady-state diffusion equation:

$$q_D = \frac{A D \Delta C}{d} \quad (3)$$

where q_D is the diffusion flux (mol/s), A is the area of the cross-section of the interface between solution and sediment (79 cm^2), D is the ion diffusion coefficient in water ($10^{-5} \text{ cm}^2/\text{s}$), ΔC is the concentration difference between bulk solution and interstitial water (mol/cm^3) and d is the diffusion distance (cm). The maximum proton flux across the stagnant water layer at a solution pH of 3, assuming a pH of 4 in the interstitial water, is $4 \times 10^{-10} \text{ mol/s}$. The proton consumption rates associated with the final dissolution rates of Al for the D-B and D-C sample in the column experiments, recalculated to the solid content (16.5 g) of the batch experiment, were $15 \times$ and $1 \times 10^{-10} \text{ mol/s}$; rates at the start of the batch experiment were $2.6 \times$ and $0.6 \times 10^{-10} \text{ mol/s}$ respectively (Table 7.3). Apparently, dissolution rates of Al in the column experiments with the D-B sample were limited by diffusion transport after transfer of the soil samples to the unstirred batch system. The overall rate of Al-release from the soil samples in the field, determined from elemental budgets (Mulder et al., 1987), and adjusted to a pH value of 3 using pH-dependent data from Bloom and Erich (1987), is about 300 times lower than for the D-B sample in the column experiment. In the field Al is released mainly from the A- and the B-horizon, where soil solutions are strongly undersaturated with respect to gibbsite (Mulder et al., 1987). Differences in rates of Al-release between column and field for the D-B sample are of similar magnitude as differences in flow rates between column (40 cm/d) and field (0.2 cm/d), also indicating that dissolution of Al in the field is limited by diffusion transport. Another factor that may cause higher rates of Al-release in the experiments than in the field may be more efficient contact between solution and solids under experimental conditions. Furthermore, the external proton supply will limit rates of Al release in the field.

| Sample | Column | Batch | Field | Column | Batch | Gibbsite |
|--------|--|-------|-------|---|-------|--|
| | "Soil" ($\text{mol} \cdot \text{kg}^{-1} \cdot \text{s}^{-1} \times 10^{10}$) | | | "Al(OH) ₃ " ($\text{mol} \cdot \text{m}^{-2} \cdot \text{s}^{-1} \times 10^{11}$) | | |
| D-B | 300 | 52 | 1 | 35 | 3 | 3 (SO ₄) 0.1 (NO ₃) |
| D-C | 20 | 12 | | 15 | 7 | |

Table 7.4 Rates of Al-release ($\text{kg}^{-1} \text{ soil}$) from the D-B and D-C sample, as observed in column and batch experiments, and as calculated from elemental field budgets. For comparison the dissolution rates ($\text{m}^{-2} \text{ Al(OH)}_3$) of gibbsite (Bloom and Erich, 1987) at pH 3 and 10 °C have been given.

Dissolution rates for the D-B and D-C sample, converted to dissolution of free Al-oxides (Table 7.1) with an assumed specific surface area of $7.7 \text{ m}^2/\text{g}$ (Bloom and Erich, 1987), are similar, but considerably higher than dissolution rates of commercial gibbsite (Bloom and Erich, 1987) (Table 7.4). This approximate comparison suggests that the reactivity of Al-oxides in different soil layers is similar. Apparently Al-oxides in soil are more amorphous or have a higher specific surface area than commercial gibbsite.

7.3.4 Application of the empirical model.

Figure 7.3 shows the cumulative dissolution of Al and K for the U-C sample at pH 3.

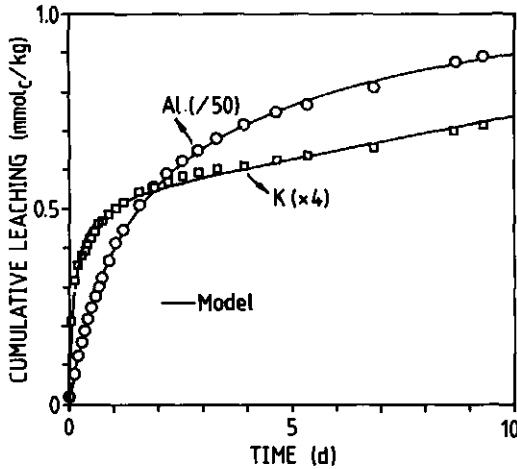


Fig. 7.3 Cumulative leaching of Al and K from the U-C sample in a column experiment at pH 3. Symbols are data points, lines fit the data according to the empirical model.

The empirical model invariably fitted the experimental data very well. Standard errors of estimate (SEE) for P_1 , P_2 and P_3 for H and Al rarely exceeded 10%. For the base cations, values of SEE for P_2 and P_3 near 100% were common. To compare different experiments, calculated values for X (Equation 1) were used, rather than individual values of P_1 and P_2 , because parameter values depended on the duration of the experiments.

Values of P_1 reflect the magnitude of reactive pools for weatherable cations. Values of P_1 for Al ranged from 10 to 100 mmol_c/kg, which is about 15% of the contents of oxalate-dithionite extractable Al (Table 7.1). Values of P_1 for the base cations ranged from 1 to 5 mmol_c/kg, which, at least in the surface horizons, were comparable to amounts of exchangeable base cations.

Values of P_2 for H, Al and Si, representing the half-life time of the non-linear dissolution stage, ranged from several hours to almost one day. Values of P_2 for K, Na, Ca and Mg, on the other hand, generally were below 30 min. Only for the U-A and D-B sample the rate of Al-release became constant during the experiment, as indicated by a larger linear dissolution rate than non-linear dissolution rate (Figure 7.4).

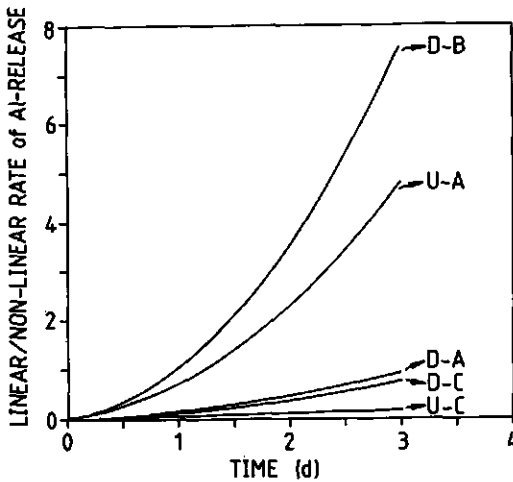


Fig. 7.4 Predicted increase of the ratio of linear release of Al over non-linear release of Al with time for all soil samples at pH 3.

Distinction between a linear and a non-linear stage of Al-dissolution in short-lasting experiments is rather arbitrary, because only a small part of the "non-linear" pools of Al is exhausted during the experiment, and dissolution of Al from "linear" pools in silicate minerals is negligible.

7.3.5 Effects of pH and depletion on the Al dissolution rate

In all soil samples, the dissolution rates of Al decreased strongly with the progress of the experiment. This decrease was nearly exponentially related to cumulative Al-leaching, as demonstrated for pH 3 in Figure 7.5.

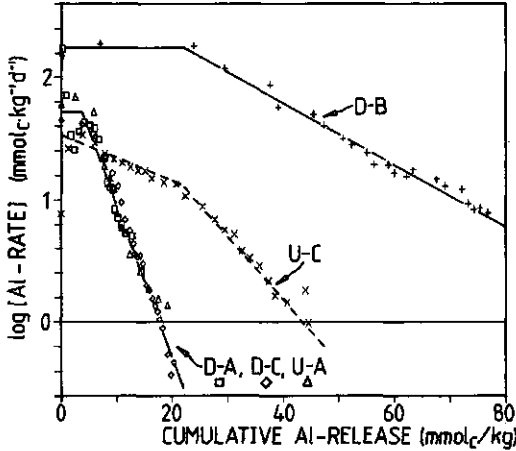


Fig. 7.5 Logarithmic decrease of the dissolution rate of Al with increasing depletion in column experiments at pH 3 for all soil samples.

Initially, rates decreased less strongly because of a simultaneous decrease of pH during percolation at the maximum possible flow rate (Figure 7.2). Dissolution rates for the B-material of the Dystrochrept and the C-material of the Udipsamment were distinctly higher than for the other samples. The dissolution kinetics of Al for the A- and C-horizon of the Dystrochrept and the A-horizon of the Udipsamment were very similar.

The non-linear dissolution capacity (P_1 ; Equation 1) increased with decreasing pH (Figure 7.6), but reached a maximum value between pH 2.9 and 3.4 for all soil samples. The dissolution rates of Al at a fixed reaction time within the non-linear dissolution stage also exhibited a maximum value between pH 2.9 and 3.4, as is predicted by Equation 2 for $t < P_2$. The observation of a maximum Al dissolution rate within the non-linear dissolution stage can be explained by the surface protonation concept (Stumm et al., 1985), which states that the mineral dissolution rate increases with the concentration of adsorbed protons

on the mineral surface. The adsorbed proton concentration for gibbsite reaches a maximum around pH 3.5 (Stumm et al., 1985).

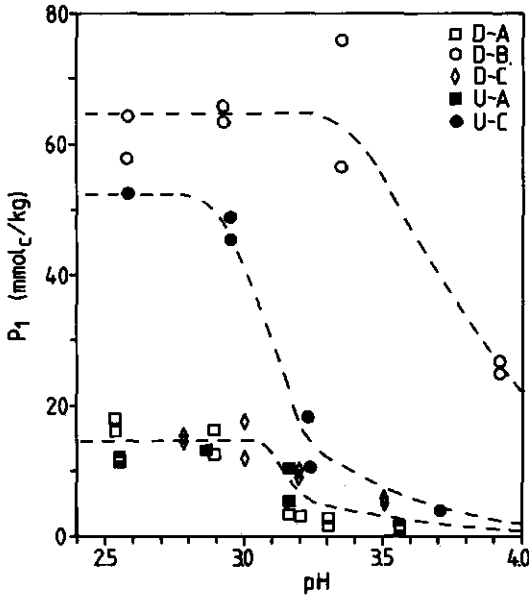


Fig. 7.6 The relationship between the non-linear dissolution capacity for Al, represented by P1 in the empirical model, and pH, for all soil samples.

The observation of a maximum dissolution rate of Al with decreasing pH may be fortuitous, because the effect of high concentrations of adsorbed protons is counteracted by faster depletion of the reactive pools of Al at low pH. The effect of depletion can be eliminated by plotting the Al dissolution rate against pH for the half-life time (P2) instead of a fixed reaction time (Figure 7.7). P2 may be considered a measure of reaction progress and depletion of Al pools. After elimination of the depletion effect no maximum dissolution rate of Al is observed. Instead, the logarithm of the Al dissolution rates for the individual soil samples seem to follow a linear relationship with pH which was also reported by Aagaard and Helgeson (1984) and Stumm and Furrer (1986):

$$\log(R_{Al}) = K + q \text{ pH} \quad (4)$$

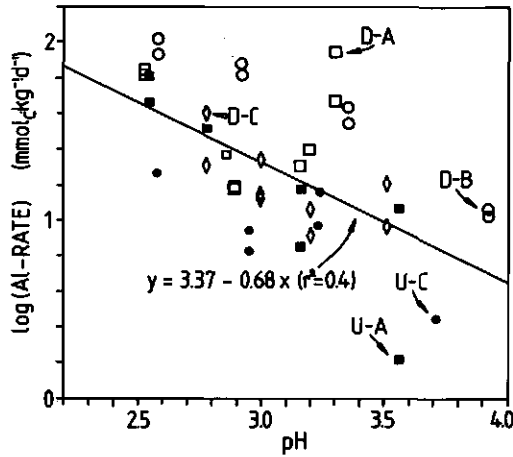


Fig. 7.7 The relationship between the dissolution rate of Al and pH at time P₂ for all soil samples, where P₂ represents a fixed degree of Al depletion of the non-linear pool.

where R_{Al} is the dissolution rate of Al, K is a constant and q is the slope. The average value of q for all samples but D-A (Figure 7.7) is -0.68 ($r^2 = 0.40$). This is in between the value of -0.4 reported by Stumm and Furrer (1986), and -1 found by Bloom and Erich (1987). Regression analysis for individual samples gave values of q between -0.5 (D-C) and -1.2 (U-A), and correlation coefficients between 0.43 (D-C) and 0.96 (D-B). Dissolution rates in the column experiments without acid addition were negligible. The rate data for the A-horizon of the Dystrochrept deviate somewhat, which may be due to the complex simultaneous action of Al-dissolution and -exchange.

7.3.6 Effect of mineral saturation on dissolution rate of Al

The increase of the rate of Al dissolution with decreasing pH not necessarily implies that higher proton activities are the only factor involved. Decreased levels of mineral saturation with respect to $Al(OH)_3$ also could play a role. If the dissolution rate of Al would respond to the proton activity only, surface protonation would be rate limiting, if it would respond to the $Al(OH)_3$ -activity product (AP), detachment of the hydrolysed Al-complex would be the rate limiting step in dissolution of Al-(hydr)oxides (Stumm et al., 1985). In an additional experiment pH was lowered independent of $Al(OH)_3$ -AP by simultaneously

increasing the Al and the proton concentration, while maintaining a constant activity product: $AP = (Al^{3+})/(H^+)^3$.

In one column experiment with a D-C sample, $\log(AP)$ was maintained at a value of 6 while pH varied between 2.7 and 3.8. In a parallel experiment without Al addition, $\log(AP)$ varied between 2.8 and 5. In the first 0.5 d at constant high AP Al-release was only half of release at lower AP (Figure 7.8).

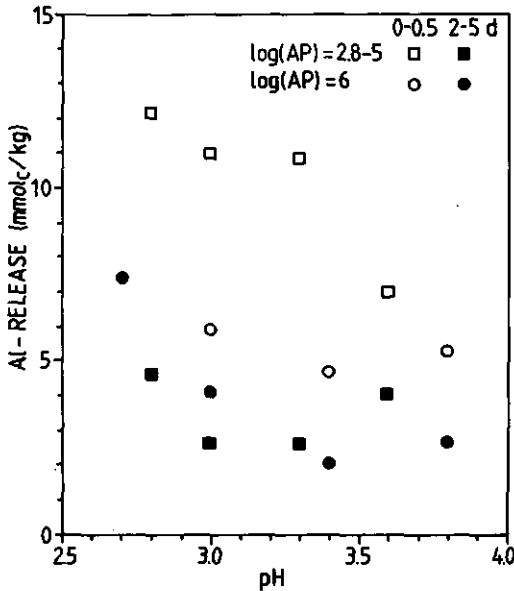


Fig. 7.8 The effect of pH on the dissolution of Al for the D-C sample, at constant ($\log AP = 6$) and variable $Al(OH)_3$ activity product.

However, from 0.5 d onwards the two experiments gave very similar Al-release. The difference in the first 0.5 d may be explained by less exchange of Al in the experiment with high AP and Al concentrations. Although the CEC of the C-horizon is small, the amount of exchangeable Al (Table 7.1) is sufficient to explain these differences in release of Al. So, we may conclude that the observed effect of pH on dissolution of Al from oxides is caused by the proton activity and not by effects of undersaturation. The AP will start to depress the dissolution rate when it approaches the AP value at equilibrium, as may be indicated by negligible dissolution of Al in the unacidified column experiments (Chapter 6: Van Grinsven et al., 1986; Velbel, 1986).

7.3.7 Pools of reactive Al

In the U-A sample exchangeable Al decreased by 16 mmol_e/kg, which is the larger part of the observed leaching of Al. Below a depth of 14 cm the fraction of easily soluble Al, represented by P₁, seems to be associated with the contents of hydrated Al-oxides rather than with exchangeable or total Al, as shown for the Dystrochrept in Table 7.5.

| Soil Depth (cm) | Exchangeable | Free Oxides (mmol _e /kg) | Total | P ₁ |
|--------------------|--------------|---|-------|-----------------|
| 2 | 27 | 280 | 1600 | 4 |
| 6 | 24 | 230 | 1700 | 21 |
| 14 | 15 | 370 | 2200 | 77 |
| 25 | 10 | 450 | 2000 | 65 |
| 35 | 7 | 450 | 2200 | -- ¹ |
| 44 | 7 | 420 | 2400 | -- |
| 54 | 4 | 180 | 2400 | -- |
| 80 | 1 | 71 | 1800 | 19 |

¹ Not Available.

Table 7.5 Pools of Al in the Dystrochrept soil profile and values of P₁ obtained from column experiments after percolation with CsCl at pH 3.

High dissolution rates in the samples for the B-horizon (8-48 cm depth) are reflected by high contents of free Al-oxides. Quantification of the decreases of the various pools of soil-Al before and after the experiments was rather inaccurate because analytical errors were of similar magnitude as the depletion itself, except for the D-B sample. For the D-B sample the decrease of dithionite extractable Al over the experiment at pH 3 was 63 ± 13 mmol_e/kg, while 77 mmol_e/kg was leached. The distinction between organic Al, amorphous oxides and crystalline oxides of Al in the free Al fraction of mineral soil horizons, by sequential extraction with pyrophosphate, oxalate and dithionite (McKeague et al., 1971) is not rigid. Separate extractions of the D-B sample showed higher amounts of Al extractable with 0.1 M pyrophosphate than with 0.2 M oxalate, which may demonstrate the ambiguous nature of the free Al fraction. The decrease of the exchangeable pools was negligible. Present pools of Al-oxides can be considered as the result of several millennia of incongruent weathering of primary aluminum silicates at pH values where Al(OH)₃ still was stable. The contents of free Al (Table 7.1) within the first 0.5 m of the studied soil profiles

corresponds to a buffer capacity between 100 to 300 kmol_c/ha. At present rates of soil acidification in these profiles near 6 kmol_c.ha⁻¹.yr⁻¹ (Van Breemen et al., 1987) pools of free Al will be depleted within the next decades, and may cause a drastic change of the buffering behaviour in acid sandy soils.

7.3.8 Effect of temperature

Column experiments were carried out between 5 and 25 °C, which is the temperature range observed in the field. Temperatures in the surface soil vary between 0 and 15 °C, quickly responding to changes in air temperature. In the subsoil temperatures are close to 10 °C and show little variation. Figure 7.9 shows the activity products for Al(OH)₃ in the percolates of unacidified column experiments between 5 and 25 °C for soil from the B-horizon of the Dystrochrept.

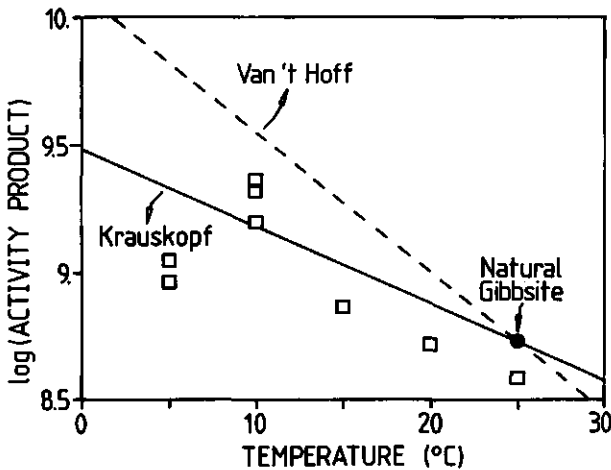


Fig. 7.9 The effect of temperature on the activity product for Al(OH)₃ after recirculation of (originally) demineralized water for 2 d through a column of the D-B sample, as compared to the theoretical effect on the dissolution constant for natural gibbsite.

The effect of temperature on the solubility constant of natural gibbsite ($\log(K_{so}) = 8.8$; Driscoll et al., 1986) can be described according to an empirical model (Equation 5; Krauskopf, 1967) or according to the classical "Van 't Hoff" formulation (Equation 6; Bolt and Bruggenwert, 1976).

$$\Delta F = \Delta H - 0.001 T \Delta S \tag{5}$$

$$\frac{d \ln(K)}{dT} = \frac{\Delta H}{R T^2} \tag{6}$$

where: ΔF is the free energy, ΔH is the reaction enthalpy, ΔS is the reaction entropy, T is absolute temperature and K is the equilibrium constant.

The value $10^{8.6}$ for the $Al(OH)_3$ activity product at 25 °C, and the fair agreement between the observed temperature dependence and that for gibbsite according to Equation 5 and 6, support control of Al-dissolution by an Al-hydroxide phase similar to natural gibbsite.

The effect of temperature on the release of Al is shown in Figure 7.10.

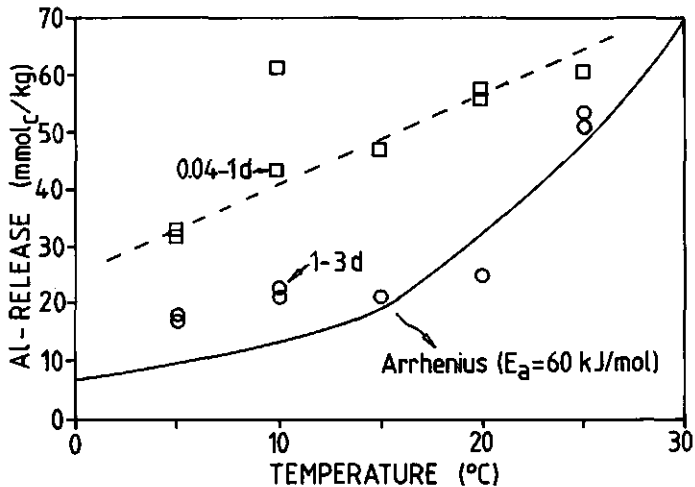


Fig. 7.10 The effect of temperature on the release of Al from the D-B sample upon percolation at pH 3, from 0.04 to 1 d, and from 1 to 3 d, as compared to the theoretical effect according to the Arrhenius model.

Cumulative release in the selected time intervals was calculated from the empirical model (Equation 1). From the first day onwards the increase of Al-release with temperature reasonably agrees with the Arrhenius model (Equation 7), assuming an activation energy of 60 kJ/mol (Bloom and Erich, 1987):

$$K = A \exp\left(-\frac{E_a}{RT}\right) \quad (7)$$

The effect of temperature on the release of Al during the first day is smaller, which may be due to a relatively important role of exchange reactions. The activation energy for exchange of Al may be expected to be lower than for dissolution of Al-oxides.

7.4 SUMMARY AND CONCLUSIONS

A new method was developed to measure weathering rates in small, packed soil columns in a controlled chemical environment. Cumulative leaching was well described with a simple, empirical three-parameter model, facilitating interpolation and extrapolation of experimental data. Samples from two acid forest soils were studied, from the A-, B-, and C-horizon of a Dystrichrept and the A- and C-horizon of a Udipsamment. Al dissolution was the main buffering process. Dissolution rates of Al were highest for the B-horizon of the Dystrichrept and the C-horizon of the Udipsamment, and were correlated with high contents of free Al-oxides. The importance of Al-oxides controlling Al-dissolution was further supported by the effect of temperature on the $\text{Al}(\text{OH})_3$ activity product and the dissolution rate Al. Dissolution rates of Al decreased exponentially with depletion and increased on average with $(\text{H}^+)^{0.7}$. Interpretation of kinetic data for Al is complicated because effects of pH and depletion occur simultaneously, which may result in apparent maximum Al-dissolution rates at decreasing pH. Depletion of the pool of hydrated Al-oxides, which at present is the main acid buffering process in acid forest soils, may be a future environmental problem if acid deposition continues at the present rate.

ACKNOWLEDGEMENTS

The authors wish to thank the Netherlands Energy Research Foundation (ECN), in particular Mr. R. Otjes and Dr. T. Lub, for their invaluable help during the development of the pH-stat column percolation technique, and for carrying out the actual experiments. Furthermore we wish to thank Hugo Denier van der Gon, who did the unstirred batch experiments as part his Msc-program, and E. Velthorst, L. Begheijn, and B. Kuiper for doing the analyses. Finally I am very grateful to Professor N. van Breemen of the Department of Soil Science and Geology and to Professor F.A.M. de Haan of Soil Science and Plant Nutrition for their indispensable guidance during the research and their critical evaluation of the manuscript.

A revised version of this chapter will be submitted to Soil Sci. Soc. Amer. J.
J.J.M. van Grinsven, W.H. van Riemsdijk and R. Otjes

Chapter 8

WEATHERING KINETICS IN ACID SANDY SOILS FROM COLUMN EXPERIMENTS

II. BASE CATIONS

ABSTRACT

Mineral weathering in samples from two acid forest soils, viz. a Dystrachrept and a Udipsamment, was studied by means of column and batch experiments at controlled pH. Dissolution of Al was the main buffering. Release of base cations in general was very low but detectable. Release of K, Ca and Mg from samples of the A-horizon was dominated by cation exchange and could be described by the Gaines-Thomas model. The Gaines-Thomas model did not fit concentration data of Al and H, presumably due to slow exchange. Weathering rates (m^2 mineral) of plagioclases were 10 to 20 times higher than of K-feldspar. Release of Mg generally was less than of other base cations, and appeared to be associated with the contents of micas and pyroboles, which were highest in the C-horizons. Weathering rates of base cations and Si, particularly Mg, increased with $(H^+)^p$, with p ranging from 0.5 to 1.4. Weathering rates of base cations and Si were up to two orders of magnitude higher than implied from field budget studies, while weathering rates in unstirred batch experiments were only slightly higher. These discrepancies cannot be the result of limiting diffusion transport but may be attributed to hydrodynamic effects of percolation rate on weathering rate. The hypothetical hydrodynamic effect is corroborated by an increase of weathering rates with increasing percolation rates in column experiments.

8.1 INTRODUCTION

Mineral weathering of K, Ca and Mg, is an essential source of plant nutrients in extensively managed soil-vegetation systems. Enhanced loss of K, Ca and Mg from both tropical and temperate forest soils, as a result of whole-tree harvesting, shifting cultivation and acid rain. Whole-tree harvesting involves a net export of nutrients (Paces, 1985). Acid rain will decrease the exchangeable pools (Halbäcken and Tamm, 1984) and cause net mineralization of cations when forest vitality declines (Van Breemen et al., 1987). Shifting cultivation carries the additional danger of erosion. Plant available pools of cations can be restored by mineral weathering, by atmospheric deposition, including deposition

of dust, and by fertilization (Miller, 1978). Fluxes of base cations in an ecosystem can be quantified by means of chemical budgets (Van Breemen et al., 1986, 1987; Nilson and Bergkvist, 1983; Pâces, 1985; Velbel, 1985). Chemical budgets are based on monitoring data on the chemistry of atmospheric water, soil solution, groundwater and surface water in combination with measurement or calculation of hydrologic fluxes over a period of several years (Chapter 3: Van Grinsven et al., 1987^b). The interpretation of such input-output budgets is complicated because several cation consuming and producing processes act simultaneously. To determine mineral weathering rates from budget studies the contribution of changes at the exchange complex and the net cation accumulation in biomass must be known. In most interpretations biomass and exchange sites are assumed to be in steady state, which is doubtful for periods of only few years (Velbel, 1986).

To analyze the behaviour of soil-vegetation systems under changing environmental factors geochemical simulation models are often used (Goldstein et al., 1984; Cosby et al., 1985^b; Chapter 11: Grinsven et al., 1987). The value of such analyses would improve when independent estimates were available for the key element fluxes, like mineral weathering rates, rates of mineralization of organic substances and cation exchange. For long-term prediction of soil acidification processes, relationships are needed between weathering rates of base cations, and pH and depletion of pools of base cations in soil.

The number of laboratory studies of mineral weathering is impressive (Helgeson et al., 1984; Velbel, 1986). These studies present relevant theories about mechanisms of mineral weathering, but contain little information regarding weathering rates useful for interpretation of chemical budgets. Weathering rates observed in the laboratory are generally one to two orders of magnitude higher than for mass balance studies (Velbel, 1985; 1986). Many factors have been proposed to explain this discrepancy including effects of sample pretreatment (Holdren and Speyer, 1985^b), overestimates of the reactive surface area (Pâces, 1983), hydrologic and hydrodynamic factors (Velbel, 1985) and biological factors (Eckhardt, 1985). In Chapter 5 (Van Grinsven and Van Riemsdijk, 1988) it was shown that there is a strong effect of stirring on the observed dissolution rates, especially for aluminum. Minimal sample pretreatment and maximum control on solution chemistry are prerequisites for reliable measurements of mineral weathering rates in soil material in the laboratory. A particular problem with soil materials is the low contents of reactive minerals in soil samples, and the relatively low solubility of these minerals. As a result long reaction times are needed to obtain detectable concentration changes from mineral weathering in soil samples.

8.2 MATERIAL AND METHODS

Soil samples were taken from two sandy acid forest soils: an Umbric Dystrochrept (Van Breemen et al., 1986) and a Typic Udipsamment (Mulder et al., 1988). For the Dystrochrept, samples were studied from the A- ("D-A"; 5 to 10), B- ("D-B"; 20 to 30) and C-horizon ("D-C"; 70 to 80 cm depth), for the Udipsamment samples from the A- ("U-A"; 0.5 to 25) and C-horizon ("U-C"; 100 to 125 cm depth). Sample preparation is described in Chapter 7 (Van Grinsven et al., 1988). Elemental analyses were carried out by X-ray fluorescence spectrometry (Begheijn, 1980), and the cation exchange complex was analyzed by an adapted unbuffered BaCl₂ extraction (Bascomb, 1986). Exchangeable acidity (H + Al) were determined by titration of the BaCl₂-extract up to pH 8.2. The average field soil solution chemistry is based on monthly, water-flux-weighted concentrations in samples, extracted by means of ceramic cups (Van Breemen et al., 1987). Heavy (specific gravity > 2.9 g/cm³) and light minerals in three particle size fractions were determined by counted optically.

Mineralogical, chemical and texture characteristics of the soil samples are given in Table 8.1. The texture of both soils is medium fine sand with little clay. The samples contain about 10% of alkali-feldspars, except for the D-C sample, which has distinctly higher feldspar contents. Feldspars are dominated by K-feldspars except for the U-A sample. Contents of mica, consisting mainly of muscovite, are higher in the Dystrochrept than in the Udipsamment. Higher contents of aggregates, and pyroboles (mainly Hornblende and Augite) occur in the D-C sample. The degree of weathering in the D-C sample, expressed by the ratio of the content of pure aluminum silicates (mainly Staurolite, Disthene, Andalusite and Sillimanite) over the content of Pyroboles (Dixon and Weed, 1977), is lower than for the other samples. Higher contents of free Al-oxides occur in the B-horizon of the Dystrochrept. All clay fractions contained kaolinite. Illite was detected only in the C-horizons. Chlorite and vermiculite were abundant throughout the Dystrochrept profile. CEC values of the surface soils are highest as a result of the presence of organic material. Base saturation is extremely low, but relatively high in the surface soils due to continuous mineralization of tree litter. The pH values of the field soil solutions range from 3.3 in the surface soil of the Dystrochrept to 4.2 in the Udipsamment. Al is the dominant ion in soil solution.

| DYSTROCHREPT: | | D-A) 5-10, D-B) 20-30, D-C) 70-80 cm depth. | | | | |
|---------------------------------|---------|---|-------|------|-----------------|-------|
| UDIPSAMMENT: | | U-A) 0.5-25, U-C) 100-125 cm depth. | | | | |
| | | D-A | D-B | D-C | U-A | U-C |
| Particle size (μm) | | Particle size distribution: (mass fraction %) | | | | |
| <2 | | 8.1 | 6.6 | 2.3 | 1.1 | 0.7 |
| 2-50 | | 12.7 | 12.7 | 1.1 | 1.4 | 1.4 |
| 50-150 | | 23.0 | 23.4 | 34.0 | 43.0 | 43.8 |
| 150-300 | | 30.1 | 29.7 | 46.5 | 50.0 | 46.8 |
| 300-420 | | 18.7 | 19.3 | 8.3 | 3.2 | 5.2 |
| 420-2000 | | 7.4 | 8.2 | 7.9 | 1.2 | 2.4 |
| | | Elemental analysis: (mass fraction %) | | | | |
| Al_2O_3 | <2 | 16.2 | 18.2 | 20.6 | -- ¹ | -- |
| | 50-150 | 2.83 | 3.13 | 6.55 | 3.09 | 3.21 |
| | 150-300 | 1.79 | 1.99 | 4.93 | 1.98 | 1.96 |
| | 300-420 | 0.80 | 0.85 | 1.55 | -- | 1.16 |
| | <2000 | 2.87 | 3.45 | 3.47 | 2.33 | 2.34 |
| K_2O | <2 | 0.82 | 0.92 | 2.48 | -- | -- |
| | 50-150 | 1.09 | 1.16 | 1.72 | 1.10 | 1.08 |
| | 150-300 | 0.92 | 0.97 | 1.61 | 1.08 | 0.86 |
| | 300-420 | 0.35 | 0.38 | 0.72 | -- | 0.63 |
| | <2000 | 0.75 | 0.83 | 1.16 | 0.89 | 0.91 |
| Na_2O | <2 | 0.26 | 0.25 | 0.30 | -- | -- |
| | 50-150 | 0.61 | 0.67 | 1.46 | 0.64 | 0.58 |
| | 150-300 | 0.24 | 0.26 | 1.10 | 0.27 | 0.25 |
| | 300-420 | <0.01 | <0.01 | 0.05 | -- | <0.01 |
| | <2000 | 0.52 | 0.58 | 0.61 | 0.48 | 0.53 |
| CaO | <2 | 0.09 | 0.10 | 0.16 | -- | -- |
| | 50-150 | 0.18 | 0.19 | 0.43 | 0.18 | 0.18 |
| | 150-300 | 0.01 | 0.03 | 0.22 | 0.03 | 0.03 |
| | 300-420 | 0.07 | 0.00 | 0.00 | -- | 0.00 |
| | <2000 | 0.17 | 0.14 | 0.14 | 0.12 | 0.12 |
| MgO | <2 | 0.84 | 1.14 | 2.26 | -- | -- |
| | 50-150 | 0.06 | 0.08 | 0.49 | 0.10 | 0.12 |
| | 150-300 | 0.04 | 0.05 | 0.25 | 0.05 | 0.07 |
| | 300-420 | 0.07 | 0.03 | 0.06 | -- | 0.02 |
| | <2000 | 0.06 | 0.07 | 0.17 | 0.05 | 0.07 |

¹ Not Available

Table 8.1 Physical, chemical and mineralogical characteristics of used soil samples and solutions.

| | Particle size (μm) | D-A | D-B | D-C | U-A | U-C |
|---|---------------------------------|---|------|------|------|------|
| | | (mass fraction Z) | | | | |
| Organic C | <2000 | 3.02 | 1.45 | 0.10 | 5.38 | 0.33 |
| Free Al_2O_3 | <2000 | 0.39 | 0.76 | 0.12 | 0.17 | 0.29 |
| Light Minerals: (specific gravity < 2.9 g/cm^3) ² | | | | | | |
| K-feldspar | 50-150 | 8.9 | 13.9 | 14.7 | 4.6 | 9.0 |
| | 150-300 | 8.8 | 12.2 | 13.3 | 5.6 | 9.3 |
| Plagioclase | 50-150 | 2.6 | -- | 6.6 | 6.5 | 1.2 |
| | 150-300 | 2.5 | -- | 3.7 | 6.8 | 0.7 |
| Mica | 50-150 | 2.0 | 3.0 | 2.2 | 0.4 | 0.5 |
| | 150-300 | 4.6 | 3.5 | 4.0 | 1.1 | 2.8 |
| Aggregate | 50-150 | 0.3 | 0.5 | 5.6 | 0.3 | 2.6 |
| | 150-300 | 1.3 | 2.7 | 4.9 | 0.4 | 1.7 |
| Heavy Minerals: (specific gravity > 2.9 g/cm^3) ² | | | | | | |
| Total | 50-420 | 0.2 | 0.3 | 0.8 | 0.7 | 0.4 |
| Pyroboles | 50-150 | 0.01 | 0.03 | 0.22 | 0.07 | 0.13 |
| | 150-300 | 0.01 | 0.03 | 0.11 | 0.01 | 0.01 |
| Weathering degree ³ | 50-420 | 1.33 | 1.10 | 0.52 | 1.15 | 1.22 |
| Exchange complex (mmol_c/kg) | | | | | | |
| K | | 0.1 | <0.1 | <0.1 | <0.1 | <0.1 |
| Na | | <0.1 | <0.1 | <0.1 | <0.1 | <0.1 |
| Ca | | 5.5 | 0.2 | <0.1 | 3 | <0.1 |
| Mg | | 1.0 | <0.1 | 0.2 | 1 | <0.1 |
| Al | | 31 | 11 | 10 | 18 | 1 |
| H | | 52 | 16 | 3 | 30 | 4 |
| Sum | | 89.5 | 27.2 | 13.2 | 52 | 5 |
| Analytical Error | | Equilibrium solutions: ($\mu\text{mol}_c/\text{L}$) | | | | |
| K | 0.2 | 53. | 9.8 | 6.6 | 22. | 8.5 |
| Na | 1.1 | 30. | 5.8 | 56. | 77. | 84. |
| Ca | 0.7 | 89. | 15. | 7.8 | 37. | 13. |
| Mg | 0.5 | 59. | 5.3 | 1.2 | 29. | 2.0 |
| Al | 2.7 | 217. | 126. | 10. | 241. | 69. |
| H | 2. | 197. | 27. | 14. | 62. | 17. |
| Field soil solution ($\mu\text{mol}_c/\text{L}$) | | | | | | |
| Depth: (cm) | | 10 | 20 | 75 | 40 | 100 |
| K | | 320 | 300 | 145 | 60 | 40 |
| Na | | 190 | 200 | 240 | 520 | 520 |
| Ca | | 400 | 550 | 390 | 110 | 90 |
| Mg | | 200 | 240 | 220 | 160 | 130 |
| Al | | 520 | 970 | 1830 | 1130 | 1520 |
| H | | 510 | 520 | 100 | 80 | 70 |

² Mass fraction (Z), assuming particle sizes within one fraction to equally distributed over all present minerals.

³ See Text

Table B.1 Continued.

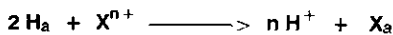
| Sample | | D-A | | D-B | | D-C | | U-A | | U-B | |
|-----------|------|-------------------------|------|------|------|------|------|------|------|------|------|
| | | Mean | S.d. | Mean | S.d. | Mean | S.d. | Mean | S.d. | Mean | S.d. |
| Component | | (mmol _c /kg) | | | | | | | | | |
| K | RE | 1.28 | 0.05 | 0.52 | 0.08 | 0.27 | 0.05 | 0.18 | 0.01 | 0.13 | 0.01 |
| | CsCl | 1.51 | -- | 0.43 | 0.07 | 0.31 | 0.22 | 0.34 | 0.05 | 0.22 | 0.05 |
| Na | RE | 0.96 | 0.04 | 2.46 | 0.99 | 0.80 | 0.21 | 0.87 | 0.04 | 0.35 | 0.03 |
| | CsCl | 0.94 | -- | 1.57 | 0.15 | 0.94 | 0.68 | 0.64 | 0.02 | 0.58 | 0.05 |
| Mg | RE | 1.40 | 0.01 | 0.51 | 0.03 | 0.12 | 0.04 | 0.30 | 0.00 | 0.04 | 0.00 |
| | CsCl | -- | -- | 0.25 | 0.02 | 0.14 | 0.10 | 0.21 | 0.00 | 0.07 | 0.01 |
| Al | RE | 11.1 | 1.3 | 65.1 | 3.4 | 13.8 | 0.6 | 15.0 | 1.1 | 26.5 | 0.8 |
| | CsCl | -- | -- | 58.4 | 1.0 | 12.6 | 8.9 | 17.7 | 0.6 | 33.3 | 1.3 |

Table 8.2 Means and standard deviations (S.d., n = 2 or n = 3) of leached quantities of K, Na, Mg and Al between 0.5 and 2 d, during percolation with recirculation extracts (RE) or with CsCl, at identical ionic strength and at pH 3.

It may be concluded that for the determination of weathering rates from column experiments at pH values which are considerably lower than in the field the application of background concentrations for the major cations need not to be applied.

8.3.3 The role of cation exchange in A-horizon of the Dystrochrept

At relatively high CEC values, as in the surface horizons, exchange reactions may contribute significantly to leaching of K, Na, Ca, Mg, and possibly Al. Cation exchange was described by the Gaines-Thomas exchange model (Equation 1; Gaines and Thomas, 1953). The general exchange equation, using H⁺ as reference ion is:



the exchange equation is:

$$K_{H,X} = \frac{(H)_n [Ca]_a}{(Ca) [H]_a^n} \quad (1)$$

where K is the selectivity coefficient, (H) and (X) are activities in solution (mol/L), and [H]_a and [X]_a are fractions of adsorbed charge equivalents. Selectivity coefficients were estimated using water-flux-weighted annual

averages of concentrations in soil solutions extracted monthly in the field and one time analyses of the adsorbed phase. Resulting selectivity coefficients using H as a reference ion, were 3.1×10^{-3} (K), 6.9×10^{-3} (Na), 3.0×10^{-4} (Ca), 1.1×10^{-4} (Mg) and 1.2×10^{-6} (Al). Cumulative desorption was predicted by calculating the changes in adsorbed concentrations from the changes in column outflow concentrations. Predicted desorption for Na, K, Ca and Mg for an experiment with the A-horizon of the Dystrochrept at pH 3 is shown in Figure 8.2.

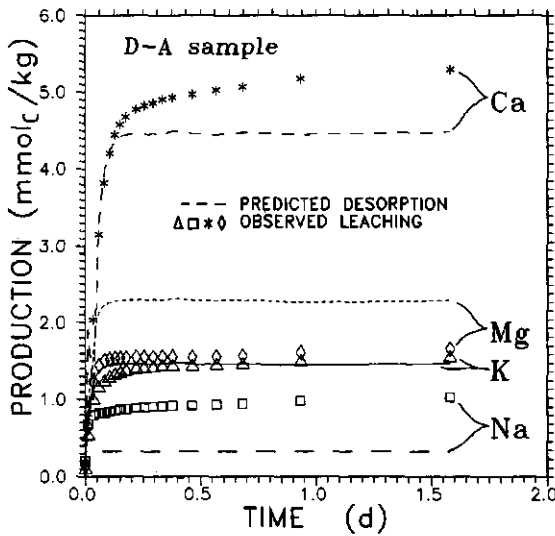


Fig. 8.2 Comparison of observed cumulative leaching and predicted desorption, using the Gaines-Thomas model, for K, Na, Ca and Mg at pH 3 from the D-A sample.

The increase of predicted desorption and observed leaching with time showed a similar pattern for K, Ca and Mg. In most cases desorption reached its maximum after about 5 h, while actual production continued. Continued release may be the result of mineral weathering, but also could indicate that equilibrium between solution and exchange sites is not instantaneous on the experimental time scale or that immobile water is present in the column. The average ratios of predicted desorption over observed leaching for all pH values was 1.07 for K, 0.29 for Na, 0.91 for Ca and 1.08 for Mg (Table 8.3). For Ca, both observed leaching and predicted desorption decreased with increasing pH values.

8.3.5 Weathering of K, Na, and Mg from the C-horizon

Only the results for samples taken from the C-horizon of the Dystrochrept and Udipsamment will be discussed because the errors in the weathering rates calculated for these samples were relatively small and interference by exchange processes was unimportant. Tables 8.5 and 8.6 summarize the weathering rates for both soils after 2 d, as calculated with Equation 1 in Chapter 7 (Van Grinsven et al., 1988^b).

| pH | K | | Na | | Mg | | Si | |
|-----|--|-----|------|-----|--|------|------|-----|
| | S.d. | | S.d. | | S.d. | | S.d. | |
| | $(\text{mol}_c \cdot \text{kg}^{-1} \cdot \text{s}^{-1} \times 10^{10})$ | | | | $(\text{mol} \cdot \text{kg}^{-1} \cdot \text{s}^{-1} \times 10^{10})$ | | | |
| 2.8 | 4.7 | 2.7 | 14.6 | 1.1 | 1.71 | 0.29 | -- | -- |
| 3.0 | 1.3 | 0.6 | 9.1 | 6.4 | 0.81 | 0.23 | 18.5 | 1.5 |
| 3.3 | 2.0 | 0.4 | 10.4 | 0.9 | 0.30 | 0.11 | 14.6 | 0.3 |
| 3.6 | 1.7 | 0.3 | 9.3 | 5.9 | 0.33 | 0.16 | 18.9 | 4.4 |
| 4.8 | 1.2 | 0.4 | 8.7 | 1.1 | 0.04 | 0.01 | 9.7 | 1.6 |

Table 8.5 Means and standard deviations (S.d., n = 2 or n = 3) of rates of release of cations and silica (kg^{-1} soil) from the D-C sample after 2 d of column leaching.

| pH | K | | Na | | Mg | | Si | |
|-----|--|-----|------|-----|--|------|------|------|
| | S.d. | | S.d. | | S.d. | | S.d. | |
| | $(\text{mol}_c \cdot \text{kg}^{-1} \cdot \text{s}^{-1} \times 10^{10})$ | | | | $(\text{mol} \cdot \text{kg}^{-1} \cdot \text{s}^{-1} \times 10^{10})$ | | | |
| 2.6 | 3.7 | -- | 20.0 | -- | 0.87 | -- | 84.8 | -- |
| 3.0 | 1.2 | 0.2 | 5.2 | 1.7 | 0.46 | 0.05 | 76.0 | 3.0 |
| 3.3 | 0.9 | 0.5 | 3.2 | 2.6 | 0.58 | 0.13 | 90.7 | 40.1 |
| 3.8 | 0.1 | 0.0 | 2.5 | 2.2 | 0.02 | 0.02 | 81.8 | 42.2 |

Table 8.6 Means and standard deviations (S.d., n = 2) of rates of release of cations and silica (kg^{-1} soil) from the U-C sample after 2 d of column leaching.

Dissolution rates of Ca are not shown, because for the Dystrochrept sample this element showed a very specific mechanism which is subject of a separate paper (Chapter 9: Van Grinsven et al., 1988^d).

Dissolution rates of Na between pH 3 and 4 from both soil samples were about 5 times higher than of K. Because contents of plagioclases were 3 (D-C) to 10 (U-C) times lower than of K-feldspars (Table 8.1), weathering rates of

plagioclases in our soil are about 15-30 times higher than of K-feldspars. Lasaga (1983) reported that the rate of Si-release from albite was 12 times higher than from K-feldspar. This difference is similar to the difference we found in our samples, considering that plagioclases are more reactive than pure albite. The rates of release of K and Na in the Dystrochrept are higher than in the Udipsamment, which probably is caused by the presence of higher contents of feldspars in the Dystrochrept (Table 8.1).

Higher rates of release of Mg in the D-C than in the U-C sample may be related to higher contents of pyroboles and micas. In spite of lower rates of release of base cations from the Udipsamment, the rate of silica release was 6 times higher than in the Dystrochrept. Also, release of silica from the Dystrochrept sample was much lower than expected from base cations release during congruent dissolution of silicate. Reprecipitation of silica in the column was unlikely because column percolates were strongly undersaturated with respect to quartz, with concentrations of Si ranging from 20 to 50 $\mu\text{mol/L}$. On the other hand, the Udipsamment released more silica than expected from the release of base cations from silicate minerals. Lower rates of release of silica than of base cations may be caused by incongruent dissolution of primary silicates to secondary aluminosilicates. Higher rates of release of silica than of base cations may result from dissolution of a pure aluminosilicate. A common product from incongruent dissolution of primary silicates, and a relevant clay mineral in the Dystrochrept sample is kaolinite. Soil solutions in the field are commonly supersaturated with kaolinite (Mulder et al., 1987), but our acidified column percolates were strongly undersaturated with kaolinite (Chapter 7: Van Grinsven et al., 1988^b). However; there is no obvious reason why kaolinite dissolution would be elevated in the Udipsamment sample, and not in the Dystrochrept. Dissolution rate of Al in our samples is mainly from dissolution of amorphous oxides (Chapter 7: Van Grinsven et al., 1988^b), but even a small contribution of aluminosilicates to the release of Al would cause a significant release of Si.

Rates of release of base cations clearly increased with decreasing pH, especially for Mg. The increase of dissolution rates with decreasing pH support the validity of the power-type relationship (Aagaard and Helgeson, 1984; Stumm and Furrer, 1986; Chapter 7: Van Grinsven et al., 1988^b).

$$\log(\text{RATE}) = K + q \text{ pH} \quad (2)$$

Significant values of q were found for Mg in the D-C ($q = -0.7$, $r^2 = -0.88$, $n = 12$) and U-C sample ($q = -1.7$, $r^2 = -0.68$, $n = 7$), and for K in the U-C-sample ($q = -1.6$, $r^2 = -0.85$, $n = 7$). For the other elements no pH effect was observed except below pH 3.

8.3.8 Hydrodynamic effect of percolation rate on weathering rate

At any time in the column experiments the percolation rate was set proportional to the overall H^+ buffer rate. In all cases but one (the C-horizon of the Dystrochrept) the H^+ consumption rate is almost equal to the Al dissolution rate. For the determination of the weathering rates of base cations it is necessary to assume that the weathering rate is independent of the percolation rate. If this assumption is correct, decreasing of the percolation rate by a factor of two causes doubling of the concentration difference of base cations and silica between inflow and outflow, as a result of doubling of the solution residence time in the column. However, in most column experiments the concentration difference decreases less than linearly with increasing residence time, as demonstrated in Figure 8.3 at pH 3 for Na.

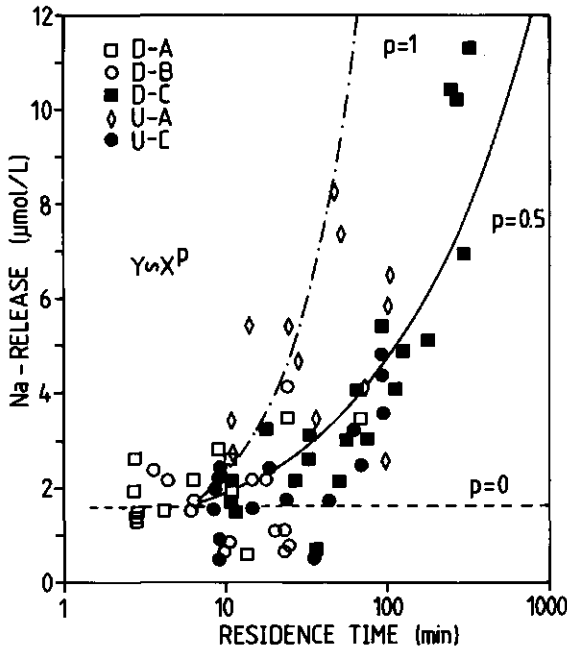


Fig. 8.3 The increase of the release of Na with increasing column residence time (decreasing percolation rate) for all soil samples. If $p = 1$ rates of release are independent of percolation rate, if $p = 0$ rates of release increase linearly with percolation rate.

A less than linear increase may also be explained by mineral depletion. Large effects of depletion, however, are unlikely as was explained before. The experimental data suggest that the concentration difference increases with residence time according to square root rather than a linear relationship. The lowest percolation rates in the column experiments are about 7 cm/d, while field percolation rate average 0.05 to 0.15 cm/d. So, the suggested square root relationship between flow rate and weathering rate could explain a factor 7 to 12 difference between weathering rates from the column experiments and in the field. The non-linear relationship between percolation rate (or residence time) and weathering rate suggests a hydrodynamic effect. In Chapter 5 (Van Grinsven and Van Riemsdijk, 1988) it was suggested that stagnant water films inside etch pits may limit diffusion transport. This hypothesis needs to be tested by further research.

8.4 SUMMARY AND CONCLUSIONS

Rates of base cation weathering in soils are important to quantify the natural availability of plant nutrients in extensively managed ecosystems. Samples from two acid forest soils were studied by means of column experiments at controlled pH. Samples were studied from the A-, B-, and C-horizon of a Dystrochrept and the A- and C-horizon of a Udipsamment. Dissolution of Al was the main buffering process. Release of base cations was detectable but the increase of concentration sometimes close to the analytical detection limit. Release of K, Ca and Mg from samples of the A-horizon was dominated by cation desorption and could be described by the Gaines-Thomas model. The exchange of Al and H was much less than predicted by the Gaines-Thomas model, presumably due to slow exchange. Weathering rates, normalized to estimated specific surface area of feldspars, of Na in the C-horizons of both soils were about 10 to 20 times higher than for K in accordance with the higher reactivity of plagioclases than of K-feldspar. Release of Mg was generally low compared to that of other base cations, and associated with contents of mica and pyroboles, which were highest in the C-horizons. Differences in weathering rates of plagioclase between both soil types, and between different depths were small. Weathering rates showed an increase with increasing (H^+), which was most apparent below pH 3. The rate increase was strongest for Mg, which rate increased nearly linear with (H^+). Observed weathering rates of base cations and Si in column experiments were

one to two orders of magnitude higher than observed in field budget studies, while rates observed in stagnant batch experiments were only slightly higher than field rates. These discrepancies cannot be the result of limiting diffusion transport or differences in mineral depletion, but may be attributed to a hydrodynamic effect of percolation rate on weathering rate. The hypothetical hydrodynamical effect is corroborated by column experiments, which showed a decrease of weathering rates with decreasing flow rate.

As long as artifacts of experimental techniques on kinetics of mineral weathering are not well understood, comparison of different types of dissolution experiments and application of rates obtained from laboratory experiments to the field should be accompanied by caution.

ACKNOWLEDGEMENTS

The authors wish to thank the Netherlands Energy Research Foundation (ECN), in particular R. Otjes and Dr. T. Lub, for their invaluable help during the development of the pH-stat column percolation technique, and for carrying out the actual experiments. Furthermore we wish to thank Hugo Denier van der Gon, who did the unstirred batch experiments as part his Msc-program, Professor L. van der Plas, T. Engelsma and B. Kuiper for assistance with the mineralogical analyses, and E. Velthorst, F. Lettink and L. Begheijn for analyses of soil solutions and exchangeable fractions. I also would like to express my gratitude to J. Mulder for providing his data of the Udipsamment soil. Finally I am very grateful to Professor F.A.M. de Haan of Soil Science and Plant Nutrition for his general support.

A revised version of this chapter will be submitted to Soil Sci Soc. Amer. J. J.J.M. van Grinsven, W.H van Riemsdijk and N. van Breemen.

Chapter 9

EVIDENCE FOR INCREASED WEATHERING OF Ca FROM PLAGIOCLASE AS A RESULT OF DISSOLUTION OF PROTECTIVE Al COATINGS IN ACID SOLUTIONS

ABSTRACT

A dissolution study was carried out with samples from the C-horizon of a Dystrachrept with ambient pH values in soil solution around 4. Both budgets of chemical input and output fluxes of Ca in the field, and of column percolation experiments in the laboratory at equilibrium pH, showed dissolution of only traces of Ca, while Al-dissolution was the main H⁺ consuming process. However, when pH was lowered, enhanced release of Ca was observed to levels comparable to those of Al. This observation could be explained by assuming the presence of small reactive anorthite domains at the surfaces of plagioclase grains, which were protected against dissolution at equilibrium pH by protective coatings of probably hydrous Al-oxides. At present, acid atmospheric deposition causes progressive dissolution of these coatings in the field, which may lead to enhanced release of Ca in the near future. The assumption that patchy coatings of secondary Al-phases cannot be protective against mineral dissolution (Berner and Holdren, 1979), may have to be reconsidered because the reactivity of mineral surfaces is also highly localized.

9.1 INTRODUCTION

In acid forest soils calcium and magnesium occur generally in low concentrations (Berden et al., 1987), often in vermiculites, amphiboles and pyroxenes (Dixon and Weed, 1977). In maritime areas it is not uncommon that atmospheric deposition is a more important source of Ca and Mg as a nutrient for trees than mineral weathering (Miller, 1978). As a result of prolonged exposition of acid forest soils to high inputs of acid atmospheric deposition, exchangeable pools of Ca and Mg have decreased considerably (Ulrich et al., 1980; Johnson et al., 1988). Ca and Mg deficiency may be involved in declined forest vitality in western and central Europe. Application of Ca and Mg fertilizers to acid forest soils may alleviate this problem, but large scale application may not be economical, and moreover may lead to temporarily increased Al-concentrations due to the salt effect, enhanced mineralization and leaching

of organic nitrogen, and the disappearance of valuable plant species and fungi. Apparently, care should be taken when applying fertilizers to extensively managed forest ecosystems, and it is preferable to rely as much as possible on natural pools of nutrients.

The kinetics of mineral weathering in relation to the supply of nutrients in forest soils is still poorly understood (Velbel, 1986; Chapter 5: Van Grinsven and Van Riemsdijk, 1988). Efforts to quantify rates of release of Ca, Mg and K from soil minerals in the field by means of laboratory experiments met little success. Estimates of mineral weathering rates of Ca, Mg and K from budget studies in the field often are very inaccurate and have no long-term predictive value (Velbel, 1986). Problems involved with the determination of weathering rates in the laboratory are discussed at length by Velbel (1985; 1986) and in Chapter 5 (Van Grinsven and Van Riemsdijk, 1988). Key problems are (1) analytical detection due to the extremely low solubility of soil minerals, (2) disturbance of the mineral surfaces before and during the experiment and (3) hydrodynamic factors.

In Chapter 7 (Van Grinsven et al. 1988^b) a new method to study mineral weathering rates in columns is presented, specifically adapted to meet these problems. This paper discusses experiments with samples from a C-horizon of a Dystrachrept, which showed a peculiar and interesting dissolution behaviour of Ca.

9.2 MATERIALS AND METHODS

9.2.1 Soil samples and chemical analysis

The soil sample for weathering experiments in the laboratory was taken between 0.7 and 0.8 m depth from a sandy, Umbric Dystrachrept, located in the Hackfort Estate, in the eastern part of the Netherlands (Van Breemen et al., 1986). The study area is a 3.2 ha woodland dominated by *Quercus robur* and *Betula pendula*. The soil parent material consists of sandy to loamy Pleistocene sediments of the river Rhine. The profile has been decalcified to a depth of 1.2 m. The hydrology and the chemistry of atmospheric water, soil solution and groundwater have been monitored from 1981 to 1987. The groundwater level fluctuates between a depth of 0.5 and 1.5 m. Annual precipitation is 0.7 m, with an excess of precipitation over evapotranspiration of 0.2 m. Annual atmospheric input of Ca and Mg are 0.4 and 0.2, annual leaching from the top 0.9 m of the soil are 0.7 and 0.5 $\text{kmol}_c \cdot \text{ha}^{-1} \cdot \text{yr}^{-1}$ respectively. Annually 2.5 kmol_c Ca and 1

kmolc Mg per ha are cycled through the vegetation. The atmospheric input of $(\text{NH}_4)_2\text{SO}_4$, causes, after nitrification in the soil, a soil acidification of 5 to 6 $\text{kmol} \cdot \text{ha}^{-1} \cdot \text{yr}^{-1}$. Most of the acid formed is buffered by dissolution of Al. Details on the soil site and monitoring are given by Van Breemen et al. (1986, 1987).

Chemical, physical and mineralogical characteristics of the subsoil sample and the surface soil are given in Table 9.1.

| Particle Size (μm) | <2 | 2-50 | 50-150 | 150-300 | 300-2000 |
|---------------------------------|-------------------|------|--------|---------|----------|
| | (mass fraction %) | | | | |
| Sample (70-80 cm) | 2.3 | 1.1 | 34.0 | 46.5 | 16.2 |
| Surface soil (0-30 cm) | 7.4 | 12.7 | 23.2 | 29.9 | 27.0 |

| | K ₂ O | Na ₂ O | CaO | MgO | Al ₂ O ₃ | Total free |
|------------------------|-----------------------------------|-------------------|------|------|--------------------------------|------------|
| | (mass fraction (%) of fine earth) | | | | | |
| Sample (70-80 cm) | 1.51 | 1.06 | 0.24 | 0.38 | 5.34 | 0.56 |
| Surface soil (0-30 cm) | 0.87 | 0.34 | 0.11 | 0.12 | 3.12 | 0.12 |

| Mineralogical composition | (mass fraction (%) of fine earth) | |
|---------------------------|-----------------------------------|-----------|
| Depth | (70-80 cm) | (0-30 cm) |
| K-feldspar | 14. | 11. |
| Plagioclase | 5.0 | 2.5 |
| Micas (muscovite) | 3. | 3. |
| Heavy minerals | 0.8 | 0.3 |
| of which pyroboles | 0.22 | 0.02 |

| | K | Na | Ca | Mg | Al | Si | H | Cl | SO ₄ | NO ₃ |
|--------------|-------------------------|------|-----|-----|-----|----|-----|----|-----------------|-----------------|
| | (mmol _c /kg) | | | | | | | | | |
| (70-80 cm) | | | | | | | | | | |
| Exchangeable | <0.1 | <0.1 | 0.1 | 0.1 | 3.9 | | 5.1 | | | |

| Solutions (70-80 cm) | (mmol _c /m ³) | | | | | | | | | |
|----------------------|--------------------------------------|-----|-----|-----|------|-----|-----|-----|------|-----|
| Average field | 145 | 240 | 390 | 220 | 1830 | 300 | 100 | 410 | 1450 | 960 |
| Equilibrium extract | 7 | 60 | 8 | 1 | 1 | 0 | 14 | 26 | 65 | 0 |

Table 9.1 Texture, chemical and mineralogical characteristics of the surface soil and the subsoil of a Dystrochrept, and chemical composition of average field soil solution and equilibrium extract.

Over 90% of the soil material is in the fine and medium fine sand fraction. The sample contains about 20% of feldspars of which 2/3 are K-feldspars. The contents of plagioclases is distinctly higher than in the surface soil. The contents in the bulk soil of K₂O is 2 times, of Na₂O are 4 times, of CaO 2 times and of MgO 3 times higher than in the surface horizons. Higher contents of CaO may be associated with higher contents of plagioclase (Dixon and Weed, 1977). Higher contents of MgO may be associated with higher amounts of pyroboles (mainly Hornblende and Augite). Contents of amorphous Al-oxides, as determined by a oxalate-dithionite extraction (Begheijn, 1980), are low compared

to contents in the surface soil. Exchangeable Ca and Mg are negligible. Soil solutions in the field are dominated by Al.

Column percolates and batch solutions were acidified before storage at room temperature. Ca and Mg were analyzed by atomic absorption spectrometry, Al and Si by inductive coupled plasma emission spectrometry.

9.2.2 Column and unstirred batch experiments

To study mineral weathering we used soil columns under nearly-controlled chemical conditions (Chapter 7: Van Grinsven et al., 1988^b). The pH of the percolate was kept constant by automatically adjusting the percolation rate of the input solution, so that the H^+ -input was proportional to the H^+ -consumption rate of the soil sample. The difference in the $[H^+]$ between inflow and outflow was maintained at about 200 $\mu\text{mol/L}$. Concentrations in the input solutions were equal to concentrations observed in recirculation extracts, except for silica which was not added. These extracts were obtained by recirculation of demineralized water for two days through columns of the same soil material, that was prewashed to remove soluble salts. The pH of the input solutions was adjusted by adding HCl. All experiments were carried out in duplicate.

When buffer rates in the column experiments became so low that flow adjustment became inaccurate, the experiments were continued in an unstirred batch system. For this purpose the soil residues were transferred to plastic containers with a diameter of 10 cm, and 150 mL of solution was added. Diffusion calculations showed that molecular diffusion was sufficient to homogenize reactant concentrations throughout the overlying solution layer (Chapter 8: Van Grinsven et al., 1988^c). A 100 mL of the solution was replaced when the H^+ concentration in the overlying solution had decreased by about 200 $\mu\text{mol/L}$.

9.3 RESULTS AND DISCUSSION

The cumulative leaching of Ca at different pH values as a function of the square root of time is shown in Figure 9.1. After about 4 d the experiments at pH 2.8, 3.2 and 3.5 were continued in an unstirred batch system. The rates of Ca release dropped considerably at the onset of the batch experiments except at pH 3.2. This decrease probably was caused by differences in hydrodynamic conditions between both types of experiments, which are discussed in detail in Chapter 5

(Van Grinsven and Van Riemsdijk, 1988) and in Chapter 8 (Van Grinsven et al., 1988°).

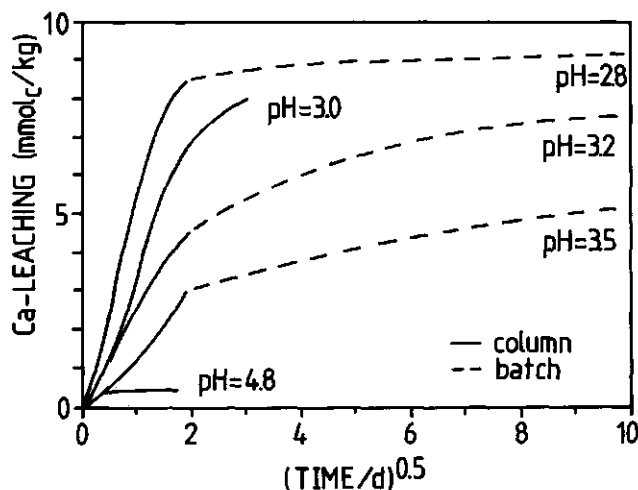


Fig. 9.1 The release of Ca with time from the soil sample in column and subsequent batch experiments at different pH values.

However, these experimental complications do not detract from the obvious conclusion from this experiment. At pH 4.8, close to the field-pH, only traces of Ca are brought into solution, while with decreasing pH, buffering by Ca becomes increasingly important. The second conclusion is that the amount of reactive Ca is limited to about 10 mmol_c/kg soil material, which is 9% of total Ca. This small pool of reactive Ca was depleted fast, which counteracted the stimulative effect of a decreasing pH on Ca-release. As a result, the highest Ca dissolution rates near the end of the batch experiment occurred at the highest pH. The reason for the sudden mobilization of Ca in subsoil material after prior acidification is not immediately clear. In the field there is no evidence whatsoever for enhanced mobilization of Ca; differences between input and output fluxes in the soil profile are small (Van Breemen et al., 1986), and can easily be accounted for by the uncertainty about the steady state condition of the pools of exchangeable and organic Ca in the overlying soil.

If we plot the cumulative Ca leaching against the Al leaching (Figure 9.2) sigmoid curves appear which are independent of pH. Apparently, regardless of pH, about 5 to 10 mmol_c/kg of Al had to be removed from the soil before Ca could be mobilized.

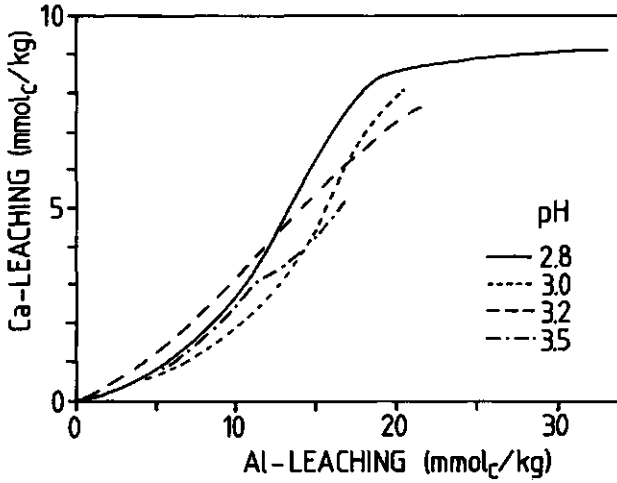
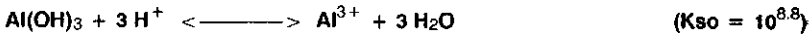


Fig. 9.2 The release of Ca as a function of the release of Al from soil in column and subsequent batch experiments at different pH values.

These observations can be explained by assuming the presence of a protective coating of an Al-rich phase, covering reactive Ca-sites. Coatings of secondary alumino-silicates on feldspar surfaces are common, both as residues of incongruent dissolution or as precipitates (Velbel, 1986). In order to be protective the diffusivity of these coatings should be in the order of 10^{-14} to 10^{-20} cm^2/s (Wollast, 1967; Velbel, 1986). A protective effect against feldspar weathering by layers of secondary Al-rich material was rejected by Berner and Holdren (1979). By SEM microphotography they showed that coatings existed, but were generally patchy and not adhered strongly to the feldspars surfaces. They assumed without convincing arguments, that diffusivities for dissolved species of these coatings were only a factor of ten lower than in water. Berner and Holdren (1979) concluded that in general weathering kinetics were controlled by surface reactions, taking place at small localized reactive sites. However, the assumption of small reactive surface sites implies that patchy coatings could play a role in protection against dissolution. Precipitation of a secondary Al-phase on top of reactive sites is even likely, because there pH values will be higher than at adjacent sites. In our sample such a hypothetical protective coating is likely to be an Al-(hydr)oxide as was pointed out earlier in Chapter 7 (Van Grinsven et al., 1988^b). The amount of Al-oxides released before Ca is liberated, is only 5% of the total amount of free Al-oxides (Table 9.1).

To test our hypothesis on protective Al-oxide coatings, and consequently the dependence of Ca release on previous release of Al, we performed two column experiments with different levels of Al-"stripping". Both experiments were carried out at an input pH of 3.5, but in one experiment dissolution of Al was suppressed by raising the activity product for dissolution of Al(OH)₃ by increasing the input concentration of Al from 1 to 200 μmol/L. The activity product for dissolution of Al:



in the experiment with the low Al input concentration, increased during column passage from 10^{4.6} to 10^{7.1}, and in the experiment with the high Al input concentration from 10^{5.6} to 10^{7.4}. The release of Al was suppressed by about 4 mmol_c/kg, mainly in the first day of the experiment. In support of our hypothesis, decreased Al-release was accompanied by distinctly lower rates of release of Ca (Figure 9.3).

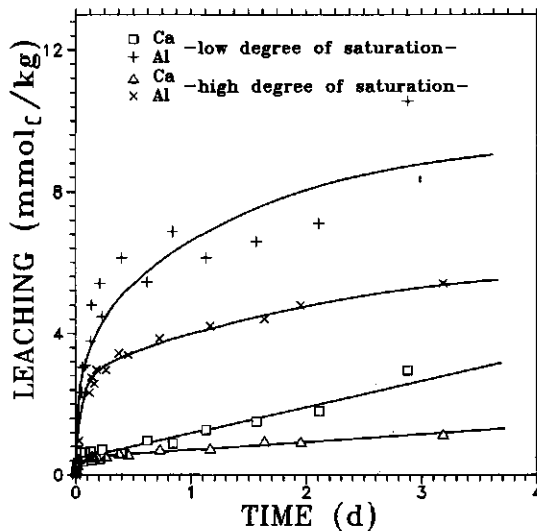


Fig. 9.3 The leaching of Ca and Al in time from soil columns at an input pH 3.5 at low and high levels of saturation with Al(OH)₃

At present, due to the increasing influence of acid atmospheric deposition, pH in the subsoil has decreased to a level where Al(OH)₃ is not stable anymore and the Al-(hydr)oxides will gradually dissolve. However, possibly less than one century ago, pH in our subsoil probably was 0.5 to 1 unit higher (Berden et al., 1987) and solutions were still in equilibrium with respect to Al(OH)₃, as is commonly observed in areas with low levels of acid deposition (David and

Driscoll, 1984). During former soil formation Al was mobilized from primary minerals in shallower soil layers and was reprecipitated in the B- and C-horizons, preferably on reactive sites upon the mineral surfaces.

A question that remains is the source of Ca. Enhanced Ca-release was not observed for samples from shallower depths than 0.7 m (Chapter 8: Van Grinsven et al., 1988^c). A possible source of Ca is plagioclase. Plagioclases are more abundant at 0.7 m depth than in the overlying soil horizons. During enhanced leaching of Ca, the molar ratios of Ca over Al, and of Ca over Si, (Figure 9.4) reached values of 1.1 and 4.5 respectively, regardless of the pH of the leachate.

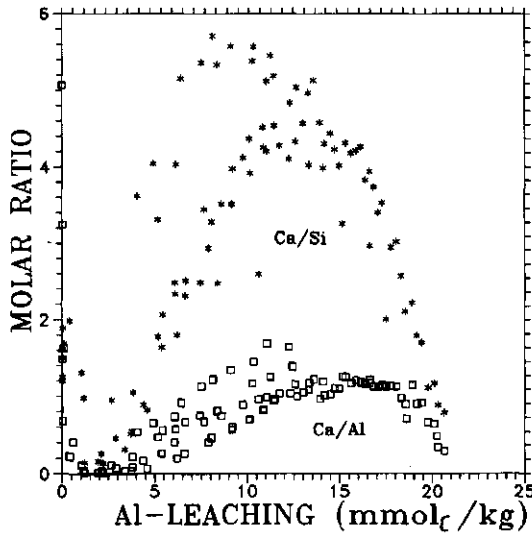


Fig. 9.4 The molar ratios of Ca over Al, and Ca over Si in the leachates of soil columns at pH values ranging from 2.8 to 3.5.

The fact that stoichiometric ratios were independent of pH, as was suggested by Holdren and Speyer (1985), proves that pH had no direct effect on the release of Ca. Congruent dissolution of anorthite in plagioclases would produce lower ratios, viz. 0.5 for Ca/Si and Ca/Al. Simultaneously release of Si and Al from K- and Na-feldspars and of Al from oxides would cause even lower ratios. The high ratios of Ca over Al and Si suggest either incongruent dissolution of anorthite or dissolution of an unknown mineral, poor in Al and Si.

Anorthite-domains, which are highly unstable and soluble at ambient soil pH, could be present at the surface of plagioclases, when covered by Al-oxide coatings. EDAX analysis of some cleaned surfaces of feldspar grains from the soil sample indeed revealed spots with elevated Ca concentrations (Table 9.2).

| Grain | Al | Si | K (%) | Na | Ca |
|-------|----|----|----------|----|----|
| 1 | 31 | 57 | 6 | 0 | 6 |
| 2 | 22 | 63 | 0 | 12 | 3 |

Table 9.2 The relative presence of Al, Si, K, Na and Ca on the surface of two feldspar aggregate grains as determined by Energy Dispersive X-ray Spectroscopy.

Feldspar grains were found both with few but large Ca-domains, and many but small Ca-domains on the feldspar surface. Apparently there is a, probably relatively short, stage in soil formation where Ca-rich plagioclases are still present while Al already is mobile. In this stage anorthite-domains may be continuously uncovered from the feldspar matrix, but are not dissolved as a result of quick formation of a protective Al-oxide coating. If in a later stage pH is lowered, enhanced Ca-release is observed due to the exposition of the accumulated uncovered anorthite-domains on the feldspar surface, after quick dissolution of the secondary Al-coatings (Figure 9.5).

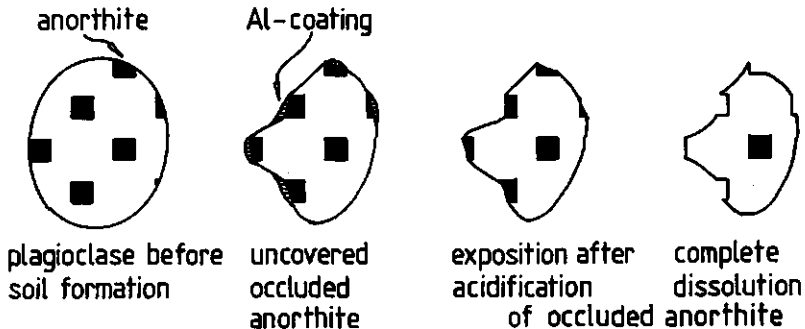


Fig. 9.5 Schematic representation of dissolution of a plagioclase with embedded anorthite-domains during soil formation and subsequent enhanced acidification.

Subordinate anorthite-domains in plagioclases are generally present as lamellae, and such unmixed plagioclases are called peristerites, which are rare in nature (Dixon and Weed, 1977).

9.4 SUMMARY AND CONCLUSIONS

Ca is an important nutrient for forest growth but is present at relatively concentrations in the mineral ensemble of large areas of acid forest soils. A dissolution study was carried out with samples from the C-horizon of a Dystrachrept profile with ambient pH values in soil solution around 4. Both budgets of chemical input and output fluxes of Ca in the field and of column percolation experiments at equilibrium pH in the laboratory, showed dissolution of only traces of Ca, while Al-dissolution was the main pH-buffering process. However when pH was lowered, enhanced release of Ca was observed to levels comparable to the release of Al. This observation was explained by assuming the presence of small reactive anorthite-domains on the surfaces of feldspar grains, which are occluded from solution by protective coatings of probably hydrous Al-oxides. Secondary Al-oxides are common in acid forest soils, and generally are adhered to surfaces of other minerals. At present these secondary Al-oxides are progressively dissolving due to continued action of acid atmospheric deposition. The removal of secondary Al-coatings, may eventually lead to exposure of reactive mineral surfaces. For the studied soil site it may lead to enhanced release of Ca in the near future. The assumption that patchy coatings of secondary Al-phases cannot be protective against mineral dissolution (Berner and Holdren, 1979) may have to be reconsidered, because the reactivity of mineral surfaces is also highly localized.

ACKNOWLEDGEMENTS

The authors wish to thank the Netherlands Energy Research Foundation (ECN), in particular R. Otjes and Dr. T. Lub for their invaluable help with the column experiments. Furthermore we would like to thank Professor L. van der Plas, B. Kuiper and T. Engelsma for carrying out the mineralogical analyses, and L. Begheijn for help with the soil analyses. We also thank C. Kooge who did the EDAX measurements as part of his MSc-programme. The first author finally would like to thank Professor F.A.M. de Haan of the Dept. of Soil Science and Plant Nutrition for his overall support.

This chapter will be submitted to *Geochim. Cosmochim. Acta*.

J.J.M. van Grinsven, H. Denier van der Gon, W.H van Riemsdijk and N. van Breemen.

Chapter 10

THE ILWAS MODEL TO ANALYZE THE RESPONSE OF AN ACID FOREST SOIL TO ACID DEPOSITION AND MITIGATION MEASURES

ABSTRACT

A modified version of the ILWAS model was calibrated for an acid sandy forest soil in the Netherlands using field data for the period between April 1981 and April 1987. ILWAS overestimated water uptake reduction, which caused overestimation of soil water fluxes by 20%, as compared to values predicted by SWATRE, which model is based on Darcy flow. ILWAS does not simulate capillary rise from the groundwater which may lead to overestimation of solute concentrations near the end of the growing season. Chemical calibration of the ILWAS model to field data was mainly confined to adjustment of the rate constants for nitrification and gibbsite dissolution. Calibration of these rate constants was complicated by cation exchange, which may modify the simulated effect of nitrification and gibbsite dissolution on fluxes and concentrations of H, NH₄ and Al over periods of several years. ILWAS appeared to be too crude to simulate the N-dynamics in the soil system, which lead to a relatively strong variation of simulated [NO₃] near the end of the growing season deeper in the soil profile. After calibration the ILWAS model was used for scenario analysis. The ILWAS model predicted that reduction of the atmospheric deposition of (NH₄)₂SO₄ by 50% would have little effect on the fluxes and concentrations of H and NO₃ for the six-year time period of simulation, but would result in rapid reduction of fluxes and concentrations of Al by nearly 40%. Fertilization with 2.6 kmol_c/ha K₂SO₄ and 8.6 kmol_c/ha MgSO₄, to restore the nutrient balance in the soil system, will cause additional exchange and leaching of 3.3 kmol_c/ha Ca and 4.9 kmol_c/ha Al. The maximum predicted concentration increases, in the summer after fertilizer addition, is 15 mmol_c/L for [Al³⁺], and 0.12 mmol/L (0.2 pH unit decrease) for [H⁺] at 40 cm depth. Removal of the forest vegetation, previous to replantation, would cause an increase of net mineralization of base cations by 15 kmol_c/ha and of NO₃ by 32 kmol_c/ha over a six year period. Concentration increases in soil solution would be smaller as a result of the concurrent increase of soil water fluxes due to reduced evapotranspiration.

10.1 INTRODUCTION

Acid atmospheric deposition is an important contributor to soil acidification (Van Breemen et al, 1984). Mathematical models for soil acidification can be useful to improve our understanding of important processes and mechanisms, or to make predictions (Reuss et al., 1986). Available soil acidification models generally are integral parts of watershed acidification models (Christophersen and Wright, 1981; Goldstein et al., 1984; Cosby et al., 1985^a). Most recently developed soil acidification models are process-oriented models, which means that formulations of actual soil processes are incorporated into the models. Proposed models, however, show a wide variation with respect to the number of distinguished processes, to the degree of simplification of process formulations, and to the degree of spatial and temporal variation. Arp (1983) lumped all weathering reactions into Freundlich-, and Booty (1984) into Langmuir-type isotherms. Bloom and Grigal (1985) extended the empirical approach by Arp (1983), including pH-dependent mineral weathering of base cations, and empirical relationships between pH and base saturation, and Al-activity in solution and pH. The soil acidification module in the RAINS model (Alcamo et al., 1987) compares the acid loading to the sequence of buffer systems proposed by Ulrich (1983). In the case of acid soils with decreasing pH, silicate weathering would be followed by cation exchange below pH 5, and below pH 4.2 also by dissolution of Al. Soil solution pH is calculated either as function of base saturation (4.2pH3) or in equilibrium with gibbsite (pH). The Trickle-Down model (Schnoor et al. 1984) is based on solution of an alkalinity balance for the watershed and surface water, lumping all buffer processes in the soil into mineral weathering, at a rate depending on acid loading. Soil acidification models by Christophersen and Wright (1981), Goldstein et al. (1984), Reuss and Johnson (1985), Cosby et al. (1985^a), Van Grinsven et al. (Chapter 11: 1987^a) and De Vries (1987) are based on explicit formulations of the key soil processes, and mathematical solution is obtained by solving the charge balance. Key soil processes may include CO₂-equilibria, cation exchange, mineral weathering, anion sorption, gibbsite equilibrium, complexation reactions, nutrient uptake by plants, decay of organic matter and water transport. The models by Christophersen and Wright (BIRKENESS, 1981), Reuss and Johnson (1985), and Cosby et al. (1985; MAGIC model) enforce equilibrium with gibbsite. However, gibbsite equilibrium is not common in acid surface soils or in situations with high acid loadings (Mulder et al., 1987; Chapter 11: Van Grinsven et al., 1987^a). The ILWAS model (Goldstein et al., 1984) allows rate limited dissolution of gibbsite, and only enforces gibbsite equilibrium at occurrence of

oversaturation. The ILWAS model is the most comprehensive acidification model to date.

Although the final purpose of all referenced models is response analysis of soil-water systems to variable acid loadings, there is a great variation in the degree of discretization in time and space. All models are one-dimensional, although overland flow and interflow are considered in the BIRKENESS and ILWAS model. The size of time steps varies between one day (ILWAS) and one year (RAINS model, Alcamo et al., 1987; Bloom and Grigal, 1985). The MAGIC model lumps the soil profile to one compartment, while eg. ILWAS distinguishes genetic soil horizons. The thickness of soil compartments for the ILWAS model was varied between 0.1 and 20 m (EPRI, 1984). The RAINS model considers homogeneous grid areas of several thousand km², while the model by Bloom and Grigal (1985) is applied for specific soil profiles.

The simulation models RAINS, BIRKENESS, MAGIC and ILWAS have been subjected to sensitivity analysis, and were used to reconstruct acidification history (Cosby et al., 1985^b) or to evaluate the response of catchments to changed acid loadings. Sensitivity analysis of the RAINS model showed particular sensitivity to initial base saturation and rates of silicate weathering. Scenario analyses with both the RAINS and the MAGIC model suggested that the pH and base saturation of soil will respond very slowly to reduced levels of atmospheric deposition of SO₄. Analysis of the response of two watersheds by the ILWAS model (Fendick and Goldstein, 1986) gave no indication of a threshold response to SO₄ loading, but instead gave continuous response curves. For loading with NO₃ a threshold response was observed, as a result of an upper limit for the uptake capabilities of the biota.

This paper describes the calibration of a modified version of the ILWAS model on an acid forest soil, followed by analysis of the response of this soil to reduced deposition of (NH₄)₂SO₄, to application of readily soluble K₂SO₄ and MgSO₄ and to removal of the forest vegetation.

10.2 MATERIALS AND METHODS

10.2.1 The ILWAS model

The ILWAS (Integrated Lake Watershed Acidification Study) model (EPRI, 1983; Goldstein et al., 1984) was originally developed to predict acidification of

surface water in the USA and Canada. The ILWAS model is considered to be the most detailed catchment acidification model present to date (Reuss et al., 1986). The ILWAS model is specifically detailed with respect to the number of included processes, while the description of transport processes in soil is rather simple. Transport is described explicitly, and no measures are taken to control numerical dispersion. In view of a time step of one day, compartment sizes of about 10 cm, and a pore water velocity of about 0.5 cm/d, the numerical dispersion length will amount to 5 cm, which is several times higher than physical dispersion lengths (Bolt, 1982). However, overestimation of physical dispersion is not necessarily a serious limitation for the use of soil acidification models, as involved vertical concentration gradients are generally small.

Figure 10.1 gives a simplified flow chart of operation of the ILWAS model, with respect to hydrologic and chemical processes.

Some key processes and their mathematical formulation are:

1) Organic matter decay.

Four types of organic matter are considered, in order of increasing stability; Litter, Fine Litter, Humus and Organic acids. Organic fraction are transformed according to first order reactions with temperature dependent rate coefficients.

$$dX/dt = K X \quad (1)$$

$$K = K_0 \exp(\ln(1.05) (T-12)) \quad (2)$$

where: X is the amount of organic matter (kg/ha), K is the first order rate constant and T is temperature (°C). The release of individual components from the distinguished organic fractions are based on contents, and leaching fractions supplied by the model user.

Decay of organic matter is confined to the first soil compartment. The first decay step is leaching of cation from fresh litter. The transformation of litter to fine litter is structural, and does not produce cations. The transformation of fine litter to humus releases the remainder of the base cations. The transformation of humus to organic acids, and the subsequent break-down of organic acids produces NH₄, SO₄, CO₂. The attribution of all decay of humus and organic acids to the first soil compartment is somewhat awkward, as the larger part of humus is present in the mineral soil and not in the litter layer. A disputable part of the module for decay of organic matter in the ILWAS model is the disregard of mass loss during transformation from litter to humus.

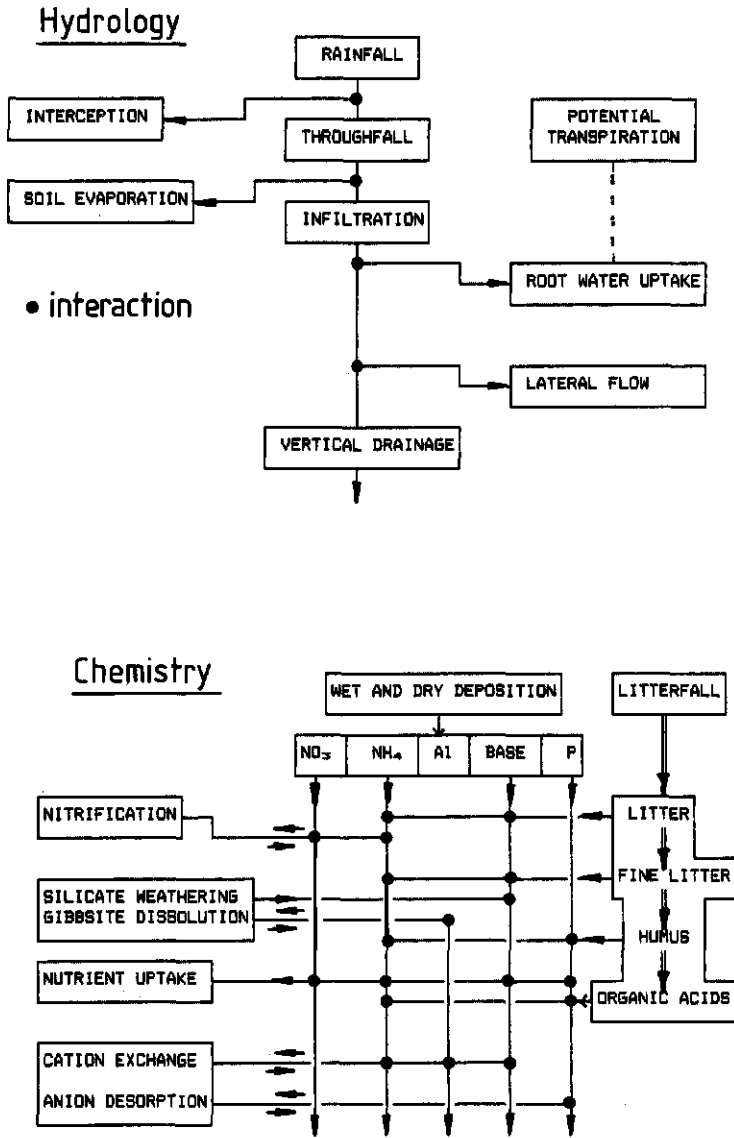


Fig. 10.1 Schematic representation of the operation of the ILWAS model with respect to soil hydrology and soil chemistry.

2) Mineral Weathering:

Separate formulations were used for weathering of base cations (K, Na, Ca and Mg) and Al. The rate equation for base cations is:

$$dM/dt = K M (H^+)^p \quad (3)$$

where: M is the actual mineral mass (mol/ha), t is time, (H⁺) is the proton activity (mol/L), p is a parameter and K is the pseudo-first order rate constant. Rates of release for individual ions are based on the reaction stoichiometry.

The rate equation for Al is:

$$r = K ([Al^{3+}]_e - [Al^{3+}]) \quad (4)$$

where: K is the rate constant for dissolution of Al(OH)₃ (L⁻¹.ha⁻¹.yr⁻¹), [Al³⁺] is the Al-concentration (mol/L), [Al³⁺]_e is the Al-concentration predicted by equilibrium with gibbsite at the prevailing pH. K depends on temperature.

3) Nitrification:

Nitrification is described by a Michaelis-Menten type of kinetic equation:

$$d[NH_4]/dt = \alpha \beta \exp(\ln(1.1) (T-20)) \frac{[NH_4]}{\gamma + [NH_4]} \quad (5)$$

where: [NH₄] is the ammonium concentration, α is a pH dependent factor, which stops nitrification below pH 2, β is the maximum nitrification rate (mol.ha⁻¹.yr⁻¹), and γ is the half saturation constant (mol/L).

4) Uptake of nutrients and water.

The nutrient demand by the plant is determined by user supplied (1) leaf and trunk composition, (2) net increase of biomass and (3) uptake distribution with month of the year and depth. Uptake reduction is determined by the component with the lowest amount in soil solution relative to the demand. Reduction of uptake will result in curtailment of growth.

The water uptake demand is determined by potential transpiration, and the water uptake distribution with depth. At water contents higher than field capacity, no reduction of water uptake is simulated. Below field capacity uptake is reduced according to:

$$d\theta/dt = -k \theta \quad (6)$$

where: θ is the volumetric water content and k is a constant. Reduction of water uptake does not cause growth curtailment.

5) Percolation

Water transport was described explicitly by a simple sequence of overflowing compartments. Below field capacity no vertical drainage takes place. Above field capacity flow to the next soil compartment is calculated according to:

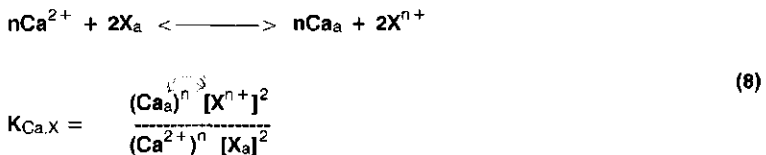
$$P = K_s \frac{(\theta - \theta_{fc})}{(\theta_s - \theta_{fc})} \quad (7)$$

where P is the percolation rate (m/d), K_s is the saturated conductivity, θ_{fc} is field capacity and θ_s is the saturated water content.

10.2.2 Modification of the ILWAS model

To simulate soil acidification processes in a Dutch acid forest soil the ILWAS model was adapted on several points:

1) The exchange of Al was included, which necessitated replacement of the original Gapon-like exchange equations by more general Gaines-Thomas-type exchange equations (Gaines and Thomas, 1953). The general formulation for Gaines-Thomas exchange, with Ca as reference ion is:



where $K_{Ca,X}$ is the selectivity coefficient, (Ca^{2+}) and (X^{n+}) are solution activities (mol/L), and $[Ca_a]$ and $[X_a]$ are adsorbed concentrations (equivalent fractions).

2) The dissolution equation for $Al(OH)_3$, was extended with a first order depletion term. The assumption that the pool of hydrous Al-oxides in Dutch acid forest soils is infinite at present rate of soil acidification, is not justified when periods of several decades are simulated (Chapter 7).

3) The ILWAS model assumes an impervious bottom soil compartment, and simulates lateral groundwater flow to generate discharge. The profile depth considered for simulation of our forest soils was one meter, and discharge was mainly caused by free drainage. Free drainage from the bottom soil compartment was built into the model, but the resulting drainage flux was converted to a lateral flux in the last line of the subroutine for simulation of hydrology, as not to interfere with the chemical and heat balance calculations in the model.

Futhermore, the simulation of canopy processes in the model, generating dry atmospheric deposition, leaf exudation and interception evaporation, and potential transpiration, was by-passed. Instead, the model was modified, to make more efficient use of the available input data from the catchment monitoring program.

10.2.3 Site characteristics and model parameterization

The soil is an Umbric Dystrachrept covered by a mixture of *Quercus robur* (L) and *Betula pendula* (L). Chemical inputs and soil solution chemistry of the Umbric Dystrachrept have been monitored since 1981, at monthly intervals. Monitoring was ended in 1987. Details on soil characteristics and field monitoring are given by Van Breemen et al. (1986, 1987, 1988). Physical and chemical model parameters are given in Table 10.1.

The soil profile was divided into 5 soil compartments (Table 10.1), representing the litter layer, the A-, B₁-, B₂- and C-horizon respectively. Field capacity is the volumetric water content at 10 kPa suction. Water uptake fractions are proportional to the compartment thicknesses, which was concluded from calibration of the SWATRE model (Chapter 3). Nutrient uptake fractions were calibrated.

Selectivity coefficients for the Gaines-Thomas exchange equation (Equation 8) were derived from annual flux-weighted mean concentrations in soil solution, and one analysis of exchangeable cations by the Bascomb method (1964).

Anion adsorption was only considered for PO₄ in order to prevent growth reduction as a result of P-shortage. SO₄ was considered to be an inert ion, except for the complexation reaction with Al.

| Soil Layer | 1 | 2 | 3 | 4 | 5 |
|--|---|---------------------|---------------------|---------------------|---------------------|
| Thickness (cm) | 5 | 10 | 10 | 20 | 60 |
| Field Capacity (vol%) | 30 | 33 | 28 | 24 | 11 |
| Saturation (vol%) | 80 | 65 | 62 | 57 | 41 |
| Water Uptake Fraction (Z) | 5 | 15 | 15 | 30 | 35 |
| Nutrient Uptake Fraction (Z) | 30 | 15 | 15 | 20 | 20 |
| N-uptake fraction (Z) | 50 | 15 | 5 | 10 | 10 |
| CEC (mmol _c /kg) | 50 | 8 | 2.8 | 2.0 | 1.0 |
| | exchangeable fractions (Z) | | | | |
| H | 26 | 52 | 50 | 52 | 49 |
| NH ₄ | 32 | 1 | 0 | 0 | 0 |
| K | 9 | 3 | 1 | 1 | 1 |
| Na | 1 | 0 | 0 | 0 | 0 |
| Ca | 16 | 8 | 2 | 1 | 2 |
| Mg | 9 | 3 | 0 | 0 | 1 |
| Al | 12 | 33 | 46 | 46 | 47 |
| | Gaines-Thomas Exchange Coefficients with Ca as reference ion | | | | |
| H | 1.3 10 ⁴ | 2.1 10 ³ | 1.5 10 ⁴ | 1.5 10 ⁵ | 3.1 10 ⁵ |
| NH ₄ | 89 | 1000 | 1000 | 1000 | 1000 |
| K | 17 | 15 | 27 | 1.7 | 1.0 |
| Na | 12 | 0.53 | 3.8 | 1.9 | 4.0 |
| Mg | 1.2 | 0.61 | 0.46 | 0.31 | 0.36 |
| Al | 0.056 | 0.045 | 16 | 2.8 | 3.2 |
| | Mineral Fractions (Z) | | | | |
| Microcline | 0.80 | 4.4 | 4.7 | 6.0 | 6.5 |
| Albite | 0.88 | 4.6 | 5.1 | 5.6 | 5.1 |
| Pseudo Ca-Mg silicate | 0.25 | 1.4 | 1.4 | 1.4 | 0.9 |
| Al(OH) ₃ | 0.07 | 0.4 | 0.7 | 0.8 | 0.2 |
| | Parameters independent of soil depth | | | | |
| Pseudo 1 st order K | | | | | |
| Microcline, Albite | | | 0.01 | | |
| Pseudo Ca-Mg silicate | | | 0.04 | | |
| Fractional order for dependence on (H ⁺) | | | 0.5 | | |
| Gibbsite dissolution K | | | 0.05 | | |
| Nitrification rate K | | | 0.30 | | |
| Gibbsite Solubility K | | | 10 ^{8.1} | | |

Table 10.1 Physical and chemical model parameters of the forest-soil system at the Hackfort estate.

| Organic Matter Decay | | | | |
|--|--------|-------------|-------|---------------|
| | Litter | Fine Litter | Humus | Organic Acids |
| Mass (t/ha) | 6.1 | 24.8 | 193 | |
| 1 st order K (yr^{-1}) | 1. | 0.2 | 0.015 | 0.10 |
| N-loss fraction | | 0.5 | 0.5 | |
| Cation leach. fraction | 0.2 | | | |

| Monthly distribution | | | | | | | | | | | | |
|----------------------|---|---|---|----|----|----|----|----|----|----|-----|----|
| | J | F | M | A | M | J | J | A | S | O | N | D |
| Litterfall (t/ha) | 0 | 0 | 0 | .1 | .1 | .3 | .5 | .5 | 1. | 2. | 1.5 | .5 |
| Uptake (Z) | 0 | 0 | 5 | 15 | 20 | 17 | 17 | 16 | 10 | 0 | 0 | 0 |

| | |
|---|-----|
| Standing biomass (t/ha) | 136 |
| Productivity ($\text{t}\cdot\text{ha}^{-1}\cdot\text{yr}^{-1}$) | 5.6 |

| | K | Ca | Mg | N | P |
|--------------------------|------|-----|-----|------|-----|
| Leaf Composition (mg/g) | 10.7 | 7.7 | 1.9 | 20.5 | 1.9 |
| Trunk Composition (mg/g) | 1.5 | 0.4 | 0.2 | 3.6 | 0.3 |

Table 10.1 (continued)

Pools of silicate minerals were based on total elemental analyses, assuming that all Na was released from albite, all K from K-feldspar (Chapter 8). A fictive mineral of similar composition as anorthite was used as a pool for Ca and Mg. All silicate minerals were assumed to dissolve incongruently to kaolinite (Chapter 8). Pseudo-first order rate constants were set equal to 0.01 yr^{-1} for K and Na and 0.04 for Ca and Mg, and the fractional exponent to 0.5 . Actual silicate weathering rates at a soil pH of 4 are 1% of the rate constant. Resulting weathering fluxes for the individual base cations range from 0.25 to $0.4 \text{ kmol}_c\cdot\text{ha}^{-1}\cdot\text{yr}^{-1}$, which is in accordance with weathering rates implied from field mass balance studies (Van Breemen, 1986; Bloom and Grigal, 1985; Velbel, 1985). Dissolution of $\text{Al}(\text{OH})_3$ was assumed to be the only mineral source of Al (Chapter 7). Rate constants for nitrification and gibbsite dissolution were calibrated.

Data for the chemical composition of tree leaves and trunk, as well as net forest growth, were obtained from De Visser (1986). Leaf exudation of particularly K, Ca and Mg were not added to the throughfall input but to litterfall, as part of the cycling of elements through the vegetation. Data on the sizes of the organic matter fractions were taken from Winkels (1985). First order decay constants were initially chosen assuming that present pools represent steady-state values. Litterfall data were obtained from Van Breemen et al. (1988).

Hydrologic input consisted of daily throughfall and the evaporative demand for the soil surface and the vegetation. Daily throughfall was derived from daily rainfall and bi-weekly throughfall according to the procedure given in Chapter 3 (Van Grinsven et al., 1987^b). Evaporative demand was obtained from Penman data provided by the Royal Dutch Meteorological Institute.

Chemical input consisted of monthly concentrations in rainfall for all ions except NH_4 , SO_4 and H. Concentrations were multiplied by the monthly ratio of rainfall over throughfall to account for evaporative concentration due to interception. Monthly concentration data for NH_4 , SO_4 and H were equal to those observed in throughfall.

10.2.4 Model calibration

For calibration and validation of the model the period from April 1981 to April 1987 was considered. Hydrologic years were considered instead of calendar years to avoid large storage changes of water and solutes. The model was not calibrated with respect to soil hydrology. Approximate chemical calibration was accomplished by comparing simulated annual chemical soil fluxes from ILWAS with fluxes obtained by multiplying measured soil solution concentrations and soil water fluxes simulated by the SWATRE model. Specific calibration of the model was obtained by superimposing simulated time series of soil solution concentrations on field observations. Model parameters which were adjusted for calibration were (1) the decay rate constant and decay stoichiometry for litter and fine litter, (2) the soil nitrification rate constant (β , Equation 5), and (3) uptake distribution with depth of nitrogen, and (4) the gibbsite dissolution rate constant (Equation 4). The period from April 1981 to April 1983 was used for calibration.

Plots of simulated time series of soil solution concentrations are based on mean values per 10 d. Flux weighted concentrations are the ratios of solute fluxes and water fluxes.

10.2.5 Scenarios

After calibration of the model, three scenarios with adjusted boundary conditions were evaluated:

- 1) A 50% reduction of atmospheric deposition of $(\text{NH}_4)_2\text{SO}_4$
- 2) Fertilization with 2.6 kmol_c/ha K_2SO_4 and 8.4 kmol_c/ha MgSO_4
- 3) Removal of the forest.

Reduction of deposition in scenario 1 was started in April 1982. Scenario 2 is based on a fertilizer experiment in Harderwijk in a stand of *Pinus Silvestris* (L) (Van Diest, 1986). The object of this experiment was to show that atmospheric deposition of N would be consumed by the vegetation provided that adequate amounts of K, Na, Ca and P were added. Ca was added as lime (93 kmol_c/ha CaO) to increase pH and to neutralize the acid effects of the sulphate fertilizers. The lime addition could not be simulated because the ILWAS model has no option yet for simulating equilibrium with CaCO_3 . Therefore, the simulation by no means evaluates the integral fertilizer experiment. In Scenario 2 the fertilizers were added in December 1982. The addition of K_2SO_4 was mimicked by wet deposition, equally distributed over a period of three months. The kieserite was added as a new mineral to the forest floor dissolving with a first order decay constant of 2 yr⁻¹.

For Scenario 3 we assumed that the forest was felled in March 1981 and that all woody parts were removed from the site. In view of the poor vitality of many coniferous forest stands in the Netherlands (Staatsbosbeheer, 1987), large scale removal of the forest vegetation and replantation may be considered. We assumed that in the following growing season the site was recovered by a ground vegetation. The assumed effects of this change of vegetation were a reduction of (1) water uptake by 50% to account for reduced transpiration and interception, (2) of nutrient demand and (3) litterfall by 50%, and of atmospheric deposition of $(\text{NH}_4)_2\text{SO}_4$ by 50%. All reductions were activated in April 1981. Uptake of water and nutrients was confined to the upper 4 soil compartments (40 cm depth). The uptake distribution for water was changed to 30%-30%-20%-20% and for nutrients to 60%-20%-10%-10% over the upper four soil compartments. Not considered were decomposition of the old tree roots. Decomposition of fine roots may cause considerable release of N (Hauhs, 1985). We also did not consider addition of fertilizer after clear-cut, which is a common practice in forestry.

10.3 RESULTS AND DISCUSSION

10.3.1 Simulation of water fluxes and [Cl]

Annual soil water fluxes simulated by the ILWAS model were compared to values obtained from the SWATRE model (Chapter 3; Van Grinsven et al., 1987^b). An additional check on hydrology was obtained by comparing measured and simulated concentrations of Cl, which is an inert ion in ILWAS, except for negligible mineralization and uptake. The precipitation surplus simulated by ILWAS (Table 10.3) is about 20% (Table 10.4) higher than that simulated by SWATRE (Table 10.2).

| | H ₂ O | H | K | Na | Ca | Mg | Al | NH ₄ | NO ₃ | SO ₄ | Cl | Si |
|-------------------|------------------|---|-------------|-------------|-------------|-------------|--------------|-----------------|-----------------|-----------------|-------------|-------------|
| Year | (mm) | Throughfall Flux (kmol_c.ha⁻¹.yr⁻¹) | | | | | | | | | | |
| 81 | 517 | 0.17 | 0.85 | 0.95 | 0.57 | 0.38 | 0.00 | 3.18 | 0.95 | 3.18 | 1.17 | 0.00 |
| 82 | 513 | 0.14 | 1.03 | 1.07 | 0.62 | 0.39 | 0.00 | 2.73 | 0.87 | 2.60 | 1.55 | 0.00 |
| 83 | 624 | 0.03 | 1.58 | 1.20 | 0.74 | 0.62 | 0.00 | 3.06 | 1.24 | 3.19 | 1.48 | 0.00 |
| 84 | 516 | 0.05 | 1.31 | 0.74 | 0.53 | 0.40 | 0.00 | 2.87 | 1.24 | 2.66 | 1.00 | 0.00 |
| 85 | 536 | 0.08 | 1.08 | 0.99 | 0.61 | 0.38 | 0.00 | 2.45 | 0.95 | 2.12 | 1.11 | 0.00 |
| 86 | 505 | 0.05 | 1.31 | 1.48 | 0.57 | 0.46 | 0.00 | 2.94 | 1.94 | 2.35 | 1.75 | 0.00 |
| Sum | 3211 | 0.52 | 7.16 | 6.43 | 3.64 | 2.63 | 0.00 | 17.23 | 7.19 | 16.10 | 8.06 | 0.00 |
| | | Soil Flux at 90 cm depth (kmol_c.ha⁻¹.yr⁻¹) | | | | | | | | | | |
| 81 | 188 | 0.05 | 0.31 | 0.45 | 0.73 | 0.52 | 2.85 | 0.09 | 1.00 | 3.00 | 0.42 | 0.72 |
| 82 | 166 | 0.18 | 0.12 | 0.53 | 0.55 | 0.38 | 3.63 | 0.01 | 1.87 | 2.35 | 0.83 | 0.46 |
| 83 | 264 | 0.30 | 0.21 | 0.71 | 0.96 | 0.48 | 4.98 | 0.02 | 2.92 | 3.53 | 1.23 | 0.75 |
| 84 | 206 | 0.19 | 0.16 | 0.65 | 0.70 | 0.39 | 4.54 | 0.05 | 3.51 | 2.32 | 0.72 | 0.67 |
| 85 | 112 | 0.12 | 0.14 | 0.32 | 0.56 | 0.32 | 3.28 | 0.00 | 3.24 | 1.04 | 0.32 | 0.33 |
| 86 | 214 | 0.22 | 0.21 | 0.58 | 0.89 | 0.45 | 4.84 | 0.00 | 3.62 | 2.35 | 1.08 | 0.93 |
| Sum | 1150 | 1.06 | 1.15 | 3.24 | 4.39 | 2.54 | 24.17 | 0.17 | 16.16 | 14.59 | 4.60 | 3.86 |
| Depth (cm) | | Mean Annual (1981-1987) Solute Flux (kmol_c.ha⁻¹.yr⁻¹) | | | | | | | | | | |
| T ¹ | 535 | 0.09 | 1.19 | 1.07 | 0.61 | 0.44 | 0.00 | 2.87 | 1.20 | 2.68 | 1.34 | 0.00 |
| 10 | 472 | 3.23 | 1.45 | 0.91 | 1.77 | 0.97 | 2.03 | 0.65 | 5.72 | 2.97 | 1.11 | 1.46 |
| 40 | 298 | 0.44 | 0.58 | 0.64 | 1.28 | 0.68 | 5.25 | 0.18 | 4.83 | 2.56 | 0.99 | 1.11 |
| 90 | 192 | 0.18 | 0.19 | 0.54 | 0.73 | 0.42 | 4.02 | 0.03 | 2.69 | 2.43 | 0.77 | 0.64 |
| | | Mean Annual (1981-1987) Flux Weighted Concentration (mol_c/m³) | | | | | | | | | | |
| T | 0.02 | 0.22 | 0.20 | 0.11 | 0.08 | 0.00 | 0.54 | 0.23 | 0.50 | 0.25 | 0.00 | |
| 10 | 0.70 | 0.31 | 0.20 | 0.38 | 0.21 | 0.44 | 0.14 | 1.22 | 0.63 | 0.24 | 0.32 | |
| 40 | 0.15 | 0.19 | 0.22 | 0.43 | 0.23 | 1.79 | 0.06 | 1.65 | 0.88 | 0.34 | 0.38 | |
| 90 | 0.09 | 0.10 | 0.28 | 0.39 | 0.23 | 2.16 | 0.01 | 1.51 | 1.25 | 0.39 | 0.33 | |

¹ T stands for values in throughfall

Table 10.2 Throughfall fluxes, and soil fluxes of water and solutes calculated by multiplying observed concentrations and observed (throughfall) or simulated (soil) water fluxes. All results are based on monthly values of

| | H ₂ O | H | K | Na | Ca | Mg | Al | NH ₄ | NO ₃ | SO ₄ | Cl | Si |
|-------------------|---|-------------|-------------|-------------|-------------|-------------|--------------|-----------------|-----------------|-----------------|-------------|-------------|
| Year (mm) | Throughfall Flux (kmol_c.ha⁻¹.yr⁻¹) | | | | | | | | | | | |
| 81 | 517 | 0.00 | 0.04 | 0.83 | 0.33 | 0.19 | 0.00 | 3.33 | 0.54 | 3.50 | 0.83 | 0.00 |
| 82 | 546 | 0.00 | 0.04 | 0.96 | 0.43 | 0.24 | 0.00 | 2.99 | 0.51 | 3.21 | 1.04 | 0.00 |
| 83 | 592 | 0.00 | 0.08 | 0.88 | 0.46 | 0.23 | 0.00 | 2.94 | 0.67 | 3.05 | 0.87 | 0.00 |
| 84 | 489 | 0.00 | 0.07 | 0.78 | 0.46 | 0.19 | 0.00 | 4.12 | 0.63 | 4.17 | 0.87 | 0.00 |
| 85 | 516 | 0.00 | 0.06 | 0.71 | 0.56 | 0.20 | 0.00 | 4.08 | 0.76 | 4.18 | 0.74 | 0.00 |
| 86 | 490 | 0.00 | 0.06 | 1.12 | 0.47 | 0.27 | 0.00 | 3.24 | 0.64 | 3.81 | 1.15 | 0.00 |
| Sum | 3150 | 0.00 | 0.35 | 5.28 | 2.71 | 1.32 | 0.00 | 20.70 | 3.75 | 21.92 | 5.50 | 0.00 |
| | Soil Flux at 100 cm depth (kmol_c.ha⁻¹.yr⁻¹) | | | | | | | | | | | |
| 81 | 221 | 0.22 | 0.64 | 0.84 | 1.23 | 0.61 | 4.46 | 0.00 | 2.77 | 3.35 | 1.03 | 1.15 |
| 82 | 236 | 0.24 | 0.74 | 0.96 | 1.52 | 0.80 | 4.69 | 0.00 | 4.36 | 3.54 | 0.96 | 1.56 |
| 83 | 297 | 0.28 | 0.82 | 0.99 | 1.62 | 0.79 | 3.74 | 0.00 | 4.26 | 2.82 | 1.00 | 1.46 |
| 84 | 237 | 0.23 | 0.53 | 0.87 | 1.26 | 0.57 | 3.37 | 0.00 | 2.44 | 3.58 | 0.70 | 1.42 |
| 85 | 223 | 0.25 | 0.55 | 1.00 | 1.32 | 0.63 | 5.08 | 0.00 | 4.61 | 3.23 | 0.94 | 1.63 |
| 86 | 225 | 0.26 | 0.54 | 1.11 | 1.15 | 0.63 | 5.77 | 0.00 | 4.08 | 4.60 | 1.00 | 1.73 |
| Sum | 1439 | 1.48 | 3.82 | 5.77 | 8.10 | 4.03 | 27.11 | 0.00 | 22.52 | 21.12 | 5.63 | 8.95 |
| Depth (cm) | Mean Annual (1981-1987) Solute Flux (kmol_c.ha⁻¹.yr⁻¹) | | | | | | | | | | | |
| T | 525 | 0.00 | 0.05 | 0.88 | 0.45 | 0.22 | 0.00 | 3.45 | 0.63 | 3.65 | 0.92 | 0.00 |
| 10 | 423 | 3.63 | 1.15 | 0.71 | 2.23 | 0.97 | 1.68 | 0.17 | 6.11 | 3.72 | 0.96 | 0.20 |
| 40 | 312 | 0.66 | 0.80 | 0.83 | 1.47 | 0.74 | 4.80 | 0.00 | 4.81 | 3.54 | 0.95 | 0.63 |
| 100 | 257 | 0.25 | 0.64 | 0.96 | 1.35 | 0.67 | 4.52 | 0.00 | 3.75 | 3.52 | 0.94 | 1.49 |
| | Mean Annual (1981-1987) Flux Weighted Concentration (mol_c/m³) | | | | | | | | | | | |
| T | 0.00 | 0.01 | 0.17 | 0.09 | 0.04 | 0.00 | 0.66 | 0.12 | 0.70 | 0.18 | 0.00 | |
| 10 | 0.86 | 0.28 | 0.17 | 0.53 | 0.23 | 0.41 | 0.04 | 1.46 | 0.89 | 0.23 | 0.05 | |
| 40 | 0.21 | 0.25 | 0.27 | 0.47 | 0.24 | 1.56 | 0.00 | 1.55 | 1.15 | 0.31 | 0.20 | |
| 100 | 0.10 | 0.26 | 0.40 | 0.56 | 0.28 | 1.92 | 0.00 | 1.57 | 1.49 | 0.40 | 0.63 | |

Table 10.3 Throughfall fluxes, soil fluxes and flux weighted concentrations simulated by the ILWAS model after calibration.

In the SWATRE model root water uptake is reduced below a water potential of -50 kPa, proportional to the reciprocal value of water potential (Chapter 3). In ILWAS, root water uptake is reduced below field capacity (exponentially with θ ; Equation 6), which for Dutch soils with shallow groundwater tables, is equivalent to reduction already below -10 kPa. Differences between soil water fluxes simulated by ILWAS and SWATRE at 10 and 40 cm depth are +12 and -5% respectively, indicating that differences in water uptake are largest in the 4th and 5th soil compartment. Reduction of water uptake by ILWAS will be most extreme when field capacity is low, as is the case for compartment 5.

| Depth H ₂ O | H | K | Na | Ca | Mg | Al | NH ₄ | NO ₃ | SO ₄ | Cl | Si | |
|--|--------------------------------|-------|-------|------|------|------|------------------|-----------------|-----------------|------|------|------|
| (cm)(mm/mm) | Ratio of Ion Equivalent Fluxes | | | | | | | | | | | |
| T ¹ | 1.02 | ERR | 20.88 | 1.21 | 1.37 | 2.00 | ERR ² | 0.85 | 1.93 | 0.75 | 1.46 | ERR |
| 10 | 1.12 | 0.97 | 1.58 | 1.31 | 0.81 | 1.02 | 3.02 | 3.88 | 0.96 | 0.81 | 1.15 | 7.68 |
| 40 | 0.95 | 0.70 | 0.74 | 0.78 | 0.86 | 0.95 | 1.11 | ERR | 1.04 | 0.74 | 1.05 | 1.80 |
| 100 | 0.79 | 0.70 | 0.31 | 0.57 | 0.55 | 0.64 | 0.93 | ERR | 0.75 | 0.72 | 0.83 | 0.44 |
| Ratio of Flux Weighted Ion Equivalent Concentrations | | | | | | | | | | | | |
| T | ERR | 17.84 | 1.14 | 1.29 | 1.89 | ERR | 0.78 | 1.58 | 0.72 | 1.35 | ERR | ERR |
| 10 | 0.78 | 1.45 | 1.25 | 0.65 | 0.86 | 2.74 | 5.56 | 0.81 | 0.73 | 1.08 | 6.01 | |
| 40 | 1.09 | 0.93 | 0.85 | 0.97 | 1.02 | 1.10 | ERR | 1.10 | 0.78 | 1.10 | 1.76 | |
| 100 | 0.97 | 0.43 | 0.74 | 0.69 | 0.83 | 1.21 | ERR | 0.96 | 0.94 | 1.04 | 0.62 | |

¹ T stands for values in throughfall
² ERR indicates denominator zero

Table 10.4 Mean annual ratios of observed over simulated values of water and solute fluxes, and flux weighted concentrations, for the period from April 1981 to April 1987. Field values are based on observed concentrations and

Simulated and measured concentrations of Cl at 90 cm depth are shown in Figure 10.3. ILWAS predicts extreme concentration peaks near the end of summer and in autumn. Such concentration peaks are not generally observed in the field, except in 1985. Isolated peak concentrations of Cl were observed in 1983, 1984 and 1986. In general ILWAS simulates no net flow of water below a depth of 40 cm throughout the growing season (Figure 10.2), which causes a

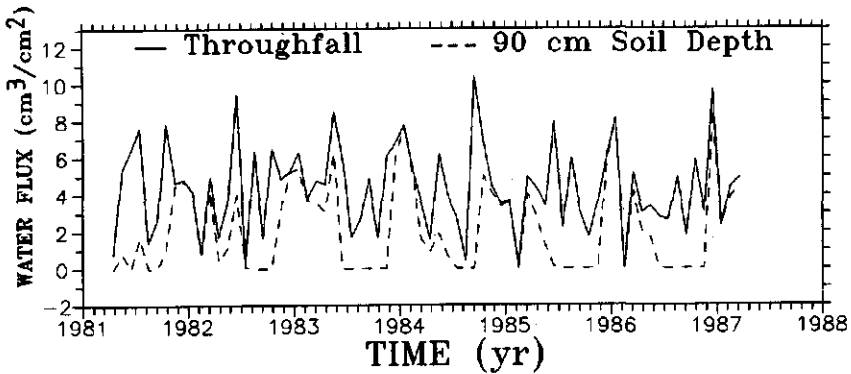


Fig. 10.2 Observed monthly water fluxes in throughfall and simulated soil water fluxes at 100 cm depth.

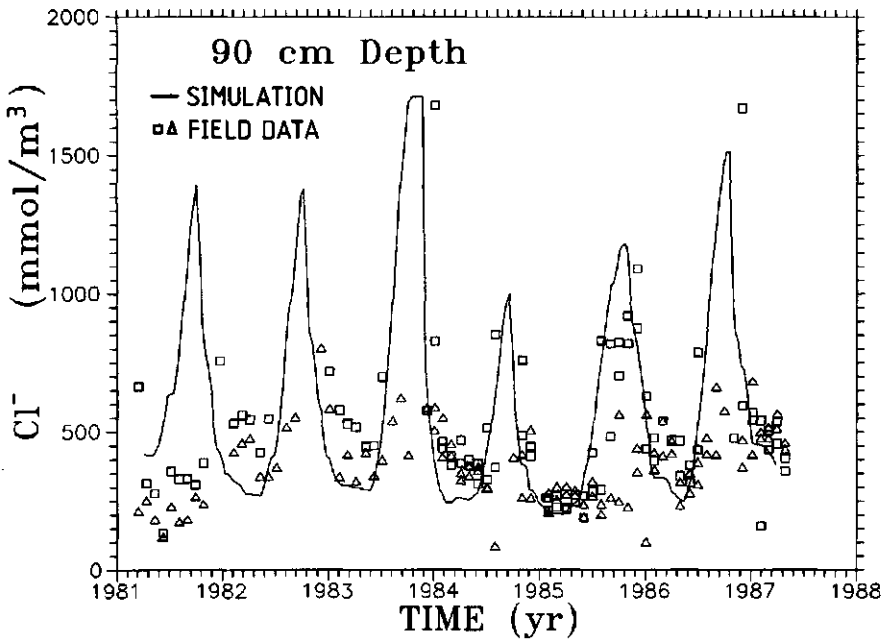


Fig. 10.3 Concentrations of Cl^- at 90 cm depth from April 1981 to April 1987 simulated by the ILWAS model and observed in two replicate field profiles.

continuous gradual decrease of the water content and increase of $[\text{Cl}]$. The SWATRE model generally simulated small upward capillary fluxes, in the order of 5 mm/month (Chapter 3), from the groundwater near the end of summer and in fall. Capillary rise of relatively dilute groundwater may explain why extremely high concentrations were not observed. In addition lysimeter cups do not always yield soil solution samples in dry periods, as indicated by fewer field data during occurrence of peak concentrations. This problem is smallest at 90 cm depth, due to the proximity of groundwater (about 1.5 m depth). However, one may doubt the representativeness of water samples in dry periods, because of the possibility of water transport from wetter dilute soil domains to the lysimeter cups. The occurrence of extremely high solute concentrations in sandy subsoils near the end of the growing season was confirmed by soil solution samples obtained by the centrifuge method (Kleijn et al., 1988). As high $[\text{Cl}]$ coincide with low or zero water fluxes, the possibly inaccurate prediction of $[\text{Cl}]$ by ILWAS in the dry season, has no great effect on fluxes of Cl.

Differences between observed and simulated annual fluxes of Cl are similar to those of the water fluxes, and differences of flux weighted concentrations are even smaller (Table 10.3 and 10.4).

10.3.2 Simulation of annual solute fluxes and flux weighted concentrations

On average predicted solute fluxes from the soil profile are 30% higher than those from field mass balances (Table 10.4). Estimates of flux weighted concentrations (FWC) at various depths by ILWAS and based on field observations (Table 10.4), generally agree within 15%, indicating that overestimation of solute fluxes is caused in part by overestimation of water fluxes. Differences between solute fluxes in field throughfall and throughfall used for ILWAS input represent the annual leaf leachate fluxes. Disagreement between predictions and field estimates of FWC are apparent for K, Si at all depths, and for NH_4 and Al (total aqueous Al assuming a charge of 3+) at 10 cm depth. Differences for Si are caused by not considering reprecipitation of Si in the ILWAS model. After its release from silicate minerals, Si is regarded as an inert component in ILWAS, resulting in a steady increase of the Si flux with depth. However, in the field the highest fluxes of Si were observed in the surface horizon. For the simulations we assumed in situ incongruent weathering of silicate minerals to kaolinite, while field observations indicated that assumed formation of secondary silicate minerals takes place at greater depths than the dissolution process.

Greater mobility of Si also implies mobilization of Al from silicate minerals in the surface horizons, which was not considered in ILWAS, and which may explain part of the underestimation of the Al-flux at 10 cm depth.

Rate constants for dissolution of gibbsite were the same for all soil compartments. Further increase of the gibbsite dissolution rate constant to simulate higher fluxes of Al at 10 cm depth, caused no increase of the convective Al-flux, but instead caused excessive exchange of Al against H. The consideration of both Al-exchange and fast dissolution of Al from gibbsite may lead to internal transfer of Al from oxides to the exchange complex, where either precipitation of gibbsite or the exchange complex may act as proton donor. This process was actually simulated in the hydrologic year 1984-1985 where gibbsite dissolution was $10.5 \text{ kmol}_e/\text{ha}$, being about twice as high as in the other five

years, and could not be explained by higher proton production from nitrification. The additional Al from gibbsite weathering was exchanged against H and Ca.

The underestimation of the NH₄-flux at 10 cm could not be solved by increasing the nitrification rate, because this caused a further overestimation of the NO₃-flux from the soil profile. The total throughfall flux of NH₄ for simulation over the six year period was 20% higher than the observed, while the total N-flux was identical. This discrepancy resulted from attributing increased NO₃-fluxes in throughfall (eg. 1984 and 1986) to dry atmospheric deposition of NH₄.

The overestimation of the K flux at 100 cm, may indicate overestimation of the weathering rate of K. Also simulated fluxes of Ca, Mg and NO₃ from the soil profiles are 25 to 35% (Table 10.4) higher than implied from the field budgets. The main causes for these discrepancies are cation exchange and net mineralization (Table 10.5).

| | H | K | Na | Ca | Mg | Al | NH ₄ | NO ₃ | SO ₄ | Cl | Si |
|----------------|-------------------------|-------------|------------|------------|------------|-------------|-----------------|-----------------|-----------------|-------------|------------|
| | (kmol _c /ha) | | | | | | | | | | |
| Deposition. | 0.0 | 0.3 | 5.3 | 2.7 | 1.3 | 0.0 | 20.7 | 3.8 | 21.9 | 5.5 | 0.0 |
| Leaching. | -1.5 | -3.8 | -5.8 | -8.1 | -4.0 | -27.1 | 0.0 | -22.5 | -21.1 | -5.6 | -9.0 |
| Exchange. | 1.3 | 0.6 | -1.6 | 1.4 | 0.2 | -9.7 | 1.1 | 0.0 | 0.0 | 0.0 | 0.0 |
| Weathering. | -45.2 | 2.4 | 2.2 | 2.0 | 1.8 | 36.7 | 0.0 | 0.0 | 0.0 | 0.0 | 8.7 |
| Net-mineralis. | -80.7 | 0.5 | 0.0 | 1.9 | 0.6 | 0.0 | 36.5 | -40.3 | -1.1 | 0.0 | 0.0 |
| Nitrification. | 118.8 | 0.0 | 0.0 | 0.0 | 0.0 | 0.0 | -59.4 | 59.4 | 0.0 | 0.0 | 0.0 |
| Storage. | -0.2 | -0.1 | -0.1 | 0.2 | 0.2 | -0.0 | 0.4 | -0.4 | 0.0 | 0.1 | 0.3 |
| Balance | -7.6 | -0.1 | 0.0 | 0.0 | 0.0 | -0.1 | -0.7 | -0.0 | -0.3 | -0.0 | 0.0 |

Table 10.5 Chemical balances for calibrated ILWAS simulation, over the period from April 1981 to April 1987.

Net mineralization of base cations was an unintentional effect of our assumption that only 90% of the N load in litterfall is taken up, to account for direct luxury uptake of N by the tree canopy. Internally, ILWAS translates reduction of uptake of N to uptake reduction of all nutrients. Net exchange of base cations is very difficult to control in the model, because yearly variation of soil solution concentrations unavoidably leads to variation of adsorbed concentrations. In this respect, the use of annual FWC for 1981 as initial condition for ILWAS may have been unfortunate. Annual FWC are artificial concentration values and, moreover, concentrations in the first year of monitoring differed somewhat (Table 10.2) from observations in the following years.

Chemical balances of H, NH₄ and NO₃ (Table 10.5) illustrate the importance of internal processes. The net flux of H⁺ from the soil system is less than 1% of the total flux, which is mainly associated with nitrification of NH₄ from mineralization. The H⁺-balance is not tight, as result of a cumulative truncation error in the modified cation exchange module in ILWAS.

10.3.3 Simulation of time series of concentration

Simulated [H⁺] in compartments 2 through 4 were generally higher than observed concentrations, which is illustrated for 10 cm depth in Figure 10.4.

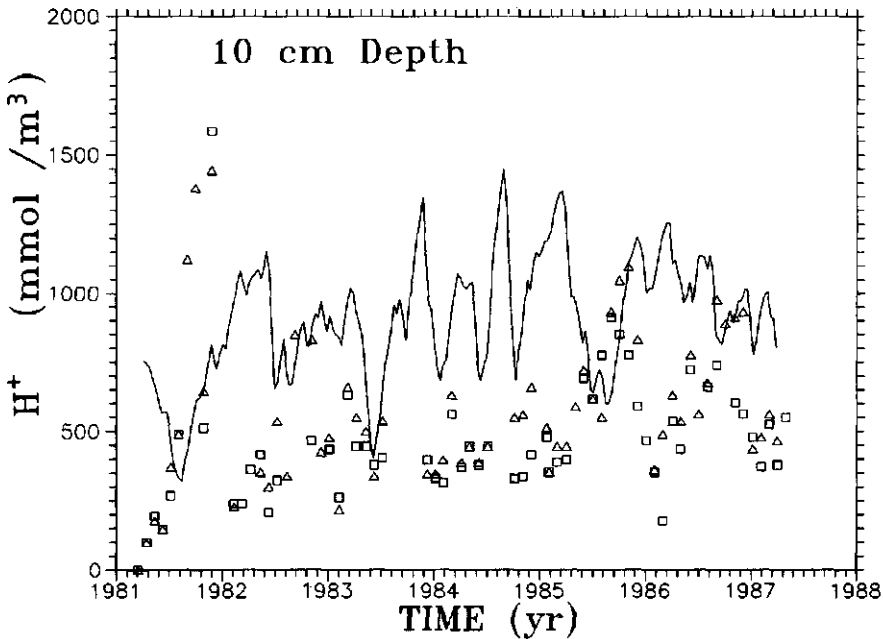


Fig. 10.4 Concentrations of H⁺ at 10 cm depth from April 1981 to April 1987 simulated by the ILWAS model and observed in two replicate field profiles.

Observed and simulated FWC compare rather well, which is mainly caused by underestimation of [H⁺] in the first hydrologic year. There is no distinct seasonal pattern for [H⁺] at 10 cm depth. Simulated short-term variation of [H⁺], which is mainly the result of variation of the nitrification of NH₄ from atmospheric deposition (Figure 10.5) and mineralization of organic matter, is more extreme

than the observed variation. Field observations suggest a very gradual increase of $[H^+]$ over the six-year period, not considering the first hydrologic year.

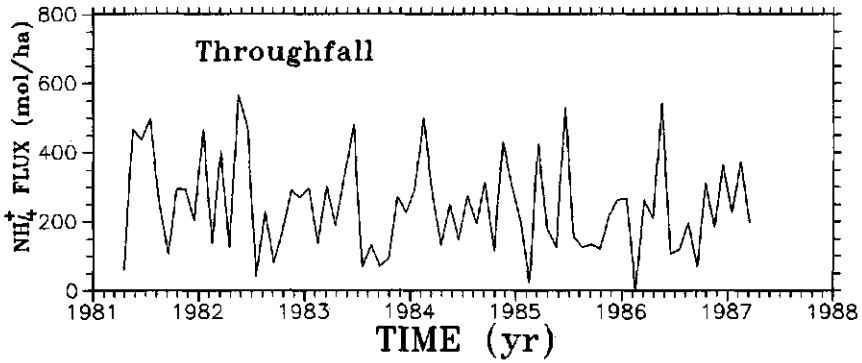


Fig. 10.5 Observed monthly total deposition of NH_4^+ in throughfall from April 1981 to April 1987.

Simulated $[Al^{3+}]$ (Figure 10.6) at 40 cm depth shows a distinct seasonal pattern which is associated with increasing concentration of the soil solution due to water uptake by roots, as was discussed for Cl.

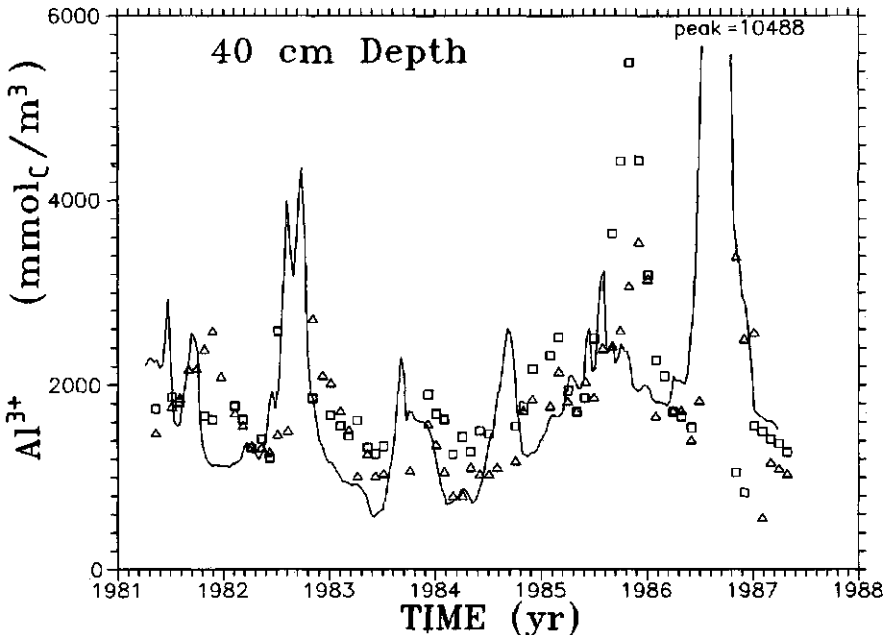


Fig. 10.6 Concentrations of Al^{3+} at 40 cm depth from April 1981 to April 1987 simulated by the ILWAS model and observed in two replicate field sites.

However, the peak height for $[Al^{3+}]$ is not correlated with the peak heights for $[Cl]$, due to the additional regulating effect of gibbsite precipitation when oversaturation occurs. Furthermore, the height of the Al-peaks is associated with the transport of Al from the upper soil compartments just before the start of the dry season. Al-transport is in part associated with transport of NO_3 , which was distinctly higher in the summer of 1985 (Figure 10.7). The summer of 1985 was the only year where a peak of Al was observed, which was distinctly higher than the simulated peak. Simulated values of $[Al^{3+}]$ compare well with field observations except for the peak values in summer. The possible causes for not observing peak concentrations were discussed for Cl. Although peak concentrations of Al are irrelevant for Al-transport, they may be relevant with respect to the biological functioning of roots and soil micro-flora and -fauna.

Concentrations of NO_3 throughout the soil profile were simulated fairly close, as illustrated for 90 cm depth (Figure 10.7) and earlier by the agreement between simulated and observed FWC (Table 10.4).

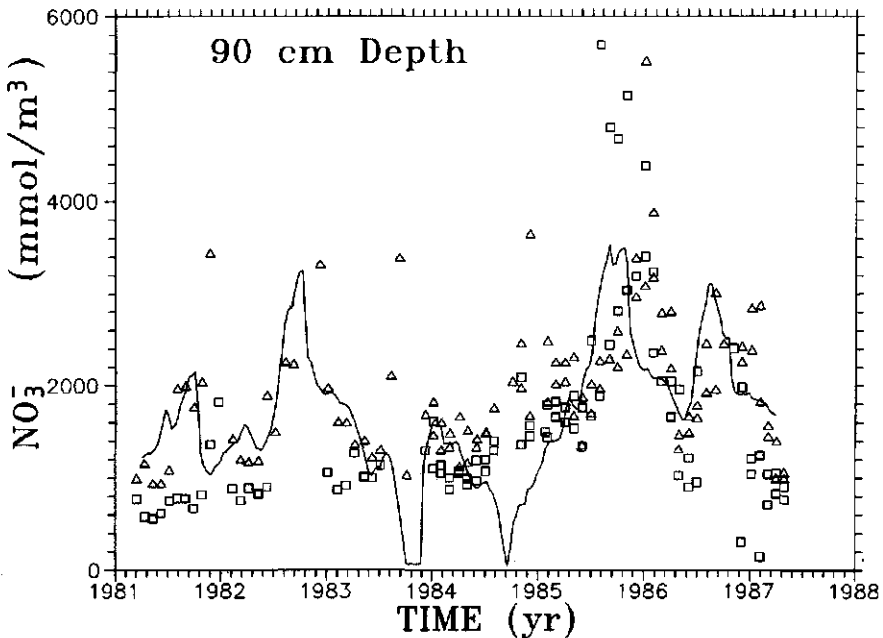


Fig. 10.7 Concentrations of NO_3^- at 90 cm depth from April 1981 to April 1987 simulated by the ILWAS model and observed in two replicate field sites.

Higher $[\text{NO}_3]$ in the summers of 1985 and 1986, relative to the other years, are both simulated and observed. The $[\text{NO}_3]$ in the subsoil towards the end of the growing season, when there is no net water transport, can become both extremely low and extremely high because of the counteracting effects of NO_3 -uptake and water uptake. Peak values of $[\text{NO}_3]$ are simulated in all summers, except in 1983 and 1984, when $[\text{NO}_3]$ become practically zero. The critical process determining the occurrence of either high or low concentration extremes is mineralization of organic N and subsequent downward transport of NO_3 just before start of the dry season. Mineralization of organic N depends on temperature according to Equation 2. Simulated soil temperatures in the forest floor vary between 6 and 15 °C (Figure 10.8), resulting in a maximum difference between mineralization rates in winter and summer of only 50%. In previous calibration runs this led to zero concentrations of NO_3 , and subsequent N-shortage for forest growth, in every growing season. To increase this difference to 500%, the temperature factor was increased to 1.2 and the no-effect temperature was decreased to 8 °C (Equation 2). Temperature correction of rate constants in ILWAS is an internal procedure which may be focussed on simulation of soil processes in alpine coniferous forest-ecosystems. Simulated soil temperatures in the winter of 1984 and the spring of 1985 were distinctly higher than in the other years (Figure 10.8), which caused a 10% increase of mineralization of organic N.

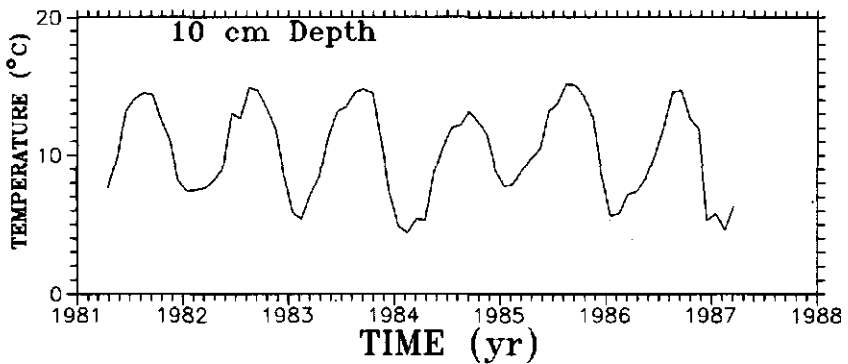


Fig. 10.8 Simulated soil temperature at 10 cm depth.

The hydrologic year 1985-1986 was the only year where mineralization of N was higher than total uptake. Simulated $[\text{NO}_3]$ in the subsoil is also extremely sensitive to the distribution of N-uptake with depth, as changing the uptake fractions by just a few percent may turn a $[\text{NO}_3]$ -maximum into a minimum. The description of N-cycling in the ILWAS, which is a key part of the model, appears to be too crude to simulate reality. The model might be improved by relating the kinetics of organic matter decay to the simulation of the microbial population dynamics, instead to instantaneous temperature effects. Further improvement of the model may be obtained by considering flexible uptake distribution of N with depth, in relation to N-availability.

10.3.4 50% reduction of atmospheric deposition of $(\text{NH}_4)_2\text{SO}_4$

Simulated solute fluxes and flux weighted concentrations after reduction of atmospheric deposition by 50% are shown in Table 10.6.

| | H | K | Na | Ca | Mg | Al | NH_4 | NO_3 | SO_4 | Si |
|---|------|------|------|------|------|-------|---------------|---------------|---------------|------|
| Soil Flux at 100 cm depth ($\text{kmol}_c\text{.ha}^{-1}\text{.yr}^{-1}$) | | | | | | | | | | |
| Year | | | | | | | | | | |
| 81 | 0.22 | 0.64 | 0.85 | 1.22 | 0.61 | 4.45 | 0.00 | 2.77 | 3.35 | 1.15 |
| 82 | 0.23 | 0.66 | 0.91 | 1.25 | 0.66 | 3.72 | 0.00 | 3.82 | 2.60 | 1.53 |
| 83 | 0.25 | 0.69 | 0.89 | 1.19 | 0.59 | 2.66 | 0.00 | 3.63 | 1.51 | 1.36 |
| 84 | 0.19 | 0.42 | 0.73 | 0.78 | 0.36 | 1.79 | 0.00 | 1.72 | 1.78 | 1.30 |
| 85 | 0.21 | 0.38 | 0.88 | 0.89 | 0.41 | 3.15 | 0.00 | 3.44 | 1.53 | 1.49 |
| 86 | 0.21 | 0.37 | 0.99 | 0.73 | 0.37 | 3.55 | 0.00 | 2.90 | 2.56 | 1.59 |
| Sum | 1.31 | 3.16 | 5.25 | 6.06 | 3.00 | 19.32 | 0.00 | 18.28 | 13.33 | 8.42 |
| Mean Annual (1982-1987) Solute Flux ($\text{kmol}_c\text{.ha}^{-1}\text{.yr}^{-1}$) | | | | | | | | | | |
| Depth (cm) | | | | | | | | | | |
| T | 0.00 | 0.00 | 0.00 | 0.00 | 0.00 | 0.00 | 1.74 | 0.00 | 1.95 | 0.00 |
| 10 | 3.21 | 1.10 | 0.64 | 1.63 | 0.68 | 0.93 | 0.16 | 5.35 | 2.10 | 0.19 |
| 40 | 0.60 | 0.64 | 0.74 | 1.18 | 0.52 | 3.37 | 0.00 | 4.12 | 2.04 | 0.66 |
| 100 | 0.22 | 0.50 | 0.88 | 0.97 | 0.48 | 2.97 | 0.00 | 3.10 | 2.00 | 1.45 |
| Mean Annual (1982-1987) Flux Weighted Concentration (mol_c/m^3) | | | | | | | | | | |
| 10 | 0.76 | 0.26 | 0.15 | 0.38 | 0.16 | 0.23 | 0.04 | 1.27 | 0.50 | 0.05 |
| 40 | 0.19 | 0.20 | 0.24 | 0.37 | 0.16 | 1.09 | 0.00 | 1.32 | 0.66 | 0.21 |
| 100 | 0.09 | 0.20 | 0.37 | 0.40 | 0.20 | 1.24 | 0.00 | 1.28 | 0.84 | 0.61 |

Table 10.6 Simulated annual solute fluxes at 100 cm soil depth, and mean annual solute fluxes and annual flux weighted concentrations in throughfall and at 10, 40 and 100 cm soil depth, after reduction of atmospheric deposition of $(\text{NH}_4)_2\text{SO}_4$ by 50% from April 1982 onwards.

A self-evident decrease of the $[H^+]$ is not predicted. The average decrease of FWC of H^+ is about 10% in all soil compartments. The decrease of $[H^+]$ at 10 cm depth (Figure 10.9) is not evenly distributed in time, but varies between 0 and 50%, depending on whether net production of H^+ is associated by nitrification of atmospheric N or organic N.

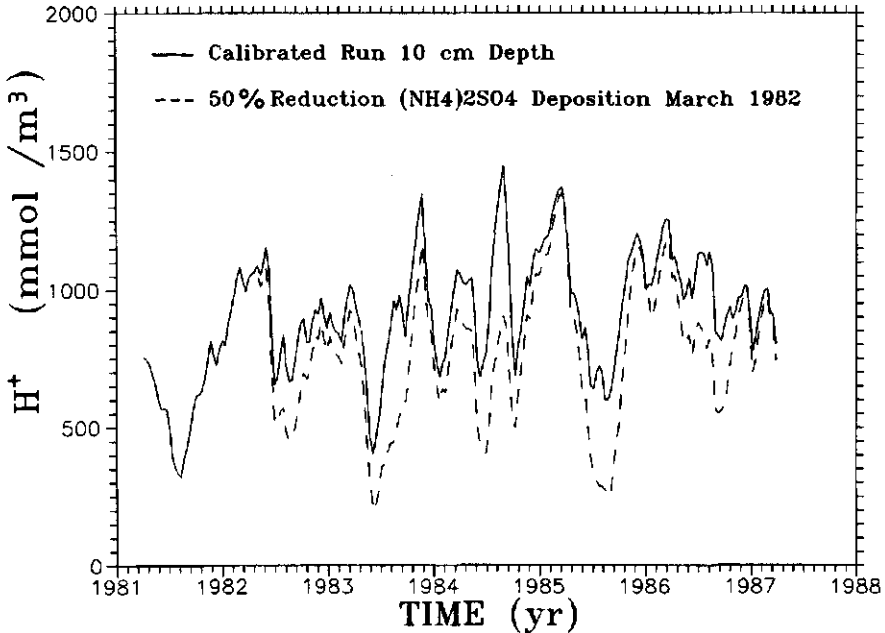


Fig. 10.9 Simulated concentrations of H^+ at 10 cm depth from April 1981 to April 1987 for present rates of atmospheric deposition of $(NH_4)_2SO_4$, and after reduction of deposition by 50% in April 1982.

The decrease of $[Al^{3+}]$ is the most apparent effect of reduced deposition. Flux weighted concentrations decrease by 44%, 30% and 35% at 10, 40 and 100 cm depth respectively. The effect is almost immediate and reaches its maximum proportion in the second year after the reduction, in accordance with a time period of about one year to flush the soil profile. The reduction of the $[Al^{3+}]$ at 40 cm depth is similar throughout all seasons (Figure 10.10). The reduction of the leaching of NO_3 from the soil profile between 1982 and 1987 is only 15%. The maximum reduction to be expected is 44% instead of 50%, because of net mineralization and net exchange of N in the calibrated run. The relatively small reduction of NO_3 leaching is caused by the strong delay of reduced leaching of atmospheric NH_4 , due to an additional loss of 3.4 kmol/ha NH_3 from the exchangeable pool between 1982 and 1987 (18%), and because part of the

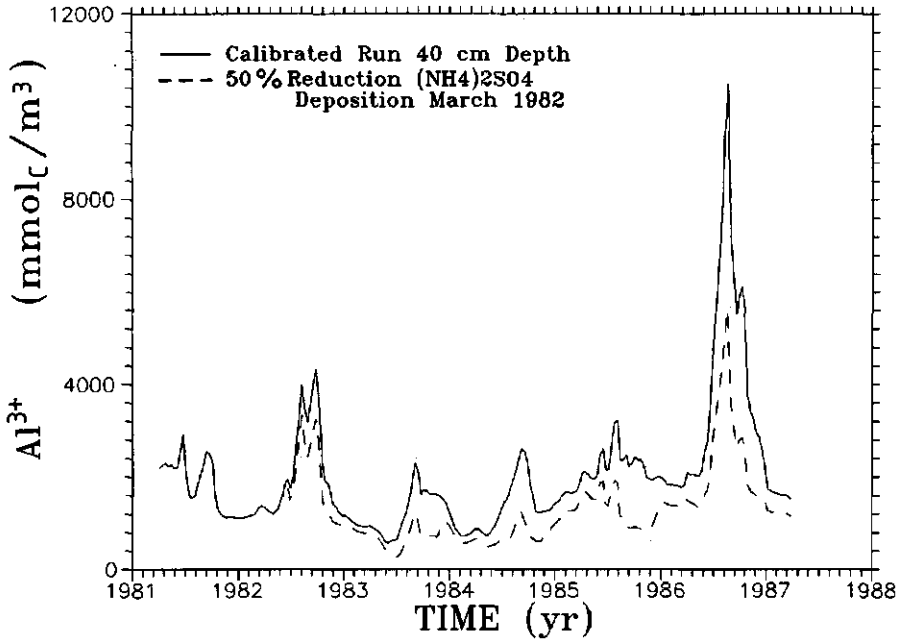


Fig. 10.10 Simulated concentrations of Al^{3+} at 40 cm depth from April 1981 to April 1987 for present rates of atmospheric deposition of $(NH_4)_2SO_4$, and after reduction of deposition by 50% in April 1982.

leaching of atmospheric N passes through the organic pools (11%). The latter effect will continue to play a role over a long period of time. In fact net leaching of N from organic pools is caused by net mineralization of N outside the growing season, which loss is compensated by net uptake of N from atmospheric deposition within the growing season.

An additional effect of reduced deposition of NH_4 is decreased losses of exchangeable base cations which amounts to 5 $kmol_c/ha$.

10.3.5 Addition of K_2SO_4 and $MgSO_4$

The added amounts of ionic K and Mg as fertilizer are initially stored on the exchange complex, while removing mainly exchangeable Ca and Al (Table 10.7). Four years after the fertilizer addition 29% of added K and 64% of added Mg are still retained on the exchange complex. Fertilizer addition has caused an additional loss of 3.25 $kmol_c/ha$ Ca from the exchange complex. Mean annual flux weighted concentrations of K, Ca and Mg are increased by 45%, 51% and 87% respectively (Table 10.8).

| Year | K | Mg | K | Ca | Mg | Al | K | Ca | Mg | Al |
|------|---------------------|------|--|-------|-------------------------------|-------|---------------------|------|------|-----|
| | | | | | (kmol_c/ha) | | | | | |
| | Fertilizer Addition | | Exchangeable Amount Relative to case with no fertilizer addition | | | | Cumulative Leaching | | | |
| 1983 | 2.80 | 4.26 | 2.33 | -1.89 | 2.97 | 1.16 | 0.07 | 0.32 | 0.18 | 1.0 |
| 1984 | | 5.18 | 1.56 | -3.34 | 6.73 | -4.93 | 0.90 | 3.04 | 1.92 | 7.7 |
| 1985 | | | 1.16 | -3.34 | 6.31 | -6.45 | 1.39 | 3.40 | 2.39 | 7.0 |
| 1986 | | | 0.88 | -3.32 | 5.86 | -5.11 | 1.75 | 3.41 | 2.84 | 5.8 |
| 1987 | | | 0.69 | -3.22 | 5.47 | -4.28 | 2.00 | 3.25 | 3.31 | 4.8 |

Table 10.7 The simulated fate of 1.4 kmol/ha K_2SO_4 and 4.7 kmol/ha MgSO_4 , added as fertilizer in December 1982, and effects on exchange and leaching of Ca and Al, as compared to a simulation without fertilizer addition.

In 1983, the year after the fertilizer was added, an enormous salt shock was predicted, when the combined addition of K and Mg exchanges against almost 5 kmol_c/ha Al. This high additional release of Al results in $[\text{Al}^{3+}]$ as high as 18 mmol_c/L in late summer at 40 cm depth (Figure 10.11), and 0.12 mmol/L (0.2 pH unit) for $[\text{H}^+]$ at 40 cm depth. A true evaluation by ILWAS of the benefit of the fertilizer operations is not possible without including soil liming. A major practical problem when liming full-grown forest stands is that the liming material can only be applied to the surface of the forest floor.

| | H | K | Na | Ca | Mg | Al | NH_4 | NO_3 | SO_4 | Si |
|------------|---|------|------|-------|------|-------|---------------|---------------|---------------|------|
| Year | Soil Flux at 100 cm depth ($\text{kmol}_c \cdot \text{ha}^{-1} \cdot \text{yr}^{-1}$) | | | | | | | | | |
| 82 | 0.26 | 0.81 | 1.10 | 4.84 | 0.98 | 5.75 | 0.00 | 4.47 | 5.15 | 1.57 |
| 83 | 0.41 | 1.65 | 1.35 | 4.34 | 2.53 | 10.44 | 0.00 | 7.22 | 12.46 | 1.75 |
| 84 | 0.26 | 1.02 | 0.88 | 1.62 | 1.04 | 2.70 | 0.00 | 2.51 | 4.28 | 1.52 |
| 85 | 0.27 | 0.91 | 0.95 | 1.33 | 1.08 | 3.83 | 0.00 | 4.18 | 3.25 | 1.66 |
| 86 | 0.28 | 0.79 | 1.06 | 0.99 | 1.10 | 4.78 | 0.00 | 3.68 | 4.60 | 1.76 |
| Sum | 1.48 | 5.18 | 5.34 | 13.12 | 6.73 | 27.50 | 0.00 | 22.06 | 29.74 | 8.26 |
| Depth (cm) | Mean Annual (1982-1987) Solute Flux ($\text{kmol}_c \cdot \text{ha}^{-1} \cdot \text{yr}^{-1}$) | | | | | | | | | |
| 10 | 3.97 | 1.73 | 0.75 | 2.75 | 1.71 | 2.68 | 0.22 | 6.81 | 6.20 | 0.22 |
| 40 | 0.71 | 1.19 | 0.87 | 2.24 | 1.48 | 5.26 | 0.00 | 5.74 | 6.08 | 0.73 |
| 100 | 0.30 | 1.04 | 1.07 | 2.62 | 1.35 | 5.50 | 0.00 | 4.41 | 5.95 | 1.65 |
| | Mean Annual (1982-1987) Flux Weighted Concentration (mol_c/m^3) | | | | | | | | | |
| 10 | 0.93 | 0.40 | 0.18 | 0.63 | 0.40 | 0.63 | 0.05 | 1.60 | 1.43 | 0.05 |
| 40 | 0.23 | 0.37 | 0.28 | 0.68 | 0.46 | 1.68 | 0.00 | 1.80 | 1.88 | 0.23 |
| 100 | 0.12 | 0.42 | 0.44 | 1.05 | 0.54 | 2.19 | 0.00 | 1.78 | 2.34 | 0.68 |

Table 10.8 Simulated annual solute fluxes at 90 cm depth, and mean annual solute fluxes and annual flux weighted concentrations at 10, 40 and 100 cm soil depth, after adding 1.4 kmol/ha K_2SO_4 and 4.7 kmol/ha MgSO_4 in December 1982.

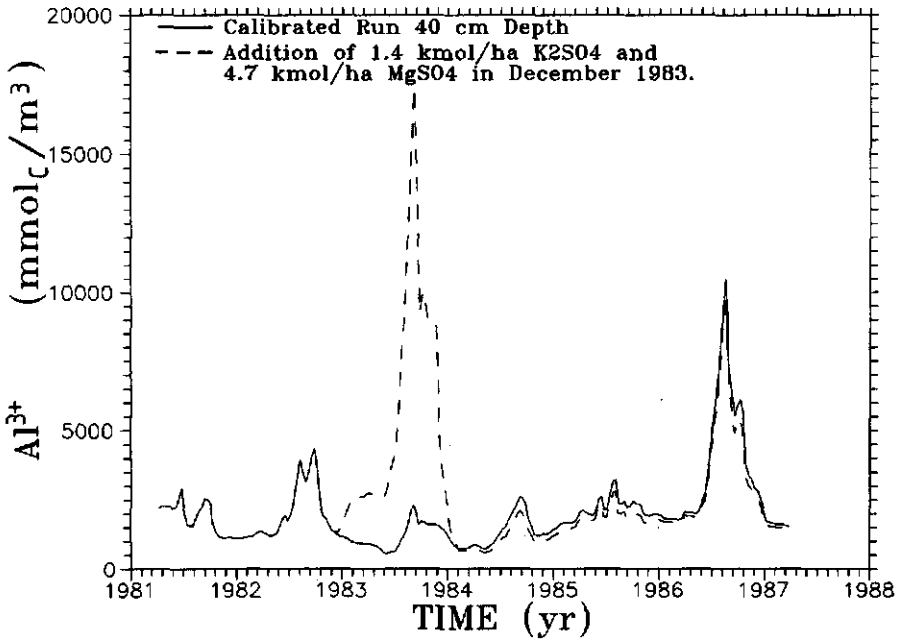


Fig. 10.11 Simulated concentrations of Al^{3+} at 40 cm depth from April 1981 to April 1987 for the calibrated model run and after addition of 1.4 kmol/ha K_2SO_4 and 4.7 kmol/ha MgSO_4 in December 1983.

Liming will increase pH in the forest floor and cause enhanced mineralization and nitrification of organic N. So in combination with addition of K_2SO_4 and MgSO_4 , a concentrated solution of nitrates and sulfates of K, Ca and Mg would infiltrate in the mineral soil and still cause a salt shock. It is not clear whether extremely high $[\text{H}^+]$ and $[\text{Al}^{3+}]$ during one growing season would cause long-term damage to the forest. Salt shocks may be prevented by adding slow release fertilizers, like eg. basalt powder, which do not produce anions of strong acids (Van Diest, 1986).

10.3.6 Removal of forest vegetation

The translation of removal of the forest vegetation into adjustments of model parameters is very approximate, and grossly simplifies the situation, but accounts for the major effects. The predominant simulated effect is a large increase of net mineralization, because element cycling for the former forest was

twice as high as for the succeeding ground vegetation. The average annual increase of the NO₃-leaching from the soil profile is 4.94 kmol/ha (Table 10.9).

| | H ₂ O | H | K | Na | Ca | Mg | Al | NH ₄ | NO ₃ | SO ₄ | Cl | Si |
|---|------------------|------|-------|------|-------|------|-------|-----------------|-----------------|-----------------|------|------|
| Soil Flux at 100 cm depth (kmol_c.ha⁻¹.yr⁻¹) | | | | | | | | | | | | |
| Year | | | | | | | | | | | | |
| 81 | 339 | 0.34 | 1.48 | 1.07 | 2.38 | 1.22 | 7.04 | 0.00 | 7.75 | 3.71 | 1.09 | 1.18 |
| 82 | 347 | 0.33 | 1.91 | 1.01 | 2.99 | 1.53 | 5.80 | 0.00 | 9.81 | 2.66 | 0.98 | 1.54 |
| 83 | 400 | 0.34 | 2.02 | 0.98 | 3.10 | 1.43 | 4.43 | 0.00 | 9.28 | 1.78 | 1.05 | 1.42 |
| 84 | 322 | 0.27 | 1.54 | 0.82 | 2.39 | 1.04 | 3.57 | 0.00 | 6.76 | 2.02 | 0.70 | 1.32 |
| 85 | 333 | 0.31 | 1.72 | 1.02 | 2.74 | 1.22 | 5.66 | 0.00 | 9.75 | 1.83 | 0.98 | 1.55 |
| 86 | 300 | 0.29 | 1.61 | 1.06 | 2.38 | 1.16 | 6.07 | 0.00 | 8.86 | 2.85 | 1.00 | 1.58 |
| Sum | 2041 | 1.88 | 10.28 | 5.96 | 15.98 | 7.60 | 32.57 | 0.00 | 52.21 | 14.85 | 5.80 | 8.59 |
| Mean Annual (1981-1987) Solute Flux (kmol_c.ha⁻¹.yr⁻¹) | | | | | | | | | | | | |
| Depth (cm) | | | | | | | | | | | | |
| T | 525 | 0.00 | 0.06 | 0.88 | 0.45 | 0.22 | 0.00 | 1.45 | 0.63 | 1.63 | 0.92 | 0.00 |
| 10 | 398 | 3.69 | 1.51 | 0.71 | 2.53 | 1.08 | 2.43 | 0.17 | 8.88 | 2.35 | 0.96 | 0.22 |
| 40 | 340 | 0.70 | 1.53 | 0.85 | 2.61 | 1.21 | 5.30 | 0.00 | 8.72 | 2.40 | 0.94 | 0.69 |
| 100 | 340 | 0.31 | 1.71 | 0.99 | 2.66 | 1.27 | 5.43 | 0.00 | 8.70 | 2.48 | 0.97 | 1.43 |
| Mean Annual (1981-1987) Flux Weighted Concentration (mol_c/m³) | | | | | | | | | | | | |
| 10 | | 0.93 | 0.38 | 0.18 | 0.63 | 0.27 | 0.63 | 0.04 | 2.24 | 0.60 | 0.24 | 0.06 |
| 40 | | 0.21 | 0.45 | 0.25 | 0.76 | 0.36 | 1.58 | 0.00 | 2.58 | 0.72 | 0.28 | 0.20 |
| 100 | | 0.09 | 0.50 | 0.29 | 0.78 | 0.37 | 1.61 | 0.00 | 2.57 | 0.74 | 0.29 | 0.42 |

Table 10.9 Simulated solute fluxes at 100 cm depth, and mean annual solute fluxes and mean annual flux weighted concentrations in throughfall and at 10, 40 and 100 cm depth, after removal of forest vegetation in March 1981.

The additional proton production due to net nitrification of organic N is buffered mainly by net mineralization of base cations at an annual average rate 2.5 kmol_c/ha. The total leaching of Al over the six year period increases by 20% in spite of the reduction of the atmospheric deposition of (NH₄)₂SO₄ by 50%, due to production of H⁺ from nitrification of organic N. Net mineralization losses of N and base cations rapidly decrease because pools of litter and fine litter gradually adjust to the new litterfall rates. At the end of simulation period the pools of litter and fine litter have decreased by 57% and 42% respectively, relative to the calibration run. Although solute fluxes increase by 20 to 50% for the major ions, the increase of FWC at 40 and 100 cm depth is much smaller due to the concurrent increase of water fluxes, which amounts to 32% at 100 cm depth.

10.4 CONCLUSIONS

The dynamics and flexibility of the ILWAS model are adequate to simulate the major features of observed seasonal and annual patterns in soil solution chemistry. Soil water fluxes calculated by ILWAS, are about 20% higher than predicted by SWATRE, due to overestimation of water uptake reduction. Not considering capillary rise from the groundwater in ILWAS may lead to overestimation of solute concentrations near the end of the growing season. Calibration of the ILWAS model to field data is mainly confined to adjustment of the rate constants of nitrification and gibbsite dissolution. Calibration of these rate constants is complicated by cation exchange which may modify the effect of nitrification and gibbsite dissolution on fluxes and concentrations of H, NH_4 and Al over periods of several years. ILWAS appears to be too crude to simulate the N dynamics in the soil system, which leads to a relatively strong variation of $[\text{NO}_3]$ near the end of the growing season deeper in the soil profile. The model may be improved by considering dynamics of the microbial populations which are responsible for mineralization and nitrification.

The ILWAS model predicted that reduction of the atmospheric deposition of $(\text{NH}_4)_2\text{SO}_4$ by 50% will result in a nearly 40% reduction of fluxes and concentrations of Al, within one year. Reduction of deposition would have little effect on the concentration of H, which is mainly determined by nitrification of organic N in the surface soil and by gibbsite equilibrium in the subsoil. Reduction of leachate fluxes of NO_3 for the six-year time period of simulation is temporarily delayed by additional production of NH_4 from the exchange complex and mineralization..

Fertilization with 2.6 kmol_c/ha K_2SO_4 and 8.2 kmol_c/ha MgSO_4 to restore the nutrient balance in the soil system would cause a strong exchange and leaching of Ca and Al. The predicted maximum concentration increases, in the summer after fertilizer addition, is 18 mmol_c/L for $[\text{Al}^{3+}]$. This salt shock would also occur when lime would have been added to the forest floor.

Removal of the forest vegetation, would lead to an increase of net mineralization of base cations by 15 kmol_c/ha and of NO_3 by 32 kmol_c/ha over a six year period. Increases of concentrations in soil solution would be smaller due to the concurrent increase of soil water fluxes due to reduced evapotranspiration.

ACKNOWLEDGEMENTS

The author is greatly indebted to Hans Kros who implemented the Gaines-Thomas exchange routine and assisted in the early simulation work with ILWAS and to Erik van Eek who contributed to acquisition of data for model input, both as part of their MSc program.

A revised version of this chapter will be submitted to the Neth. J. Agric. Sci. J.J.M. van Grinsven, N. van Breemen, W.H. van Riemsdijk, H. Kros and E. van Eek.

Chapter 11

THE SENSITIVITY OF ACID FOREST SOILS TO ACID DEPOSITION

ABSTRACT

A simple simulation model is used to evaluate the sensitivity of two Dutch acid sandy soils to acid atmospheric deposition. Processes considered are atmospheric deposition, biocycling, net uptake of nutrients, cation exchange, base cation weathering, dissolution of $Al(OH)_3$ and water balance. Present soil chemical conditions are obtained from long-term field monitoring programs, involving a podzol under pine and a chemically rich, sandy inceptisol under oak. A simulated reconstruction of the present soil solution chemistry shows the importance of the biocycle. Scenario analysis shows that the chemical status of the soil will further deteriorate slowly under present levels of atmospheric deposition. However the soil acidity would decrease quickly upon lowering of the atmospheric deposition. Forest dieback would cause a rapid increase of concentrations and leaching of base cations. Application of calcium fertilizer could only be effective if given in a slowly dissolving form. Application of readily soluble Ca would strongly increase dissolved acidity. The exhaustion of the fast buffering amorphous Al-(hydr)oxide and of Ca-containing soil minerals are potential future problems in poor sandy soils.

11.1 INTRODUCTION

Most efforts to simulate soil acidification are integrated in watershed studies (Christophersen and Wright, 1981; Goldstein et al., 1984; Cosby et al., 1985^a). Only recently long-term monitoring data have become available to specifically study the soil processes (Ulrich and Matzner, 1983; Van Breemen et al., 1986). In watershed acidification models lumped soil chemical parameters were derived from stream data by reverse modelling (Cosby et al., 1985^a) and gibbsite equilibrium is used to describe the behaviour of Al and H. In areas with low to moderate levels of acid deposition (around $1 \text{ kmol} \cdot \text{ha}^{-1} \cdot \text{yr}^{-1}$ H), gibbsite equilibrium indeed does apply in surface water, groundwater and soil water deeper in the soil profile. However in shallow soil horizons in areas with high rates of acid atmospheric deposition soil solutions are undersaturated with gibbsite. Nevertheless, fast dissolution of Al from relatively large pools of amorphous Al, will be an important mechanism of proton consumption, although

exchange processes may be equally important. However the mathematical description of exchange processes is complicated and uncertain (Reuss, 1983), especially for the adsorption of hydrogen and aluminum to the largely organic exchangers in surface horizons of sandy soils.

The use of computer models to predict the future response of soils to different scenarios of acid deposition and mitigation measures has increased strongly during the past three years (Cosby et al., 1985^b; Bloom and Grigal, 1985; Levine and Ciolkosz, 1986). The value of model predictions is limited due to uncertainties about model formulations, model parameters and initial conditions. Furthermore the response of biochemical processes, like mineralization and nutrient uptake, to a changing chemical environment can only be guessed. Present efforts to simulate soil acidification focus on the chemical output of the soil and not on the internal chemical status. The ILWAS model (Goldstein et al., 1984) is the most complete soil acidification model presently available, but it requires a large number of model parameters and it does not describe aluminum exchange.

Here we present a simple model which describes all relevant soil chemical processes. Field data from long-term monitoring programs are used to calibrate the model. Present soil chemical conditions are reconstructed with the model by simulating the soil chemistry over the past century. The reconstructed conditions are used to initiate some scenario analyses for the next two to fifty years.

11.2 THE MODEL

The model is written as a LOTUS-spreadsheet (1983), and describes a soil profile of 1 m thickness divided into three horizons. The model describes the behaviour of H, monovalent (m1) and bivalent (m2) cations, Al, NH₄, NO₃ and (SO₄ + Cl). Hydrology (infiltration, water uptake and drainage), mass transport, atmospheric deposition, biocycle (litterfall, mineralization, uptake), net uptake of nutrients, incongruent dissolution of m1 and m2 from primary minerals, dissolution and precipitation of Al(OH)₃ and exchange of m1 and m2 and Al (Table 11.1) are simulated.

| COMPONENT | H | m1 | m2 | Al | NH ₄ | NO ₃ | SO ₄ +Cl |
|---------------------|---|----|----|----|-----------------|-----------------|---------------------|
| PROCESS | | | | | | | |
| MASS TRANSPORT | + | + | + | + | + | + | + |
| ATM. DEPOSITION | + | + | + | - | + | + | + |
| BIOCYCLE | - | + | + | - | + | + | - |
| NET UPTAKE | - | + | + | - | + | + | - |
| MINERAL DISSOLUTION | + | + | + | + | - | - | - |
| PRECIPITATION | + | - | - | + | - | - | - |
| ADSORPTION | - | + | + | + | - | - | - |

Table 11.1 Summary of simulated processes and ionic species involved in each process.

By approximation the component (SO₄ + Cl) is chemically inert as the studied soil profiles are poor in sesquioxides. Complexation reactions and activity corrections were not considered.

The rate of release of m1 and m2 from primary minerals is described by:

$$r = K_1 \frac{M_t}{M_0} \tag{1}$$

- with: r = dissolution rate (kmol_c.ha⁻¹.yr⁻¹.m⁻¹)
- M₀ = initial pool of M (mass fraction)
- M_t = actual pool of M
- K₁ = constant

Dissolution and precipitation of Al is described by:

$$r = -K_2 \frac{M_t}{M_0} \log(Q/K_{so}) \tag{2}$$

- with: Q = (Al³⁺) (H⁺)⁻³ (L²/mol²)
- K_{so} = solubility constant of Al(OH)₃
- K₂ = constant: dissolution rate for LOG(Q/K_{so}) = 1

The dissolution rate of Al according to Equation 2 will decrease when saturation with Al(OH)₃ is approached. Supersaturation will result in

precipitation. Formation of fresh $\text{Al}(\text{OH})_3$ from incongruent dissolution of primary minerals was not considered.

Cation exchange was assumed to be a linear adsorption process within small concentration ranges:

$$X_{\text{ads}} = K_D X_{\text{sol}} \quad (3)$$

with: X_{ads} = adsorbed concentration (mmol_c/L)

X_{sol} = concentration in solution (mmol_c/L)

K_D = Distribution constant.

Adsorption of NH_4^+ was not considered as no adsorbed NH_4^+ could be detected.

Proton concentrations follow from the charge balance:

$$\text{In solution: } H_{\text{sol}} = \text{NO}_3 + \text{SO}_4 + \text{Cl} - \text{NH}_4 - m_1 - m_2 - \text{Al} \quad (4)$$

$$\text{On the exchange complex: Initially: } H_{\text{ads}} = \text{CEC} - m_1 - m_2 - \text{Al}, \quad (5)$$

$$\text{Afterwards: } H_{\text{ads}} = H_{\text{tot}} - H_{\text{sol}}, \quad (6)$$

in which H_{tot} is the total proton concentration.

The uptake of nutrients and water is coupled by means of an uptake fraction for all three soil compartments. Mineralization is treated in the same way as atmospheric deposition.

The final mass balance equations is solved implicitly:

$$C_{i,t+1} = \frac{\{(K_D + 1) C_{i,t} + [(C_{i-1,t+1}) S - U + W] R\}}{(K_D + 1 + R)} \quad (7)$$

with: C = concentration (mmol_c/L)

i = compartment number

t = time step (yr)

U = total uptake (mmol_c/L)

W = total weathering (mmol_c/L)

S = salt concentration factor for water from compartment i-1 infiltrating in compartment i:

$$S = J_i/J_{i-1}$$

J = percolation flux ($\text{mm}^3 \cdot \text{mm}^{-2} \cdot \text{yr}^{-1}$)

R = number of times the solution in compartment i is replaced within one time step:

$$R = \frac{(J_i t)}{(T \theta)}$$

T = thickness of compartment i (mm)

θ = volumetric water fraction in compartment i

Long time steps (up to one year) can be used because calculations are carried out with the total (solution + adsorbed) concentration. The model does not consider seasonal fluctuations.

11.3 FIELD DATA AND MODEL PARAMETERS

Two soil profiles were studied; (I) an Aquic Udipsamment (Hackfort B) and (II) a Typic Haplorthod (Tongbersven) (USDA, 1975). Vegetation on soil I is oak (*Quercus robur* (L.)), on soil B pine (*Pinus silvestris* (L.)). Data on chemical composition and quantity of bulk precipitation, throughfall, soil water and groundwater have been collected since 1981 for soil I and since 1983 for soil II. The three soil compartments considered for both soils correspond to the A-, B- and C-horizon. Details on the soil sites and field monitoring procedures are given elsewhere (Van Breemen et al., 1988; Van Grinsven et al., 1987^b; Van Dobben and Mulder, 1988).

Soil properties that serve for model input and model initiation are summarized in Tables 11.2 and 11.3.

The biocycling was assumed to be equal to the annual litterfall. The net uptake was determined in a tree biomass study (Van Breemen et al., 1988).

The value of M_0 for Al_2O_3 (Equation 2) refers to "free" Al as determined by the oxalate-dithionite extraction. The M_0 values for m1 and m2 were calculated from total elemental analysis (X-ray fluorescence spectroscopy), adding all Na_2O to K_2O and all MgO to CaO .

| SOIL I: HACKFORD B. | | | | | | | | | | |
|-----------------------------|--|-----------------|------------------|--------------------|------------------------|---|---------------------|-----|-----|-----|
| COMPONENT | H | m1 | m2 | Al | NH ₄ | NO ₃ | SO ₄ +Cl | | | |
| BOUNDARY FLUX | (kmol _c .ha ⁻¹ .yr ⁻¹) | | | | | | | | | |
| Atmosph. Deposition | 0.10 | 0.90 | 0.60 | 0.00 | 3.00 | 0.50 | 4.10 | | | |
| Biocycle | 0.00 | 2.20 | 3.40 | 0.00 | 2.20 | 7.80 | 0.00 | | | |
| Net uptake | 0.00 | 0.30 | 0.50 | 0.00 | 0.20 | 1.00 | 0.00 | | | |
| SOIL SOLUTION CONCENTRATION | (mmol _c .L ⁻¹) | | | | | | | | | |
| A-horizon | 0.49 | 0.49 | 0.57 | 0.49 | 0.25 | 1.43 | 0.85 | | | |
| B-horizon | 0.31 | 0.41 | 0.70 | 1.16 | 0.15 | 1.25 | 1.48 | | | |
| C-horizon | 0.09 | 0.39 | 0.72 | 1.80 | 0.07 | 1.12 | 1.95 | | | |
| | K _D | CEC | | M ₀ | | r | | | | |
| | m ¹⁺ | m ²⁺ | Al ³⁺ | m ₂ O | mO | Al ₂ O ₃ | m1 | m2 | Al | |
| | - (mmol _c .kg ⁻¹) - | | | - (mass%) - | | (kmol _c .(ha.m.yr) ⁻¹) | | | | |
| A-horizon | 5 | 21 | 129 | 70 | 1.66 | 0.26 | 0.50 | 0.4 | 0.4 | 5.0 |
| B-horizon | 4 | 4 | 40 | 23 | 1.91 | 0.28 | 0.72 | 0.4 | 0.4 | 5.0 |
| C-horizon | 4 | 14 | 24 | 10 | 2.06 | 0.29 | 0.16 | 0.4 | 0.4 | 5.0 |
| | Thickness (cm) | Theta | Uptake Fraction | Infiltration: | 55 cm.yr ⁻¹ | | | | | |
| A-horizon | 10 | 0.35 | 0.20 | Transpiration: | 34 cm.yr ⁻¹ | | | | | |
| B-horizon | 30 | 0.25 | 0.60 | Rooting depth: | 50 cm | | | | | |
| C-horizon | 60 | 0.15 | 0.20 | Bulk Density: | 1.2 g.cm ⁻³ | | | | | |
| | | | | Nitrification: | 95 % | | | | | |
| | | | | Biocycle Litterl.: | 40 % | | | | | |

Table 11.2 Overview of soil chemical and soil physical properties of soils I, averaged up for 1981-1986.

Adsorbed concentrations were determined by an unbuffered BaCl₂ extraction (Bascomb, 1964). Distribution constants were calculated from adsorbed concentrations and average annual, water flux-weighted soil solution concentrations.

11.4 SIMULATION PROCEDURES

A standard set of simulations was carried out.

A: Calibration of actual transpiration and fraction of biocycling within litter-layer.

The litter-layer was not considered. The actual transpiration was calculated by fitting the average measured electrolyte concentration in the third

compartment (which lies beyond the influence of the biocycling and nutrient uptake). The distribution of nutrient uptake was assumed to be independent of depth in a fixed root zone. The fraction of biocycling which takes place within the litter-layer was calculated by fitting the electrolyte concentration in the first soil compartment.

| SOIL II: TONGBERSVEN | | | | | | | | | | |
|-----------------------------|--|-----------------|------------------|--------------------|------------------------|--------------------------------|---|-----|-----|------|
| COMPONENT | H | m1 | m2 | Al | NH ₄ | NO ₃ | SO ₄ +Cl | | | |
| BOUNDARY FLUX | (kmol _c ·ha ⁻¹ ·yr ⁻¹) | | | | | | | | | |
| Atmosph. Deposition | 0.10 | 0.70 | 0.40 | 0.00 | 4.00 | 0.10 | 5.10 | | | |
| Biocycle | 0.00 | 1.20 | 1.60 | 0.00 | 1.50 | 4.30 | 0.00 | | | |
| Net uptake | 0.00 | 0.10 | 0.30 | 0.00 | 0.00 | 0.40 | 0.00 | | | |
| SOIL SOLUTION CONCENTRATION | (mmol _c ·L ⁻¹) | | | | | | | | | |
| A-horizon | 0.81 | 0.70 | 0.26 | 0.25 | 0.31 | 1.10 | 1.22 | | | |
| B-horizon | 0.10 | 0.39 | 0.14 | 1.71 | 0.32 | 1.12 | 1.52 | | | |
| C-horizon | 0.13 | 0.32 | 0.18 | 2.21 | 0.32 | 1.16 | 2.02 | | | |
| | K _D | | CEC | | M ₀ | | r | | | |
| | m ¹⁺ | m ²⁺ | Al ³⁺ | m ₂ O | mO | Al ₂ O ₃ | m1 | m2 | Al | |
| | - (mmol _c ·kg ⁻¹) - | | | - (mass%) - | | | (kmol _c ·(ha·m·yr) ⁻¹) | | | |
| A-horizon | 5 | 10 | 150 | 25 | 0.29 | 0.01 | 0.06 | 0.2 | 0.2 | 1.0 |
| B-horizon | 5 | 10 | 245 | 127 | 0.89 | 0.05 | 1.17 | 0.2 | 0.2 | 20.0 |
| C-horizon | 5 | 10 | 10 | 10 | 1.10 | 0.13 | 0.19 | 0.2 | 0.2 | 5.0 |
| | Thickness (cm) | Theta | Uptake Fraction | Infiltration: | 50 cm·yr ⁻¹ | | | | | |
| A-horizon | 20 | 0.25 | 0.33 | Transpiration: | 25 cm·yr ⁻¹ | | | | | |
| B-horizon | 20 | 0.30 | 0.33 | Rooting Depth: | 60 cm | | | | | |
| C-horizon | 60 | 0.12 | 0.33 | Bulk Density: | 1.3 g·cm ⁻¹ | | | | | |
| | | | | Nitrification: | 80 % | | | | | |
| | | | | Biocycle Litterl.: | 50 % | | | | | |

Table 11.3 Overview of soil chemical and soil physical properties of soils II, averaged for 1983-1986.

B: Reconstruction of the stationary soil chemical status in 1888.

The stationary soil solution concentrations belonging to an assumed atmospheric deposition of (NH₄)₂SO₄ of 0.25 kmol_c·ha⁻¹·yr⁻¹ in 1888 were calculated. The dissolution rates of m1 and m2 were calculated according to:

$$r = (\text{DRAINAGE OUTPUT}) - (\text{ATMOSPHERIC DEPOSITION}) + (\text{NET UPTAKE}) \quad (8)$$

Mineral pools were assumed to be unlimited. The dissolution rate of m_2 in compartment 3 of soil I was assumed to be dependent on pH according to:

$$r = K_3 \frac{M_t}{M_0} (H^+)^{0.5} \quad (9)$$

because present drainage outputs of m_2 are higher than $0.5 \text{ kmol}_c \cdot \text{ha}^{-1} \cdot \text{yr}^{-1}$. Dissolution experiments (Chapter 8 and 9) confirm the validity of a pH dependent dissolution rate of Ca.

C: Reconstruction of the acidification history from 1888 to 1986.

The acidification during the past century due to increased atmospheric deposition was simulated assuming an annual increase of acid deposition by a constant factor. Factors of 1.0215 and 1.0184 respectively yielded the present deposition rates of 1.5 (soil I) and 2.0 (soil II) $\text{kmol} (\text{NH}_4)_2\text{SO}_4 \text{ ha}^{-1} \cdot \text{yr}^{-1}$. In this stage of calculation the dissolution rate of Al was adjusted to simulate the present concentrations of H and Al.

The scenario analyses were initiated with the simulated rather than the measured present soil chemical status. This was done to prevent artifacts in predicted future soil chemical parameters. Because the model only approximates the soil chemical processes that have lead to the present concentrations in soil solution, measured initial concentrations will also change during predictive simulation as an adjustment to inadequate model formulations and parameters.

Five scenarios were simulated. The rate of acid deposition was:

- D) maintained 50 years,
- E) reduced annually by a constant factor, amounting to 50% reduction after 50 years,
- F) maintained 50 years while reducing nutrient uptake annually by a constant factor, amounting to 50% after 50 years,
- G) maintained 10 years, after application of a slowly dissolving Ca-silicate (which consumes protons),
- H) maintained 2 years, while 20 kmol_c of gypsum was added gradually over that period.

11.5 RESULTS AND DISCUSSION

Calculated soil solution concentration of H, Al, m1, and m2 for simulation case A to H, for both soil profiles are shown in Figure 11.1.

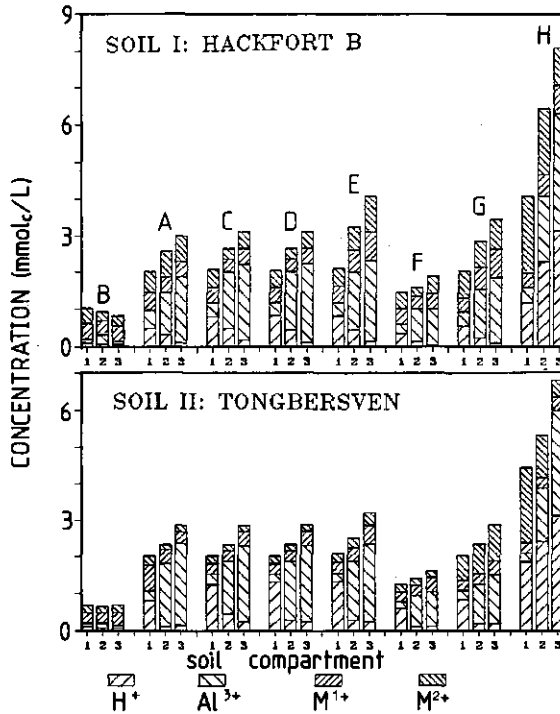


Fig. 11.1 Simulated soil solution concentrations of H⁺, Al³⁺, m¹⁺ and m²⁺ for the year 1888 (B), 1986 (A and C) and for five scenarios: in 2035 for; (D) unchanged deposition, (E) forest dieback, and (F) 50% decreased deposition; in 1996 after application of calcium-silicate (G) and in 1988 after application of gypsum (H).

The reconstructed present condition (C) compares well to the measured condition (A), except for the concentration of m1 for soil II. This concentration can not possibly be explained by present levels of atmospheric deposition and biocycling. Fast mineral dissolution is also unlikely as concentrations in the second compartment are reasonably reconstructed. Reconstructed concentrations of base cation in soil II for 1888 (B) are identical to the present conditions because the situation in 1888 was stationary and because rates of

atmospheric deposition and mineral weathering of base cations are constant (Tables 11.2 and 11.3). For soil I the m2 concentration in 1986 is higher than in 1888 due to the pH dependent dissolution rate. Reconstructed pH values in 1888 vary between 4 in the first and 4.4 in the third soil compartment.

Changes in soil chemistry in 2035 after 50 years of constant deposition levels (D) are very small. However in compartment 1 of soil II the mineral pool of m2 is depleted by 30% and of "free" Al_2O_3 by 50%. In soil I the corresponding values are 1% and 26% respectively. This depletion will cause a further decrease of pH and m2 concentrations. Forest dieback (F) leads to an increasing surplus of mineralization over nutrient uptake. As a result the concentrations of base cations and NO_3 will increase.

Concentration increases in soil II are slower due the presence of a larger exchange complex. Initially a large part of the mobilized cations will be retained by the adsorption complex. Eventually however, these cations will be leached from the soil system. The soil system responds immediately to decreased levels of acid deposition: After 50 years pH in soil I increases by 0.4 unit in compartment 1 to more than 1 unit in compartment 3. In soil II the pH increase in the third compartment is less distinct. The application of a calcium-source to mitigate soil conditions, strongly depends on the form of the fertilizer. Application of a slowly dissolving calcium-silicate (G) is most effective. Concentrations of m2 will slowly increase, while concentrations of H and Al will slowly decrease. The application of readily soluble gypsum (H) will have adverse effects. High concentrations of Ca will cause desorption of H which is not immediately buffered. The H concentration shows a maximum a few months after the start of the gypsum addition. After two years, the pH in soil I decreases to 2.9, 2.65 and 2.45, in soil II to 2.74, 2.62 and 2.51, in compartment 1, 2 and 3 respectively.

The presented simulation model is only suitable to extrapolate soil solution concentrations under constant or slowly changing rates of atmospheric deposition or fertilizer application. The total number of required parameters is about 70, of which the distribution and dissolution constants are most difficult to obtain. The assumption that the drainage outputs of base cations in 1888 are equal to present average drainage outputs is not realistic, especially when only a few years of field monitoring data are available. Also cation desorption and net mineralization can contribute to drainage outputs. These contributions are not considered as we assume a closed biocycle and a stationary state between present concentrations, deposition rates and dissolution rates of base cations.

This chapter is published in the Proc. of the international symposium "Acidification and Water Pathways", Bolkesjo, May 4-8, 1987: p. 365-374.
J.J.M van Grinsven, N. van Breemen, W.H. van Riemsdijk, and J. Mulder.

Chapter 12

THE EFFECT OF PERCOLATION RATE ON WEATHERING KINETICS

ABSTRACT

Soil columns were percolated at rates varying by a factor of 50, using sandy soil samples with very low CEC and organic matter contents. A linear decrease of concentrations of base cations and Si after column passage with increasing percolation rate, which may be expected if mineral weathering is the dominant process, was observed only by way of exception. In general the leachate concentrations increased less than proportional with the square root of residence time, which implies an increase of weathering rate with at least the square root of the percolation rate. An increase of weathering rates with percolation rate may explain part of the discrepancies between weathering rates observed in the laboratory and in the field.

12.1 INTRODUCTION

Rates of mineral weathering are essential to quantify the natural availability of K, Ca and Mg for plant growth, and to evaluate the long-term potential of regolith and soil to buffer pH. Weathering rates can be estimated from chemical budgets of catchments or soil profiles in the field, or from dissolution studies in the laboratory. However, discrepancies up to two orders of magnitude for one type soil or rock material, are commonly observed between rate values from field and laboratory studies on the one hand, and from different dissolution techniques in the laboratory on the other hand (Chapter 5). A large part of these discrepancies could be attributed to mechanical disturbance before and during laboratory experiments, which increase the reactivity of the minerals. In the absence of effects of mechanical disturbance, discrepancies up to one order of magnitude, persist between weathering rates from chemical field budgets, column experiments and unstirred batch experiments. This remaining discrepancy was attributed to effects of percolation rate (Chapter 5 and 8). An increase of weathering rate with percolation rate was observed, which was explained by a hypothetical decrease of the thickness of stagnant water films inside etch pits. This effect was observed for dissolution of base cations from silicate minerals at controlled pH, and therefore could not be caused by an effect of percolation rate

on the degree of mineral saturation, as may be expected for dissolution of calcite (Berner, 1978). The earlier observation of an effect of percolation rate on weathering rate (Chapter 5 and 8) was not unambiguous, because percolation rate was not an independent variable. Instead, the percolation rate was lowered progressively during the experiments, in proportion to the H^+ -consumption rate, in order to control pH. As a result, the effect of percolation rate was interfered by a, probably small, effect of depletion of mineral pools of cations.

This paper discusses dissolution experiments in columns, while imposing, in a random order, one of five fixed percolation rates, ranging from 20 to 2000 L/d.

12.2 MATERIALS AND METHODS

12.2.1 Soil samples and chemical analysis

Soil samples were taken from the C-horizons of an Umbric Dystrachrept (75 cm depth; Van Breemen et al., 1986), and a Typic Udipsamment (110 cm depth; Mulder et al., 1988). Details on sample pretreatment are given in Chapter 8. Subsamples (300 g) of the soil were percolated beforehand by 4 L of 0.1 mol/L HCl, in order to remove soluble salts and to exhaust highly reactive pools of cations. Experiments were carried out at room temperature. Selected chemical characteristics of both soil samples are given in Table 12.1.

| Sample | Mass fraction of fine earth (%) | | | |
|--------------|---------------------------------|-----------------------------|---------------------|------|
| | K ₂ O | Na ₂ O | CaO | MgO |
| Dystrachrept | 1.16 | 0.61 | 0.14 | 0.17 |
| Udipsamment | 0.91 | 0.53 | 0.12 | 0.07 |
| Sample | Organic C (%) | CEC (mmol _c /kg) | Base Saturation (%) | |
| | | | | |
| Dystrachrept | 0.12 | 13 | 2 | |
| Udipsamment | 0.29 | 5 | <5 | |

Table 12.1 Selected chemical characteristics of soil samples

Before storage, leachate samples were passed over a 0.45 μ m filter, and acidified. Si was determined by Colorimetry and K, Na, Ca and Mg were

determined by Atomic Absorption Spectrometry. Analytical errors for Ca and Si were less than $1 \text{ mmol}_{(c)}/\text{m}^3$, and for Mg was $0.2 \text{ mmol}_{(c)}/\text{m}^3$.

12.2.2 Column experiments

The column percolation technique is described in detail in Chapter 7. Columns were percolated with $3 \times 10^{-4} \text{ mol/L}$ HCl. Prior to experiments the soil columns were flushed thoroughly with the $3 \times 10^{-4} \text{ mol/L}$ HCl solution to remove the concentrated strong acid solution. The range of pH in the leachate between the highest and the lowest percolation rate, was 3.9 ± 0.2 to 4.1 ± 0.1 for the Dystrochrept and $3.80.1$ to $3.90.1$ for the Udipsamment sample. One peristaltic pump controlled percolation rates in two duplicate columns. Selected percolation rates were 2000, 650, 320, 80 and 40 mL/d. Selected percolation rates were applied three times in a random order, but not before the other four rates had been applied. Percolation rates were maintained until at least 10 pore volumes had passed the column. Chemical analysis was carried on the last pore volumes, collected during application of one percolation rate.

12.2.3 Computational procedures

The hypothesis to be tested is that weathering rate is independent of percolation rate, which implies that the concentration increase of base cations and Si due to mineral weathering is inversely proportional to the percolation rate, or proportional to residence time of pore water in the column. A precondition for testing this hypothesis is that production of base cations and Si in the column from cation exchange and mineralization of organic matter is negligible. This assumption seems justified in view of a small CEC (about $10 \text{ mmol}_{(c)}/\text{kg}$) and undetectable amounts of exchangeable base cations, and low contents of organic C with negligible amounts of structural base cations. Consumption of base cations from mineral weathering by exchange may play a role in batch experiments, but probably is insignificant in the column experiments because continuous flushing prevent build-up of concentrations. Concentration contributions from colloidal material, mobilized by physical weathering, may play a role, in particular for Si, but this effect was reduced by filtration over $0.45 \text{ }\mu\text{m}$.

A simple formulation for the relationship between the concentration increase from weathering in the soil column, dC (mol/m^3), and the pore water residence time, s (s), is:

$$dC = \alpha \tau^\beta \quad (1)$$

$$\tau = V/P$$

where P is the percolation rate (m^3/s), V is the pore volume of the soil core (m^3), and α ($\text{mol}\cdot\text{m}^{-3}\cdot\text{s}^{-1}$) and β are parameters. The weathering rate R (mol/s) is obtained by multiplying dC and P :

$$R = \alpha P^{(1-\beta)} \quad (2)$$

If R is independent of percolation rate, the parameter has the value 1. Equation 1 was fitted to the concentration data for fixed values of β of 0, 0.5 and 1 by linear regression. The goodness-of-fit for the different regression analyses was evaluated by examining a Normalized Standard Error of Regression (Steel and Torrie, 1986):

$$\text{NSER} = (\text{SSQ}_r/n)^{0.5}/m \quad (3)$$

where SSQ_r is the sum of residual squares about regression, n is number of degrees of freedom and m is the sample mean.

12.3 RESULTS AND DISCUSSION

Concentrations of K and Mg for both samples, and of Ca for the Udipsamment sample in the leachate were only a few times higher than the detection limit. However, coefficients of variation for duplicate experiments, averaged for all percolation rates, generally were less than 20%, also for Mg (Table 12.2). In Figure 12.1^a and 12.1^b the NSER for regression analyses with $\beta = 0$, $\beta = 0.5$ and $\beta = 1$ is plotted against NSER for $\beta = 1$.

For the majority of the elements, NSER's for $\beta = 0$ or $\beta = 0.5$ are smaller than for $\beta = 1$. This means that $(1-\beta)$ in Equation 2 is larger than zero, and that the weathering rate increases with percolation rate. In terms of scoring, giving 2 points, for the lowest NSER, 1 point for the second lowest NSER and 0 points for highest NSER, scores for the regression analyses on the data for the

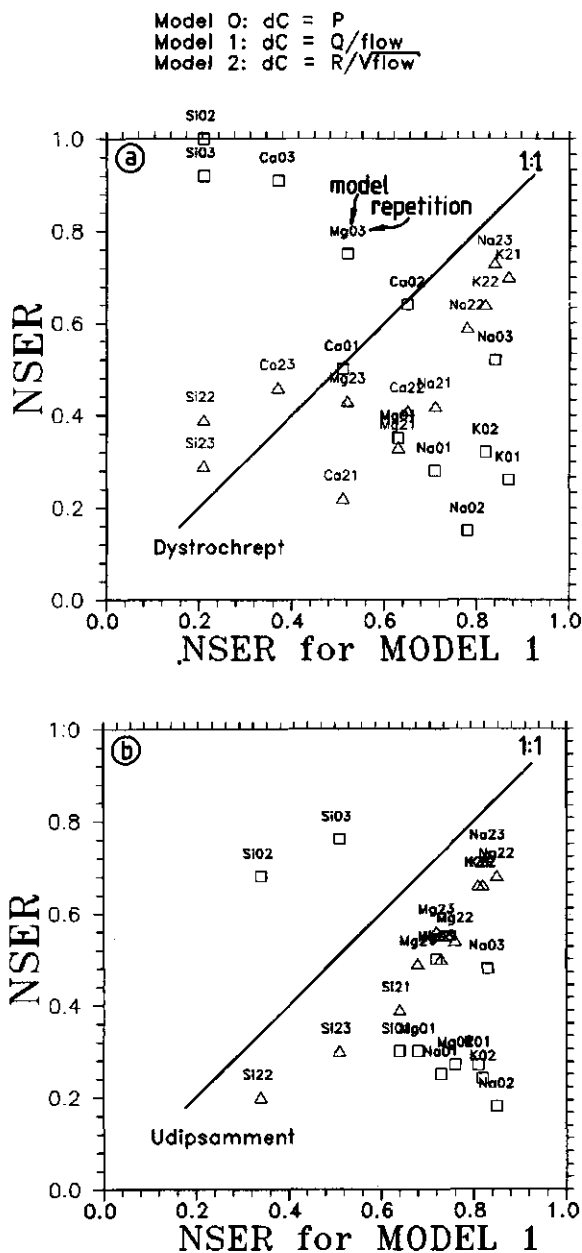


Fig. 12.1 The normalized standard error of regression (NSER) for fits of leachate concentrations as a function of residence time by a power-type relationship with a fixed exponent (β) of 0 (model 0), 1 (model 1) and 0.5 (model 2), plotted as a function of NSER for model 1, using data for (a) the Dystrochrept sample and (b) the Udipsammet sample.

| | Dystrochrept Sample | | | | Udipsamment Sample | | | |
|---------------|---------------------|---------|----------|---------|--------------------|---------|----------|---------|
| | Ca | | Mg | | Si | | Mg | |
| | α | β | α | β | α | β | α | β |
| Repetition 1 | 2.48 | 0.43 | 0.24 | 0.19 | 6.44 | 0.22 | 0.30 | 0.09 |
| Repetition 2 | 0.67 | 0.59 | 0.13 | 0.27 | 0.96 | 0.42 | 0.27 | 0.06 |
| Repetition 3 | 1.48 | 0.42 | 0.04 | 0.44 | 0.37 | 0.59 | 0.13 | 0.17 |
| Average CV(Z) | 8.4 | | 10.3 | | 2.6 | | 9.4 | |

Table 12.2 Regression coefficients for a power-type relationship between concentration increase after column passage and percolation rate, and average coefficients of variation (CV) of concentrations from duplicate observations.

Dystrochrept sample are 16, 18 and 8, and for Udipsamment sample 20, 14, 1, for values of β of 0, 0.5 and 1 respectively. Values of NSER were not considered when they were larger than 1 for all values of β , which indicates strong variation of the concentration data. Values of β lower than 1 were most apparent for Ca and Mg for the Dystrochrept sample and, for Mg and Si for the Udipsamment sample. Results of the regression analysis for these cases are shown in Figures 12.2^a to 12.2^d and in Table 12.2.

For Si and Ca there is a distinct, but less than linear increase of concentration with increasing residence time (Figure 12.2^a and 12.2^c). For Mg there is hardly an effect of residence time on the

concentration increase although the residence time is varied by a factor of 50 (Figure 12.2^b and 12.2^d). A less than linear effect of percolation rate on the concentration increase due to weathering, strongly indicates an effect of percolation rate on weathering kinetics, but might also be related to variation of pH with percolation rate or to cation exchange.

Increase of percolation rate will cause a decrease of pH in the pore water which will accelerate weathering reactions and counteract the net increase of concentration in the leachate. Assuming a square root increase of weathering rate with (H^+) (Chapter 8), the observed variation of (H^+) by a factor of 3 (0.5 pH unit) would cause a variation of weathering by a factor 1.7. This effect of pH is negligible compared to an expected variation of leachate concentrations due to variation of the percolation rate by a factor of 50.

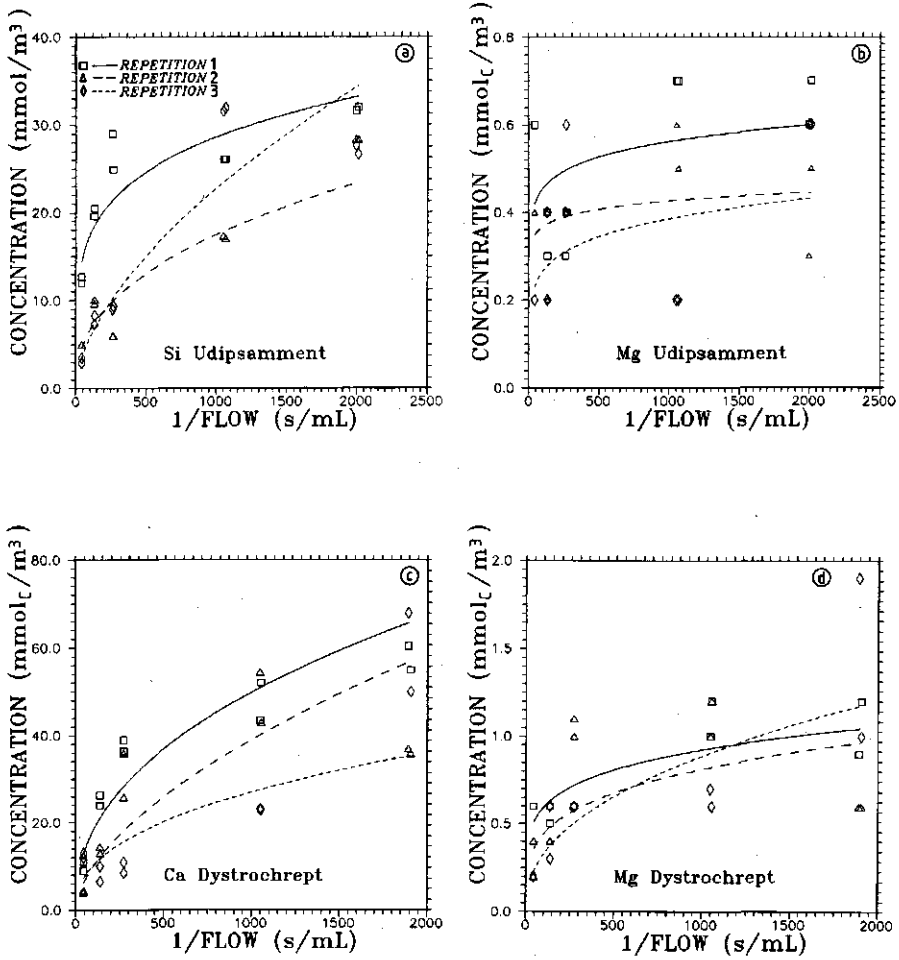


Fig. 12.2 The concentration increase of (a) Si and (b) Ca for the Udipsamment sample, and (c) Ca and (d) Mg for the Dystrochrept sample after leaching with 3×10^{-4} mol/L HCl at varying percolation rates.

The CEC for the column sample (40 g) was about 0.4 mmol_c, and initial exchangeable base cations were less than 0.004 mmol_c, on a total percolated volume of about 4 L. In view of the previous leaching step with 0.1 M HCl, net production from cation exchange can be ruled out completely. However, the CEC is sufficiently large to modify changes of cation concentrations, but then it is still remarkable that only downward modifications of the concentration were observed. Furthermore, cation exchange cannot explain the effect of percolation rate on the weathering rate of Si.

Most experiments showed a decrease of production rates of cations and Si in time. Important depletion effects may be considered unlikely because of the pretreatment with strong acid (pH 1) and in view of relatively constant base cation weathering rates which were observed in long-term column (9 months) experiments (Chapter 13).

12.4 CONCLUSIONS

A linear decrease of concentrations of base cations and Si with increasing percolation rate in leachates from column experiments, which may be expected if mineral weathering is the dominant process, was observed only by way of exception. In general the leachate concentrations increased less than proportional with the square root of residence time, which implies an increase of weathering rate with at least the square root of the percolation rate. Cation exchange may have modified an expected linear relationship between percolation rate and concentration increase in the leachate due to weathering. However, the general observation of a less than linear effect, irrespective of the direction of the changes of percolation rate, cannot be explained by effects of cation exchange. An increase of weathering rates with percolation rate may explain part of the discrepancies between weathering rates observed in the laboratory and in the field. For elucidation of the mechanism underlying this effect of percolation rate experiments with pure, well-defined minerals, may give further support to our conclusions.

ACKNOWLEDGEMENTS

The author wishes to thank Hans van den Dool, who took care of the experimental work in this study as part of his MSc program.

Chapter 13

WEATHERING RATES FROM LONG-TERM COLUMN EXPERIMENTS

ABSTRACT

Undisturbed soil cores and packed soil cores were leached with 3 mmol/L HCl at a percolation rate of 42 ml/d over a period of 267 d. Dissolution of Al from the crystalline oxide pool was the dominant proton consuming process. With progress of reaction the dissolution rate of Al showed two distinct plateaux, which could not be associated with depletion of specific fractions of extractable Al. Rates of cation release both increased in time (Mg), decreased in time (Ca), or remained constant (Na), in relation to the counteracting effects of increasing mineral depletion and increasing (H^+).

13.1 INTRODUCTION

Mineral weathering and atmospheric deposition are the major natural sources of base cations (K, Ca and Mg) for forest growth. Rates of mineral weathering in acid forest soils are generally low, due to low contents and low reactivity of feldspars. Dissolution experiments in the laboratory are the easiest way of determining weathering rates. The kinetics of feldspar weathering depend on pH and the reactivity of the surfaces. Particularly in the initial stage of dissolution experiments, rates of release of cations tend to decrease rapidly, partly because of salt effects and cation exchange, but also due to a rapid depletion of pools of most reactive minerals. The weathering kinetics are sensitive to experimental conditions, in particular to mechanical disturbance, due to sample pretreatment or stirring. In case of column experiments weathering kinetics also depend on percolation rate (Chapter 5, 8 and 12). As a result, observed weathering rates in different types of batch experiments and column experiments may vary over several orders of magnitude, and are generally far higher than observed in field mass balance studies (Chapter 5 and 8). In general the agreement between weathering rates from laboratory studies and field studies will increase with increasing resemblance between experimental conditions and field conditions. Therefore, best laboratory estimates of weathering rates in the field are obtained in unstirred batch experiment and column experiments at low flow rates. However, an important remaining difference between soils in the field and soil

samples in laboratory experiments concerns the degree of saturation with water. In most laboratory experiments samples will be saturated, while soils in the field are generally partially saturated with water.

This paper describes results of column experiments at low flow rates (45 mL/d which is equivalent to 20 mm/d) which were continued for nine months. Low flow rates resulted in incomplete saturation of the pore volume with water. Packed columns were compared with undisturbed soil cores, excavated in the field.

13.2 MATERIALS AND METHODS

Soil samples were taken at 65 cm depth, in the C-horizon of an Umbric Dystrochrept. The soil sample had a low CEC of about 10 mmol_c/kg. Exchangeable base cations were undetectable (<0.1 mmol_c/kg). Fine earth contained 1.16% K₂O, 0.61% NaO, 0.14% CaO and 0.17% MgO. Examination of feldspars in the fine sand fraction (50-420 μm) by means of the optical microscope revealed contents of 12% of K-feldspars and 6% of plagioclases. Undisturbed soil samples were excavated in the field with stainless steel boxes, from which undisturbed soil cores were obtained in the laboratory. The soil material for the packed soil cores was sieved to remove roots and stones, and freeze-dried for storage. These mild pretreatments were used in earlier dissolution studies to allow long-term storage of the soil material and to prepare the soil material for column experiments at high flow rates (Chapter 5 and 7). Duplicate column experiments were carried out with disturbed, packed cores and with undisturbed cores. Soil cores were 5 cm high and 5 cm in diameter, weighed about 120 g, and were enclosed in between 2 cm thick layers of inert quartz, to obtain homogeneous throughflow. Columns were percolated at a nearly constant rate of about 42 mL/d with 3 mmol/L HCl (pH = 2.5), which was withdrawn from one 10 L vessel, and applied through syringe needles by means of one peristaltic pump. The pump tubing and stock solution were replaced every 2 to 3 months. Column outflow was collected daily by means of an automatic sampler. Until d 30 daily leachate samples were pooled every 2 d, from d 31 to 70 daily samples were analyzed, from d 71 to 184 samples were pooled every three d, and from d 185 onwards every 5 d. Samples were analyzed for pH by potentiometry, for Ca, Mg, K and Na by Atomic Absorption Spectrometry, and for Al and Si by colorimetric methods.

At the end of the experiment (d 267), samples of the untreated soil material, and samples of the upper, middle and low part of the leached soil cores, were extracted with 1 M KCl, 0.1 M NH₄-oxalate and Na-dithionite (Begheijn, 1980)

Extraction with KCl gives exchangeable Al, extraction with NH₄-oxalate releases exchangeable Al, organically complexed Al and Al in amorphous oxides, while extraction with Na-dithionite also dissolves crystalline Al-oxides.

13.3 RESULTS AND DISCUSSION

13.3.1 Aluminum and hydrogen

The percolation rates with time for the disturbed and undisturbed soil column are shown in Figure 13.1.

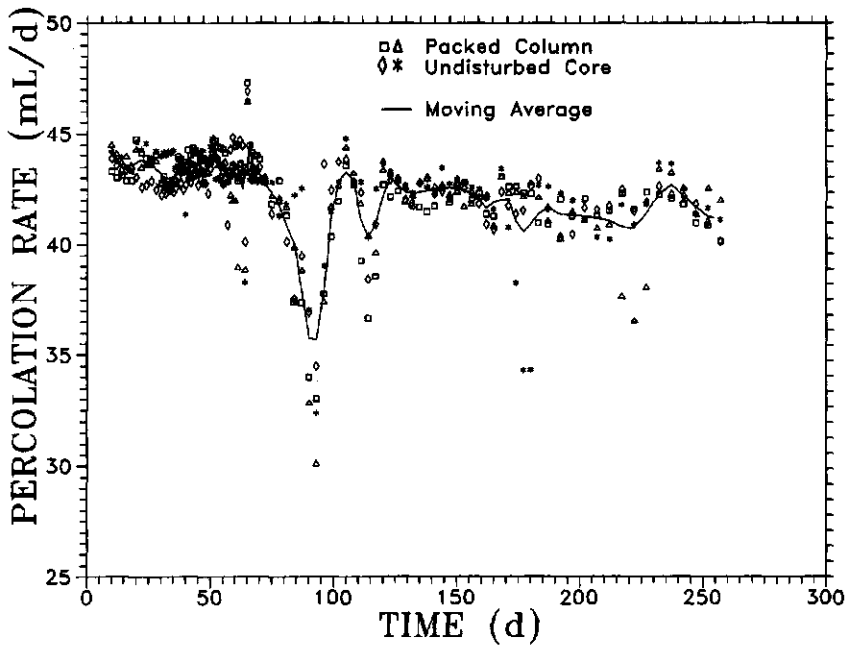


Fig. 13.1 Percolation rates for duplicate column leaching experiments using packed cores and undisturbed soil cores.

Lower percolation rates between d 70 and d 100 were caused by clogging of the tubing for column inflow. In spite of the regular replacement of the pump tubing, there was a gradual decrease of the pumping rate from 44 mL/d initially to 41 mL/d at the end of the experiment. Leaching rates of H and Al are shown in Figure 13.2.

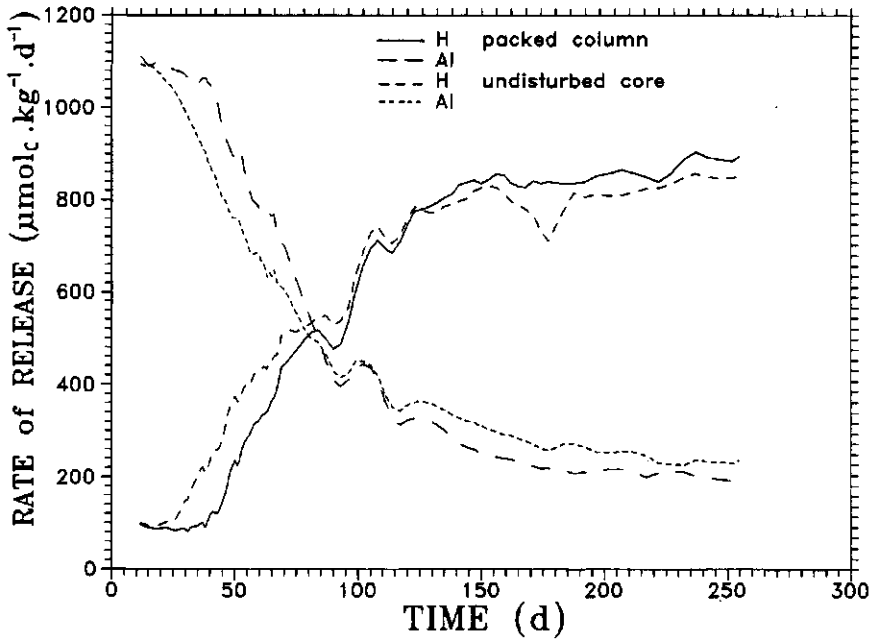


Fig. 13.2 Rates of release of H and Al during percolation of packed and undisturbed soil cores with 3 mmol/L HCl.

Rates of release were obtained using moving averages per 6 observations (three observations in time for duplicate experiments). The decrease of the leaching rates of H^+ was almost perfectly inversely proportional to the increase of the leaching rates of Al^{3+} , indicating that dissolution of Al is the main buffering process. The rate of Al release showed two apparent plateaux, one near $1100 \mu\text{mol}_c \cdot \text{kg}^{-1} \cdot \text{d}^{-1}$ from day 5 to 40 and at the other near $200 \mu\text{mol}_c \cdot \text{kg}^{-1} \cdot \text{d}^{-1}$ from about day 160 onwards. The occurrence of the first plateau coincided with high degrees of saturation ($\log(Q_{50}) = 8$) with respect to $\text{Al}(\text{OH})_3$ in the leachates. After about 40 d leaching rates of Al started to decrease rapidly until d 120. The occurrence of the first inflection point corresponds to a total leaching of approximately $40 \text{ mmol}_c/\text{kg}$ Al. The second inflection point corresponds to $110 \text{ mmol}_c/\text{kg}$ Al leaching. These values of Al depletion do not clearly correspond to one of the extractable fractions of Al (Table 13.1). Crystalline Al-oxides form the dominant fraction of reactive Al. The Al-fractions extractable with KCl and Na-oxalate, both on average decreased by 56% during the experiments. The decrease of the dithionite extractable fraction for the disturbed soil cores (31%) was markedly higher than for the undisturbed soil cores (13%).

| | KCl | $(\text{NH}_4)_2\text{C}_2\text{O}_4$ (mmol _c /kg) | $\text{Na}_2\text{S}_2\text{O}_4$ | Leached |
|----------|-------------|--|-----------------------------------|----------|
| | Untreated | | | |
| | 16.1 ± 0.1 | 2 41.0 ± 0.0 | 2 257.2 ± 8.0 | 6 |
| | Disturbed | | | |
| Column 1 | 6.8 ± 0.7 | 6 17.5 ± 1.6 | 6 198.2 ± 22.8 | 12 120.7 |
| Column 2 | 6.2 ± 0.5 | 6 13.8 ± 2.3 | 6 158.2 ± 14.1 | 12 119.0 |
| | Undisturbed | | | |
| Column 1 | 7.6 ± 1.4 | 6 20.3 ± 3.5 | 6 221.5 ± 30.9 | 8 121.3 |
| Column 2 | 7.6 ± 1.0 | 6 20.5 ± 1.9 | 6 214.8 ± 18.3 | 12 120.5 |

Table 13.1 Fractions of Al extractable with 1 M KCl, 0.2 M NH_4 -oxalate and $\text{Na}_2\text{S}_2\text{O}_4$ before and after the column leaching experiments.

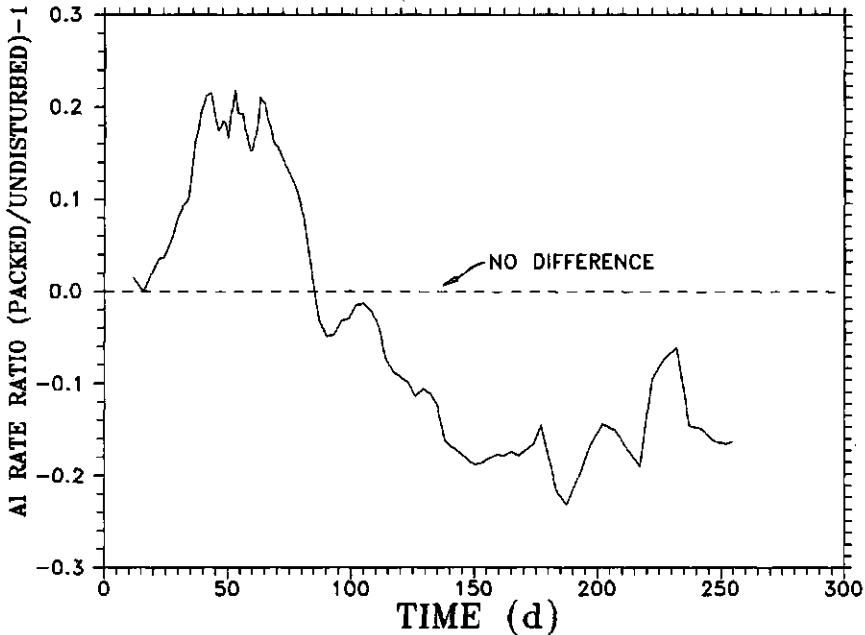


Fig. 13.3 The ratio of the rate of Al-release from packed soil cores over that from undisturbed soil cores during percolation with 3 mmol/L HCl.

The total decrease of the dithionite pool was 81 mmol_c/kg for the disturbed cores, explaining 70% of total leaching, and 35 mmol_c/kg for the undisturbed cores, explaining only 29% of total leaching. Although the determination of the dithionite extractable fractions was not very accurate (Table 13.1), results suggest that the average size of the dithionite extractable fraction in the undisturbed sample was higher than for the disturbed material. The untreated sample for extraction was obtained from mixed soil material. The Al leaching, which cannot be explained by a decrease of extractable fractions, probably is caused by dissolution of alumino-silicates. The effect of sample pretreatment and packing on the reactivity of the Al-pools is illustrated by the fact that the first rate plateau is maintained 20 d longer for the packed columns, and rates of release remained higher until d 90. However, from d 120 onwards rates in the undisturbed experiments were higher again and total leaching of Al after 267 d for both disturbed and undisturbed soil cores is almost identical. This is more clearly illustrated by plotting the ratio between the rate of Al-release from the disturbed soil core over that from the undisturbed soil core (Figure 13.3). Apparently sample pretreatment has caused rather a transference of moderately reactive Al to highly reactive Al, than a creation of additional reactive Al.

13.3.2 Base cations and silica

The rates of release of Ca, Mg, Na, and Si are shown in the Figures 13.4^a to 13.4^d. Total release of all base cations (Table 13.2) was at least ten times as high as may be expected from exchangeable pools, which were below the detection limit.

With increasing time, and not considering the initial strong decrease due to displacement of the original pore water, rate of release slowly decreased (Ca), slowly increased (Mg), remained unchanged (Na) or showed a maximum value (Si). This large variation of response for individual elements can be explained by considering two counteracting effects, increasing depletion of reactive pools of cations and a gradually increasing proton concentration. In general the dependence of mineral weathering rates on (H^+) is described by a fractional order dependence (Chapter 8), with an average exponent of 0.5. Considering the increase of (H^+) from 0.2 to 2.5 mmol/L, an increase of weathering rate by a factor of 3.5 would be expected. The increase for Mg in the disturbed cores between d 20 and d 240 was 3.3, and 2.9 for the undisturbed cores. The strongest increase of rates of Mg release between d 20 and d 60 ran parallel to the increase of (H^+).

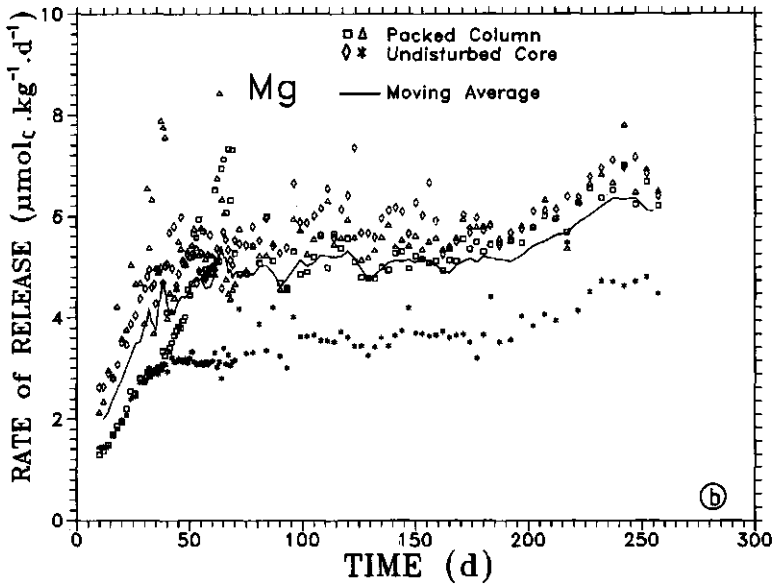
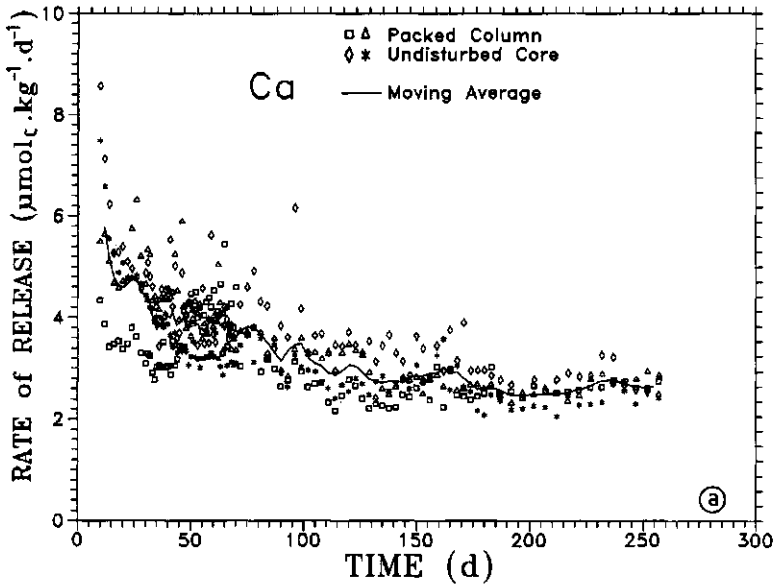


Fig. 13.4 Rates of release of (a) Ca, (b) Mg, (c) Na and (d) Si during percolation of packed and undisturbed soil cores with 3 mmol/L HCl. The moving average is based on 3 subsequent leachate samples for all columns ($n = 12$).

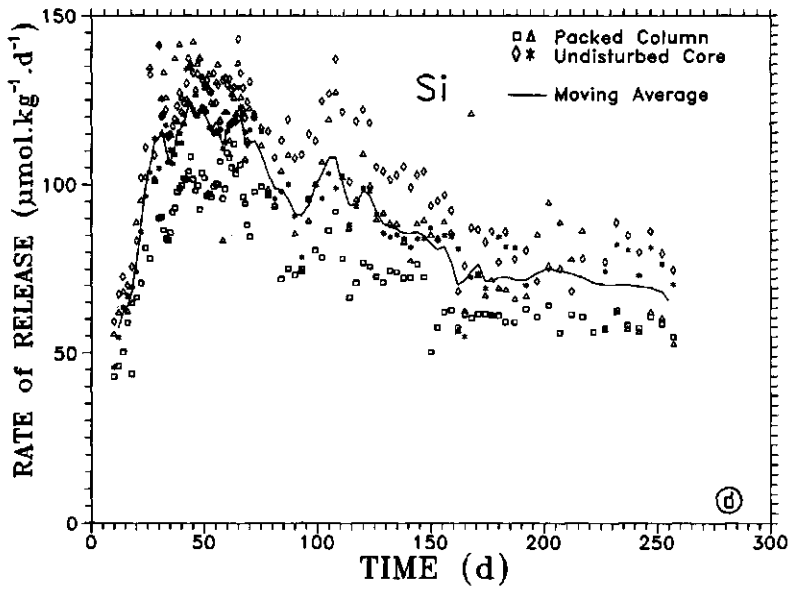
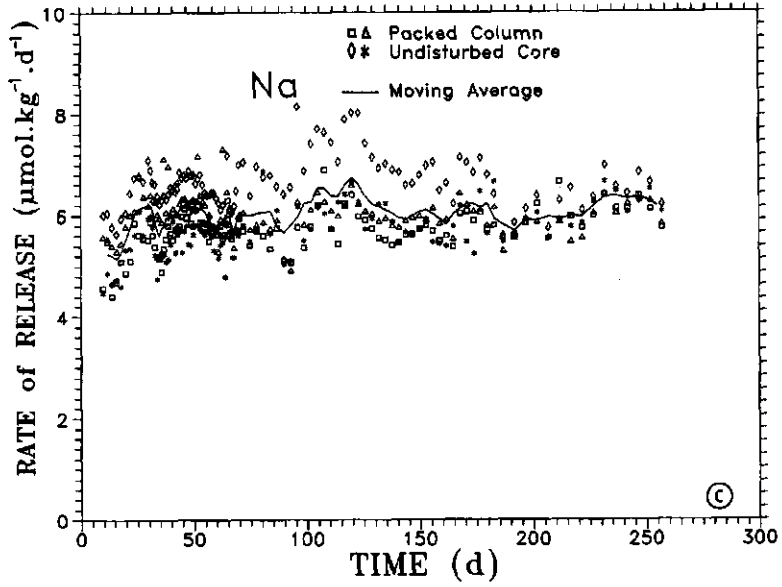


Fig.13.4 (continued)

Column experiments at constant pH (Chapter 8) showed a relatively stronger dependence of Mg on (H^+) than for other cations. The decreasing rates of release of Ca indicate dominance of the depletion effect and the presence of a relatively constant rate for Na suggests exact balance of the depletion and pH effect.

| | Flow (mL) | H | Al | K | Na | Ca | Mg | Si |
|---|-------------------|--------|-------|-------------------|------|------|------|------|
| Disturbed | | | | | | | | |
| Column 1 | | | | | | | | |
| Total leaching (mmol _c /kg) | 10940 | -125.4 | 120.7 | -- | 1.50 | 1.00 | 1.29 | 18.2 |
| Mean Concentration (μmol _c /L) | 41.9 [†] | | | 12.0 [‡] | 20.7 | 10.4 | 18.4 | 268 |
| Standard deviation | 2.4 [†] | | | 0.8 [‡] | 5.8 | 2.7 | 2.2 | 55 |
| Column 2 | | | | | | | | |
| Total leaching | 10940 | -124.6 | 119.0 | -- | 1.64 | 1.21 | 1.50 | 23.6 |
| Mean Concentration* | 41.7 | | | 12.3 [‡] | 21.6 | 11.5 | 20.1 | 355 |
| Standard deviation | 2.7 | | | 1.3 [‡] | 2.5 | 2.7 | 1.3 | 124 |
| Undisturbed | | | | | | | | |
| Column 1 | | | | | | | | |
| Total leaching | 10990 | -125.3 | 14.56 | -- | 1.75 | 1.23 | 1.49 | 25.9 |
| Mean Concentration | 42.4 | | | 10.4 [‡] | 18.1 | 9.6 | 15.6 | 287 |
| Standard deviation | 1.8 | | | 0.5 [‡] | 1.5 | 2.0 | 1.9 | 49 |
| Column 2 | | | | | | | | |
| Total leaching | 11030 | -129.3 | 14.46 | -- | 1.53 | 1.13 | 0.97 | 22.7 |
| Mean Concentration | 42.6 | | | 10.2 [‡] | 17.3 | 8.5 | 10.8 | 276 |
| Standard deviation | 2.2 | | | 0.4 [‡] | 1.6 | 1.2 | 1.7 | 48 |

[†] in units of mL/d

* mean concentrations are based on samples collected from d 50 onwards (n=74)

[‡] based on unpolluted leachate samples collected from d 207 onwards (n=12)

Table 13.2 Summary of results of column leaching experiments at a constant percolation rate of 3 mmol/L HCl over a period of 267 d.

The presence of a maximum rate for release of Si shows that both effects are non-linear with respect to reaction time, causing initial dominance of the effect of pH. Results for K were not considered because experiments suggested K pollution in the common input solution.

The experiments do not provide information on the separate effects of depletion and (H^+), for which purpose experiments at controlled pH are required (Chapter 7 and 8). The experiment illustrates that long-term changes of weathering rates of base cations are difficult to predict. However, when simulating effects of soil acidification over several decades the assumption of constant weathering rates is not a bad guess because in general a decrease of soil solution pH will be accompanied by, and will be the result of, mineral depletion, in particular of pools of reactive Al.

Extrapolated rates of release, averaged for all four experiments are 0.88, 1.52, 0.78, 1.27 $\text{kmol}_c.\text{ha}^{-1}.\text{yr}^{-1}$ for K, Na, Ca and Mg respectively and 23.2 $\text{kmol}.\text{ha}^{-1}.\text{yr}^{-1}$ for Si, for a 5 cm long soil core. When considering a soil profile of 90 cm, rates should be multiplied by a factor of 18. Resulting rates of cation release are about forty times higher than values implied from field mass balance studies for a 90 cm profile: 0.4, 0.7 and 0.3 for K, Ca and Mg respectively (Van Breemen et al., 1986; Chapter 5 and 10). The larger part of this discrepancy is associated with the use of high percolation rates (2 cm/d) relative to the field (0.05 cm/d) (Chapter 4, 8, 12) and to the difference of pH between the percolate (3.5 to 2.6) and the field soil solution (pH near 4). The estimated increase of weathering rate due to percolation rates is a factor 6 and due to pH is a factor 4.

13.4 CONCLUSIONS

Dissolution of Al from the crystalline oxide pool was the dominant proton consuming process. With progress of reaction the dissolution rate of Al showed two distinct plateaux, which could not be associated with depletion of specific fractions of extractable Al. Rates of cation release both increased in time (Mg), decreased in time (Ca), or remained constant (Na), in relation to the counteracting effects of increasing mineral depletion and increasing (H^+). Rates of release are about 40 times higher than implied from field studies because of the lower pH values and because of the higher percolation rates.

ACKNOWLEDGEMENTS

I am very obliged to Mr. Egbert Nab who build the experimental setup, maintained the actual experiments and did the chemical analyses.

SUMMARY

Soil acidification may be defined as a decrease of the Acid Neutralizing Capacity (ANC) of the soil. Soil acidification is a natural process, where CO_2 , organic acids and the living biomass may act as sources of protons. By its definition, the ANC of the soil will decrease upon external supply of protons. Atmospheric deposition of SO_x , NO_x and NH_x , will become an external source of protons, after oxidation in precipitation, on the vegetation or in the soil, to sulfuric and nitric acid. After infiltration of these mineral acids in the soil the chemical composition of the soil solution will undergo major changes, of which the nature and extent will depend on the chemical reactions with the solid phase of the soil. There is substantial evidence that changes in soil solution composition, in particular increased concentrations of Al, NH_4 and H, as compared to concentrations of K, Ca and Mg, have adverse effects on root functions and consequently on vitality of the vegetation. With respect to the response of soil to acid atmospheric deposition and to the resulting composition of the soil solution, mineral weathering of Al and base cations, cation exchange, nitrification, and transformation of organic matter are key processes.

In this thesis three major issues related to soil acidification are addressed:

- Quantification of soil acidification in actual field sites, as part of an overall quantification of chemical fluxes and soil chemical processes. The basis of soil acidification research is long-term monitoring of chemical and physical parameters in the field.
- The formulation of explicit relationships between the output, the input and environmental factors of key soil processes. Formulations are based on experimental research.
- The integration of process and transport formulations into a general simulation model for soil acidification. Calibration and validation of such a model against field data. Analysis of the response of the soil system under maintained or changing boundary conditions.

Chemical fluxes are determined by combination of hydrologic fluxes and chemical concentrations in atmospheric water and soil water. At present, hydrologic fluxes in soil can be measured only by way of exception, and therefore are generally determined by simulation. The determination of chemical fluxes in

the unsaturated soil is complicated by the inaccuracy of simulation of unsaturated soil water fluxes and by spatial variability of soil solution concentrations. Errors in annual chemical fluxes in soil profiles at the Hackfort estate, ranged from 10 to 30%, increasing with depth. Spatial variability was the largest source of uncertainty. Errors of annual unsaturated soil water fluxes did not exceed 10%, but can be much larger for small annual precipitation surpluses or for specific months in summer.

The uncertainty in vertical chemical fluxes in soil profiles would be much smaller if unsaturated soil water fluxes could be measured directly by "in situ" interception, and if soil solution concentrations were determined directly in the intercepted water. Both features were combined in a new type of flux meter, which could intercept soil water fluxes at a similar accuracy as obtained by numerical simulation, but without requiring labour intensive field monitoring. Interception of soil water is controlled by a microprocessor which automatically adjusts the vacuum imposed on a porous filter cloth, such that identical matric potentials are maintained just above the cloth and at the same depth in the neighboring soil. The flux meter depends on the proper operation of tensiometers, which is doubtful in extremely sandy or clayey soils, particularly under dry conditions.

Mineral weathering is responsible for a major part of the buffering of proton inputs to the soil and supplies a relevant part of cation nutrients for plant growth. Mineral weathering reactions can be quantified in terms of reaction stoichiometry and reaction rate. Reaction rates are most easily obtained from batch experiments. However, weathering rates for soil material from stirred batch experiments appeared to be more than one order of magnitude higher than those from column experiments, as a result of mechanical disturbance of mineral surfaces. Weathering rates from column experiments were still one order of magnitude higher than those implied from field mass balance studies and from unstirred batch experiments. These discrepancies could be explained by assuming reaction rate control by stagnant water films inside etch pits, of which the thickness will decrease upon increasing percolation rate. An approximately square root increase of weathering rate with percolation rate was derived from column experiments at various percolation rates.

In principle the rate of weathering reactions is determined by the chemical composition of the solution. The mechanism of rate control depends on the reaction progress. In well homogenized systems, reaction rate is determined by the rate of the surface reactions. Far from equilibrium ($\log(Q/K) < -3$) the rate of surface complexation is rate-limiting, resulting in an increase of reaction rate with

the hydrogen ion activity according to $(H^+)^p$. Closer to equilibrium, the rate of detachment of the surface complex into solution is rate limiting. This will result in a dependency of the reaction rate on the degree of mineral saturation, which may be expressed by $(1-(Q/K)^p)$, where Q is the ionic activity product and K is the equilibrium constant. Results from a stirred batch experiments on samples of the C-horizon of a Dystrachrept, could be described by congruent dissolution of illite until saturation with gibbsite was reached, followed by incongruent dissolution of illite and gibbsite precipitation. The congruent illite dissolution rate could be fitted as a function of $(1-(Q/K)^p)$, in accordance with transition state theory.

To study weathering rates at controlled pH, without causing mechanical disturbance, a new column percolation technique was developed, where H^+ supply to the column and the H^+ consumption in the column were balanced by adjusting the percolation rate. Soil samples were taken from the A-, B- and C-horizon of an Umbric Dystrachrept and from the A- and C-horizon of a Typic Udipsamment. Dissolution of Al was the main buffering process for all soil samples. The dominant pool of reactive pool of Al was present in fraction which could be extracted with Na-dithionite, which consist of amorphous and crystalline (hydr)oxides of Al together with organic compounds. On average Al-dissolution rate increase proportional with $(H^+)^{0.7}$. The Al-dissolution decreased exponentially with depletion of soil-Al. Depletion of the reactive Al-pool as a result of acid atmospheric deposition, is a realistic future problem in acid forest soils.

Weathering rates of base cations (K, Na, Ca and Mg) from column experiments at controlled pH were two to three orders lower than those of Al. K and Na are specifically released from alkali-feldspars, but sources of Ca and Mg are more diverse. An increase of weathering rates of base cations with decreasing pH was generally observed, in particular below a pH of 3. The increase was strongest and most apparent for Mg, which rate increased almost proportional with (H^+) . After initial exhaustion of small reactive mineral pools of base cations, relatively constant rates of release of base cations were observed even when leaching over 9 months at pH below 3. Weathering rates from column experiments at much higher percolation rates than prevail in the field (0.5-2 mm/d), lead to an overestimation of weathering rates under field conditions, because of the assumed effect of percolation rate on diffusion transport of weathering products from etch pits, mentioned earlier.

In surface soils with high CEC values, associated with the presence of high organic matter contents, cation exchange is the main source of cations. Base cation release could be predicted by the Gaines-Thomas exchange equilibrium

model. Release of Al was much less than predicted by the Gaines-Thomas model, indicating slow exchange of Al against H.

The rates of Ca-release from samples of the C-horizon of one of the soils studied (a Dystrochrept) markedly increased after lowering the input pH in column experiments. In the field release of Ca in the C-horizon was negligible. The enhanced Ca-release was associated with removal of a small fraction of Al, and led to the hypothesis that upon acidification, anorthite-domains in plagioclases started to dissolve because of removal of protective coatings of Al-oxides. This hypothesis suggests that patchy coatings of secondary Al-rich material can be protective if dissolution of primary minerals is confined to a small fraction of the mineral surface.

The ILWAS simulation model was adapted to simulate transport and chemical interactions in an acid forest soil profile, viz. the Umbric Dystrochrept under mixed vegetation of oak (*Quercus robur*) and birch (*Betula pendula*). The model was calibrated by data on solution chemistry, which were collected between 1981 and 1987. The first two measuring years were used for calibration, and the following years for validation. The most important calibration parameters were the rate constants for nitrification, dissolution of gibbsite and decay of organic matter. After calibration, the model was used to analyze the response of the forest soil to 50% reduction of deposition of $(\text{NH}_4)_2\text{SO}_4$, the application of K_2SO_4 and MgSO_4 as fertilizers, and to removal of the forest vegetation, considering the period from 1981 to 1987. Reduction of acid atmospheric deposition by 50% will result in a reduction of concentration of Al by about 40% within one year. The effect on pH would be small as pH in the surface soil is mainly determined by nitrification and mineralization of organic N and in the subsoil by equilibrium with gibbsite. The reduction of the concentration of NO_3 would be strongly delayed due to additional nitrification of NH_4 from temporary net desorption and mineralization. Addition of 2.6 kmol_c/ha K and 8.2 kmol_c/ha Mg as readily soluble fertilizers would lead to a significant increase of concentrations of K (45%) and Mg (85%) in soil solution. An additional effect would be a short-lasting desorption and leaching of Ca (3.3 kmol_c/ha). Exchange of Mg against Al would cause high concentration peaks of Al (18 mmol_c/L) in the year following fertilizer addition, irrespective of addition of lime. Removal of the forest vegetation would increase mineralization and nitrification of organic N, which would almost double leachate fluxes of base cations and NO_3 in the six-year period. The effect on concentrations would be minor because drainage fluxes would also increase due to a concurrent reduction of evapotranspiration.

For evaluation of the long-term (in the order of decades) response of soil-ecosystems detailed simulation models with small time steps are not necessarily suitable tools, because such detailed models require many, often poorly available, input parameters, are uneconomic with respect to computer-time requirements, and may generate excessive numerical dispersion. To simulate annual averages of soil solution concentrations under slowly changing boundary conditions, it is not strictly necessary to distinguish between aqueous and adsorbed concentrations. For simple simulation models the sum of both concentrations may be considered, which comprises the directly available pool of ions. In general, these directly available pools of ions, are many times larger than annual ion fluxes and allow the use of long time steps (month or year), thus preventing excessive numerical dispersion. A simulation model based on this principle proved to be appropriate to simulate annual concentration averages in an Umbric Dystrachrept under a mixed oak-birch forest, and in a Typic Haplorthod under a pine forest (*Pinus silvestris*).

SAMENVATTING

Bodemverzuring kan worden gedefinieerd als een afname van het Zuur-Bindend Vermogen (ZBV) van de bodem. Bodemverzuring is een natuurlijk proces, waarbij CO_2 , organische zuren en een groeiende vegetatie kunnen optreden als zuurbronnen. Per definitie, zal het zuurbindend vermogen van de bodem afnemen bij toevoer van protonen van buitenaf. Atmosferische depositie van SO_x , NO_x en NH_x wordt een externe bron van protonen, nadat deze stoffen op de vegetatie of in de bodem zijn geoxideerd tot zwavelzuur en salpeterzuur. Wanneer deze sterke zuren met het regenwater in de bodem infiltreren, zal de chemische samenstelling van de bodemoplossing belangrijke veranderingen ondergaan, waarvan de aard en de omvang afhangen van de chemische reactie tussen de bodemoplossing en de vaste bodemdelen. In de afgelopen jaren hebben experimenten op overtuigend wijze aangetoond, dat verhoging van concentraties van Al, NH_4 en H in het bodemvocht, bij gelijkblijvende of verlaagde concentraties van K, Ca en Mg, zal leiden tot een verminderd functioneren van het wortelstelsel en een algehele verlaging van de vitaliteit van de vegetatie. Mineraalverwerking, kationenomwisseling, nitrificatie en afbraak van organische stof zijn sleutelprocessen met betrekking tot de reactie van de bodem met extern aangevoerd zuur, en de totstandkoming van de samenstelling van de bodemoplossing in het algemeen.

In dit proefschrift worden drie, aan bodemverzuring gerelateerde, onderwerpen behandeld:

- De bepaling van de grootte van bodemverzuring in reële veldsituaties, als een integraal onderdeel van de kwantificering van stoffluxen en chemische processen. Het fundament voor dit bodemverzuringsonderzoek wordt gevormd door een meetserie van fysische en chemische parameters in het veld over een periode van zes jaar.
- De formulering van expliciete relaties tussen de invoerproducten, uitvoerproducten en omgevingsfactoren voor de eerder genoemde sleutelprocessen in de bodem. Deze formuleringen zijn gebaseerd op experimenteel onderzoek.

- De integratie van proces- en transportvergelijkingen in een algemeen simulatiemodel voor bodemverzuring. Calibratie en validatie van een dergelijk model met behulp van veldgegevens. Analyse van het gedrag van het bodemsysteem bij gehandhaafde of veranderde randvoorwaarden.

Stoffluxen worden bepaald door vermenigvuldiging van waterfluxen met chemische concentraties, in atmosferische water of bodemvocht. Tot nu toe is directe meting van waterfluxen in de onverzadigde bodem alleen bij uitzondering mogelijk, en worden deze fluxen in het algemeen bepaald door middel van simulatie. De bepaling van stoffluxen in de onverzadigde bodem wordt bemoeilijkt door de onnauwkeurigheid van de simulatie van onverzadigde bodemwaterfluxen en door de ruimtelijke variabiliteit van bodemvochtconcentraties. Hierdoor ontstonden fouten in de stoffluxen voor bodemprofielen in het landgoed Hackfort ter grootte van 10 tot 30%, welke toenamen met de diepte. Ruimtelijke variabiliteit was de grootste bron van onzekerheid. Op jaarbasis, waren de fouten voor de onverzadigde bodemwaterfluxen niet groter dan 10%. Deze fouten kunnen sterk toenemen in geval van kleinere neerslagoverschotten of bij berekening op maandbasis voor het groeiseizoen.

De fout bij de bepaling van stoffluxen voor een een-dimensionaal bodemprofiel zou veel kleiner zijn, wanneer de onverzadigde bodemwaterfluxen direct gemeten konden worden door in situ interceptie van het bodemvocht. Hierbij kunnen de concentraties in het bodemvocht direct in het geïntercepteerde water bepaald worden. Deze verbetering kon gerealiseerd worden met een nieuw ontwerp voor een fluxmeter, met behulp waarvan waterfluxen bepaald konden worden met een vergelijkbare nauwkeurigheid als voor numerieke simulatie. In tegenstelling tot numerieke simulatie, vereist de fluxmeter geen arbeidsintensieve veldmetingen van neerslag, verdamping, vochtgehalte en vochtspanning. De werking van de fluxmeter berust op automatische aanpassing van de onderdruk op een poreus filter, zodanig dat er vlak boven het filterdoek eenzelfde bodemvochtspanning heerst als op gelijke diepte in de ongestoorde bodem. De fluxmeter is sterk afhankelijk van de juiste werking van een aantal tensiometers, welke twijfelachtig is in extreem grof of fijn bodemmateriaal, met name onder droge omstandigheden.

Verwerking van mineralen is verantwoordelijk voor een belangrijk deel van de buffering van extern aangevoerd zuur, en speelt een belangrijke rol bij de voorziening van voedingsstoffen voor de vegetatie. Verweringsprocessen kunnen worden uitgedrukt in termen reactiostoichiometrie en reactiesnelheid. Verweringsnelheden worden het meest eenvoudig verkregen door middel van schud-

experimenten. Verwerkingssnelheden van K, Na, Ca en Mg in bodemmateriaal, verkregen door middel van schudexperimenten, bleken echter ruim een orde van grootte hoger te zijn dan snelheden bepaald door middel van kolomexperimenten, waarschijnlijk als gevolg van mechanische aantasting van de mineraaloppervlakken. Verwerkingssnelheden uit kolomexperimenten bleken echter ook weer ruim een orde van grootte hoger dan verwerkingssnelheden uit oplosexperimenten met een stagnante waterfase en schattingen van verwerkingssnelheden uit massabalansen voor veldproeven. Het merendeel van dit verschil kon worden verklaard door aan te nemen dat de verwerkingssnelheid werd gecontroleerd door stagnante waterlaagjes in en op zogenaamde etch pits. Op grond van kolomexperimenten bij variabele percolatiesnelheden, werd bij benadering een wortel-verband gevonden tussen de toename van de verwerkingssnelheid en de toename van de percolatiesnelheid.

In principe wordt de verwerkingssnelheid bepaald door de samenstelling van de oplossing. De aard van het mechanisme voor snelheidsregulering hangt van de voortgang van de reactie. Vooropgesteld dat de oplossing goed is gemengd, wordt de verwerkingssnelheid bepaald door de snelheid van de oppervlakte-reactie. Wanneer de oplossing sterk onderverzadigd is met betrekking tot het oplossende mineraal ($\approx \log(Q/K) < -3$, waarbij Q staat voor het ionen-activiteitsprodukt en K voor de evenwichtconstante), wordt de oplosnelheid gelimiteerd door de vormingssnelheid van het geactiveerd oppervlaktecomplex. Dit kan resulteren in een toename van de verwerkingssnelheid met de activiteit van het waterstof-ion volgens een machtsfunctie, $(H^+)^p$, met p kleiner dan 1. Wanneer de oplossing evenwicht nadert met het oplossend mineraal, wordt de verwerkingssnelheid bepaald door de snelheid waarmee het geactiveerde oppervlaktecomplex in oplossing wordt gebracht. Dit kan zich uiten in een verband tussen de verwerkingssnelheid en de mate van onderverzadiging, uitgedrukt als $(1 - (Q/K)^p)$. De resultaten van schudexperimenten met bodemmateriaal van de C-horizont van het Hackfort B profiel (Umbric Dystrachrept) konden worden beschreven door aanname van congruente oplossing van illiet met een snelheid, welke gerelateerd was aan de mate van onderverzadiging met illiet. Congruente oplossing werd gevolgd door incongruente oplossing nadat verzadiging met gibbsiet werd bereikt.

Om verweringsprocessen te kunnen bestuderen bij constante pH en zonder mechanische aantasting van de minerale oppervlakken, werd een nieuwe techniek voor kolompercolatie ontwikkeld. De pH in het effluent werd constant gehouden door de percolatiesnelheid, en hierdoor de toevoer van H^+ aan de kolom, automatisch aan te passen aan consumptie van H^+ in de kolom. Bodemonsters voor het onderzoek waren afkomstig uit de A-, B- en C-horizont van

het Hackfort B profiel en uit de A- en C-horizont van het Gerritsfles profiel onder bos (Typic Udipsamment). In alle monsters was buffering door oplossing van Al het belangrijkste proces. De belangrijkste bron van reactief Al in de vaste fase wordt gevormd door de fractie extraheerbaar met Na-dithioniet, welke bestaat organische verbindingen en amorge en cristallijne (hydr)oxiden van Al. Gemiddeld werd een toename van de verwerkingssnelheid van Al gevonden evenredig met $(H^+)^{0.7}$. De snelheid van Al-verwerking nam exponentieel af met voortgang van de uitspoeling van Al. Totale uitputting van de reactieve voorraad van Al kan in een reëel probleem gaan vormen in zure bosgronden in de komende eeuw.

Verwerkingssnelheden van K, Na, Ca en Mg in kolomexperimenten bij constante pH zijn over het algemeen twee tot drie orden van grootte lager dan voor Al. Veldspaten zijn de voornaamste bronnen van K en Na, terwijl de bronnen voor Ca en Mg meer divers zijn. Een toename van de verwerkingssnelheden van deze kationen werd algemeen waargenomen, met name beneden een pH van 3. De toename was het meest uitgesproken voor Mg, waarvan de verwerkingssnelheid vrijwel evenredig met de (H^+) toenam. Na een snelle initiële uitputting van kleine reactieve voorraden van Ca, Mg, K en Na, werden relatief constante verwerkingssnelheden waargenomen, zelfs na percolatie over een periode van 9 maanden bij een pH beneden de 3. Metingen van verwerkingssnelheden in kolomproeven bij veel hogere percolatiesnelheden dan aanwezig in het veld (0.5-2 mm/d), overschatten verwerkingssnelheden onder veldomstandigheden, met name door het eerder genoemde effect van percolatiesnelheid op diffusief transport van verwerkingsproducten vanaf de selectieve verwerkingsplekken op het mineraal oppervlak.

In oplosexperimenten met monsters van de A-horizont, welke een relatief hoge CEC bezitten in samenhang met hoge gehalten aan organische stof, wordt de afgifte van kationen bepaald door kationenuitwisseling. Voor deze monsters kon de afgifte van Ca, Mg en K voorspeld worden met behulp van het Gaines-Thomas evenwichtsmodel voor omwisseling. De afgifte van Al was echter veel lager dan voorspeld door dit model, hetgeen wijst op langzame uitwisseling van Al tegen H.

In één van de onderzochte bodemlagen, namelijk de C-horizont van het Hackfort B profiel, werd een opvallend sterke toename waargenomen van de Ca-afgifte, na verlaging van de pH van de kolompercolaten. In het veld is de afgifte van Ca uit deze bodemlaag gering. Deze versnelde afgifte van Ca werd geconstateerd na oplossing van een vaste hoeveelheid Al. Dit leidde tot de hypothese dat na verlaging van de pH, anorthiet-kristallen in het oppervlak van plagioclasen in oplossing gebracht konden worden door verwijdering van beschermende laagjes van Al-(hydr)oxiden. Deze hypothese impliceert dat fragmenta-

rische huidjes van secundaire, Al-rijke, mineralen wel degelijk het onderliggende mineraal tegen oplossing kunnen beschermen, aangezien oplossing van primaire mineraal plaatsvindt op een slechts een klein deel van het oppervlak.

Het waterverzuringmodel ILWAS werd aangepast voor de simulatie van transport en chemische interacties in het Hackfort B profiel, en de daarop aanwezige vegetatie van eik (*Quercus robur*) en berk (*Betula pendula*). Het model werd gecalibreerd met behulp van bodemvochtconcentraties en stoffluxen verzameld in de periode van april 1981 tot april 1987. De belangrijkste parameters voor calibratie waren de snelheidsconstanten voor nitrificatie, oplossing van gibbsiet en afbraak van organische stof. Het model werd gecalibreerd op de eerste twee meetjaren en werd gevalideerd op de latere jaren. Het gecalibreerde model werd gebruikt voor analyse van de respons van het bodemsysteem over de meetperiode van 6 jaar op verlaging van 50% van de depositie van $(\text{NH}_4)_2\text{SO}_4$, op toediening van K_2SO_4 en MgSO_4 als meststof en op kap van de bosvegetatie.

Reductie van de depositie van $(\text{NH}_4)_2\text{SO}_4$ met 50% zou resulteren in een 40% reductie van de Al-concentraties binnen een jaar. Het effect op pH zou gering zijn, omdat de pH in de bovengrond voornamelijk wordt bepaald door mineralisatie en nitrificatie van organisch N, en in de ondergrond door evenwicht met gibbsiet. De reductie van uitspoeling van NO_3 zou sterk vertraagd worden door een tijdelijke netto afgifte van NH_4 van het omwisselcomplex en door mineralisatie. Bemesting met 2.6 kmol_c/ha K_2SO_4 en 8.2 kmol_c/ha MgSO_4 zou leiden tot een aanzienlijke verhoging van de concentraties van K (45%) en Mg (85%) in de bodemoplossing, maar zou tevens een zoutschok veroorzaken. Als gevolg van deze zoutschok zou er een extra uitspoelingsverlies van 3.3 kmol_c/ha Ca optreden. Ook zou er een extreme verhoging (18 mmol_c/L) van de concentratie van Al optreden in het jaar van toediening. Verwijdering van de bosvegetatie zou leiden tot een tijdelijke verdubbeling van de uitspoeling van NO_3 , als gevolg van mineralisatie en nitrificatie van organisch N, welke gepaard zou gaan met extra uitspoeling van K, Ca en Mg. De veranderingen van concentraties in het bodemvocht zouden relatief gering zijn als gevolg van een gelijktijdige toename van de waterfluxen door verminderde evapotranspiratie.

Voor de evaluatie van de respons op lange termijn (tientallen jaren) van bos-bodem-ecosystemen op veranderende randvoorwaarden, zijn gedetailleerde simulatiemodellen zoals ILWAS, welke rekenen met kleine tijdstappen, niet noodzakelijkerwijs het meest geschikte middel. Dergelijke gedetailleerde modellen vragen meestal een groot aantal, moeilijk beschikbare invoergegevens, vragen

veel rekentijd en geven soms aanleiding tot excessieve numerieke dispersie. Voor de simulatie van jaar-gemiddelde concentraties in de bodemoplossing, bij langzaam veranderende randvoorwaarden, is een strikte scheiding tussen geadsorbeerde en vrije ion-concentraties niet noodzakelijk. In plaats hiervan zou gerekend kunnen worden met de som van beiden, welke equivalent is met de onmiddellijk beschikbare voorraad van ionen. Deze som van ionen is, in tegenstelling tot de vrije ion-concentratie, in het algemeen vele malen groter dan de jaarlijkse netto veranderingen, hetgeen de toepassing van grote tijdstappen mogelijk maakt. Een eenvoudig simulatiemodel, gebaseerd op dit principe, bleek geschikt om de jaar-gemiddelde bodemvochtconcentraties in het Hackfort B profiel en in het Tongbersven-profiel (Typic Haplorthod) onder grove den (*Pinus Silvestris*) te voorspellen.

MAJOR CONCLUSIONS

- 1: Weathering of Al from hydrated oxides is the main acid neutralizing process in acid sandy soils. The weathering rate increases nearly proportional to (H^+) , which strongly stabilizes pH in soil solution. The pool of hydrated oxides is limited and may be exhausted within the next century, if rates of acid atmospheric deposition are maintained at their present levels. Depletion of the reactive pool of hydrated Al-oxides will eventually lead to a large concentration increase of either H or NH_4 , depending on the rate of nitrification.
- 2: Weathering of K, Ca and Mg are relevant sources of nutrients for plant growth. In general weathering rates of these base cations increase less strongly with increasing (H^+) than the rate of Al weathering, causing a decrease of base cation concentrations relative to concentrations of H, Al or NH_4 . Such a decrease will have an adverse effect on plant growth. Mineral pools of K are practically infinite, and weathering rates of K will remain constant for millennia. Mineral pools of Ca and Mg are limited, and may be depleted considerably in the next century, because of enhanced dissolution due to soil acidification.
- 3: It is practically impossible to obtain unbiased estimates of field weathering rates from short-lasting dissolution experiments in the laboratory. In general the relevance of weathering rates from laboratory studies improves with increasing similarity between experimental conditions and field conditions, in particular with respect to mechanical disturbance of mineral surfaces and hydrodynamical conditions. In this respect column experiments at controlled pH appear appropriate, but an increase of weathering rates with, by approximation, the square root of the percolation rate was demonstrated.
- 4: Research into the effects of acid atmospheric deposition on soils strongly depends on long-term monitoring of field parameters. Understanding of soil acidification processes greatly increases by considering chemical fluxes and budgets in the soil, which are obtained by combination of simulated hydrologic fluxes and chemical concentrations. Calculation of chemical budgets is not frustrated by large uncertainty about simulated soil water fluxes in summer, or about potential transpiration. The determination of chemical fluxes and budgets in the field may be greatly improved and simplified, by a new technique which measures in situ unsaturated soil water fluxes.

5: Process oriented simulation models for transport and interactions of chemical constituents in soil are useful tools to interpret data from field monitoring and to analyze the response of soils to changing boundary conditions. Meaningful simulation of average annual soil chemical properties can be carried out by using simple approximate models, while analysis of seasonal pattern requires detailed deterministic models. The ILWAS model proved to be adequate to simulate the major soil chemical features of an acid forest soil, which was monitored at monthly intervals. Scenario analysis demonstrated that upon 50% reduction of the deposition of $(\text{NH}_4)_2\text{SO}_4$, fluxes and concentrations of Al would be reduced correspondingly within one year, while effects on pH were minor and effects on NO_3 were strongly delayed. Furthermore, the ILWAS model proved very helpful to evaluate the effects of drastic mitigation measures in acid forest systems, like addition of readily soluble K- and Mg-bearing fertilizers and removal of the forest vegetation.

REFERENCES

- Aagaard P. and H.C. Helgeson, 1982. Thermodynamic and kinetic constraints on reaction rates among minerals and aqueous solutions. I. Theoretical considerations. *Amer. J. Sci.* 282, p. 237-285.
- Abrahamsen, G. and A.O. Stuanes, 1986. Lysimeter study of effects of acid deposition on properties and leaching of gleyed dystric brunisolic soil in Norway. *Water, Air and Soil Pollut.* 31: p. 865-878.
- Alcamo, J., M. Amann, J.P. Hettelingh, M. Holmberg, L. Hordijk, J. Kamäri, L. Kauppi, P. Kauppi, G. Kornai and A. Mäkelä, 1987. Acidification in Europe: A simulation model for evaluating control strategies. *Ambio* 16 (5): p. 232-245.
- Andersson, F. and J.M. Kelly. (eds.) 1984. Aluminum toxicity to trees. *Int. Workshop, Uppsala, Sweden, 16-17 May, Swedish University of Agricultural Sciences, Uppsala, Sweden.*
- Arp, P.A., 1983. Modelling the effects of acid precipitation on soil leachates: a simple approach. *Ecological Modell.* 19: p. 105-117.
- Bascomb, C.L., 1964. Rapid method for the determination of cation exchange capacity of calcareous and non-calcareous soils. *J. Sci. Food Agric.*: 12, p. 821-823.
- Begheijn, L.Th., 1980. *Methods of chemical analysis for soils and waters.* Agricultural University Wageningen, The Netherlands.
- Belmans, C., J.G. Wesseling and R.A. Feddes. 1983. Simulation model of the water balance of a cropped soil: SWATRE. *J. Hydrol.* 63, 3/4: p. 271-286.
- Berden, M., S.I. Nilson, K. Rosen and G. Tyler, 1987. Soil acidification; extent, causes and consequences. *Nat. Swedish Environm. Prot. Board Rep.* 3292. Modin-Tryck A.B., Stockholm. (ISBN 91-620-3292-5).
- Berner, R.A., 1978. Rate control of mineral dissolution under earth surface conditions. *Amer. J. Sci.* 278: p. 235-252.
- Berner, R.A. and G. R. Holdren, 1979. Mechanism of feldspar weathering. II. Observations of feldspars from soils. *Geoch. Cosmoch. Acta.* 43: p.1173-1186.
- Berner, R.A., G.R. Holdren and J. Schott, 1984. Critical comment; Surface layers on dissolving silicates. *Geoch. Cosmoch. Acta* 49: p. 1657-1658.
- Bloom, P.R. and D.F. Grigal, 1985. Modeling soil response to acidic deposition in nonsulfate adsorbing soils. *J. Environ. Qual.* 14 (4): p. 489-495.
- Bloom, P.R., and M.S. Erich, 1987. Effect of solution composition on the rate and mechanism of gibbsite dissolution in acid solutions. *Soil Sci. Soc. Am. J.* 51: p. 1131-1136.
- Blum, A.E. and A.C. Lasaga, 1986. Monte Carlo simulations of surface reaction rate laws. In: Colman, S.M. and Dethier, D. (eds.), *Rates of chemical weathering of rocks and minerals*, Academic Press, New York: p. 255-291.
- Bolt, G.H., 1967. Cation exchange equations used in soil science - A review. *Neth. J. Agric. Sci.* 15: p. 81-103.
- Bolt, G.H. and M.G.M. Bruggenwert, 1976. *Soil chemistry. A. Basic Elements. Developments in Soil Science 5a.* Elseviers Scientific Publishing Company, Amsterdam, the Netherlands.

- Bolt, G.H. (ed.), 1982. Soil Chemistry. B. Physico-chemical models. Developments in soil science 5B. Elsevier Sci. Publ. Co. Amsterdam.
- Booty, W.G., 1983. Watershed acidification model and the soil acid neutralization capacity concept. PhD-thesis. McMaster University, Hamilton, Ontario, Canada.
- Brakke, T.W., S.B. Verma and N.J. Rosenberg. 1978. Lowland regional components of sensible heat advection. *J. Appl. Meteor.* 17: p. 955-963.
- Busenberg, E. and C.V. Clemency, 1976. The dissolution kinetics of feldspars at 25 °C and 1 atm CO₂ partial pressure. *Geochim. Cosmochim. Acta* 40: p. 41-49.
- Byrne, G.F., J.E. Drummond and C.W. Rose. 1967. A sensor for water flux in soil. "Point source" instrument. *Water Resour. Res.* 3: p. 1073-1078.
- Byrne, G.F., J.E. Drummond and C.W. Rose. 1968. A sensor for water flux in soil. 2. "Line source" instrument. *Water Resour. Res.* 4: p. 607-611.
- Cary, J.W. 1968. An instrument for in situ measurement of soil moisture flow and suction. *Soil Sci. Soc. Amer. Proc.* 32: p. 3-5.
- Cary, J.W. 1970. Measuring unsaturated soil water flow with a meter. *Soil Sci. Soc. Amer. Proc.* 34: p. 24-27.
- Cary, J.W. 1973. Soil water flow meters with thermocouple outputs. *Soil Sci. Soc. Amer. Proc.* 37: p. 176-180.
- Chou, L. and R. Wollast, 1984. Study of the weathering of albite at room temperature and pressure with a fluidized bed reactor. *Geoch. Cosmoch. Acta* 48: p. 2205-2217.
- Chou, L. and R. Wollast, 1985. Steady-state kinetics and dissolution mechanisms of Albite. *Amer. J. Sci.* 285: p. 963-993.
- Christoffersen, N., and R.F. Wright, 1981. A model for streamwater chemistry at Birkeness Norway. *Water Resour. Res.* 18: p. 977-996.
- Correns, C.W., and W. von Engelhardt, 1938. Neue Untersuchungen über die Verwitterung des Kalifeldspates. *Chemie der Erde* 12: p. 1-22.
- Cosby, B.J., R.F. Wright, G.M. Hornberger and J.N. Galloway, 1985^a. Modelling the effects of acid deposition: Assessment of a lumped-parameter model of soil and stream water chemistry. *Water Resour. Res.* 21: p. 51-63.
- Cosby, B.J., R.F. Wright, G.M. Hornberger and J.N. Galloway, 1985^b. Modeling the effects of acid deposition: Estimation of long-term water quality responses in a small forested catchment. *Water Resour. Res.* 21: p. 1591-1601.
- Cronan, C.S., 1985. Chemical weathering and solution chemistry in acid forest soils: Differential influence of soil type, biotic processes, and H⁺ deposition. **In:** *The chemistry of weathering*, J.I. Drever (ed.), D. Reidel Publ. Co.: p. 175-195.
- Cronan, C.S., W.J. Walker and P.R. Bloom, 1986. Predicting aqueous aluminium concentrations in natural waters. *Nature* 324: p. 140-143.
- David, M.B., and C.T. Driscoll, 1984. Aluminum speciation and equilibria in soil solutions of a Haplorthod in the Adirondack Mountains, *Geoderma* 33: p. 297-318.
- De Visser, P.H.B., 1986. Interactions between soil, vegetation and atmospheric deposition. Dutch Priority Programme on Acidification, Rep. no. 02-01, RIVM, Bilthoven, the Netherlands.

- De Vries, W. and A. Breeuwsma, 1984. Gevolgen van de Zure Regen voor de bodem. 2. Aandeel in de bodemverzuring in Nederland. STIBOKA Rep. no. 1787 STIBOKA, Wageningen, the Netherlands.
- De Vries, W., 1987. A conceptual model for analyzing soil and groundwater acidification on a regional scale. In: Proc. Int. Sympos. Acidification and water pathways, Bolkesjo 4-5 May, Norwegian National Committee for Hydrology (ISBN 82-554-0486-4), p. 185-194.
- Dirksen, C. 1972. A versatile soil water flux meter. p. 425-442. In: Proc. 2nd Symp. on fundamentals of transport phenomena in porous media, Vol. 2. IAHR, ISSS. Guelph, Ontario Canada.
- Dirksen, C. 1974. Field test of soil water flux meters. Trans. ASAE 17: p. 1038-1042.
- Dixon, J.B. and S.B. Weed (eds.), 1977. Minerals in the soil environment. Soil Sci. Soc. Amer., Madison.
- Driscoll C.T. and J.J. Bisogni, 1984. Weak acid/base systems in dilute lakes and streams of the Adirondack region of New York State. In: J.L. Schnoor (ed.) Modeling impacts of total acid precipitation. Acid precipitation series, vol. 9: p. 53-71. Butterworth Publishers, Boston.
- Duke, H.R. and H.R. Haise. 1973. Vacuum extractors to assess deep percolation losses and chemical constituents of soil water. Soil Sci. Soc. Amer. Proc. 37: p. 963-964.
- Eckhardt, F.E.W., 1985. Solubilization, transport and deposition of mineral cations by microorganisms - efficient rock-weathering agents. In: The chemistry of weathering, J.I. Drever (ed.), D. Reidel Publ. Co.: p. 161-175.
- EPRI, 1983. The Integrated Lake-Watershed Acidification Study. Volume 1. Model principles and application procedures. Rep. EA-3221. TETRA TECH Inc., Lafayette, Calif., USA.
- EPRI, 1984. The Integrated Lake-Watershed Acidification Study. Volume 4. Summary of major results. Rep. EA-3221. TETRA TECH Inc., Lafayette, Calif., USA.
- Feddes, R.A., P.J. Kowalik and H. Zaradny. 1978. Simulation of field water use and crop yield. Simulation Monographs. PUDOC, Wageningen.
- Federer, C.A., and J.W. Hornbeck, 1985. The buffer capacity of forest soils in New England. Water, Air Soil Pollut. 26: p. 163-173.
- Fendick, E.A. and R.A. Goldstein, 1986. Response of two Adirondack watersheds to acidic deposition. Water Air Soil Pollut. 33: p. 43-56.
- Gaines, G.L. and H.C. Thomas, 1953. Adsorption studies on clay minerals. II. A formulation of the thermodynamics of exchange adsorption. J. Chem. Phys. 21: p. 714-718.
- Galoux, A. 1981. Radiation, heat, water and carbon dioxide balances. p. 87-205. In: D.E. Reichle (ed.) Dynamic properties of forest ecosystems. IBP 23. Cambridge Univ. Press, Malta.
- Gash, J.H.C. and J.B. Stewart. 1977. The evaporation from Thetford forest during 1975. J. Hydrol. 35: p. 385-396.
- Goldstein, R.A., S.A. Gherini, C.W. Chen, L. Mak and R.J.M. Hudson, 1984. Integrated acidification study (ILWAS): A mechanistic ecosystem analysis. Philos. Trans. R. Soc. London, Ser. B 305: p. 409-425.

- Halbäck, L. and C.O. Tamm, 1986. Changes in soil acidity from 1927-1982-1984 in a forest area of south-west Sweden. *Scand. J. For. Sci.* 1: p. 219-232.
- Hauhs, M., 1985. Wasser- und Stoffhaushalt im Einzugsgebiet der Langen Bramke (Harz). *Berichte des Forschungszentrums Waldökosysteme/Waldsterben*, Bd. 17, Göttingen, FRG.
- Helgeson, H.C., 1971. Kinetics of mass transfer among silicates and aqueous solutions. *Geoch. Cosmoch. Acta* 35: p. 421-469.
- Helgeson, H.C., W.M. Murphy and P. Aagaard, 1984. Thermodynamic and kinetic constraints on reaction rates among minerals and aqueous solutions. II. Rate constants, effective surface area and the hydrolysis of feldspar. *Geoch. Cosmoch. Acta* 48: p. 2405-2432.
- Hillel, D. *Fundamentals of soil physics*, 1980. p. 152-155. Academic Press, New York.
- Hoeks, J., 1983. *Verzuring van bodem en grondwater als gevolg van atmosferische depositie*. Instit. voor Cultuurtechniek en Waterhuishouding, Nota 1480, Wageningen, the Netherlands.
- Hoeks, J., 1985. *Proc. Int. Conf. on Water Quality Modelling in the Inland Natural Environment*, Bournemouth, England, June 10-13, 1986, BHRA, Fluid Eng. Centre, Cranfield, Bedford, MK430AJ England. 9 p.
- Holdren, G.R. and P.M. Speyer, 1985^a. pH dependent changes in the rates and stoichiometry of dissolution of an alkali feldspar at room temperature. *Amer. J. Sci.* 285: p. 994-1026.
- Holdren, G.R. and P.M. Speyer, 1985^b. Reaction rate-surface area relationship during the early stages of weathering. I. Initial observations. *Geoch. Cosmoch. Acta.* 49: p. 675-681.
- Holdren, G.R. and P.M. Speyer, 1985^c. Stoichiometry of alkali feldspar dissolution at room temperature and various pH values, *In: Colman, S.M. and Dethier, D. (eds.), Rates of chemical weathering of rocks and minerals*, Academic Press, New York: p. 61-81.
- Holdren, G.R. and P.M. Speyer, 1987. Reaction rate-surface area relationships during early stages of weathering. II. Data on eight additional feldspars. *Geoch. Cosmoch. Acta.* 51: p. 2311-2318.
- Ingestad, T. 1987. *New concepts on soil fertility and plant nutrition as illustrated by research on forest trees and stands*. *Geoderma* 40: 237-252.
- Jackson, R.D. and F.D. Whisler. 1970. Equations for approximating vertical non-steady drainage of soil columns. *Soil Sci. Soc. Amer. Proc.* 34: p. 715-718.
- James, B.R. and S.J. Riha; 1986. pH buffering in forest soil organic horizons: Relevance to acid precipitation. *J. Environ. Qual.* 15: p. 229-234.
- Johnson, D.W., G.S. Henderson and D.E. Todd, 1988. Changes in nutrient distribution in forests and soils of Walker Branch watershed, Tennessee, over an eleven-year period. *Biogeochemistry: (In press)*.
- Jordan, C.F. 1982. The nutrient balance of an Amazonian rain forest. *Ecology* 63: p. 647-654.
- Journel, A.G. and C.J. Huijbregts. 1978. *Mining Geostatistics*. Academic Press, London.

- Kilsdonk, A.C.M., 1977. Non-Linear Optimization package OPTPAC 3. Program description and reference manual. ISA-DSA Scientific Computer Application, no UDV-DSA/SCA/TU/77/054/ap, N.V. Philips, Eindhoven, The Netherlands.
- Kinniburgh, D.G., 1986. Towards more detailed methods for quantifying the acid susceptibility of rocks and soils. *J. Geol. Soc. London* 143: p. 679-690.
- Kleijn, G.E., G. Zuidema and W. de Vries. 1988. De indirecte effecten van atmosferische depositie op de vitaliteit van Nederlandse bossen. 2. De bodemvochtsamenstelling in 8 Douglasopstanden. STIBOKA rep. no. 2050.
- Klute, A. 1972. The determination of the hydraulic conductivity and the diffusivity of unsaturated soils. *Soil Sci.* 113: p. 264-276.
- Koorevaar, P., G. Menelik and C. Dirksen. 1983. Elements of soil physics. Developments in soil science 13. Elsevier, Amsterdam.
- Krauskopf, K.B., 1967. Introduction to geochemistry. Mc. Graw-Hill Inc.
- Kwong, R.F., Ng Kee, and P.M. Huang, 1979. Surface reactivity of aluminum hydroxides precipitated in the presence of low molecular weight organic acids. *Soil Sci. Soc. Amer. J.* 43: p. 1107-1113.
- Lasaga, A.C., 1983. Kinetics of silicate dissolution. Proc. 4th Int. Conf. Water Rock Interaction: p. 269-274.
- Levine, E.R. and Ciolkosz, E.J. 1986. A computer simulation model for soil genesis applications. *Soil Sci. Soc. Amer. J.* 50 (3): p. 661-667.
- Lotus. 1983. Lotus Development Corpor. 161 First Street. Cambridge, MA 02142, USA.
- May, H.M., P.A. Helmke and M.L. Jackson, 1979. Gibbsite solubility and thermodynamic properties of hydroxy-aluminum ions in aqueous solutions at 25 C. *Geochim. Cosmochim. Acta*, 43: p. 861-868.
- McKeague, J.A., J.E. Brydon and N.M. Miles, 1971. Differentiation of forms of extractable iron and aluminum in soils. *Soil Sci. Soc. Amer. Proc.* 35: p. 33-38.
- Miller, H.G., 1978. The nutrient budgets of even-aged forests. In: D.C. Malcolm and J. Afferson (eds.) The ecology of even-aged forest plantations. Proc. Meeting of Divis. 1, IUFRO Edinburgh 1978.
- Mitscherlich, G. 1971. Forest, growth and environment (in German). Part II, Sauerländer's Verlag, Frankfurt a.M.
- Monteith, J.L. 1965. Evaporation and environment. *Proc. Symp. Soc. Exp. Biol.* 19: p. 205-234.
- Montgomery, B.R., L. Prunty and J. Bauder. 1987. Vacuum Trough Extractors for measuring drainage and nitrate flux through sandy soils. *Soil Sci. Soc. Am. J.* 51: p. 271-276.
- Mulder, J., J.J.M. van Grinsven and N. van Breemen, 1987. Impacts of acid atmospheric deposition on woodland soils in the Netherlands: III. Aluminum Chemistry. *Soil Sci. Soc. Amer. J.* 51: p. 1640-1645.
- Mulder, J., N. van Breemen, L. Rasmussen and C.T. Driscoll, 1988. Aluminum chemistry of acidic sandy soils with various inputs of acidic deposition in the Netherlands and in Denmark. *Amer.* (submitted to *Geoderma*).
- Nilsson, S.I., and B. Bergkvist. Aluminum chemistry and acidification processes in a shallow podzol on the Swedish westcoast. *Water Air Soil Pollut.*: 20, p. 311-329.
- Paces, T., 1973. Steady-state kinetics and equilibrium between ground water and granitic rock. *Geoch. Cosmoch. Acta* 37: p. 2641-2663.

- Paces, T., 1983. Rate constant of dissolution derived from the measurements of mass balance in hydrological catchments. *Geochim. Cosmochim. Acta* 47: p. 1855-1863.
- Paces, T., 1985. Sources of acidification in central Europe estimated from elemental budgets in small basins. *Nature* 315: p. 31-36.
- Paces, T., 1986^a. Weathering rates of gneiss and depletion of exchangeable cations in soils under environmental acidification. *J. Geol. Soc. London* 143, p. 673-677.
- Paces, T., 1986^b. Rates of weathering and erosion derived from mass balances in small drainage basins. **In:** Colman, S.M. and Dethier, D. (eds.), *Rates of chemical weathering of rocks and minerals*, Academic Press, New York: p. 531-551
- Peck, A.J. 1969. Entrapment, stability and persistence of air bubbles in soil water. *Austr. J. Soil Res.* 7: p. 79-90.
- Penman, M.L. 1948. Natural evaporation from open water, bare soil and grass. *Proc. R. Soc. London*, 193: p. 120-145.
- Petrovic, R., R.A. Berner and M.B. Goldhaber, 1976. Rate control in dissolution of alkali feldspars. I. Study of residual feldspar grains by X-ray photo-electron spectroscopy. *Geoch. Cosmoch. Acta* 40: p. 537-548.
- *Petrovic, R., 1976. Rate control in feldspar dissolution. II. The protective effects of precipitates. *Geoch. Cosmoch. Acta* 40: p. 1509-1521.
- Press, W.H., B.P. Flannery, S.A. Teukolsky and W.T. Vetterling. 1986. *Numerical Recipes. The art of scientific computing*. Cambridge University Press, New York.
- Reuss, J.O. 1983. Implications of the calcium-aluminium exchange system for the effect of acid precipitation on soils. *J. Environ. Qual.* 12: p. 591-595.
- Reuss, J.O. and D.W. Johnson, 1985. Effect of soil processes on the acidification of water by acid deposition. *J. Environ. Qual.* 14: p. 26-31.
- Reuss, J.O., N. Cristophersen and H.M. Seip, 1986. A critique of models for freshwater and soil acidification. *Water, Air Soil Pollut.* 30: p. 909-930.
- Roberts, J. 1983. Forest transpiration: a conservative hydrological process? *J. Hydrol.* 66: p. 133-141.
- Rutter, A.J. 1968. Water consumption by forests. p. 23-84. **In:** T.T. Kozlowski (ed.) *Water deficit and plant growth*, Vol. II. Academic Press, New York.
- Schnoor, J.L., W.D. Palmer and G.E. Glass, 1984. Modelling impacts of acid precipitation for northeastern Minnesota. **In:** J. Schnoor (ed.) *Modelling of total acid precipitation impacts*. Acid precipitation series, vol. 9. Butterworth Publ. Inc. Boston: p. 155-173.
- Singh, B. and G. Sceicz. 1979. The effect of intercepted rainfall on the water balance of a hardwood forest. *Water Resour. Res.* 15: p. 131-138.
- Skeffington, R.A. and K.A. Brown, 1986. The effect of five years acid treatment on leaching, soil chemistry and weathering of a humo-ferric podzol. *Water, Air and Soil Pollut.* 31: p. 891-900.
- Soil Survey Staff, 1975. *Soil Taxonomy: A basic system of soil classification for making and interpreting soil surveys*. USDA-SCS Agric. Handb. 436. U.S. Government Printing Office, Washington DC.
- Staatsbosbeheer, 1987. *De vitaliteit van het Nederlandse bos; 5. Verslag van de landelijk inventarisatie*. Rep. 1987-27. Afdeling Bosontwikkeling. Utrecht, the Netherlands.

- Steel, R.G.D., and J.H. Torrie, 1981. Principles and procedures of statistics. A biometrical approach. 2nd Ed., McGraw-Hill, Singapore.
- Stumm, W., G. Furrer, E. Wieland, and B. Zinder, 1985. The effects of complex-forming ligands on the dissolution of oxides and aluminosilicates. **In:** The Chemistry of Weathering, J.I. Drever (ed.), D. Reidel Publ. Co., Dordrecht, the Netherlands: p. 1997-2016.
- Stumm, W. and G. Furrer, 1986. The dissolution of oxides and aluminum silicates; Examples of surface coordination controlled kinetics. **In:** Colman, S.M. and Dethier, D. (eds.), Rates of chemical weathering of rocks and minerals, Academic Press, New York: p. 197-219.
- Ulrich, B., R. Mayer and P.K. Khanna, 1980. Chemical changes due to acid precipitation in a loess-derived soil in central Europe. *Soil Science* 130: p. 193-199.
- Ulrich, B. and Matzner, E. 1983. Abiotische Folgewirkungen der weiträumige Ausbreitung von Luftverunreinigungen. *Luftreinhaltung Forschungsbericht* 104 02 615.
- Ulrich, B., 1983. Soil acidity and its relation to acid deposition. **In:** Ulrich, B. and J. Pankrath (eds.) Effects of accumulation of air pollutants in forest ecosystems. Proc. Workshop. Göttingen, FRG, May 16-19, 1982. D. Reidel Publ. Co., Dordrecht: p. 127-146.
- *Van Breemen, N., P.A. Burrough, E.J. Velthorst, H. van Dobben, Toke de Wit, T.B. Ridder and H.F.R. Reijnder, 1982. Soil acidification from atmospheric ammonium sulphate in forest canopy throughfall. *Nature* 299: p. 548-550.
- *Van Breemen, N., J.J.M. van Grinsven and E.R. Jordens, 1983. H⁺ budgets and nitrogen transformations in woodland soils in the Netherlands influenced by high inputs of atmospheric ammonium sulphate. Proc. Int. Conf. Acid Precipitation - Origin and effect. VDI, Düsseldorf, Germany.
- Van Breemen, N., J. Mulder and C.T. Driscoll, 1983. Acidification and alkalization of soils. *Plant and Soil* 75: p. 283-308.
- Van Breemen, N., C.T. Driscoll, and J. Mulder, 1984. Acidic deposition and internal proton sources in acidification of soils and waters. *Nature* 307: p. 599-604.
- Van Breemen, N., P.H.B. de Visser and J.J.M. van Grinsven, 1986. Nutrient and proton budgets in four soil-vegetation systems underlain by Pleistocene alluvial deposits. *J. Geol. Soc. London* 143: p. 659-666.
- Van Breemen, N., J. Mulder and J.J.M. van Grinsven, 1987. Impacts of acid atmospheric deposition on woodland soils in the Netherlands: II. Nitrogen transformations. *Soil Sci. Soc. Amer. J.* 51: p. 1634-1640.
- Van Breemen, N., W.J.F. Visser and Th. Pape (eds.). 1988. Biogeochemistry of an oak woodland affected by acid atmospheric deposition. Agric. Res. Rep. no. 930 (ISBN 90 220 0942-4), PUDOC, Wageningen, the Netherlands.
- Van Diest, A., 1986. Aanvullende bemesting met mineralen in Nederlandse bossen. *Meststoffen* 2/3: p. 4-9.
- Van Dobben, H.F. and Mulder, J. 1988. Impact of acid atmospheric deposition on oligotrophic ecosystems part II: Biogeochemistry and hydrobiology of moorland pools and surrounding upland areas. Report in preparation.
- Van Genuchten, M.Th. 1981. A closed form equation for predicting the hydraulic conductivity of unsaturated soils. *Soil Sci. Soc. Am. J.* 44: p. 892-898.

- *Van Grinsven, J.J.M., J. Mulder and N. van Breemen, 1984. Hydrochemical budgets of some dutch woodland soils with high inputs of atmospheric acid deposition. Mobilization of aluminium: **In:** Eriksson, E. (ed.), Hydrochemical balances of freshwater systems. IAHS Publication No 150: p. 237-247.
- Van Grinsven, J.J.M., G.D.R. Kloeg and W.H. van Riemsdijk, 1986. Kinetics and mechanism of mineral dissolution in a soil at pH values below 4. *Water, Air and Soil Pollut.* 31: p. 981-990.
- Van Grinsven, J.J.M., F.A.M. de Haan and W.H. van Riemsdijk, 1986. Effects of acidic deposition on soil and groundwater. **In:** T. Schneider (ed.), Acidification and its policy implications. Elsevier Sci. Publ., Amsterdam, the Netherlands.
- Van Grinsven, J.J.M., N. van Breemen, W.H. van Riemsdijk and J. Mulder, 1987^a. The sensitivity of acid forest soils to acid deposition. *Proc. Int. Sympos. Acidification and water pathways*, Bolkesjo 4-5 May, Norwegian National Committee for Hydrology (ISBN 82-554-0486-4), p. 365-374.
- Van Grinsven, J.J.M., N. van Breemen and J. Mulder, 1987^b. Impacts of acid atmospheric deposition on woodland soils in the Netherlands: I. Calculation of hydrologic and chemical budgets. *Soil Sci. Soc. Amer. J.* 51: p. 1629-1634.
- Van Grinsven, J.J.M., H.W.G. Booltink, C. Dirksen, N. van Breemen, N. Bongers and N. Waringa, 1988^a. Automated in situ measurement of unsaturated soil water flux. *Soil Sci. Soc. Amer. J.* (In press).
- Van Grinsven, J.J.M., and W.H. van Riemsdijk, 1988. A comparison between batch and column techniques to measure weathering rates in soils. Discrepancies with rates from field mass balance studies. (submitted to *Geoderma*).
- Van Grinsven, J.J.M., W.H. van Riemsdijk and R. Otjes, 1988^b. Weathering kinetics in acid sandy soils from column experiments: I. Aluminum. (submitted to *Soil Sci. Soc. Amer. J.*).
- Van Grinsven, J.J.M., W.H. van Riemsdijk and N. van Breemen, 1988^c. Weathering kinetics in acid sandy soils from column experiments: II. Base cations. (submitted to *Soil Sci. Soc. Amer. J.*).
- Van Grinsven, J.J.M., H. Denier van der Gon, W.H. van Riemsdijk and N. van Breemen, 1988^d. Evidence for increased weathering of Ca from plagioclases as a result of dissolution of protective Al-coatings in acid solutions. (submitted for publ. in *Geochim. Cosmochim. Acta*)
- Van Riemsdijk, W.H., and A.M.A. van der Linden, 1984. Phosphate sorption by soils: II. Sorption measurement technique. *Soil Sci. Soc. Amer. J.* 48: p. 541-544.
- Velbel, M.A., 1985. Geochemical mass balances and weathering rates in forested watersheds of the Southern Blue Ridge. *Amer. J. Sci.* 283: p 904-930.
- Velbel, M.A., 1986. Influence of surface area, surface characteristics, and solution composition on feldspar weathering rates. In *Geochemical processes at mineral surfaces*, J.A. Davis and K. F. Hayes (eds), ACS Symposium series No. 323, Amer. Chem. Soc.: p. 615-634.
- Wagenet, R.J. 1986. Water and solute flux. **In:** A. Klute (ed.) *Methods of soil analysis. Part 1. Physical and mineralogical methods.* Agron. Monogr. no. 9. ASA-SSSA, Madison.
- Wilson, M.J., 1975. Chemical weathering of some primary rock-forming minerals. *Soil Sci.* 119: p. 349-354.

- Winkels, H., 1985. Kwantitatieve aspecten van de koolstof en stikstof huishouding van de strooisellaag in de gronden van het Hackfortprojekt. Msc thesis, Agricultural University, Wageningen, the Netherlands.
- Wollast, R., 1967. Kinetics of the alteration of K-feldspar in buffered solutions at low temperature. *Geoch. Cosmoch. Acta* 31: p. 635-648.
- Wollast, R. and L. Chou, 1985. Kinetic study of the dissolution of albite with a continuous flow-through fluidized bed reactor. **In:** *The chemistry of weathering*, J.I. Drever (ed.), D. Reidel Publ. Co., Dordrecht, the Netherlands: p. 75-96.

* Not referred to in thesis but of general interest to subject

Curriculum Vitae

Hans van Grinsven werd geboren op 11 maart 1958 te Cuijk (Noord Brabant) als één van vijf zonen van Theo van Grinsven en Hubertha Jacobs. In 1976 behaalde hij het diploma atheneum-B aan het Elzendaalcollege te Boxmeer. In hetzelfde jaar begon hij met de studie aan de Landbouwhogeschool te Wageningen, en koos hij voor de studierichting Bodemkunde en Bemestingsleer (N33). Gedurende de periode van September 1979 tot Juli 1980 volbracht hij de praktijk en een drie-maands doctoraalvak Bodemchemie op de University of Florida bij Dr. Jimmy Street. De doctoraalstudie bestond verder uit een zes-maands vak Kolloïdchemie bij Dr. Rob Cleven en Dr. Herman van Leeuwen, en een zes-maands vak Bodemnatuurkunde bij Dr. Chris Dirksen. In mei 1982 verkreeg hij het ingenieursdiploma met lof.

Van juni 1982 tot juli 1988 was hij werkzaam als wetenschappelijk assistent bij de Vakgroep Bodemkunde en Geologie in het project "Effekten van zure atmosferische depositie op de bodem" onder leiding van Professor Nico van Breemen. Voor het onderzoek was hij gedetacheerd op de Vakgroep Bodemkunde en Plantenvoeding, waar nauw werd samengewerkt met Dr. Willem van Riemsdijk en Professor Frans de Haan van de sectie Bodemhygiëne en Bodemverontreiniging, en met Dr. Chris Dirksen van de sectie Bodemnatuurkunde. Het onderzoek was gericht op watertransport in de onverzadigde zône, de kinetiek van mineraalverwerking en simulatie van bodemverzuringprocessen. Van 1982 tot 1985 werd zijn aanstelling gefinancierd door de EEG en van, 1985 tot en met 1988 door VROM, als onderdeel van het Het Nationaal Programma Zure Regen. In het onderzoek werd verder samengewerkt met het Energie Centrum Nederland te Petten en met het Staatliches Amt für Wasser und Abfall Wirtschaft te Münster (BRD).